UNIVERSIDAD D SEVILLA

FACULTAD DE FÍSICA

DEPARTAMENTO DE FÍSICA
ATÓMICA, MOLECULAR Y NUCLEAR

Quantum correlations and graphs

Memoria presentada por

Antonio José López Tarrida

para optar al grado de Doctor en Física

Sevilla, 30 de junio de 2014

DEPARTAMENTO DE FÍSICA ATÓMICA, MOLECULAR Y NUCLEAR
Facultad de Física
Universidad de Sevilla

Quantum correlations and graphs

Memoria presentada al Departamento de Física Atómica, Molecular y Nuclear, y a la Comisión de Doctorado de la Universidad de Sevilla en cumplimiento de los requisitos para optar al grado de Doctor en Física

El Director:

Dr. D. Adán Cabello Quintero

El Tutor:

Dr. D. Joaquín José Gómez Camacho

El Doctorando:

D. Antonio José López Tarrida

Sevilla, 30 de junio de 2014

Requisitos para la Mención Internacional en el Título de Doctor

La memoria de tesis doctoral que presentamos cumple los siguientes requisitos para la optar a la *Mención Internacional en el Título de Doctor*:

- Durante el período de investigación del Doctorado, el doctorando ha realizado una estancia de investigación de tres meses fuera de España en una institución de enseñanza superior o centro de investigación de prestigio realizando trabajos de investigación directamente relacionados con su tesis. En concreto, entre el 25 de septiembre y el 23 de diciembre de 2011 fue estudiante de doctorado visitante en el grupo de investigación Kvantinformation & Kvantoptik (KIKO), de la Stockholms Universitet, dirigido por el Prof. Dr. Mohamed Bourennane y bajo la supervisión directa del mismo.

- Parte de la tesis doctoral, al menos el resumen y las conclusiones, se ha redactado en una de las lenguas habituales para la comunicación científica en su campo de conocimiento, distinta a cualquiera de las lenguas oficiales en España (en inglés). La disertación en defensa de la tesis, igualmente, será realizada parcial o totalmente en inglés.

- La tesis ha sido informada por un mínimo de dos expertos pertenecientes a alguna institución de educación superior o instituto de investigación no español. Han emitido informe positivo acerca de la tesis doctoral y en apoyo de la Mención Internacional los profesores

  - Dr. Jan-Åke Larsson, de la Linköpings Universitet, Suecia.
  - Dr. Marcelo Terra-Cunha, de la Universidade Federal de Minas Gerais, Brasil.

- Formará parte del tribunal evaluador de la tesis al menos un experto con título de Doctor perteneciente a alguna institución de educación superior o instituto de investigación no español. Ha confirmado su participación el Prof. Dr. Otfried Gühne, de la Universität Siegen, Alemania.

Agradecimientos

La tesis que hoy concluyo con estas líneas, cierra una historia que comenzó... con otra tesis doctoral, allá por los primeros años 90 del siglo pasado, siendo yo otro yo, mucho más joven. Tras los cursos de doctorado, aquella tesis, de temática y naturaleza bien diferentes a ésta, quedó abruptamente interrumpida —y finalmente abandonada— antes de tomar cuerpo y densidad por la inesperada visita de la enfermedad, que me obligó a replantearme mis prioridades. Hoy, dos décadas más tarde, más viejo y experimentado aunque no sé si más sabio, tras un feliz matrimonio, dos hijos, dolorosas desapariciones de familiares y amigos queridos, concursos y oposiciones, innumerables horas de trabajo como docente, miles de alumnos, el desempeño de un cargo académico en la universidad, cumplimiento de fechas, presión y estrés, reconocimientos y sinsabores, azares y vicisitudes, luces y sombras, cierro una etapa y confío en abrir otra, no necesariamente mejor, pero quizá más plena y más tranquila.

Es momento de mirar atrás con agradecimiento, y tener un recuerdo para aquellas personas que han ayudado en el último lustro, a veces sin saberlo, a que esta tesis haya pasado de ser una entelequia a materializarse por fin, tras un considerable esfuerzo de comprensión y compresión (más si cabe en alguien tan proclive como el que escribe a dejarse llevar por el frenesí del verbo), en una memoria de poco más de doscientas páginas que encierran muchos sacrificios. Sin la influencia, consejo y apoyo explícitos o implícitos de esas personas, el producto final habría sido bien distinto, a buen seguro peor: cualquier demérito que aun así persista en esta memoria es enteramente achacable al autor, y no a sus supervisores, colaboradores, compañeros, familiares y amigos. Cualquier relación de éstos a buen seguro pecará de incompleta, por lo que de entrada pido disculpas si alguien se siente postergado u olvidado, esperando con ello que sea indulgente y no me lo tenga en cuenta.

La génesis, desarrollo y materialización de este trabajo de investigación no hubieran sido posibles sin el estímulo de mi director de tesis, compañero y amigo, Adán Cabello Quintero. Soy consciente de que yo, ya entrado en la cuarentena, algo oxidado, con obligaciones académicas y familiares sin cuento y con muy poco tiempo disponible, no encajaba en el modelo ideal de estudiante de doctorado *full-time* recién licenciado que Adán tenía en mente cuando me propuso el reto ("Un estudiante de doctorado debe trabajar 24 horas al día... Y si no es suficiente, debe trabajar también de noche", Asher Peres. Mensaje enviado por Adán por correo-e o por Skype..., varias veces en cinco años). Le debo gratitud por atreverse, asumir el riesgo y tener paciencia con mis otras obligaciones. Su pasión y entusiasmo contagiosos por la Mecánica Cuántica, sus misterios, perplejidades y sorpresas, que me ha transmitido a través de jugosas discusiones cuyo tiempo hemos robado al poco del que ya disponíamos, han hecho posible culminar la empresa. Hacerme partícipe de sus hallazgos y avances en sus trabajos en solitario

o con otros autores, permitiéndome intervenir en numerosas discusiones aportando mi punto de vista, ha sido un regalo enormemente enriquecedor, que de paso me ha brindado la posibilidad de conocer e interaccionar con algunos de los investigadores más destacados en nuestro campo de estudio. Recuerdo en particular, con especial afecto, al Dr. Fabio Sciarrino, de la Universitá di Roma La Sapienza, a quien Adán me presentó en la XXXIII Bienal de la RSEF en Santander, en septiembre de 2011, con quien mantuve cordiales e interesantes conversaciones, y que me dio buenos consejos ante mi inminente marcha a Estocolmo. Precisamente, la oportunidad de realizar una estancia de investigación en Estocolmo se concretó gracias a Adán, merced a sus contactos y su implicación personal en las gestiones. Otra ocasión singular que se hizo realidad gracias a Adán fue la asistencia al *FQXi Workshop on Quantum Contextuality and Sequential Measurements*, celebrado en Sevilla en noviembre de 2013. Allí Adán me presentó a investigadores a quienes admiraba por sus trabajos pero a los que no conocía personalmente: Marek Żukowski, Karl Svozil, Otfried Gühne, Jan-Åke larsson, Matthias Kleinmann, Dagomir Kaszlikowski, Pawel Kurzyński, Mateus Araújo, entre otros. Todo un privilegio.

Espero, en el balance final, no haberle defraudado en exceso. Yo finalizo mi viaje enriquecido por tantas memorables experiencias. Por todo ello y mucho más, gracias de nuevo, Adán.

Quiero manifestar mi agradecimiento a los miembros del Departamento de Física Atómica, Molecular y Nuclear de la Facultad de Física de la Universidad de Sevilla, tanto a su personal docente como de administración y servicios, porque durante el tiempo que compartí con ellos en una primera etapa hace años (aquel remoto proyecto de tesis...), y recientemente en este último quinquenio de reencuentro, siempre me han dispensado una cordial acogida. Quiero en particular agradecer su disponibilidad, su atención y su tiempo a José Miguel Arias Carrasco, Director del Departamento, y a Joaquín José Gómez Camacho, mi tutor en el programa de doctorado de Física Nuclear, ambos con una agenda muy apretada en la que siempre han hecho hueco generosamente cuando he necesitado su consejo y apoyo. Tengo un recuerdo agradecido también para Miguel Ángel Respaldiza Galisteo, que pudo ser mi director de tesis si la rueda de la fortuna hubiese girado de otra forma, y que presidió en diciembre de 2009 el tribunal evaluador de mi Diploma de Estudios Avanzados en Física Nuclear. Y cómo no, a Pepe Díaz, siempre tan servicial, por su ayuda en el laboratorio hace años, y por su interés en cómo me han ido yendo las cosas últimamente.

Las fructíferas conversaciones e intercambios "e-epistolares" (por correo-e) con mis colaboradores en trabajos de investigación, cuyas coordenadas mentales tanto difieren en algunos aspectos de las mías para beneficio de todos, me han hecho ponerme al día, reciclarme, motivarme, mejorar, profundizar..., ¡y divertirme! Quiero recordar aquí con cariño innumerables charlas mantenidas a lo largo de cuatro años con Pilar Moreno Martín, compañera de doctorado en el Grupo de Investigación de Fundamentos de Mecánica Cuántica, en las que compartimos no sólo lo meramente científico, sino también inquietudes en un terreno más personal, aquí en Sevilla, en Ciudad Real y en Roma. Vaivenes de la vida tras la defensa de su tesis doctoral han hecho que perdamos el contacto: le deseo lo mejor en sus aspiraciones de futuro. Con Lars Eirik Danielsen, de la Universidad de Bergen (Noruega), que trabaja ahora en el ámbito privado, he mantenido contacto a distancia: ha sido un admirable colaborador, eficaz y brillante, un auténtico especialista, de trato cordial y educado por escrito, y jucio certero. Para mí ha sido un auténtico privilegio trabajar con él. En cuanto a José Ramón Portillo Fernández, "José-Ra", nuestro matemático residente, especialista en Matemática Discreta y Teoría de Grafos, qué

puedo decir: me he sentido en todos estos años muy identificado con su manera altamente creativa de abordar los problemas, dosificando adecuadamente orden y caos, todo ello con un fino e irónico sentido del humor, con el que simpatizo visceralmente. Guardo gran cantidad de correos-e que atestiguan la buena sintonía y la sinergia positiva de nuestra colaboración, de la que yo a buen seguro he obtenido más de lo que haya podido aportarle. Le agradezco especialmente su apoyo y comprensión en los momentos grises que, como toda empresa de largo recorrido, tiene la realización de una tesis doctoral. Gracias, amigo José-Ra, por el ánimo constante y el optimismo militante. Un apartado especial merece también Carmen Santana, quien desinteresadamente, pues es completamente ajena a nuestro campo de investigación —aunque por motivos personales lo sigue de cerca—, tuvo a bien prestarnos ayuda gráfica en uno de nuestros artículos: a su experta mano con las herramientas de diseño gráfico debemos las figuras 4.1 y 4.2 de esta tesis doctoral, por las cuales le estamos enormemente agradecidos (de la calidad de su trabajo da fe el que la segunda de ellas acabó siendo figura de portada del volumen 45, número 28, de 20 de julio de 2012 en la revista *Journal of Physics A: Mathematical and Theoretical*).

Entre el 25 de septiembre y el 23 de diciembre de 2011 realicé una estancia de investigación de tres meses como estudiante de doctorado visitante en el grupo de investigación Kvantinformation & Kvantoptik (KIKO), de la Stockholms Universitet, dirigido por el Prof. Dr. Mohamed Bourennane, bajo la directa supervisión de éste y de Adán Cabello. Dicha estancia, a la que tanto debe la primera parte de esta tesis doctoral (la última, cronológicamente), fue una experiencia irrepetible. Separarme tres meses de mi familia, con mis hijos en una edad crítica en que necesitaban a su padre cerca (aunque Skype haga milagros) fue una apuesta importante, en que mi mujer jugó un papel esencial, al darme la tranquilidad necesaria para poder marchar a Estocolmo sin inquietudes. Desde el día de mi llegada, el Prof. Bourennane fue simplemente Mohamed, un supervisor cercano, cordial, amigable y divertido al par que duro y exigente, que me hizo fácil la estancia: se puso completamente a mi disposición aquel primer lunes en el AlbaNova Universitetscentrum, me presentó uno por uno a todos los miembros del grupo, y no cejó hasta que quedé perfectamente equipado, conectado e instalado en mi silla en el extremo izquierdo de la mesa corrida de la sala A3001, la de los *PhD students*, en la tercera planta del edificio, a un tiro de piedra de su despacho. Estoy en deuda de gratitud con el Prof. Bourennane por su inestimable apoyo y consejo, y por las numerosas discusiones sobre la Mecánica Cuántica, sus fundamentos y aplicaciones, tanto en los muchos almuerzos compartidos con Adán Cabello y con él en *Le Due Fratelli* o en el comedor del AlbaNova, como en los encuentros en el acogedor seminario con cristalera orientada al oeste, mirando al lago Brunnsviken. En una de esas ocasiones, por mediación de Adán, conocí a Piotr Badziąg, y disfruté viéndoles a él, a Adán y Mohamed discutir, discrepar y debatir los pormenores de un artículo en ciernes, que a la postre acabaría presentando las tres desigualdades pentagonales de Bell. Tres temperamentos fuertes, y toda una experiencia.

Quiero dejar constancia de mi agradecimiento a todos los miembros del grupo del Prof. Bourennane, en especial a Hannes Hübel e Isabel Herbauts, que me obsequiaron con su agradable compañía y cálida conversación en el almuerzo del primer día y en muchas otras ocasiones, y se interesaron por mi situación en Estocolmo, solventando mis dudas y brindándome su tiempo cuando necesité ayuda con trámites o con problemas informáticos de diversa índole. También a Elias Amselem, brillante investigador, estupendo compañero, agradable y gran conversador, con quien mantuve cordial relación desde el primer momento. Lo mismo puedo decir de Kate

Blanchfield y Johan Ahrens, y por idénticas razones. Alley Hameedi y Muhamad Sadiq me depararon buenos ratos de camaradería: paciente y amablemente, tuvieron a bien enseñarme el laboratorio y mostrarme en detalle los experimentos que estaban llevando a cabo, y fueron muy cordiales y entrañables el día de mi vuelta a casa. Con el Prof. Ingemar Bengtsson compartí un interesante almuerzo en un restaurante con comida local, y una aún más interesante discusión en compañía de Adán y Kate sobre la desigualdad de Yu-Oh, recién descubierta. He dejado para el final al estudiante de máster Mojtaba Taslimitehrani, "Mo": éramos casi siempre los primeros en llegar y los últimos en irnos. Con él compartí té, inquietudes, charlas reposadas al mediodía y a la caída temprana de la noche nórdica, planes de futuro, sus desvelos con la gravitación cuántica, y de cuando en cuando parte del recorrido diario de regreso a casa, desde el AlbaNova hasta la estación de metro de Odengatan. Sé que anda ahora por la Chalmers University of Technology, en Göteborg: le deseo la mejor de las suertes en su carrera investigadora, y en la vida.

Estocolmo resultó una ciudad acogedora, lo que favoreció que no tuviese que preocuparme de otra cosa que no fuera la investigación, con algunos momentos de ocio y esparcimiento. Ello fue posible gracias entre otras cosas al propietario del piso en que alquilé mi habitación durante los tres meses: Carlos Sanz, sudamericano afincado en Suecia desde hace años, un hombre respetuoso, afable y servicial, con el que fue muy fácil entenderse. Durante el primer mes y medio compartí piso con un alemán de voz grave y risa resonante, Sascha Tiede, doctor en Química que a la sazón estaba realizando un postdoc en la Stockholms Universitet. Recuerdo nítidamente el día de mi llegada, a las 4 p.m. del 25 de septiembre de 2011: tal como solté la maleta, tras las oportunas formalidades, me agarró del brazo, me metió en el metro de Bergshamra, y me enseñó Gamla Stan en una hora y media, llevándome con la lengua fuera, según él para aclimatarme a la ciudad cuanto antes. Lo cierto es que fue un buen compañero de piso, con el que simpaticé desde primera hora, y al que eché de menos a su marcha. Le reemplazó un joven y políglota cocinero holandés, Cornelis van der Plas (o "Cor", como le gustaba que le llamaran), cuyo horario era disjunto respecto al mío, salvo dos días en semana, en que departíamos en los desayunos y acordábamos una mínima coordinación. Puedo decir que con ambos tuve suerte, y la convivencia fue civilizada. Esta ausencia de problemas domésticos fomentó la concentración en el piso, donde el trabajo y el estudio continuaban hasta bien entrada la noche, preparando la jornada siguiente. En definitiva, guardo de mi estancia en Estocolmo un magnífico recuerdo.

La estancia de investigación en el extranjero es uno de los requisitos que deben cumplirse para que esta tesis pueda optar a la Mención Internacional en el Título de Doctor. Otro requisito indispensable es el informe positivo por parte de dos expertos pertenecientes a alguna institución de educación superior o instituto de investigación extranjero. Debo manifestar mi profundo agradecimiento a los profesores Dr. Jan-Åke Larsson, de la Linköpings Universitet (Suecia), y Dr. Marcelo Terra-Cunha, de la Universidade Federal de Minas Gerais (Brasil), por su amabilidad a la hora de ofrecerse para leer el manuscrito de la tesis y emitir el correspondiente informe. Les doy las gracias, no sólo por el tono y contenido de los informes, sino por haber hecho un hueco en sus apretadas agendas entre tránsito, vuelo y congreso, para ocuparse del trabajo de un doctorando acuciado por plazos inminentes que cumplir, que irrumpió en sus programas de actividades alterándolos irremisiblemente.

Ya de vuelta en Sevilla, y prosiguiendo con los reconocimientos, agradezco vivamente a muchos compañeros del claustro de profesores de la Escuela Técnica Superior de Ingeniería

de Edificación, su interés por saber de mis progresos y su insistencia en que no decayera en mi ánimo, cuando aún el final estaba lejos. En particular a los más persistentes en diversas épocas: José María Calama Rodríguez, Antonio Ramírez de Arellano Agudo, Juan Jesús Gómez de Terreros, Enrique Herrero Gil, Amparo Graciani García, Valeriano Lucas Ruiz, Rosa María Domínguez Caballero y Juan Jesús Martín del Río. Retrospectivamente, lo valoro mucho más ahora que el final ya se vislumbra.

Me siento especialmente en deuda con todos mis compañeros del Departamento de Física Aplicada II. En la sección de Arquitectura todos merecen un hueco en estas líneas: José Pablo Baltanás, Diego Frustraglia, Rafael García-Tenorio, Francisco Gascón, Pilar Gentil, Sara Girón, Aureliano Gómez, Guillermo Manjón, Juan Mantero, Jesús Martel, Rafael Morente, Francisco Nieves, Juan Lucas Retamar e Ignacio Vioque, cada uno a su manera ha sido un apoyo y un estímulo durante todo este tiempo. Pero he de destacar singularmente a una gran, excelente persona: Teófilo Zamarreño García, siempre dispuesto a interesarse por mis avances, y a darme constantemente ánimos y consejo durante años, siempre con la palabra justa, siempre tan cercano. Quizá no lo sabías ni lo sospechabas, Teo, pero te estoy muy, muy agradecido.

En cuanto a mis compañeros de Física Aplicada II en la E. T. S. de Ingeniería de Edificación... Estas palabras no pueden hacerles justicia. Sin ellos este trabajo podría haber descarrilado por falta de tiempo, o haberse alargado *sine die*. Me han cubierto las espaldas en los asuntos del día a día siempre que lo he necesitado durante los últimos dos o tres años, lo que me ha permitido sacar más tiempo y concentrarme en esta tarea, y han soportado estoicamente mis digresiones, limítrofes con la obsesión monomaníaca, acerca de las luces y sombras del trabajo de investigación, y lo han hecho con una sonrisa amable, exenta de diplomacia. Gracias (por orden de antigüedad creciente en el grupo, que no de mérito) a Sheila López, María Villa, Manuel Espín, Adán Cabello, Miguel Galindo, Agustín Fernández, Helena Moreno, Paco Pontiga, Leoncio García y Martín Muñoz. Mi recuerdo más sentido a nuestro buen Antonio Ramírez Pérez, que nos dejó antes de tiempo, y al que a buen seguro le habría gustado verme en este trance. Todos sois no sólo compañeros, sino amigos. A cada uno de vosotros debo algo:

Sheila y María, que han aportado aires nuevos al grupo, me han dado valiosísimos consejos de toda índole, y han hecho que renueve mis energías y mi ilusión en momentos de desánimo. A las dos, gracias por ese desbordante y contagioso entusiasmo. Espero compartir con vosotras muchos años de amistad, colaboración y compañerismo.

Manuel, en relativamente poco tiempo, se ha convertido en un auténtico amigo, merecedor de mi más absoluta confianza y respeto. Te agradezco tu permanente y desinteresada oferta de apoyo y ayuda, el estar al quite en todo lo que ha ido surgiendo durante la elaboración de esta tesis, y tu aguda perspicacia en todos los problemas que te he consultado.

De Adán..., ya ha quedado dicho todo al principio: sólo deseo que sigamos colaborando y disfrutando, más si cabe, en la docencia, la investigación y en el día a día.

Miguel, con su aparentemente despreocupada manera de tomarse lo que la vida va trayendo, me ha enseñado a desdramatizar ante las adversidades, a asumirlas con naturalidad, y a no tomarse a uno mismo demasiado en serio, todo un ejercicio de salud mental y una gran lección de cara a la redacción de la memoria de la tesis. Gracias, maestro.

A ti Agustín, amigo fiel y constante, he de agradecerte tu bonhomía, tu carácter afable, y tu absoluta e incondicional disponibilidad para todo lo que pudiera necesitar. E instarte, con aprecio, a que pongas proa al puerto de su tesis, con buen viento.

Helena, mi amiga desde hace más de veinte años, siempre está ahí, siempre tiene tiempo que concederme aun cuando le agobien sus muchas tareas. Gracias por escucharme, aunque últimamente sea tan pesado y me repita demasiado con mis desvelos sobre la tesis. Gracias por la amistad que compartimos y que ha ido acendrándose con el paso del tiempo.

A Leoncio, entrañable amigo al que echamos mucho en falta en el día a día por su buen humor contagioso, le agradezco sus sabios consejos, y la lección continua que nos da con su manera de enfocar la vida. Sabes bien que todos, de mayores, queremos ser (y haber sido) como tú. Gracias por recordarme, en los agobios de la tesis, cuáles eran las auténticas prioridades.

Con Martín, gran amigo en horas bajas, con quien tantas cavilaciones sobre la tesis y sobre un sinfín de temas he compartido antes de su retiro pasajero, mi deuda de gratitud es enorme, imposible de saldar. Te deseo un pronto y feliz restablecimiento, que nos permita compensar el tiempo que se fue en una nueva etapa de mayor densidad vital.

Y Paco... El pasado 31 de enero, con ocasión de una de sus providenciales actuaciones, Adán me dijo por correo-e: "Hablamos poco de ello: Paco es estupendo". Y llevaba toda la razón. Va siendo hora de que quede consignado por escrito: querido Paco, contigo se rompió el molde. Creo que todos estamos de acuerdo en que no puede haber mejor compañero. Gracias mil, Paco, por tu tiempo, por tu entrega, por tu ayuda, por tu serenidad, por tu capacidad y por tu pericia puesta al servicio de todos y mío. Esta tesis sería muy distinta, lo sabes bien, sin tus atinados consejos sobre los misteriosos caminos del LaTeX y otras herramientas, cuando nada parecía funcionar. Y, por supuesto, tampoco sería la misma tesis sin los desayunos en que a diario la irrepetible Susana, tú y yo arreglamos el mundo. Susana, la de verbo apasionado y preciso, mente privilegiada, mil y un intereses y temas de conversación, consejo oportuno y buenos sentimientos. En lo práctico, le agradezco su sensato punto de vista sobre las vicisitudes que un doctorando atraviesa en la génesis y desarrollo de una tesis doctoral, que ha sido muy valioso para mí. Pero me quedaría muy corto limitándome sólo a eso: es mucho más lo que hemos compartido. Sobre todas las cosas he de agradecerle... que sea como es. Gracias, amiga.

Termino con mi círculo más íntimo:

Gracias a todos mis otros amigos, los de fuera del trabajo, y muy singularmente a Alberto (mi amigo más antiguo) y su mujer Rocío, y a "los seis magníficos" de los últimos veinte años: Eva y Pepe, Chary y Manolo, Helena y Manuel. Vosotros, quizá sin ser conscientes de ello, habéis jugado un papel muy importante, habéis sido una válvula de escape, un bálsamo de las tensiones acumuladas durante la escritura de esta memoria. Me habéis recordado todos estos años, en jornadas memorables de camaradería y eutrapelia, que sí, que es cierto, que hay vida más allá de la tesis...

Finalmente, gracias a mi familia, la carnal y la extendida:

A Feli, Enrique, Mariló, Luis y Amparo, por preguntar desinteresadamente por mis progresos, y animarme. A mis cuñados Pedro y Jorge, por muchas estimulantes conversaciones en torno a la tesis.

Y a mis hermanos: Alicia, Inmaculada, Patricio Luis, Ángela y Cristina, que transitan conmigo por la vida desde siempre, por su firme apoyo en esta empresa todos estos años, sus constantes palabras de ánimo, y su cariño incondicional. No se necesitan más palabras...

A todos los citados y a los omitidos involuntariamente, muchas gracias.

Los que están permanentemente en mi pensamiento: mis padres, mi mujer, mis hijos, mi maestro, merecen una dedicatoria aparte...

Dedicatoria

Esta tesis doctoral, esta larga empresa de reflexión y crecimiento interior que tantas horas de sueño y vigilia me ha robado, está dedicada a quienes más la han sufrido y disfrutado conmigo en todos estos años. Con vosotros lo celebro:

A mis padres, Antonio y Filli, las personas más rectas que he conocido nunca, mi modelo de conducta en la vida, mi referente ético, mi apoyo incondicional, raíces y savia de mi árbol. Siempre os estaré en deuda por vuestro cariño y vuestros sacrificios, sin los cuales no sería posible haber llegado hasta aquí. Esta tesis doctoral es también vuestra. Os quiero.

A mi esposa Maribel, por ser y estar, *hic et nunc, nunc et semper*. La bella hechicera de todos los días, magia cotidiana que lo hace todo posible. Mi inspiración, mi reposo, mi bálsamo, mi hogar, mi amor, agua, aire y sol de mi árbol. Por sufrirme y entenderme. Por tu entrega. Por todo lo compartido, por todo lo que tú sabes.

Y a mis hijos Antonio José y María Celeste, mis tesoros más preciados, mi ilusión renovada a diario, mi aventura más estimulante, mi arco iris tras la tormenta, prometedores frutos de mi árbol. Por ser tan comprensivos para su tierna edad cuando comencé esta empresa, y entender que su padre tenía que robarles un poco de su tiempo para dedicarlo a menesteres más prosaicos. Y, ahora que han crecido, por haber sabido esperarme con una sonrisa expectante al final del camino.

Por último, una dedicatoria especial a una persona irrepetible. Cuando empecé esta tesis doctoral, no imaginaba que tendría que formularla de esta manera, lamentablemente:

A mi maestro, D. Luis Rey Romero (1935–2009), la primera persona que me habló de esa extraña disciplina llamada Mecánica Cuántica, en agradecimiento por la pasión que siempre puso en la docencia y la investigación. Maestro en el aula y en la vida, tanto en la salud como, especialmente, en la enfermedad que no pudo doblegar su espíritu. Mi amigo. Con admiración, respeto, y ya desgraciadamente con irreversible nostalgia de los momentos compartidos.

In memoriam.

Contents

Agradecimientos 3

Dedicatoria 9

Requisitos para la Mención Internacional en el Título de Doctor 15

Introducción y resumen 17

Introduction and summary 27

I Exclusivity graphs of non-contextuality inequalities 35

1 Graph-theoretic approach to quantum correlations 37

1.1 Specker's observation and the exclusivity principle within a general framework of operational theories . . . 37

1.1.1 Preparations and tests . . . 38

1.1.2 States and observables . . . 38

1.1.3 Joint measurability of observables . . . 38

1.1.4 Events . . . 39

1.1.5 Mutual exclusivity of events . . . 39

1.1.6 Specker's observation and the E principle . . . 40

1.2 Correlations . . . 40

1.2.1 General correlations . . . 41

1.2.2 No-signaling correlations . . . 43

1.2.3 Local correlations . . . 45

1.2.4 Quantum correlations . . . 45

1.2.5 Commutativity, no-disturbance and joint measurability . . . 47

1.3 Quantum contextuality. Non-contextual correlations . . . 48

1.4 Cabello-Severini-Winter's graph-theoretic approach to quantum correlations . . . 49

1.4.1 Exclusivity graph of an experiment . . . 49

1.4.2 Compatibility and exclusivity graphs of a non-contextuality inequality . . . 50

1.4.3 Correlations in theories satisfying the exclusivity principle . . . 52

1.4.4 The limits of the correlations in NCHV theories, quantum theory and theories satisfying the E principle . . . 54
1.4.5 The Lovász number as a physical limit and the set of quantum correlations 55
1.4.6 Suggested developments and connections to our work . . . 56
1.5 Classification of contextual exclusivity graphs . . . 58
1.5.1 Results . . . 59

2 Basic exclusivity graphs in quantum correlations 63
2.1 Introduction . . . 63
2.2 The exclusivity graph of a non-contextuality inequality . . . 64
2.3 Basic exclusivity graphs . . . 64
2.4 Basic exclusivity graphs and the dimension of the quantum system . . . 67
2.5 NC inequalities represented by basic exclusivity graphs . . . 68
2.6 The exclusivity principle enforces the quantum violation of the NC inequalities represented by basic exclusivity graphs . . . 70
2.7 Appendix: Basic exclusivity graphs inside the exclusivity graphs of some NC inequalities . . . 73

3 Quantum fully contextual correlations 75
3.1 Introduction . . . 75
3.2 Non-contextual content. Quantum fully contextual correlations . . . 76
3.3 Graph approach . . . 77
3.3.1 Quantum fully contextual exclusivity graphs . . . 78
3.4 Experimental quantum fully contextual correlations . . . 79

4 Quantum social networks 83
4.1 Introduction . . . 84
4.2 Quantum social networks . . . 87
4.3 Social networks with no-better-than-quantum advantage . . . 88
4.4 Final remarks . . . 89
4.5 Appendix . . . 90
4.5.1 Finding graphs in which QSNs can outperform CSNs . . . 90
4.5.2 State-independent QSNs . . . 91

II Graph states: Classification and optimal preparation 93

5 Introduction: Stabilizer formalism and graph states 95
5.1 Stabilizer formalism . . . 95
5.1.1 The Pauli group . . . 97
5.1.2 Stabilized states and stabilizing operators . . . 99
5.1.3 Stabilizers and stabilizer states . . . 101
5.1.4 Unitary operations and stabilizer formalism . . . 102
5.1.5 Measurements in the stabilizer formalism . . . 105
5.2 Graph states . . . 108

5.2.1 Definitions . . . 109
5.2.2 Graph states as a "theoretical laboratory" for multipartite entanglement . 111

6 Entanglement in eight-qubit graph states 121
6.1 Introduction . . . 121
6.2 Criteria for the classification . . . 122
6.2.1 Minimum number of controlled-Z gates for the preparation . . . 122
6.2.2 Schmidt measure . . . 123
6.2.3 Rank indexes . . . 124
6.3 Procedures and results . . . 124
6.3.1 Orbits under local complementation . . . 124
6.3.2 Bounds to the Schmidt measure . . . 125
6.4 Final remarks, open problems, and future developments . . . 128

7 Compact set of invariants characterizing graph states of up to eight qubits 133
7.1 Introduction and main goal . . . 133
7.2 Basic concepts . . . 135
7.2.1 Supports and classes of equivalence related to supports . . . 136
7.2.2 Invariants of Van den Nest, Dehaene, and De Moor . . . 136
7.3 Results and discussion . . . 139

8 Optimal preparation of graph states 145
8.1 Introduction . . . 145
8.1.1 Graph states: the graph as a blueprint for preparation . . . 146
8.1.2 Preparation using only controlled-Z gates . . . 146
8.1.3 Optimum preparation . . . 148
8.2 Classification of graph states in terms of entanglement . . . 150
8.3 Optimum representative . . . 152
8.4 One-qubit gates . . . 154
8.5 Example . . . 154
8.6 Further developments: Hypergraph states as generalizations of graph states . . . 155

9 Proposed experiment for the quantum "Guess My Number" protocol 159
9.1 Introduction . . . 159
9.1.1 Reduction of communication complexity in a nutshell . . . 160
9.2 The original *Guess My Number* protocol. Experimental requirements . . . 163
9.3 The modified *Guess My Number* protocol . . . 164
9.3.1 Maximum classical probability of winning . . . 165
9.3.2 Best entanglement-assisted strategy . . . 166
9.4 Results and discussion . . . 168

Exclusivity graphs and graph states: What is the connection? 171
A connection between exclusivity graphs and graph states . . . 171

Conclusiones 175

Conclusions **185**

Publications and contributions directly related to the thesis **193**
Articles published in peer-reviewed journals 193
Other contributions 194

Index of acronyms **197**

Bibliography **199**

Introducción y resumen

Esta tesis doctoral trata de diversos aspectos de la teoría cuántica (TC), que abarcan desde el campo de los fundamentos de la disciplina (en particular, la búsqueda de un conjunto de principios que seleccionen y distingan a la TC en el panorama de las teorías probabilísticas generales) hasta el reino de las aplicaciones en información y computación cuánticas.

Todos los problemas que hemos abordado en nuestra investigación tienen un rasgo distintivo común: la teoría de grafos parece ser especialmente adecuada para describirlos y tratarlos. Y no sólo eso: el lenguaje y las herramientas de la teoría de grafos proporcionan una poderosa y nueva percepción que permite arrojar luz sobre tales problemas, y representan además un importante impulso para futuros desarrollos.

Precisamente, uno de los problemas que tuvimos que plantearnos en esta tesis, desde el primer momento, fue decidir su título. El alcance de la tesis era demasido amplio como para poderlo comprimir en un título que fuese significativo, preciso y relativamente corto, y esto explica nuestra elección final: *Quantum correlations and graphs*, es decir, *Correlaciones cuánticas y grafos*, una declaración intencionadamente de amplio espectro y algo vaga con la que intentamos capturar los principales aspectos de nuestra investigación, quizá sin éxito.

En lo que concierne a la alusión a los *grafos* en el título, la principal razón para nuestra concisión es la siguiente: la tesis está dividida en dos partes en las que los grafos constituyen la herramienta matemática ubicua y versátil sobre la cual hemos basado toda nuestra investigación. Sin embargo, hemos de hacer notar que los grafos *significan cosas muy distintas* y juegan papeles bien diferentes en cada parte de la tesis. En la Parte I, que está dedicada a los grafos de exclusividad de desigualdades no contextuales (NC), los grafos dan cuenta de experimentos en los cuales algunas medidas se llevan a cabo sobre ciertos estados: los vértices de uno de tales grafos representan eventos, en tanto que las aristas describen relaciones de exclusividad mutua entre eventos, y sobre la base de dichos grafos nosotros construimos desigualdades NC y calculamos sus valores límite a partir de algunos números combinatorios propios de los grafos. En la Parte II, que está dedicada específicamente a los denominados estados grafo, los grafos por el contrario representan estados cuánticos entrelazados de muchos qubits. El grafo no sólo proporciona una ayuda para escribir el generador del estado grafo, sino que también sirve por así decir como una plantilla o guía para su preparación: los vértices representan qubits, y las aristas describen subsiguientes operaciones de entrelazamiento cada una de la cuales involucra a dos qubits. Todo esto prueba cuán fructífera y versátil llega a ser la teoría de grafos cuando se aplica a algunos problemas fundamentales en TC, lo que constituye una de la principales ideas que alientan la tesis.

Entre estas dos partes de la tesis, en apariencia desligadas, hay no obstante una profunda conexión, que se explica con detalle al final de la tesis, en la p. 171. En pocas palabras: hay

una construcción que partiendo de cualquier grafo conexo de tres o más vértices que describe a un estado grafo lleva a un grafo de mayor orden y tamaño, siendo éste último un grafo de exclusividad cuyos vértices representan todos los posibles eventos consistentes con el grupo estabilizador del estado grafo original, y cuyas aristas conectan eventos mutuamente excluyentes. Tal procedimiento transcribe en términos de teoría de grafos la conexión existente entre un estado grafo y una desigualdad de Bell violada máximamente por la TC.

Otro comentario importante tiene que ver con *correlaciones cuánticas*, el otro elemento que aparece con concisión en el título: proporcionamos una definición general de correlaciones cuánticas en la Sec. 1.2.4, a la que referimos al lector para más detalle. Nosotros seleccionamos dos tipos de correlaciones cuánticas: correlaciones cuánticas proyectivas, y correlaciones cuánticas tipo Bell. Debemos enfatizar el hecho de que en la primera parte de esta tesis, a menos que se diga expresamente lo contrario, por correlaciones cuánticas se entenderá que se trata de correlaciones cuánticas *proyectivas*, es decir, *correlaciones entre los resultados de medidas conjuntas de observables cuánticos proyectivos*. Las razones para esta elección se aportan en la p. 46. Por otro lado, nuestro principal interés en la segunda parte de la tesis es la clasificación y preparación óptima de estados grafo. En este caso, las correlaciones cuánticas (en particular, correlaciones cuánticas tipo Bell) aparecen implícitamente al discutir la conexión existente entre los grafos de exclusividad, los estados grafo y una clase de desigualdades de Bell violada máximamente por los estados grafo.

Con todas estas consideraciones en mente, pasamos a continuación a hacer una descripción resumida de nuestro trabajo de investigación. La tesis que presentamos, como ha quedado dicho, está estructurada en dos partes:

1. La Parte I se titula **Grafos de exclusividad de desigualdades no contextuales**, y está organizada en cuatro capítulos:

   - Capítulo 1: **Aproximación a las correlaciones cuánticas mediante teoría de grafos.**

     Éste es un capítulo introductorio, cuyo principal propósito es proporcionar el mínimo trasfondo teórico necesario para discutir los problemas y resultados de la primera parte de la tesis, además de presentar nuestros primeros resultados más básicos.

     Comenzamos en la Sec. 1.1 con una descripción concisa y autocontenida del marco general de las teorías operacionales, siguiendo las Refs. [1, 2]. Esta introducción concluye con la definición de exclusividad mutua entre eventos, en términos operacionales. Ello nos permite conectar la observación de Specker acerca de la mensurabilidad dos a dos y la mensurabilidad conjunta en TC con el principio de exclusividad (E), es decir, con el hecho de que la suma de las probabilidades de un conjunto de eventos mutuamente excluyentes dos a dos no puede exceder de 1. En la Sec. 1.2 pasamos revista a diferentes tipos de correlaciones entre resultados de medidas realizadas en un sistema, según las predicciones de ciertas teorías físicas. Seguimos las Refs. [3, 4, 5] en la discusión de las correlaciones locales, cuánticas, *no-signaling* and generales. Nos ocupamos de dos tipos de correlaciones cuánticas: proyectivas y tipo Bell, y seguidamente centramos nuestra atención en las correlaciones cuánticas proyectivas, proporcionando razones para dicha elección en la primera parte de la

tesis. En la Sec. 1.3 definimos correlaciones no contextuales, e introducimos el concepto de desigualdad NC. La Sec. 1.4 se dedica a presentar la aproximación a las correlaciones cuánticas mediante teoría de grafos de Cabello-Severini-Winter (CSW), recogida en las Refs. [6, 7], atendiendo específicamente a dos resultados principales y varias propuestas de posible desarrollo ulterior de dichos autores, en las cuales se basa nuestra investigación. Presentamos nuestros primeros resultados básicos en la Sec. 1.5, relativos a la clasificación de los llamados grafos cuánticos contextuales (QCG), y concluimos resumiendo las conexiones entre esta clasificación y los problemas abordados en capítulos subsiguientes.

- Capítulo 2: **Grafos de exclusividad básicos en correlaciones cuánticas.**

  En este capítulo nos ocupamos de un problema fundamental: entender por qué la TC viola únicamente ciertas desigualdades NC, e identificar los principios físicos que impiden violaciones mayores que las producidas por la TC.

  Utilizamos, como herramienta principal a lo largo del capítulo, el grafo de exclusividad de una desigualdad NC que ya se ha introducido previamente en la Sec. 1.4.2. En la Sec. 2.3, presentamos una condición necesaria para la existencia de correlaciones cuánticas contextuales: demostramos que la TC viola únicamente aquellas desigualdades NC cuyos grafos de exclusividad contienen, como subgrafos inducidos, ciclos impares de cinco o más vértices y/o sus complementos. En la Sec. 2.4, mostramos que se puede obtener una cota inferior de la dimensión (i. e., del número de estados perfectamente distinguibles) del sistema cuántico utilizado para violar la desigualdad NC mediante la identificación de subgrafos inducidos en el grafo de exclusividad de la desigualdad NC. El resultado de la Sec. 2.3 sugiere que las desigualdades NC cuyos grafos de exclusividad son o bien un ciclo impar o bien su complemento son especialmente importantes para entender la manera en que la TC viola desigualdades NC. En la Sec. 2.5 mostramos que los ciclos impares son los grafos de exclusividad de una familia bien conocida de desiguladades NC, y que hay también una familia de desigualdades NC cuyos grafos de exclusividad son los complementos de los ciclos impares. Además, caracterizamos los valores máximos no contextual y cuántico de estas desigualdades NC y proporcionamos los estados cuánticos y las medidas que conducen a sus violaciones cuánticas máximas. Finalmente, en la Sec. 2.6 presentamos algunos resultados que ofrecen evidencias que apoyan la conjetura de que el principio E selecciona exactamente la máxima violación cuántica de la desigualdades NC discutidas en la Sec. 2.5. Finalizamos el capítulo con material adicional en la Sec. 2.7, en la que presentamos una tabla que cuenta el número de subgrafos de exclusividad básicos inducidos en los grafos de exclusividad de algunas desigualdades NC y demostraciones de Kochen-Specker (KS) conocidas.

- Capítulo 3: **Correlaciones cuánticas completamente contextuales.**

  Las correlaciones cuánticas son contextuales. Sin embargo, en general, nada impide la existencia de correlaciones incluso más contextuales aún. El propósito del Capítulo 3 es identificar y poner a prueba una desigualdad NC en la cual la violación cuántica no pueda ser mejorada por ninguna hipotética teoría post-cuántica, y utilizarla para obtener experimentalmente correlaciones en las que la fracción de correlaciones no

contextuales sea lo más pequeña posible. Tales correlaciones se generan experimentalmente a partir de los resultados de test secuenciales compatibles realizados sobre un sistema cuántico de cuatro estados codificado en la polarización y el camino de un solo fotón.

Para abordar dicho propósito, utilizamos una de las ideas clave del Capítulo 1 (en particular, las Secs. 1.4.6 y 1.5.1): la aplicación de la aproximación de CSW mediante teoría de grafos a las correlaciones cuánticas (Ref. [7]) sobre la base de nuestra clasificación de los QCG (Ref. [8]) permite diseñar experimentos con contextualidad cuántica "a la carta", mediante la selección de grafos con las propiedades deseadas.

El Capítulo 3 presenta un destacado ejemplo de este programa: utilizamos el enfoque teórico-gráfico de CSW a fin de identificar y realizar un experimento con test cuánticos secuenciales y compatibles, que produce correlaciones con la mayor contextualidad permitida por la suposición de *no-disturbance* (ND) (véase Ec. (1.20)), cuya validez se asume también para teorías post-cuánticas. Con ese objetivo, en la Sec. 3.2 introducimos en primer lugar una medida de contextualidad de las correlaciones, el llamado contenido no contextual W_{NC}, de modo que el valor $W_{\mathrm{NC}} = 0$ corresponde a la contextualidad máxima. A continuación, mostramos cómo obtener experimentalmente cotas superiores medibles de W_{NC}. Más tarde, en la Sec. 3.3, mostramos en qué modo la teoría de grafos nos permite identificar experimentos en que la cota superior de W_{NC} predicha por la TC es igual a cero, y aplicamos ese método para seleccionar un experimento para el cual $W_{\mathrm{NC}} = 0$. Esto implica a su vez utilizar nuestra clasificación de los QCG para seleccionar un grafo con las propiedades combinatorias deseadas, i. e., un grafo cuántico completamente contextual (QFCG). Encontramos que hay únicamente cuatro QFCG con menos de 11 vértices, e identificamos aquél que requiere un sistema cuántico con la dimensión mínima necesaria para producir la máxima violación cuántica de la desigualdad NC asociada a dicho grafo de exclusividad. Además, proporcionamos la desigualdad NC, el estado cuántico y las medidas conducentes a la máxima violación cuántica. Finalmente, en la Sec. 3.4, describimos y llevamos a cabo el experimento que pone a prueba dicha desigualdad NC, y discutimos los resultados obtenidos, que ponen de manifiesto correlaciones para las que $W_{\mathrm{NC}} < 0.06$.

- Capítulo 4: **Redes sociales cuánticas.**

  Para cerrar la primera parte de la tesis, este capítulo propone una interesante aplicación de las ideas expuestas en los capítulos precedentes. Consideramos una tarea de teoría de la información, en concreto la maximización de cierta probabilidad promedio, para la cual el enfoque de CSW basado en teoría de grafos constituye un marco natural. Para dicha tarea, la TC no sólo supera a las teorías clásicas, sino que también en algunos casos no puede ser mejorada utilizando hipotéticas teorías post-cuánticas. El aspecto novedoso aquí es que el enfoque se hace más atractivo al tender un puente con otra disciplina, la de las ciencias sociales, en la que la teoría de grafos proporciona una herramienta principal en el análisis, y esta conexión abre la posibilidad a posteriores aplicaciones insospechadas.

  Enfocamos nuestra atención en las redes sociales (RS), un objeto de estudio tradi-

cional en las ciencias sociales. Empezamos con la observación de que, si bien una RS viene típicamente descrita por un grafo en que los vértices representan actores de la red y las aristas representan el resultado de su mutua interacción, dicho grafo no captura la naturaleza de las interacciones ni explica por qué un actor está conectado o no a otros actores de la RS. Desde esta perspectiva, el grafo da una descripción incompleta de la RS. El objetivo de este capítulo es discutir las RS sobre la base de las interacciones generales que pueden dar lugar a ellas.

En la Sec. 4.1 introducimos un enfoque físico a las RS en que cada actor está caracterizado por un test sí-no sobre un sistema físico. Este enfoque permite considerar RS más generales (RSG), más allá de aquéllas generadas por interacciones basadas en propiedades pre-existentes, como ocurre en las RS clásicas (RSC). También ponemos de manifiesto la diferencia entre una RSG y una RSC descritas por el mismo grafo, por medio de una tarea simple para la cual la probabilidad promedio de éxito está acotada superiormente de manera diferente dependiendo de la naturaleza de las interacciones que definen la RS. En la Sec. 4.2 introducimos las RS cuánticas (RSQ), como un ejemplo de RS más allá de las RSC. En una RSQ, un actor i está caracterizado por un test acerca de si el sistema está o no en un estado cuántico $|\psi_i\rangle$. Nosotros demostramos que las RSQ superan a las RSC para la tarea previamente mencionada y en ciertos grafos. Identificamos los más simples de entre dichos grafos, y mostramos que los grafos en que las RSQ superan a las RSC son cada vez más frecuentes a medida que crece el número de vértices. En la Sec. 4.3 consideramos grafos para los que las RSQ superan a las RSC, pero ninguna RSG supera a la mejor RSQ, e identificamos todos los grafos con menos de 11 vértices con esa propiedad. Es más, analizamos también el hecho de que, mientras que la ventaja cuántica usualmente requiere la preparación del sistema en un estado cuántico específico, según crece la complejidad de la red este requerimiento llega a ser innecesario: existen grafos para los cuales la ventaja cuántica es independiente del estado cuántico. Nosotros identificamos el grafo más simple de esta clase. El capítulo finaliza con algunas observaciones acerca de las posibles implicaciones prácticas de estas ideas, en la Sec. 4.4; y con un breve apéndice con detalles técnicos acerca de las herramientas y procedimientos necesarios para alcanzar nuestros resultados, en la Sec. 4.5.

2. La Parte II lleva por título **Estados grafo: Clasificación y preparación óptima**, y está estructurada en cinco capítulos:

   - Capítulo 5: **Introducción: Formalismo de estabilizador y estados grafo.**

     Es éste un capítulo introductorio, cuyo propósito es proporcionar las definiciones principales, y el mínimo trasfondo teórico necesario para sentar las bases para la discusión de los resultados de la segunda parte de la tesis. El capítulo se organiza en dos secciones:

     La Sec. 5.1 se dedica a introducir el formalismo de estabilizador. Presentamos, en una forma autocontenida y compacta, algunos conceptos básicos y definiciones junto con la notación y las técnicas que se utilizarán en los siguientes capítulos. Discutimos brevemente el grupo de Pauli, y consideramos estados estabilizados y operadores

estabilizadores, en general; y a continuación ponemos énfasis específicamente en los conceptos de estabilizador y generador, y en estados de estabilizador, que serán utilizados con profusión más tarde. Entre las operaciones unitarias destacamos el papel importante de las operaciones pertenecientes al grupo de Clifford, que serán de mucha utilidad cuando más tarde tratemos con los estados grafo y sus propiedades de entrelazamiento.

La Sec. 5.2 enfoca la atención sobre los estados grafo, ejemplos particulares de estados de estabilizador que constituyen el objeto de estudio en esta parte de nuestra investigación. Presentamos una lista condensada de posibles aplicaciones de los estados grafo en teoría cuántica de la información. Se dan dos definiciones de estado grafo en la Sec. 5.2.1: la primera constituye una receta para la preparación de un estado grafo, que utiliza el grafo correspondiente como una plantilla o modelo. La segunda constituye una caracterización algebraica del generador del estado grafo sobre la base del propio grafo. En la Sec. 5.2.2 nos ocupamos de los estados grafo entendidos como un "laboratorio teórico" para el entrelazamiento multipartito, y describimos algunos resultados relevantes obtenidos previamente por otros autores en relación con el problema general de la clasificación del entrelazamiento en estados cuánticos puros, que proporcionan el escenario conceptual para nuestras contribuciones. Terminamos la exposición con un resumen sucinto acerca de la clasificación de los estados grafo de hasta 7 qubits en clases de equivalencia bajo operaciones locales de Clifford (LC), que fue llevada a cabo por nuestros predecesores Hein, Eisert y Briegel (HEB) en la Ref. [9], la cual puede considerarse el punto de partida de nuestro trabajo sobre estados grafo.

- Capítulo 6: **Entrelazamiento en estados grafo de ocho qubits.**

  En este capítulo extendemos hasta ocho qubits la clasificación de los estados grafo de acuerdo a la equivalencia LC llevada a cabo en la Ref. [9], con la que cerramos el capítulo precedente.

  Van den Nest, Dehaene y De Moor (VDD) encontraron en la Ref. [10] que la aplicación sucesiva de una transformación con una descripción gráfica simple es suficiente para generar la clase de equivalencia completa de estados grafo bajo operaciones locales unitarias (LU) pertenecientes al grupo de Clifford, también conocida como *órbita*. Esta transformación simple recibe el nombre de complementación local, transformación que en definitiva permite generar las órbitas de todos los estados grafo de n qubits no equivalentes bajo operaciones LC; en particular, las 101 órbitas correspondientes a los estados grafo de 8 qubits, cuya clasificación es la meta de este capítulo.

  Para establecer un orden entre las clases de equivalencia nosotros utilizamos los criterios propuestos en las Refs. [9, 11], es decir, (a) número de qubits, (b) mínimo número de puertas controlled-Z necesario para la preparación, (c) la medida de Schmidt, y (d) los índices de rango. Estos criterios se introducen y describen en la Sec. 6.2. En la Sec. 6.3 presentamos nuestros resultados: para cada una de estas clases de equivalencia obtenemos un representante que requiere el mínimo número de puertas controlled-Z para su preparación y mínima profundidad de preparación. Además, calculamos la medida de Schmidt para la partición 8-partita, y los rangos de Schmidt

para todas las particiones bipartitas. En la Sec. 6.4 presentamos nuestras conclusiones y señalamos algunos problemas pendientes, que atañen principalmente a las limitaciones del uso de los criterios precedentes como etiquetas que distingan de forma no ambigua entre cualquier par de clases de equivalencia bajo LC de estados grafo de hasta ocho qubits. Este asunto es abordado en el siguiente capítulo.

- Capítulo 7: **Conjunto compacto de invariantes que caracteriza a estados grafo de hasta ocho qubits.**

  El conjunto de medidas de entrelazamiento propuesto por HEB en la Ref. [9] para estados grafo de n qubits falla a la hora de distinguir entre clases de equivalencia bajo operaciones LC (clases LC) que no son equivalentes entre sí, para $n \geq 7$. Por tanto, no podemos utilizar estos invariantes para decidir a qué clase de entrelazamiento pertenece un estado grafo dado. Recíprocamente, si dispusiésemos de un conjunto de invariantes con esas características, entonces podríamos utilizarlo para etiquetar de manera no ambigua cada una de las clases.

  Por otro lado, el conjunto de invariantes propuesto por VDD en la Ref. [12] distingue entre clases no equivalentes, pero contiene demasiados invariantes (más de 2×10^{36} para $n = 7$) para ser práctico.

  En este capítulo resolvemos el problema de decidir a qué clase de entrelazamiento pertenece un estado grafo de $n \leq 8$ qubits mediante el cálculo de algunas propiedades intrínsecas del estado, por tanto sin necesidad de generar la clase LC completa. La Sec. 7.1 es un resumen condensado de ideas y conceptos que ya se han presentado en capítulos previos, y que permiten seguir las discusiones subsiguientes. En la Sec. 7.2, por conveniencia, empezamos recordando la definición de estado grafo a través de la caracterización algebraica del generador, y repasamos el efecto de la complementación local sobre los operadores de estabilización. Luego, en la Sec. 7.2.1, introducimos un nuevo concepto básico del formalismo de estabilizador, a saber, el soporte de un operador de estabilización, y las clases de equivalencia relativas a los soportes. Estos conceptos son necesarios en la Sec. 7.2.2, donde analizamos algunos de los resultados acerca de invariantes propuestos por VDD que serán útiles en nuestra discusión. En la Sec. 7.3 presentamos y discutimos los resultados de nuestra investigación: confirmamos la conjetura formulada en la Ref. [12] de que los invariantes de VVD tipo $r = 1$ son suficientes para distinguir entre las 146 clases de equivalencia LC para estados grafo de hasta ocho qubits. Además, introducimos un nuevo conjunto compacto de invariantes relacionado con los propuestos por VDD, los llamados invariantes cardinalidad-multiplicidad (C-M), y demostramos que cuatro de tales invariantes C-M son suficientes para distinguir entre todas las clases LC no equivalentes para estados grafo con $n \leq 8$ qubits.

- Capítulo 8: **Preparación óptima de estados grafo.**

  En este capítulo aprovechamos tanto la clasificación de los estados grafo en clases de equivalencia LC (Cap. 6) como la identificación de tales clases sobre la base de un conjunto compacto de invariantes bajo operaciones LC (Cap. 7). Mostramos cómo preparar cualquier estado grafo de hasta 12 qubits con: (a) el mínimo número de puertas controlled-Z, y (b) la mínima profundidad de preparación. Asumimos en

la preparación sólo puertas de un qubit, y puertas controlled-Z. El método explota el hecho de que cualquier estado grafo pertenece a una clase de equivalencia bajo operaciones LC: si uno necesita preparar un estado grafo $|G\rangle$ y sabe que dicho estado pertenece a una clase específica, entonces uno puede preparar $|G\rangle$ mediante la preparación del estado $|G'\rangle$, equivalente bajo operaciones LC, que requiere el menor número de puertas entrelazadoras y la menor profundidad de preparación de esa clase LC (Refs. [9, 11, 13]), y a continuación transformando $|G'\rangle$ en $|G\rangle$ por medio de operaciones unitarias de un qubit.

En la Sec. 8.1, por comodidad, recordamos la definición de estado grafo en la que se usa el grafo como una plantilla o modelo para su preparación a través de la aplicación de una serie de puertas controlled-Z. Definimos el concepto de profundidad de preparación, y a continuación discutimos cómo el problema de la profundidad de preparación está relacionado con un problema clásico en teoría de grafos, el de la determinación del índice cromático o número cromático de aristas de un grafo: el mínimo número de colores requerido para conseguir un coloreado propio de aristas del grafo.

En la Sec. 8.2, extendemos hasta 12 qubits la clasificación de los estados grafo de acuerdo con sus propiedades de entrelazamiento (en clases LC), e identificamos cada clase utilizando para ello únicamente un conjunto reducido de invariantes (invariantes C-M). En la Sec. 8.3, proporcionamos un representante de la clase con las dos propiedades (a) y (b), si éste existe, o en caso contrario uno con la propiedad (a) y otro con la propiedad (b). Todos estos resultados, que ocupan varios cientos de megabytes, se organizan en dos tablas, una para $n < 12$ y otra para $n = 12$, que se presentan como material suplementario en la Ref. [14]. En la Sec. 8.4 explicamos cómo obtener las puertas de un qubit necesarias, y proporcionamos como material suplementario en la Ref. [15] un programa de ordenador para, dado el grafo G correspondiente al estado grafo que uno desea preparar, generar una secuencia de operaciones de complementación local que conecte G con el correspondiente (o los correspondientes) grafo(s) óptimo(s). Finalmente, en la Sec. 8.5 ilustramos el método completo con un ejemplo.

Como material para terminar este capítulo, hemos añadido la Sec. 8.6, donde discutimos sucintamente una generalización de los estados grafo conocida como *estados hipergrafo*, de la cual los anteriores constituyen un subconjunto. Tras presentar las definiciones principales, y describir algunos de los resultados más recientes acerca de la exploración de las propiedades de entrelazamiento y características no clásicas de los estados hipergrafo, señalamos posibles futuras extensiones de nuestras contribuciones en relación con los estados grafo, en particular el análisis de la profundidad de preparación de un estado hipergrafo dado y su posible procedimiento óptimo de preparación.

- Capítulo 9: **Propuesta experimental para el protocolo cuántico "Guess My Number".**

  El objetivo de este capítulo es presentar, de una manera sencilla y directa, un protocolo experimental de reducción de la complejidad de la comunicación basado en el

uso de recursos cuánticos, conocido como el protocolo "Guess My Number" (GMN). El punto clave radica en que los participantes en el protocolo GMN comparten un estado cuántico entrelazado, y este estado cuántico es precisamente un estado grafo, el estado Greenberger-Horne-Zeilinger (GHZ) de tres (o de cuatro) qubits.

En los Caps. 6–8 hemos centrado nuestra atención en los estados grafo desde el punto de vista de la teoría del entrelazamiento. También hemos presentado resumidamente muchas de las principales aplicaciones de los estados grafo en teoría cuántica de la información en la Sec. 5.2. Entre ellas mencionamos la complejidad de la comunicación, para la cual los estados grafo constituyen recursos interesantes y ventajosos debido a su genuino entrelazamiento multipartito.

Comenzamos en la Sec.9.1.1 pasando revista de manera resumida a algunos conceptos básicos relacionados con la complejidad de la comunicación, a fin de proporcionar el mínimo trasfondo conceptual necesario. Enfatizamos el hecho de que los estados grafo, como otros estados cuánticos entrelazados, constituyen un valioso recurso que puede ser compartido por los participantes en aquellos escenarios correspondientes al denominado modelo de entrelazamiento de la complejidad de la comunicación. Nuestro propósito en las siguinetes secciones es presentar en detalle uno de esos escenarios, que involucra un protocolo de comunicación basado en el juego GMN, con la peculiaridad de que los participantes comparten específicamente un estado grafo.

Describimos el protocolo original GMN asistido por entrelazamiento para la reducción de la complejidad de la comunicación, introducido por Steane y van Dam, en la Sec. 9.2, y a continuación analizamos las dificultades de una realización experimental de dicho protocolo: ésta requeriría producir y detectar estados GHZ de tres qubits con una eficiencia $\eta > 0.70$, lo que a su vez requeriría detectores de un fotón de eficiencia $\sigma > 0.89$.

Presentamos nuestra versión modificada del protocolo GMN en la Sec. 9.3: proponemos ciertos cambios que hacen que el protocolo GMN modificado sea experimentalmente factible. Discutimos seguidamente la mejor estrategia clásica (que implica intercambio de bits, utilizando aleatoriedad compartida), la estrategia cuántica alternativa (intercambio de bits sobre la base del uso ingenioso de un estado grafo compartido), y luego hacemos una comparación entre sus rendimientos para determinar la ventaja cuántica respecto a la variante clásica, a través del análisis de la probabilidad de éxito en el juego GMN. Finalmente, en la Sec. 9.4, discutimos los requisitos de eficiencia de detección de fotones necesarios para realizar el experimento en el laboratorio, y realizamos una propuesta experimental concreta para tal experimento. En el experimento propuesto, la reducción cuántica de la complejidad de la comunicación multipartita requeriría una eficiencia $\eta > 0.05$, que se puede lograr con detectores con $\sigma > 0.47$, para cuatro participantes, y $\eta > 0.17$ ($\sigma > 0.55$) para tres participantes. Concluimos el capítulo dando cuenta de la subsiguiente realización del experimento por parte de Zhang *et al.* en la Ref. [16], con los resultados esperados: los participantes separados entre sí que comparten el estado (grafo) entrelazado, pueden computar una función de inputs distribuidos mediante el intercambio de menos información clásica que la requerida utilizando cualquier estrategia clásica.

La tesis termina con una sección separada en la p. 171, donde explicamos en cierto detalle la conexión entre las Partes I y II. En la p. 185 se recoge un resumen con las conclusiones de la tesis. Los artículos en que se basa esta tesis, junto con otras contribuciones, se relacionan en la p. 193. Por comodidad, se proporciona un índice con los acrónimos más frecuentemente utilizados a lo largo de la tesis en la p. 197. Finalmente, tras la bibliografía, presentamos un anexo con los artículos originales que dan soporte a la tesis.

Introduction and summary

This thesis is concerned with several topics in quantum theory (QT), that range from the field of the foundations of the discipline (in particular, the quest for a set of principles that single out QT from the landscape of general probabilistic theories) to the realm of applications in quantum information and computation.

All the issues we have addressed in our research have a common flavor: graph theory seems to be perfectly suited to describe and deal with them. And not only this: the language and tools from graph theory provide a powerful insight that sheds light on such issues and represent an important boost for future developments.

Incidentally, one of the problems we had to address in this thesis, from the very first moment, was to decide its title. The scope of the thesis was too wide to be captured in a meaningful, precise and relatively short title, and this fact accounts for our final choice: *Quantum correlations and graphs*, an intentionally broad-range and somewhat vague declaration with which we try to capture the main aspects of our research, perhaps unsuccessfully.

Concerning the allusion to *graphs* in the title, the main reason for our conciseness is this: the thesis is divided into two parts where graphs constitute the ubiquitous and versatile mathematical tool upon which we have based all our research. However, graphs *mean very different things* and play diverse roles in either part of the thesis. In Part I, which is devoted to exclusivity graphs of non-contextuality (NC) inequalities, graphs account for experiments in which some measurements are carried out on states: vertices represent events while edges describe relations of mutual exclusivity between events, and on the basis of such graphs we construct NC inequalities and calculate their bounds from some combinatorial numbers specific of the graphs. In Part II, specifically devoted to graph states, graphs represent entangled multi-qubit quantum states. The graph not only provides an aid to write the generator of a graph state, but also serves as a blueprint for its preparation: vertices represent qubits and edges describe subsequent entangling 2-qubit operations. This proves how fruitful and versatile graph theory becomes when applied to some fundamental problems in QT, one of the main thrusts of the thesis.

Nevertheless, between these apparently non-linked parts of the thesis there is in fact a profound connection, which is explained in detail at the end of the thesis, on p. 171. In a nutshell: there is a construction that maps any connected graph on three or more vertices representing a graph state into a larger graph, which is an exclusivity graph whose vertices represent all possible events consistent with the stabilizer group of the graph state and where mutually exclusive events are adjacent. Such procedure translates into graph-theoretic terms the connection between a graph state and a Bell inequality maximally violated by quantum mechanics.

Another important remark has to do with *quantum correlations*, the other concise element

of the title: a general definition of quantum correlations is provided in Sect. 1.2.4, where we refer the reader for further details. We single out two kinds of quantum correlations: projective quantum correlations and Bell-type quantum correlations. We must emphasize the fact that in the first part of this thesis, unless otherwise noted, by quantum correlations we mean *projective* quantum correlations, i.e., *correlations between the outcomes of jointly measurable projective quantum observables*. The reasons for this choice are given on p. 46. On the other hand, the main concern of the second part of the thesis is the classification and optimal preparation of graph states. In this case, quantum correlations (in particular, Bell-type quantum correlations) are implicit when we discuss the connection between exclusivity graphs, graph states, and a class of Bell inequalities maximally violated by graph states.

With these considerations in mind, let us give an outline of our work below. This thesis is structured as follows:

1. Part I is titled **Exclusivity graphs of non-contextuality inequalities**, and is organized in four chapters:

   - Chapter 1: **Graph-theoretic approach to quantum correlations.**

     This is an introductory chapter, whose main purpose is to provide the minimum necessary theoretical background for discussing the problems and results of the first part of this thesis, along with our first basic results.

     We begin in Sect. 1.1 with a concise and self-contained description of the general framework of operational theories, following Refs. [1, 2]. This introduction concludes with the definition of mutual exclusivity of events in operational terms. This allows us connect Specker's observation about pairwise and joint measurability in QT with the exclusivity (E) principle, namely, the fact that the sum of the probabilities of a set of pairwise exclusive events cannot exceed 1. In Sect. 1.2 we review different kinds of correlations between outcomes of measurements performed on a system, as predicted by certain physical theories. We follow Refs. [3, 4, 5] in the discussion of local, quantum, no-signaling and general correlations. We single out two kinds of quantum correlations: projective and Bell-type quantum correlations, and then focus the attention on projective quantum correlations, providing reasons for that choice throughout the first part of the thesis. In Sect. 1.3 we define non-contextual correlations, and introduce the concept of NC inequality. Sect. 1.4 is devoted to presenting the graph-theoretic approach to quantum correlations by Cabello-Severini-Winter (CSW) from Refs. [6, 7], focusing our attention on two main results and several proposals of further development, on which our research is based. We present our first basic result in Sect. 1.5, the classification of the so-called quantum contextual graphs (QCGs), and we conclude summarizing the links between this classification and the problems addressed in the subsequent chapters.

   - Chapter 2: **Basic exclusivity graphs in quantum correlations.**

     In this chapter we address a fundamental problem: to understand why QT only violates some NC inequalities and identify the physical principles that prevent higher-than-quantum violations.

We use, as a main tool throughout the chapter, the exclusivity graph of an NC inequality which was already introduced in Sect. 1.4.2. In Sect. 2.3, we present a necessary condition for the existence of quantum contextual correlations: We prove that QT violates only those NC inequalities whose exclusivity graphs contain, as induced subgraphs, odd cycles on five or more vertices and/or their complements. In Sect. 2.4, we show that a lower bound of the dimension (i.e., of the number of perfectly distinguishable states) of the quantum system that is used to violate an NC inequality can be obtained by identifying induced subgraphs in the exclusivity graph of the NC inequality. The result in Sect. 2.3 suggests that NC inequalities whose exclusivity graph is either an odd cycle or its complement are especially important for understanding the way QT violates NC inequalities. In Sect. 2.5, we show that odd cycles are the exclusivity graphs of a well-known family of NC inequalities, and that there is also a family of NC inequalities whose exclusivity graphs are the complements of odd cycles. Moreover, we characterize the maximum non-contextual and quantum values of these NC inequalities and also provide the quantum states and measurements leading to their maximum quantum violation. Finally, in Sect. 2.6 we present some results that provide evidence supporting the conjecture that the maximum quantum violation of the NC inequalities discussed in Sect. 2.5 is exactly singled out by the E principle. We finish the chapter with additional material in Sect. 2.7, where we present a table that counts the number of induced basic exclusivity subgraphs inside the exclusivity graphs of some NC inequalities and Kochen-Specker (KS) proofs.

- Chapter 3: **Quantum fully contextual correlations.**

  Quantum correlations are contextual yet, in general, nothing prevents the existence of even more contextual correlations. The purpose of Chapter 3 is to identify and test a NC inequality in which the quantum violation cannot be improved by any hypothetical post-quantum theory, and use it to experimentally obtain correlations in which the fraction of non-contextual correlations is as small as possible. Such correlations are experimentally generated from the results of sequential compatible tests on a four-state quantum system encoded in the polarization and path of a single photon.

  For that purpose, we use one of the key ideas of Chapter 1 (in particular, Sects. 1.4.6 and 1.5.1): the application of CSW's graph-theoretic approach in Ref. [7] on the basis of our classification of QCGs in Ref. [8] allows to design experiments with quantum contextuality on demand, by selecting graphs with the desired properties.

  Chapter 3 presents a remarkable example of this programme: we use CSW'S graph-theoretic approach in order to identify and perform an experiment with sequential quantum compatible tests, which produces correlations with the largest contextuality allowed under the no-disturbance (ND) assumption (1.20), which is assumed to be valid also for post-quantum theories. For this purpose, in Sect. 3.2 we first introduce a measure of contextuality of the correlations, the so-called non-contextual content W_{NC}, so that $W_{\mathrm{NC}} = 0$ corresponds to the maximum contextuality. Then, we show how to experimentally obtain testable upper bounds to W_{NC}. Next, in Sect. 3.3, we show how graph theory allows us to identify experiments in which the upper bound

to W_{NC} predicted by QT is zero, and apply this method to single out an experiment for which $W_{\mathrm{NC}} = 0$. This implies using our classification of QCGs to select a graph with the desired combinatorial properties, i.e., a quantum fully contextual graph (QFCG). There are only four QFCGs with less than 11 vertices, and we identify the one requiring a quantum system with the minimum dimension needed for the maximum quantum violation of the NC inequality associated to the graph. Moreover, we provide the NC inequality, the quantum state and the measurements leading to the maximum quantum violation. Finally, in Sect. 3.4, we describe and perform the experiment testing the NC inequality, and discuss the results obtained, which reveal correlations in which $W_{\mathrm{NC}} < 0.06$.

- Chapter 4: **Quantum social networks.**

  To close the first part of the thesis, this chapter proposes an appealing application of the ideas previously presented in the foregoing chapters. We consider an information-theoretic task, namely, the maximization of certain average probability, for which CSW's graph-theoretic approach is a natural framework. For this task, QT not only outperforms classical theories, but also in some cases cannot be improved by using hypothetical post-quantum theories. The novel point is that the approach is made more attractive by building a bridge to another discipline, social sciences, in which graph theory provides a major tool in the analysis, and this connection opens the possibility of further unforeseen applications.

  We focus our attention on social networks (SNs), a traditional subject of study in social sciences. We start with the observation that, while a SN is typically described by a graph in which vertices represent actors and edges represent the result of their mutual interactions, the graph does not capture the nature of the interactions or explain why an actor is linked or not to other actors of the SN. From this perspective, the graph gives an incomplete description. The aim of the chapter is to discuss SNs on the basis of general interactions which can give rise to them.

  In Sect. 4.1, we introduce a physical approach to SNs in which each actor is characterized by a yes-no test on a physical system. This approach allows us to consider more general SNs (GSNs) beyond those originated by interactions based on pre-existing properties, as in a classical SN (CSN). We also highlight the difference between a GSN and a CSN described by the same graph, by virtue of a simple task for which the average probability of success is upper bounded differently depending on the nature of the interactions defining the SN. In Sect. 4.2 we introduce quantum SNs (QSNs) as an example of SNs beyond CSNs. In a QSN, an actor i is characterized by a test of whether or not the system is in a quantum state $|\psi_i\rangle$. We show that QSNs outperform CSNs for the aforementioned task and some graphs. We identify the simplest of these graphs and show that graphs in which QSNs outperform CSNs are increasingly frequent as the number of vertices increases. In Sect. 4.3 we consider graphs for which QSNs outperform CSNs but no GSN outperforms the best QSN, and identify all the graphs with less than 11 vertices with that property. Furthermore, we analyze the fact that, while the quantum advantage usually requires the preparation of the system in a specific quantum state, as the complexity of the network increases

this requirement becomes unnecessary: there are graphs for which the quantum advantage is independent of the quantum state. We identify the simplest graph of this kind. The chapter ends with some final remarks about possible practical implications of these ideas, in Sect. 4.4; and a brief appendix with technical details relating the tools and procedures needed to achieve our results, in Sect. 4.5.

2. Part II is titled **Graph states: Classification and optimal preparation**, and is organized in five chapters:

   - Chapter 5: **Introduction: Stabilizer formalism and graph states.**

     This is an introductory chapter, whose purpose is to provide the main definitions and minimum necessary theoretical background to pave the way for discussing the results of the second part of this thesis. The chapter is organized in two sections:

     Sect. 5.1 is devoted to introducing the stabilizer formalism. We present, in a rather self-contained and compact fashion, some basic concepts and definitions along with the notation and techniques that will be used in the subsequent chapters. We briefly describe the Pauli group, and consider stabilized states and stabilizing operators, in general; and then we put emphasis specifically on the concepts of stabilizer and generator, and on stabilizer states, that will be profusely used later. Among unitary operations, the important role of the operations belonging to the Clifford group, which will be useful when dealing with graph states and their entanglement properties, is also highlighted.

     Sect. 5.2 focuses the attention on graph states, a particular instance of stabilizer states which constitute the subject of study in this part of our research. We present a condensed list of possible applications in quantum information theory. Two definitions of graph states are given in Sect. 5.2.1: the first is a recipe for the preparation of a graph state, which uses the corresponding graph as a blueprint. The second one constitutes an algebraic characterization of the graph state's generator on the basis of the graph. In Sect. 5.2.2 we deal with graph states as a "theoretical laboratory" for multipartite entanglement, and describe some relevant results previously obtained by other authors in relation to the general problem of the classification of entanglement in pure quantum states, which provide the conceptual scenario for our contributions. We finish the exposition with a succinct outline of the classification of graph states of up to 7 qubits in classes of equivalence under local Clifford (LC) operations carried out by our predecessors Hein, Eisert and Briegel (HEB) in Ref. [9], which can be considered the starting point of our work on graph states.

   - Chapter 6: **Entanglement in eight-qubit graph states.**

     In this chapter, we extend up to eight qubits the classification of graph states according to LC equivalence in Ref. [9] that closed the previous chapter.

     Van den Nest, Dehaene, and De Moor (VDD) found that the successive application of a transformation with a simple graphical description is sufficient to generate the complete equivalence class of graph states under local unitary (LU) operations within the Clifford group, also known as *orbit*, Ref. [10]. This simple transformation is local

complementation, which allows to generate the orbits of all LC-inequivalent n-qubit graph states; in particular, the 101 orbits corresponding to 8-qubit graph states, whose classification is the goal of this chapter.

To establish an order between the equivalence classes we use the criteria proposed in Refs. [9, 11], namely, (a) number of qubits, (b) minimum number of controlled-Z gates needed for the preparation, (c) the Schmidt measure, and (d) the rank indexes. These criteria are introduced an reviewed in Sect. 6.2. In Sect. 6.3 we present our results: for each of these classes we obtain a representative which requires the minimum number of controlled-Z gates for its preparation and minimum preparation depth, and calculate the Schmidt measure for the 8-partite split, and the Schmidt ranks for all bipartite splits. In Sect. 6.4 we present our conclusions and point out some pending problems, mainly about the limitations in the use of the previous criteria as labels that distinguish unambiguously among any pair of LC classes of equivalence of graph states up to eight qubits. This issue is tackled in the following chapter.

- Chapter 7: **Compact set of invariants characterizing graph states of up to eight qubits.**

  The set of entanglement measures proposed by HEB in Ref. [9] for n-qubit graph states fails to distinguish between inequivalent classes under LC operations if $n \geq 7$. Therefore, we cannot use these invariants for deciding which entanglement class a given state belongs to. Reciprocally, if we have such a set of invariants, then we can use it to unambiguously label each of the classes.

  On the other hand, the set of invariants proposed by VDD in Ref. [12] distinguishes between inequivalent classes, but contains too many invariants (more than 2×10^{36} for $n = 7$) to be practical.

  In this chapter we solve the problem of deciding which entanglement class a graph state of $n \leq 8$ qubits belongs to by calculating some of the state's intrinsic properties, thus without generating the whole LC class. Sect. 7.1 is a condensed outline of ideas and concepts already presented in foregoing chapters, allowing to follow the subsequent discussions. In Sect. 7.2, for the sake of convenience, we start recalling the definition of graph state through the algebraic characterization of the generator, and review the effect of local complementation on the stabilizing operators. Then, in Sect. 7.2.1, we introduce a new basic concept of the stabilizer formalism, namely, the support of a stabilizing operator, and the classes of equivalence related to supports. This concepts are necessary in Sect. 7.2.2, where we analyze some of the results about the invariants proposed by VDD that will be useful in our discussion. In Sect. 7.3 we present and discuss the results of our research: we confirm the conjecture in Ref. [12] that VVD's invariants of type $r = 1$ are enough for distinguishing between the 146 LC equivalence classes for graph states up to eight qubits. Moreover, we introduce a new compact set of invariants related to those proposed by VDD, the so-called cardinality-multiplicity (C-M) invariants, and show that four C-M invariants are enough for distinguishing between all inequivalent classes with $n \leq 8$ qubits.

- Chapter 8: **Optimal preparation of graph states.**

  In this chapter we take advantage of both the classification of graph states in LC

equivalence classes (Chap. 6) and the identification of such classes on the basis of a compact set of LC invariants (Chap. 7). We show how to prepare any graph state of up to 12 qubits with: (a) the minimum number of controlled-Z gates, and (b) the minimum preparation depth. We assume only one-qubit and controlled-Z gates. The method exploits the fact that any graph state belongs to an equivalence class under LC operations: If one needs to prepare a graph state $|G\rangle$ and knows that it belongs to one specific class, then one can prepare $|G\rangle$ by preparing the LC-equivalent state $|G'\rangle$ requiring the minimum number of entangling gates and the minimum preparation depth of that class (Refs. [9, 11, 13]) and then transform $|G'\rangle$ into $|G\rangle$ by means of simple one-qubit unitary operations.

In Sect. 8.1, for convenience, we recall the definition of graph state using the graph as a blueprint for its preparation through the application of a series of controlled-Z gates. We define the concept of preparation depth, and then discuss how the preparation depth problem is related to an old problem in graph theory, namely, the determination of the chromatic index or edge chromatic number: the minimum number of colors required to get a proper edge coloring of the graph.

In Sect. 8.2, we extend up to 12 qubits the classification of graph states according to their entanglement properties, and identify each class using only a reduced set of invariants (C-M invariants). In Sect. 8.3, we provide a representative of the class with both properties (a) and (b), if it exists, or, if it does not, one with property (a) and one with property (b). All these results, which occupy several hundreds of megabytes, are organized in two tables, one for $n < 12$ and one for $n = 12$, and presented as supplementary material in Ref. [14]. In Sect. 8.4, we explain how to obtain the one-qubit gates needed, and provide as supplementary material a computer program in Ref. [15] to, given the graph G corresponding to the state we want to prepare, generate a sequence of local complementations which connect G to the corresponding optimum graph(s). Finally, in Sect. 8.5, the whole method is illustrated with an example.

As ending material for this chapter, we have added Sect. 8.6, where we succinctly discuss a generalization of graph states known as *hypergraph states*, of which the former ones constitute a subset. After presenting the main definitions, and describing some of the most recent results about the exploration of the entanglement properties and nonclassical features of hypergraph states, we consider possible future extensions of our contributions regarding graph states, in particular the analysis of the preparation depth of a given hypergraph state and its possible optimal preparation procedure.

- Chapter 9: **Proposed experiment for the quantum "Guess My Number" protocol.**

  The goal of this chapter is to present, in a straightforward manner, an experimental protocol of reduction of communication complexity based on the use of quantum resources, known as the "Guess My Number" (GMN) protocol. The key point is that the participants in the GMN protocol share an entangled quantum state, and this quantum state is precisely a graph state, the 3-qubit or 4-qubit Greenberger-Horne-Zeilinger (GHZ) state.

  In Chaps. 6–8 we have focused our attention on graph states from the point of view

of the theory of entanglement. We also outlined many of the main applications in quantum information science in Sect. 5.2. Among them, we mentioned communication complexity, for which graph states constitute interesting and advantageous resources due to their genuine multipartite entanglement.

We begin in Sect.9.1.1 with a summarized review of some basic concepts relating communication complexity, in order to provide the necessary background. We emphasize that graph states, like other entangled quantum states, constitute a valuable resource that may be shared by the participants in those scenarios corresponding to the entanglement model of communication complexity. Our purpose in the next sections is to present in detail one of those scenarios, involving a communication protocol based on the GMN game, with the peculiarity that the contestants share specifically a graph state.

We describe the original entanglement-assisted GMN protocol for the reduction of communication complexity, introduced by Steane and van Dam, in Sect. 9.2, and then analyze the difficulties of an experimental realization of this protocol: it would require producing and detecting three-qubit GHZ states with an efficiency $\eta > 0.70$, which in turn would require single photon detectors of efficiency $\sigma > 0.89$.

Our modified version of the GMN protocol is presented in Sect. 9.3: we propose certain changes that make the modified GMN protocol experimentally feasible. We discuss the best classical strategy (exchanging bits and using shared randomness), the alternative quantum strategy (exchanging bits on the basis of a clever use of the shared graph state), and then make a comparison between their yields to determine the quantum versus classical advantage, through the analysis of the probability of success in the game. Finally, in Sect. 9.4, we discuss the photon detection efficiency requirements needed to perform the experiment in the laboratory, and make a concrete proposal for such an experiment. In the proposed experiment, the quantum reduction of the multiparty communication complexity would require an efficiency $\eta > 0.05$, achievable with detectors of $\sigma > 0.47$, for four parties, and $\eta > 0.17$ ($\sigma > 0.55$) for three parties. In a final remark, we account for the subsequent realization of the experiment by Zhang *et al.* in Ref. [16], with the expected results: the separated parties sharing the entangled (graph) state can compute a function of distributed inputs by exchanging less classical information than it is required by using any classical strategy.

The thesis ends with a separate section on p. 171, where we explain in certain detail the connection between Parts I and II. A summary of conclusions of the thesis is collected on p. 185. The articles this thesis is based on, and other contributions, are listed on p. 193. For the sake of convenience, an index of acronyms frequently used throughout the thesis is provided on p. 197. Finally, after the bibliography, we present an addendum of enclosed publications, which support the thesis.

Part I

Exclusivity graphs of non-contextuality inequalities

Chapter 1

Graph-theoretic approach to quantum correlations

The purpose of this chapter is to provide the minimum necessary theoretical background for discussing the results of the first part of this thesis. We will briefly present some basic concepts and definitions, along with the notation and techniques that will be used in the subsequent chapters. Some relevant results previously obtained by other authors, on which our research is based, will also be described here. We will finish the exposition with some basic results of ours, and their links to the contents and developments of the following chapters.

We begin in Sect. 1.1 with a concise and self-contained description of the general framework of operational theories, following Refs. [1, 2]. This introduction concludes with the definition of mutual exclusivity of events in operational terms. This allows us connect Specker's observation about pairwise and joint measurability in quantum theory (QT) with the exclusivity (E) principle. In Sect. 1.2 we review different kinds of correlations between outcomes of measurements performed on a system, as predicted by certain physical theories. We follow Refs. [3, 4, 5] in the discussion of local, quantum, no-signaling and general correlations. In Sect. 1.3 we define non-contextual correlations, and introduce the concept of non-contextuality (NC) inequality. Sect. 1.4 is devoted to presenting the graph-theoretic approach to quantum correlations by Cabello-Severini-Winter (CSW) in Refs. [6, 7], focusing our attention on two main results and several proposals of further development, on which our research is based. We present our first basic result in Sect. 1.5, the classification of the so-called quantum contextual graphs, and we conclude summarizing the links between this classification and the problems addressed in the subsequent chapters.

1.1 Specker's observation and the exclusivity principle within a general framework of operational theories

In this section, we formulate Specker's observation about QT (Refs. [17, 18]) and the E principle (Refs. [19, 20, 21]) within a general framework of operational theories and prove that the E principle holds in any theory in which Specker's observation holds.

1.1.1 Preparations and tests

Preparations and tests are taken as primitive notions with the following meaning:

A *preparation* is a sequence of unambiguous and reproducible experimental procedures.

A *test* is a preparation followed by a step in which outcome information is supplied to an observer. This information is not trivial since tests that follow identical preparations may not have identical outcomes.

An *operational theory* is one that specifies the probabilities of each possible outcome X of each possible test M given each preparation P. We denote these probabilities by $p(X|M;P)$.

The presented framework is independent of the interpretation of probability used; the reader is free to use, e.g., frequentist, propensity, or Bayesian interpretations.

1.1.2 States and observables

Two preparations are operationally equivalent if they yield identical outcome probability distributions for either test. Each equivalence class of preparations is called a *state*. For instance, the state associated with a particular preparation P_1 is

$$\rho_1 \equiv \{P \mid \forall M : p(X|M;P) = p(X|M;P_1)\}. \tag{1.1}$$

Two tests are operationally equivalent if they yield identical outcome probability distributions for either preparation. Each equivalence class of tests is called an *observable*. For instance, the observable associated with a particular test M_1 is

$$\mu_1 \equiv \{M \mid \forall P : p(X|M;P) = p(X|M_1;P)\}. \tag{1.2}$$

1.1.3 Joint measurability of observables

Two observables μ_1 and μ_2 are *jointly measurable* if there exists an observable μ such that: (i) the outcome set of μ, $\sigma(\mu)$, is the Cartesian product of the outcome sets of μ_1 and μ_2, i.e.,

$$\sigma(\mu) \equiv \{(X_i, X_j) \mid X_i \in \sigma(\mu_1), X_j \in \sigma(\mu_2)\}, \tag{1.3}$$

and (ii) for all states ρ, the outcome probability distributions for every measurement of μ_1 or μ_2 are recovered as marginals of the outcome probability distribution of μ, i.e.,

$$\forall \rho, \forall X_i \in \sigma(\mu_1) : \quad p(X_i|\mu_1;\rho) = \sum_{X_j \in \sigma(\mu_2)} p((X_i, X_j)|\mu;\rho), \tag{1.4a}$$

$$\forall \rho, \forall X_j \in \sigma(\mu_2) : \quad p(X_j|\mu_2;\rho) = \sum_{X_i \in \sigma(\mu_1)} p((X_i, X_j)|\mu;\rho). \tag{1.4b}$$

N observables $\mu_1, \ldots, \mu_N$ are *jointly measurable* if there exists an observable μ such that: (i') the outcome set of μ is the Cartesian product of the outcome sets of $\mu_1, \ldots, \mu_N$ and (ii') for all states ρ, the outcome probability distributions for every joint measurement of any subset

$S \equiv \{\mu_i | i \in I\} \subset \{\mu_1, \ldots, \mu_N\}$ are recovered as marginals of the outcome probability distribution of μ. Denoting by μ_S an observable associated with a joint measurement of the subset S, its outcome set by $\sigma(\mu_S)$ and one of its outcomes by X_S, the condition can be expressed as

$$\begin{aligned} &\forall S,\ \forall \rho, \forall X_S \in \sigma(\mu_S) : \\ &\qquad p(X_S|\mu_S;\rho) = \sum_{X_t : t \notin I} p((X_1, \ldots, X_N)|\mu;\rho). \end{aligned} \tag{1.5}$$

Joint measurability of a set of observables implies pairwise joint measurability of them (i.e., joint measurability of any pair of them). The converse is not necessarily true.

A *joint probability distribution* for N observables $\mu_1, \ldots, \mu_N$ exists if, for all subsets $S \equiv \{\mu_i | i \in I\} \subset \{\mu_1, \ldots, \mu_N\}$, for all states ρ and for all $X_S \in \sigma(\mu_S)$, where μ_S is an observable associated with a joint measurement of S, there exists a probability distribution $p(X_1, \ldots, X_N|\rho)$ such that

$$p(X_S|\mu_S;\rho) = \sum_{X_t : t \notin I} p(X_1, \ldots, X_N|\rho). \tag{1.6}$$

If some observables are jointly measurable then there exists a joint probability distribution for them. The existence of a joint probability distribution for some observables does not imply that they are jointly measurable. The non-existence of a joint probability distribution for some observables indicates the impossibility of jointly measuring them.

1.1.4 Events

We are interested in a specific type of preparations: those resulting from a test M with outcome X on a previous preparation P. We denote these preparations by $P' \equiv X|M;P$.

Two of these preparations are operationally equivalent if they yield identical outcome probability distributions for either subsequent test M'. Each equivalence class of these preparations is called an *event*. For instance, the event associated with a particular preparation $P'_1 \equiv X_1|M_1;P_1$ is

$$\epsilon_1 \equiv \left\{P' \mid \forall M' : p(X'|M';P') = p(X'|M';P'_1)\right\}. \tag{1.7}$$

Notice that the term "event", which is usually restricted to designate the *outcome* X of test M on preparation P, here designates the *state* after test M with outcome X on preparation P. The probability of an event is therefore the probability of *transforming* one state (e.g., the one associated with P_1) into another (e.g., the one associated with P'_1). In a given NC inequality (see Sect. 1.3, and Eq. (1.22)), all probabilities (of events) are probabilities of different transformations of the *same* state.

1.1.5 Mutual exclusivity of events

Two events ϵ_1 and ϵ_2 are *mutually exclusive* if there exist two jointly measurable observables μ_1, univocally defined for ϵ_1 (i.e., independent of ϵ_2), and μ_2, univocally defined for ϵ_2, that distinguish between them, i.e., if there exists an observable μ associated with a joint measurement

of μ_1 and μ_2 such that there are $X_1 \subset \sigma(\mu)$ and $X_2 \subset \sigma(\mu)$ with $X_1 \cap X_2 = \emptyset$ such that

$$p(X_1|\mu;\epsilon_1) = 1, \tag{1.8a}$$
$$p(X_2|\mu;\epsilon_2) = 1. \tag{1.8b}$$

The N events of a set $\mathcal{E} = \{\epsilon_1, \ldots, \epsilon_N\}$ are *jointly exclusive* if there exists a set of N jointly measurable observables $\mathcal{M} = \{\mu_1, \ldots, \mu_N\}$ that distinguish between the events in any subset of $\mathcal{E}$.

Joint exclusivity of a set of events implies mutual exclusivity of any pair of them. The converse is not necessarily true.

1.1.6 Specker's observation and the E principle

Specker's observation. Specker pointed out that, in QT, pairwise joint measurability of a set $\mathcal{M}$ of observables implies joint measurability of $\mathcal{M}$, while in other theories this implication does not need to hold (Ref. [17]). Later, Specker conjectured that this is "the fundamental theorem" of QT (watch video in Ref. [18]).

The E principle states that any set of pairwise mutually exclusive events is jointly exclusive. Therefore, from Kolmogorov's axioms of probability, the sum of their probabilities cannot be higher than 1.

Lemma: In any theory in which pairwise joint measurability of observables implies joint measurability of observables, pairwise mutual exclusivity of events implies joint exclusivity of events.

Proof: If the events in a set $\mathcal{E} = \{\epsilon_1, \ldots, \epsilon_N\}$ are pairwise exclusive, there exists a set $\mathcal{M} = \{\mu_1, \ldots, \mu_N\}$ of pairwise jointly measurable observables that permits to distinguish between any two events in $\mathcal{E}$. If pairwise joint measurability of $\mathcal{M}$ implies joint measurability of $\mathcal{M}$, then $\mathcal{M}$ permits to distinguish between the events in any subset of $\mathcal{E}$. ■

The converse implication, namely, that in any theory in which pairwise mutual exclusivity implies joint exclusivity also pairwise joint measurability implies joint measurability, is not necessarily true.

1.2 Correlations

Any experimental scenario, where some measurements are performed on a physical system, and for which it is desirable to avoid any assumptions regarding the kind of system or the specific way the measurements are implemented, can be rephrased in an more abstract but equivalent way by means of a device-independent or "black-box" (or simply box) formalism: we model the scenario by a black box for which there are some admissible sets of inputs $\{M_1, M_2, \ldots, M_k\}$, chosen from a set $\mathcal{M}$ of possible inputs. By admissible set of inputs we mean settings or measurements corresponding to some jointly measurable observables, in the sense of 1.1.3. For each input M_j the black box returns an output a_j from a set of possible outputs $\mathcal{A}_j$. We can picture this situation as some experimentalist (or team of experimentalists) in the laboratory pressing appropriate buttons of the box to select the inputs, and then registering the results depicted by some built-in flashing lights or mobile pointers indicating values in a dial. We must remark

that not all possible combinations of buttons might, in principle, be pushed, depending on the specific experiment to be modeled, which is an abstract way to describe the joint measurability of observables.

Let us note that this formalism is able to account for more restricted scenarios, those where a physical system is not viewed as a single entity but as a set of physical subsystems, upon which several parties carry out measurements: in this case the black box is just a collection of black sub-boxes, for each of which the previous description is still valid. The setting chosen by one of the parties in the corresponding sub-box could be constrained or not by the functioning of the sub-box and even by another party's box's setting selection, giving rise to sets of admissible inputs. The sub-boxes might be space-like separated, if needed, like in Bell-type scenarios, where n space-like separated parties have access to k measurements each, and each of these measurements has m possible outcomes (we would assign a sub-box per party, with the appropriate number of buttons and lights). In such a case, we admit the parties can choose their settings regardless of the other parties' selection.

The inner functioning of such a box (or sub-boxes) is in principle irrelevant for our purposes: no matter how the outputs are produced (either by actual measurements carried out on physical systems or by some rules derived from an unknown theory), we can assume the inner mechanism as inaccessible in practice. That being the case, and considering that the outcomes can be correlated in an arbitrary fashion, a general way to describe the box's behavior from the viewpoint of these correlations, independently of the physical model, is through the joint probability distributions of the resulting outputs, conditioned on the selected inputs, $p(a_1, a_2, \ldots, a_k|M_1, M_2, \ldots, M_k)$, where $\{M_1, \ldots, M_k\}$ is any admissible set of inputs (note that for sets of jointly measurable observables the existence of well defined joint probability distributions is guaranteed, according to 1.1.3).

In the following subsections we will summarize the most relevant types of correlations on the basis of the properties fulfilled by the corresponding joint probability distributions of the outcomes generated by such black boxes.

1.2.1 General correlations

Let us consider a physical system modeled by a black box, and let $\{M_1, \ldots, M_N\}$ be a jointly measurable set of inputs. Denote by a_j the outcome corresponding to the measurement M_j on the physical system.[1] Without loss of generality, we will assume that there is only a finite number of possible discrete outcomes for M_j. As we have said before, the outcomes obtained can be arbitrarily correlated, and the joint probability distribution of the outcomes conditioned on the settings, $p(a_1, a_2, \ldots, a_N|M_1, M_2, \ldots, M_N)$, is an adequate way to describe the correlations. These joint probability distributions must obey the positivity condition

$$p(a_1, a_2, \ldots, a_N|M_1, M_2, \ldots, M_N) \geq 0, \forall a_1, \ldots, a_N, \forall M_1, \ldots, M_N, \tag{1.9}$$

[1] This is a generalization of an scenario in which there are N parties, each of them possessing a physical system. Party j has a finite set of different observables at disposal, among which he/she can choose one at will. M_j is the observable (alternatively, the setting) chosen by party j, and a_j is the corresponding outcome the party obtains when measuring M_j on the physical system.

and the normalization condition

$$\sum_{a_1,\ldots,a_N} p(a_1, a_2, \ldots, a_N|M_1, M_2, \ldots, M_N) = 1, \forall M_1, \ldots, M_N. \tag{1.10}$$

The fact that these probabilities cannot be greater than 1 is derived from (1.9) and (1.10).

The set of all possible joint probability distributions satisfying the positivity and normalization conditions constitutes a convex set, since convex combinations of them are legitimate probability distributions too. It is useful to consider these conditioned probability distributions as points in a large dimensional real space:[2] the set of all these points is a convex polytope, that we can refer to as the *general correlations polytope*, $\mathcal{G}$.

In order to deal with more specific types of correlations, it is necessary to consider further restrictions besides conditions (1.9) and (1.10). The procedure usually followed consists of obtaining marginal probabilities for each setting and outcome from the joint probabilities (by summing over the outcomes of the other settings), and then introducing constraints upon these marginal probabilities motivated by more or less plausible physical considerations. For the sake of simplicity, let us illustrate this procedure with a simple case:

Imagine two sets of inputs $S_1 = \{A_1, B_1\}$ and $S_2 = \{A_2, B_2\}$ with the following property: the inputs in S_1 are not jointly measurable, and the same is true for those in S_2; nevertheless, choosing one input from S_1 and another input from S_2 results in a jointly measurable pair of inputs (we can visualize S_1 and S_2 as two switches with only two positions A and B, that can be manipulated independently). Let us denote an outcome corresponding to A_i (or B_j) by a_i (or b_j). If we choose the setting A_1 from S_1, there are two possible jointly measurable pairs involving A_1, namely $\{A_1, A_2\}$ and $\{A_1, B_2\}$, and the marginal probabilities of an outcome a_1 for each of the two possible settings from S_2 are given by

$$p_{A_2}(a_1|A_1) = \sum_{a_2} p(a_1, a_2|A_1, A_2), \tag{1.11a}$$

$$p_{B_2}(a_1|A_1) = \sum_{b_2} p(a_1, b_2|A_1, B_2). \tag{1.11b}$$

The same can be said for B_1 in relation to jointly measurable settings from S_2, and likewise for the marginal probabilities of outcomes corresponding to settings chosen from S_2 regarding jointly measurable settings from S_1.

Note that, for general correlations (those described by joint probability distributions fulfilling only (1.9) and (1.10)), the marginal probabilities $p_{A_2}(a_1|A_1)$ and $p_{B_2}(a_1|A_1)$ *might be different*. In case $p_{A_2}(a_1|A_1) \neq p_{B_2}(a_1|A_1)$, this would imply that the choice of setting in S_2 could change the marginal probability distribution of outcomes of measurements belonging to S_1 (and vice versa, by switching the roles of S_1 and S_2): the term *signaling* is conventionally used to refer to this behavior.

It is interesting to note that signaling is often described taking for granted the existence of two space-like separated parties $\{1, 2\}$ that can choose freely between two settings from $S_1 = \{A_1, B_1\}$ and $S_2 = \{A_2, B_2\}$, respectively. In this scenario, space-like separation provides

[2] For instance, for the N-party scenario mentioned in footnote 1, we need a space of dimension $d = \prod_{j=1}^{N} n_{M_j} n_{a_j}$, where n_{M_j} and n_{a_j} are, respectively, the number of settings and the number of outcomes per setting for party j.

the joint measurability of two observables belonging to different parties: party 1 could signal to party 2 just by selecting different settings from S_1 thereby disturbing party 2's marginal probability distributions, and vice versa.

Nevertheless, from the point of view of this thesis, the existence of parties and the space-like separation between them are extra assumptions that lead to a specific kind of signaling, namely, *super-luminal* signaling.[3] The former two-party (or multi-party) scenario is nothing but a particular instance of the more general and less constrained framework we are considering here, where the only assumption is the *joint measurability of certain observables*. Therefore, signaling must be understood as the fact that the marginal probability distribution of outcomes of a measurement M might be affected by different possible choices of measurements that can be jointly performed with M, without presupposing the reason for their joint measurability.

Of course, signaling need not be the case for more restrictive types of correlations, like those we deal with in the following subsections.

1.2.2 No-signaling correlations

Once again, consider the previous two sets of inputs $S_1 = \{A_1, B_1\}$ and $S_2 = \{A_2, B_2\}$ with the same joint-measurability relationships between them. If the marginal probability distributions of outcomes of a measurement belonging to one of the sets do not depend on the choice of a jointly measurable setting made in the other set, then the correlation between their outcomes is a *no-signaling correlation*: so to say, both sets cannot signal to each other by means of the choice of setting, so that no one is able to tell what setting from S_2 was chosen and measured (or whether any measurement at all was performed) by looking at the statistics of the outcomes of measurements from S_1, and vice versa. Mathematically, the marginal probabilities $p_{M_2}(a_1|A_1)$ and $p_{M_2}(b_1|B_1)$ are independent of the choice $M_2 \in \{A_2, B_2\}$, and analogously for $p_{M_1}(a_2|A_2)$ and $p_{M_1}(b_2|B_2)$ with respect to the choice $M_1 \in \{A_1, B_1\}$, namely,

$$p_{M_2}(a_1|A_1) = p(a_1|A_1), \forall a_1, \forall M_2 \in S_2, \tag{1.12a}$$
$$p_{M_2}(b_1|B_1) = p(b_1|B_1), \forall b_1, \forall M_2 \in S_2, \tag{1.12b}$$
$$p_{M_1}(a_2|A_2) = p(a_2|A_2), \forall a_2, \forall M_1 \in S_1, \tag{1.12c}$$
$$p_{M_1}(b_2|B_2) = p(b_2|B_2), \forall b_2, \forall M_1 \in S_1. \tag{1.12d}$$

This is the mathematical content of the so-called *no-signaling principle*. Let us recall that our only assumption here is the joint measurability between an observable selected from S_1 and another observable selected from S_2. When no additional assumptions are made, some authors (see Ref. [22], v.g.) prefer to denominate this principle as *no-disturbance principle*,[4] and

[3] With more detail, super-luminal signaling entails a notion of space-time structure, whereas signaling does not: we can define the event of measuring an observable as the space-time region comprising the volume in space where the measurement takes place and the interval of time between the choice of setting and the obtention of the corresponding outcome. Space-like separation between such measurement events implies that the observers who perform the measurements are sufficiently distant from each other, and the measurement processes are brief enough so that the measurement events are outside each other's light cone in any inertial reference frame. The relativistic principle of constancy of the speed of light in any reference frame entails that no signal carrying information can travel faster than light, and hence provides the threshold for super-luminal influences.

[4] Alternatively, Gleason's property, like in Ref. [6], since it is the condition underlying Gleason's theorem.

reserve the term "no-signaling" for scenarios in which the sets of measurements S_1 and S_2 are performed on space-like separated physical systems. From our point of view, such distinction is unnecessary.

We can generalize the definition of no-signaling correlations to the case in which there are N sets of observables $S_1, S_2, \ldots, S_N$: by hypothesis, let us assume that any collection of N observables, one from each set S_i, is jointly measurable (although the observables belonging to the same set S_i need not be jointly measurable). In case of no-signaling correlations, one cannot signal to a given subset of these sets of observables from the remaining sets by changing the latter's selected measurement settings.[5] Therefore, the marginal probability distributions of outcomes of observables for each subset of input sets only depend on the corresponding observables measured within the subset.

Mathematically, take any subset $\{S_1, S_2, \ldots, S_p\}$, and select the settings $A_1, A_2, \ldots, A_p$, with $A_i \in S_i, \forall i$. Then, the condition that the rest of the sets $\{S_{p+1}, \ldots, S_N\}$ cannot signal to $\{S_1, S_2, \ldots, S_p\}$ by switching their settings implies that, for all outcomes $a_{p+1}, \ldots, a_N$:

$$p(a_1, \ldots, a_p|A_1, \ldots, A_N) = p(a_1, \ldots, a_p|A_1, \ldots, A_p). \tag{1.13}$$

In fact, conditions (1.13) derive from a single statement: from a given set of observables S_k one cannot signal to the rest of the sets $\{S_1, S_2, \ldots, S_{k-1}, S_{k+1}, \ldots, S_N\}$ by switching between settings in S_k. In mathematical terms, following Refs. [3, 4] and adapting the language appropriately, for each $k \in \{1, \ldots, N\}$ the marginal probability distribution that is obtained when tracing out set S_k's outcomes is independent of what observable (A_k, B_k, etcetera) is measured in S_k. Namely:

$$\sum_{a_k} p(a_1, \ldots, a_k, \ldots, a_N|A_1, \ldots, A_k, \ldots, A_N) = \sum_{b_k} p(a_1, \ldots, b_k, \ldots, a_N|A_1, \ldots, B_k, \ldots, A_N), \tag{1.14}$$

for all outcomes $a_1, \ldots, a_{k-1}, a_{k+1}, \ldots, a_N$ and all settings $A_1, \ldots, A_k, B_k, \ldots, A_N$. This allows to define the marginal probability distribution for the $N-1$ sets not including set S_k,

$$p(a_1, \ldots, a_{k-1}, a_{k+1}, \ldots, a_N|A_1, \ldots, A_{k-1}, A_{k+1}, \ldots, A_N), \tag{1.15}$$

in a way which does not depend on the settings chosen in S_k, as required.

The set of joint probability distributions arising from no-signaling correlations, considered as points in the real space, constitutes a convex polytope, the so-called *no-signaling polytope*, $\mathcal{P}$. The facets of $\mathcal{P}$ that follow from the positivity conditions (1.9) can be considered as trivial, whereas those following from the no-signaling requirements (1.14) are non-trivial ones: a point violating an inequality describing a non-trivial facet of $\mathcal{P}$ would correspond to experimental data which cannot be reproduced using only a no-signaling model, implying the necessity of some kind of signaling.

Obviously, $\mathcal{P} \subset \mathcal{G}$.

[5] Note again that each set S_i of settings could be assigned to a different party j, space-like separated from the others, although this restriction is not necessary.

1.2.3 Local correlations

The set of no-signaling correlations that we have just presented can in turn be divided into two types: local and non-local. In the black-box description, local correlations are those generated by a local box, consisting of a collection of sub-boxes that share classical information, i.e., the only resources at disposal are local operations and shared randomness. Usually, each sub-box is assigned to an observer who locally chooses its settings (for instance, following certain rules on the basis of shared randomness) and obtains the corresponding outcomes (that can be communicated to other parties by classical means). Consequently, local correlations are those described by joint probability distributions of the form

$$p(a_1,\ldots,a_N|A_1,\ldots,A_N)=\sum_{\lambda} p(\lambda)p(a_1|A_1,\lambda)\cdots p(a_N|A_N,\lambda), \tag{1.16}$$

where λ (sometimes called *local hidden variable*) is a random variable that stands for the information shared among the parties; $p(\lambda)$ is the probability that a particular value of λ occurs, and $p(a_j|A_j,\lambda)$ is the (locally generated) probability that party j outputs a_j given that the shared random data was λ and the input was chosen to be A_j.

A model that provides only local correlations is usually called a local hidden-variable (LHV) model. The joint probability distributions that cannot be written similarly to (1.16) correspond to non-local correlations.

When we represent joint probability distributions satisfying (1.16) as points in a real space we obtain the set of local correlations, which is a convex polytope, the so-called *local polytope*, frequently denoted by $\mathcal{L}$. Such local polytope is delimited by two kinds of facets: firstly, trivial facets described by the positivity conditions (1.9), which are trivial facets of the no-signaling polytope $\mathcal{P}$ as well. Secondly, non-trivial facets corresponding to Bell-type inequalities, whose violation by certain point implies that such a point lies outside the local polytope, and thus corresponds to non-local correlations. The latter facets are not facets of $\mathcal{P}$.

Note that local correlations are no-signaling, since one can define their marginal probability distributions the same way as it was done previously for no-signaling correlations, i.e., like in (1.15). Accordingly, the set-inclusion relationship between the correlation polytopes presented so far is $\mathcal{L}\subset\mathcal{P}\subset\mathcal{G}$.

For a complete review of Bell inequalities, polytopes and related topics, see Ref. [23].

1.2.4 Quantum correlations

Quantum correlations constitute the main subject of this thesis. A precise definition of what is meant by quantum correlations in our work requires us to introduce some previous concepts:

Without loss of generality, in QT we can represent the state of a quantum system by a unit vector $|\psi\rangle$ in a Hilbert space $\mathcal{H}$, and a quantum measurement A_i by a set of orthogonal projectors $\{\Pi_{a_i}^{(A_i)}\}_{a_i}$, where each projector corresponds to an outcome a_i, fulfilling $\Pi_{a_i}^{(A_i)}\Pi_{a_j}^{(A_j)}=\delta_{a_i,a_j}\Pi_{a_i}^{(A_i)}$ and $\sum_{a_i}\Pi_{a_i}^{(A_i)}=\mathbb{1}_{\mathcal{H}}$. The probability of obtaining outcome a_i when measurement A_i is performed on a system in state $|\psi\rangle$ is

$$p(a_i|A_i)=\langle\psi|\Pi_{a_i}^{(A_i)}|\psi\rangle. \tag{1.17}$$

Notice that, from the point of view of an observer having access only to a subspace $\mathcal{H}_S$ of $\mathcal{H}$ (i.e., $\mathcal{H} = \mathcal{H}_S \bigoplus \mathcal{H}_S^{\perp}$), the state is represented by a density operator $\rho = \mathrm{tr}_{\mathcal{H}_S^{\perp}}(|\psi\rangle\langle\psi|)$, where $\mathrm{tr}_{\mathcal{H}_S^{\perp}}$ denotes the partial trace over subspace $\mathcal{H}_S^{\perp}$, and the measurement A_i is represented by the positive-operator-valued measure (POVM) elements $\{M_{a_i}^{(A_i)}\}_{a_i}$, where $M_{a_i}^{(A_i)} = \Pi_S \Pi_{a_i}^{(A_i)} \Pi_S$, and Π_S is the orthogonal projection taking $\mathcal{H}_S \bigoplus \mathcal{H}_S^{\perp}$ to $\mathcal{H}_S$.[6]

Two quantum measurements A_i and A_j are compatible if and only if $[\Pi_{a_i}^{(A_i)}, \Pi_{a_j}^{(A_j)}] = 0, \forall a_i, a_j$. A set of quantum measurements $\{A_1, \ldots, A_N\}$ is compatible if each pair $\{A_i, A_j\}$ is compatible. Such a set is called a *context*.

We define quantum correlations as those that can be written as

$$p(a_1, \ldots, a_N | A_1, \ldots, A_N) = \langle\psi|\Pi_{a_1}^{(A_1)} \ldots \Pi_{a_N}^{(A_N)}|\psi\rangle, \tag{1.18}$$

where $|\psi\rangle$ is a quantum state in $\mathcal{H}$, $\Pi_{a_i}^{(A_i)}$ are orthogonal projectors, and $\{A_1, \ldots, A_N\}$ is a context.

Two types of quantum correlations are of particular interest:

(I) *Projective* quantum correlations: those for which all quantum measurements A_i are projective in $\mathcal{H}_{\mathcal{S}}$.

(II) *Bell-type* quantum correlations: in this case, the quantum system is composed of N spatially separated subsystems, and the joint Hilbert space is $\mathcal{H} = (\mathcal{H}_1 \bigoplus \mathcal{H}_1^{\perp}) \otimes \cdots \otimes (\mathcal{H}_N \bigoplus \mathcal{H}_N^{\perp})$.

Quantum mechanics fulfills the no-signaling principle. Therefore, quantum correlations (1.18) constitute a type of no-signaling correlations: the corresponding marginal probability distributions are defined in the same way as it was done in (1.15) for no-signaling correlations. Taking now the joint probability distributions (1.18) as points in the real space, the set of quantum correlations ends up still being a convex set but with a more subtle geometry, not a polytope (since the number of its extremal points is not finite and, correspondingly, the number of its bounding halfplanes is infinite): this set is usually named as the *quantum set* or *quantum body*, and denoted by $\mathcal{Q}$. Note also that, since the correlations allowed by quantum mechanics can violate Bell inequalities, the set $\mathcal{Q}$ includes points corresponding to correlations that are non-local. Trivially, the local polytope is a subset of the quantum set.

In a nutshell, the set-inclusion relationship between the general correlations, no-signaling and local polytopes as defined in the previous subsections, and the quantum set we have just introduced, is the following: $\mathcal{L} \subset \mathcal{Q} \subset \mathcal{P} \subset \mathcal{G}$. Such strict set-inclusion relationship is illustrated in Fig. 1.1.[7].

An important remark: in the following sections of this chapter, and also in the rest of this thesis unless otherwise stated, *we will focus on projective quantum correlations*. Hereafter, as a consequence, by quantum correlations we will mean *correlations between the outcomes of jointly measurable projective quantum observables*. Note that these correlations are less restrictive than Bell-type correlations. There are two fundamental reasons for this choice: (i) In Bell-type scenarios (where the emphasis is put on non-locality) it is assumed that experiments involving

[6] The other way round, any POVM can be understood as a projection-valued measure (PVM), i.e., a set of mutually orthogonal projections that sum to 1, in an enlarged Hilbert space by virtue of Neumark's theorem. See for instance Ref. [24], Sect. 9.6. Also Ref. [25].

[7] We encourage the reader to compare his figure with Fig. 1.4, where another set-inclusion relationship is depicted, for sets of correlations associated to an arbitrary exclusivity graph G.

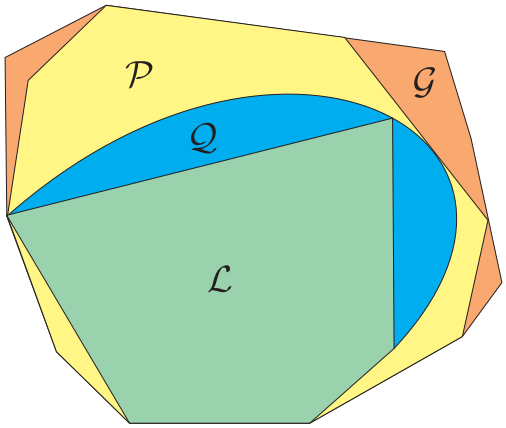

Figure 1.1: Schematic representation of the inclusion relationship among the sets of general ($\mathcal{G}$), no-signaling ($\mathcal{P}$), quantum ($\mathcal{Q}$) and local ($\mathcal{L}$) correlations, as defined in previous subsections. All of them are polytopes, except for $\mathcal{Q}$, which is in general a convex set but not a polytope. Recall that $\mathcal{L}$ is delimited by trivial facets described by the positivity conditions (1.9), and non-trivial facets corresponding to Bell-type inequalities. In the figure, the two hyperplanes delimiting $\mathcal{L}$ and $\mathcal{Q}$ represent Bell inequalities.

space-like separated tests are more fundamental than other types of correlation experiments. Nevertheless, apparently nothing in the rules of QT supports this assumption. In fact, quantum correlations can also occur in experiments involving jointly measurable observables in systems in which no parts can be identified and, consequently, where space-like separation plays no role (Ref. [26]). (ii) The basic quantum correlations (those corresponding to basic exclusivity graphs, see Chap. 2) *do not* attain their maximum values in Bell-type scenarios, whereas these maxima are achieved in less restricted scenarios, in which parts are not taken into account, and where only jointly measurable projective quantum observables are involved. An example can be found in Ref. [27] (see also Sect. 1.4.5, and footnote 22, on p. 55).

1.2.5 Commutativity, no-disturbance and joint measurability

We will finish this section with a brief comment on the mutual implications between some of the concepts presented so far, specifically with regard to QT. According to Ref. [28], two of the main features of QT, in sharp contrast with classical physics, are the impossibility of jointly measure some observables and the fact that measurements of different observables usually disturb each other, properties that often come along with non-commutativity of the operators representing such observables. Strictly speaking, however, no-disturbance (ND), joint measurability (JM) and commutativity (COM) are different concepts. Whereas joint measurability and no-disturbance can easily be understood in operational terms, as we have seen before, commutativity seems to rely more on the underlying mathematical representation of quantum

observables.[8] The connections between all these properties are well studied for pairs of general quantum observables, which are given in terms of POVMs. In general, it is known that

$$\text{COM} \Rightarrow \text{ND} \Rightarrow \text{JM}, \tag{1.19}$$

and that the first two implications are strict in the sense that the reverse implications do not hold in general. Nonetheless, if the POVMs are PVMs then all three notions turn out to be coincident with one another. Given that this thesis focuses on projective measurements, we will use such notions as equivalent and interchangeable, unless noted otherwise.

1.3 Quantum contextuality. Non-contextual correlations

Quantum contextuality (Refs. [17, 29, 30]) refers to the fact that the predictions of quantum mechanics cannot be reproduced assuming non-contextuality of results (i.e., that the results are predefined and independent of other compatible tests) or, equivalently, non-contextual hidden variable (NCHV) theories.[9] By compatible tests we mean jointly measurable tests, according to definition of joint measurability in Sect. 1.1.3 (for other definitions of compatibility, see Ref. [24], p. 203; Ref. [31], Sect. 6.3; and also Ref. [32]). In quantum mechanics, two tests represented by self-adjoint operators A and B are compatible when A and B commute.[10] This guarantees that the quantum predictions for compatible tests are given by a single probability measure on a single probability space. Compatibility implies that the probability $p(a_i|x_i)$ of obtaining the result a_i for the test x_i is independent of other compatible tests $x_1, \ldots, x_{i-1}, x_{i+1}, \ldots, x_n$, i.e.,

$$p(a_i|x_i) = \sum_{a_1,\ldots,a_{i-1},a_{i+1},\ldots,a_n} p(a_1, \ldots, a_n|x_1, \ldots, x_n), \tag{1.20}$$

for all sets $x_1, \ldots, x_n$ of compatible tests, and where $p(a_1, \ldots, a_n|x_1, \ldots, x_n)$ is the joint probability of obtaining the results $a_1, \ldots, a_n$ for the compatible tests $x_1, \ldots, x_n$, respectively. Assumption (1.20) is formally equivalent to the no-signaling principle (or, alternatively, no-disturbance principle, as some authors refer to the no-signaling principle when it involves compatible tests —like in this case— instead of space-like separated tests; see p. 43).

The assumption of the non-contextuality of results states that the result a_i of test x_i is the same regardless of other compatible tests being performed; it only depends of x_i and some hidden variables λ. This implies that the correlation among the results of compatible tests can be expressed as

$$p(a_1, \ldots, a_n|x_1, \ldots, x_n) = \sum_{\lambda} p(\lambda) \prod_{i=1}^{n} p(a_i|x_i, \lambda), \tag{1.21}$$

[8] In Ref. [28], the concept of *coexistence* of observables is also defined, and its implications regarding commutativity, joint measurability and no-disturbance are discussed. We will set it aside, since it will not be necessary for our purposes.

[9] The terms "contextuality" and "contextual" come from *context*, which is a set of mutually compatible observables.

[10] Recalling (1.19), commutativity between the self-adjoint operators implies joint-measurability of the observables represented by them. Hence, a context can be defined, alternatively, as a set of jointly-measurable observables.

for some common distribution $p(\lambda)$. Such correlations are called *non-contextual* correlations.

NC inequalities are expressions of the form

$$S \equiv \sum T_{a_1,\ldots,a_n,x_1,\ldots,x_n} p(a_1,\ldots,a_n|x_1,\ldots,x_n) \overset{\text{NC}}{\leq} \Omega_{\text{NC}}, \tag{1.22}$$

where $T_{a_1,\ldots,a_n,x_1,\ldots,x_n}$ are real numbers and $\overset{\text{NC}}{\leq} \Omega_{\text{NC}}$ denotes that the maximum value of S for any non-contextual correlations [therefore satisfying (1.21)] is Ω_{NC}. Quantum contextuality is experimentally observed through the violation of NC inequalities (Refs. [33, 34, 35, 36]).

Quantum non-locality (Ref. [37]) is a particular form of quantum contextuality which occurs when the tests are not only compatible but also space-like separated. In this case, NC inequalities are called Bell inequalities (Ref. [37]). In addition to applications such as device-independent quantum key distribution (Refs. [38, 39]) and random number generation (Ref. [40]), which require space-like separation, quantum contextuality also offers advantages in scenarios without space-like separation. Examples are communication complexity (Ref. [41]), parity-oblivious multiplexing (Ref. [42]), zero-error classical communication (Ref. [43]), and quantum cryptography secure against specific attacks (Refs. [44, 45]).

1.4 Cabello-Severini-Winter's graph-theoretic approach to quantum correlations

The experimental violation of NC inequalities reveals contextual correlations that cannot be explained with NCHV theories, i.e., theories in which outcomes are predefined and do not depend on which combination of jointly measurable observables is considered. A novel approach to quantum correlations within this general framework of contextual correlations is presented in Refs. [6, 7]: the main feature of this approach is the use of graphs to characterize correlations arising in three different classes of theories, namely, NCHV theories, QT, and more general probabilistic theories. The first part of this thesis is directly based on this graph-theoretic approach, and develops some of the proposals in Refs. [6, 7]: for instance, the classification of graphs according to some of their combinatorial numbers, which consequently provides a classification of all possible forms of quantum contextuality; or the identification of experimental scenarios with specific correlations on demand (e.g., fully contextual quantum correlations). The aforementioned reasons justify that we dedicate the present section to summarize the fundamental concepts that underlie the graph-theoretic approach, and the main results obtained in Refs. [6, 7].

1.4.1 Exclusivity graph of an experiment

Given any correlation experiment, one can associate it with a graph $\mathcal{G}$ in which events are represented by vertices and pairs of exclusive events[11] are represented by adjacent vertices. We will refer to $\mathcal{G}$ as the *exclusivity graph of the experiment*.

For example, let us consider the Clauser-Horne-Shimony-Holt (CHSH) experiment, Ref. [46], in which there are four tests A_0, B_0, A_1, and B_1, each of them with two possible outcomes: -1

[11] See the operational definition of mutual exclusivity in 1.1.5. In practice, two events are mutually exclusive if they cannot be simultaneously true: at most, one of them can occur.

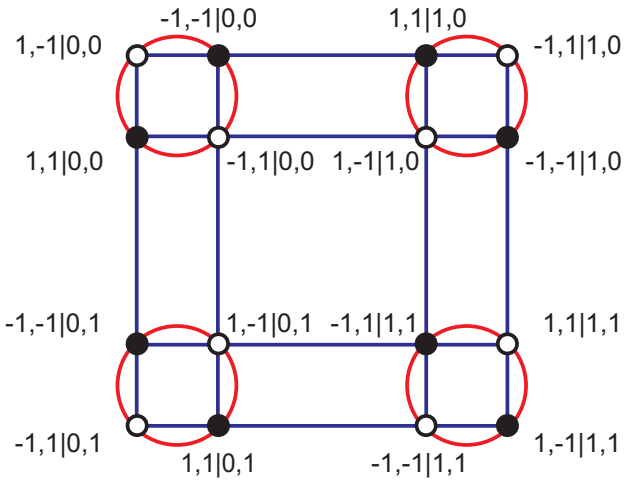

Figure 1.2: Simplified representation of the exclusivity graph of the CHSH experiment, $\mathcal{G}_{\text{CHSH}}$. Events are represented by vertices. Here, for simplicity, sets of 4 pairwise exclusive events are represented by 4 vertices lying on the same straight line (blue) or circumference (red), rather than by cliques. Each vertex belongs to three cliques. Black vertices correspond to the 8 events depicted in Fig. 1.3 (b). Figure taken from Ref. [7] and slightly modified, with permission of the authors.

and 1. All possible pairs of them are compatible except for the pairs (A_0, A_1) and (B_0, B_1). The experiment consists of performing the pairs of tests (A_0, B_0), (A_0, B_1), (A_1, B_0), and (A_1, B_1) on systems in the same quantum state. The exclusivity graph of the CHSH experiment, $\mathcal{G}_{\text{CHSH}}$, is represented in Fig. 1.2, where a vertex labeled by $a, b \,|\, i, j$ corresponds to the event "the result a has been obtained when measuring A_i and the result b has been obtained when measuring B_j". It is a 16-vertex graph with 12 cliques of size 4 (sets of 4 pairwise adjacent vertices).

1.4.2 Compatibility and exclusivity graphs of a non-contextuality inequality

As it is pointed out in Refs. [6, 7], the correlations in any NC inequality are expressed as a linear combination of probabilities of a subset of events of the corresponding experiment. The fact that the sum of probabilities of outcomes of a test is 1 can be used to express these correlations as a *positive* linear combination of probabilities of events e_i, $S = \sum_i w_i p(e_i)$, with $w_i > 0$ (recall that in the general expression for a NC inequality (1.22), the coefficients $T_{a_1,\ldots,a_n,x_1,\ldots,x_n}$ accompanying the probabilities are real numbers, without restrictions).

Two different graphs can be associated to any given NC inequality:

(I) On one hand, the graph in which vertices represent the observables measured in the NC inequality and adjacent vertices represent those which are compatible (Ref. [47]). This graph is

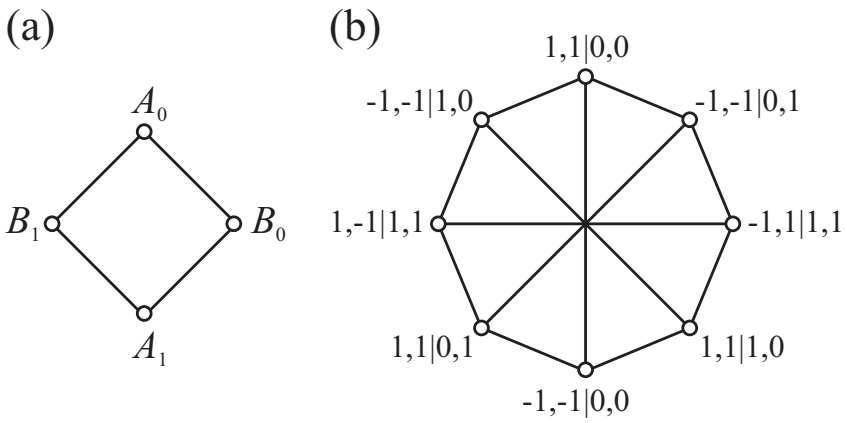

Figure 1.3: (a) The compatibility graph of the local observables in the CHSH experiment. (b) The exclusivity graph G_{CHSH} of the CHSH inequality (1.25).

the so-called *compatibility graph*. For example, consider the CHSH inequality in Ref. [46],

$$\beta = \langle A_0 B_0 \rangle + \langle A_0 B_1 \rangle + \langle A_1 B_0 \rangle - \langle A_1 B_1 \rangle \overset{\text{NCHV}}{\leq} 2, \tag{1.23}$$

where $\langle A_i B_j \rangle$ denotes the mean value of the product of the results of measuring the observables A_i and B_j, each of them with possible results either -1 or 1, and $\overset{\text{NCHV}}{\leq}$ 2 indicates that 2 is the maximum value for β for NCHV theories. As we have said before, all possible pairs of observables in the CHSH experiment are compatible except for the pairs (A_0, A_1) and (B_0, B_1). Therefore, the compatibility graph[12] is the one depicted in Fig. 1.3 (a).

(II) On the other hand, by taking into account that

$$\pm \langle A_i B_j \rangle = 2[p(1, \pm 1 \,|\, i, j) + p(-1, \mp 1 \,|\, i, j)] - 1, \tag{1.24}$$

where $p(a, b \,|\, i, j)$ is the probability of the event "the result a has been obtained when measuring

[12] Remarkably, there is a connection between the compatibility graph of a set of observables and the existence of a joint probability distribution for them. In Refs. [48, 22] the authors prove that for any set of observables whose corresponding compatibility graph is a *chordal* graph (i.e., a graph which does not contain induced cycles of size greater than 3), there always exists a joint probability distribution reproducing the quantum marginals. They also provide a graph theoretical method to construct such joint probability distribution on the basis of the compatibility graph. Let us note that the CHSH compatibility graph of Fig. 1.3 (a) is the 4-cycle, C_4, which is not a chordal graph: this entails the lack of a joint probability distribution for the set of observables $\{A_0, A_1, B_0, B_1\}$, a reason behind the violation of the NC inequality (1.23).

A_i and the result b has been obtained when measuring B_j," inequality (1.23) can be written as

$$\begin{aligned} S_{\text{CHSH}} = \frac{\beta}{2} + 2 = p(1,1\,|\,0,0) + p(-1,-1\,|\,0,0) + p(1,1\,|\,0,1) + p(-1,-1\,|\,0,1) \\ + p(1,1\,|\,1,0) + p(-1,-1\,|\,1,0) + p(1,-1\,|\,1,1) + p(-1,1\,|\,1,1) \overset{\text{NCHV}}{\leq} 3, \end{aligned} \tag{1.25}$$

where the left-hand side is now a convex sum of probabilities of events. A new graph can be associated to the set of events, one in which the vertices represent the events and adjacent vertices represent events that cannot occur simultaneously (i.e., exclusive events). This is the so-called *exclusivity graph* (see Ref. [6]). For example, the exclusivity graph for the CHSH inequality (1.25), denoted as G_{CHSH}, is depicted in Fig. 1.3 (b). Let us note that the set of 8 events appearing in (1.25) constitutes a subset of the 16 events of the whole CHSH experiment (those corresponding to the black vertices in Fig. 1.2): G_{CHSH} is the induced subgraph[13] of $\mathcal{G}_{\text{CHSH}}$ obtained by removing all but the 8 black vertices.[14] G_{CHSH} is isomorphic to the 8-vertex circulant $(1,4)$ graph, $Ci_8(1,4)$.

Whereas in the previous CHSH example and in other NC inequalities (like, for instance, Wright's inequality in Ref. [49]) all probabilities have weight 1, that need not be the case in general: in an arbitrary NC inequality, expressed as a linear combination of probabilities of events $S = \sum_i w_i p(e_i)$ with $w_i > 0$, each probability $p(e_i)$ may have a different weight w_i, and hence the exclusivity graph associated to S will be a *vertex-weighted* graph[15] (G, w), where $G \subseteq \mathcal{G}$. For such graph, a vertex $i \in V(G)$ represents an event e_i such that $p(e_i)$ is in S, adjacent vertices represent exclusive events, and the vertex weights represent the weights w_i of the probabilities $p(e_i)$.

In the following subsections we present the two main results obtained in Refs. [6, 7] on which this part of our thesis is based.

1.4.3 Correlations in theories satisfying the exclusivity principle

Quantum theory (QT) is the most successful scientific theory of all times. However, it is still not known how to derive it from fundamental physical principles. Recently, this problem has been addressed from different perspectives. One consists of reconstructing QT from information-theoretic axioms (see Refs. [50, 51, 52, 53, 54, 55]). However, these reconstructions fail to

[13] An induced subgraph H of a given graph F is obtained by selecting a subset of the vertices of F and their incident edges in such a way that for any pair of vertices i and j of H, ij is an edge of H if and only if ij is an edge of F. Alternatively, it is a subgraph obtained by deleting a subset of the vertices of F along with their incident edges.

[14] Note that taking the 16 events, the normalization of the probabilities, namely,

$$p(1,1\,|\,i,j) + p(1,-1\,|\,i,j) + p(-1,1\,|\,i,j) + p(-1,-1\,|\,i,j) = 1, \forall\, i,j = 0,1, \tag{1.26}$$

and no-signaling conditions between the pairs (A_0, A_1) and (B_0, B_1), namely,

$$p(a\,|\,i) = p(a,1\,|\,i,j) + p(a,-1\,|\,i,j), \forall\, a = -1,1; \forall\, i,j = 0,1, \tag{1.27a}$$

$$p(b\,|\,j) = p(1,b\,|\,i,j) + p(-1,b\,|\,i,j),\ \forall\, b = -1,1; \forall\, i,j = 0,1, \tag{1.27b}$$

determine the probabilities of the "white events" given the probabilities of the "black events".

[15] A vertex-weighted graph (G, w) is a graph G with vertex set $V(G)$ and weight assignment $w : V(G) \to \mathbb{R}_+$.

capture the "*physical* assumptions that give rise to the theory", according to Refs. [56, 57]. Another approach, initiated by the work of Popescu and Rohrlich in Ref. [58], tries to identify the principles behind quantum nonlocal correlations (Refs. [59, 60, 61, 62, 63, 64, 65, 66]). Here one problem is that principles such as information causality (Ref. [61]) and macroscopic locality (Ref. [62]) have been proved to fail to exclude non-quantum correlations in tripartite scenarios (see Refs. [63, 64]). However, the main limitation of this approach is that it renounces to explain quantum correlations between experiments that are not space-like separated, while quantum correlations are ubiquitous.

Nothing in the known rules of QT supports the previous supposition according to which experiments with space-like separation are more fundamental than other types of correlation experiments. As pointed out in Refs. [6, 7], a more general approach to account for quantum correlations follows from the question of whether there exists a joint probability distribution that gives the marginal probabilities predicted by QT, which is equivalent to the question of whether a specific set of linear correlation inequalities is satisfied (Bell inequalities, for experiments with space-like separated tests; and NC inequalities, for more general scenarios).

As we have said before, the experimental violation of NC inequalities reveals contextual correlations that cannot be explained by NCHV theories. In this sense, QT is contextual. In order to account for such contextual quantum correlations, QT is contrasted in Ref. [7] with NCHV theories and with a general class of theories assigning probabilities to events, namely, probabilistic theories satisfying the *E principle* (see 1.1.6), according to which the sum of probabilities of any set of pairwise exclusive events cannot be higher than 1. This class has been previously considered in Refs. [17, 49]. Specker noticed that classical theories and QT satisfy this principle, but that there are theories that do not (Refs. [17, 1]).

Given an NC inequality S and its pertaining exclusivity graph (G, w), it is convenient to denote by E1 those theories satisfying the E principle applied to the probabilities assigned to the vertices of G alone (or, as it is usually said, to "one copy of G"). Here, the index 1 in E1 is used to distinguish these theories from those satisfying the E principle applied jointly to G and other independent graphs, Refs. [19, 20, 67, 2] (for instance, by En we would designate theories satisfying the E principle applied to the entire set of probabilities assigned independently to the vertices of n copies of a given graph G).

In Refs. [6, 7], the set of correlations obeying E1, denoted by $\mathcal{E}^1(G)$, is defined as

$$\mathcal{E}^1(G) := \left\{ p \in \mathbb{R}_+^{|V|} : \sum_{i \in C} p_i \leq 1 \text{ for all cliques } C \right\}. \tag{1.28}$$

Moreover, $\mathcal{E}^1(G)$ is exactly the fractional stable set polytope (or clique-constrained stable set polytope) of G, QSTAB(G), introduced in Ref. [68].

Let us emphasize that if (G, w) is the exclusivity graph of an NC inequality, then a clique $C \in V(G)$ corresponds to a set of pairwise exclusive events, and the condition $\sum_{i \in C} p_i \leq 1$ formulates the E principle (see 1.1.6) applied to one copy of G. For our purposes, the important assertion is this: *correlations obeying E1 also obey the no-signaling principle* . In fact, the set of E1-correlations, $\mathcal{E}^1(G)$, is a proper or strict subset of $\mathcal{P}(G)$, the no-signaling polytope[16] of

[16] For the proof of these statements we refer the reader to Ref. [6] (Appendix, [ii]); and also to Ref. [65], where

G. We refer the reader to Figs. 1.1 and 1.4 for a pictorial representation of the relationships of inclusion for the different sets of correlations.

1.4.4 The limits of the correlations in NCHV theories, quantum theory and theories satisfying the E principle

The exclusivity graph of S can be used to calculate the limits of the correlations in NCHV theories, QT and theories satisfying E1. Three combinatorial numbers characteristic of (G, w) provide such limits: the independence number, the Lovász number and the fractional packing number. We give the definitions below.

Let (G, w) be a vertex-weighted graph with vertex set V, and w_i the weight corresponding to vertex $i \in V$. An independent or stable set of G[17] is a set of pairwise nonadjacent vertices of G. The independence number of (G, w), denoted by $\alpha(G, w)$, is the maximum of $\sum_i w_i$ taken over all stable sets of vertices of G (Ref. [69]). When all the vertices have weight 1 (unweighted graph) the independence number is denoted as $\alpha(G)$, and is equal to the cardinality of the largest independent set of G (Ref. [70]).

An orthonormal representation (OR) in $\mathbb{R}^d$ of a graph G with vertex set V assigns a nonzero unit vector $|v_i\rangle \in \mathbb{R}^d$ to each $i \in V$ such that $\langle v_i|v_j\rangle = 0$ for all pairs i, j of nonadjacent vertices. A further unit vector $|\psi\rangle \in \mathbb{R}^d$, usually called *handle* (Ref. [71]), is sometimes specified together with the OR. The definition of OR does not require that different vertices be mapped onto different vectors nor that adjacent vertices be mapped onto nonorthogonal vectors.[18] The complement $\overline{G}$ of a graph G is the graph with vertex set V such that two vertices i, j are adjacent in $\overline{G}$ if and only if i, j are not adjacent in G. The Lovász number of (G, w) can be defined following Refs. [71, 72, 69] as

$$\vartheta(G, w) := \max \sum_{i \in V} w_i |\langle \psi | v_i \rangle|^2, \tag{1.29}$$

where the maximum is taken over all ORs of $\overline{G}$ and handles in any dimension.

The fractional packing number (or fractional stability number) of (G, w) (Refs. [72, 69, 68]), denoted by $\alpha^*(G, w)$, is defined as

$$\alpha^*(G, w) := \max \sum_{i \in V} w_i p_i, \tag{1.30}$$

where the maximum is taken over all $p_i \geq 0$ and for all cliques C of G, under the restriction $\sum_{i \in C} p_i \leq 1$.[19]

---

the authors introduce the so-called *local orthogonality* (LO) principle —which may be seen as the E principle restricted to Bell scenarios— and prove that, while the set of LO correlations coincides with the set of no-signaling correlations in the bipartite case, it is strictly smaller for more than two parties. That is, the LO principle is more restrictive than the no-signaling principle in the multipartite case. Recall that quantum correlations fulfill the E (or LO, in Bell scenarios) principle.

[17] Since the adjacency relationship between vertices does not depend on the vertex weight assignment, and for the sake of simplicity, we omit reference to weights when it is not necessary.

[18] If these conditions also hold, the OR is called *faithful*.

[19] Recall that, when (G, w) is the exclusivity graph of an NC inequality, this last restriction imposes that the sum of the probabilities of any set of pairwise exclusive events in S (such sets correspond to cliques in G) cannot exceed 1, which is the content of the E principle, in 1.1.6.

The independence number is a lower bound of the Shannon capacity $\Theta(G)$ of a graph G (Ref. [68]), whereas the Lovász number and the fractional packing number are upper bounds of $\Theta(G)$. The comparison between one another gives (Ref. [71])

$$\alpha(G) \leq \vartheta(G) \leq \alpha^*(G), \tag{1.31}$$

and this relationship also holds for the weighted versions of these combinatorial numbers (Ref. [69]).

Result 1 (Ref. [7]): Given S corresponding to a Bell or NC inequality, the maximum value of S for classical (LHV and NCHV) theories, QT, and theories satisfying E1 is given by

$$S \overset{\text{LHV,NCHV}}{\leq} \alpha(G,w) \overset{\text{QT}}{\leq} \vartheta(G,w) \overset{\text{E1}}{\leq} \alpha^*(G,w), \tag{1.32}$$

where (G,w) is the exclusivity graph of S.

For example, applying Result 1 to S_{CHSH} (1.25), whose exclusivity graph is the one in Fig 1.3 (b), one obtains $\alpha(G_{\text{CHSH}}) = 3$, $\vartheta(G_{\text{CHSH}}) = 2+\sqrt{2}$, and $\alpha^*(G_{\text{CHSH}}) = 4$, which correspond to the maximum for LHV (Ref. [46]) and NCHV theories, QT (Ref. [73]), and no-signaling[20] theories (Ref. [58]), respectively.

1.4.5 The Lovász number as a physical limit and the set of quantum correlations

Note that $\vartheta(G,w)$ might be only an upper bound to the maximum quantum value of S in cases in which the particular physical settings of the experiment testing S add further constraints.[21] A typical example of this circumstance is a Bell inequality, which is a particular instance of NC inequality satisfied by LHV theories, where compatible settings are assumed to correspond to different space-like separated parties (in a general NC inequality, however, compatibility of measurements does not have to follow from the space-like separation of observers). This additional constraint could prevent the maximum quantum value of S from reaching $\vartheta(G,w)$.[22]

In the light of this, a natural question is whether, given G, there is a NC inequality that reaches $\vartheta(G)$.

Result 2 (Ref. [7]): For any graph G, there is always a NC inequality such that the quantum maximum is *exactly* $\vartheta(G)$ and the set of quantum probabilities is *exactly* the Grötschel-Lovász-Schrijver theta body $\text{TH}(G)$ (Ref. [69]).

The proof, that we transcribe here almost literally, is the following (Ref. [7]): given G, by definition (1.29), there is always an OR of $\overline{G}$ in $\mathbb{R}^d$, $\{|v_i\rangle\}$, and a handle $|\psi\rangle$ such that $\vartheta(G) = \sum_{i\in V} |\langle\psi|v_i\rangle|^2$ [i.e, an OR of $\overline{G}$ providing $\vartheta(G)$]. Let D be the minimum dimension d in

[20] Recall the previous comment about no-signaling correlations and correlations obeying E1, in 1.4.3, p. 53. For a 2-party Bell scenario, like CHSH, E1 and no-signaling principles define the same set of correlations.

[21] We have dealt with a similar issue when discussing no-signaling correlations and the rather *ad hoc* distinction between the no-signaling and no-disturbance principles. See p. 43.

[22] For example, as we have just mentioned, the maximum quantum value of S_{CHSH} in (1.25) is equal to $2+\sqrt{2}$, which is exactly $\vartheta(G_{\text{CHSH}}) = \vartheta[Ci_8(1,4)]$, and this value is achievable regardless of the possible space-like separation between measurements A_i and B_j. On the contrary, if G is a pentagon, C_5, although there exist NC inequalities for which the maximum quantum value is $\vartheta(C_5) = \sqrt{5}$ (see Refs. [49, 74]), there is no Bell inequality reaching $\vartheta(C_5)$ (Ref. [27]).

which this OR exists. Then, consider the following positive linear combination of probabilities of events:

$$S = \sum_{i \in V} P(1, 0, \ldots, 0 | i, i_1, \ldots, i_{n(i)}), \tag{1.33}$$

where test i is defined as $\Pi_i = |v_i\rangle\langle v_i|$, with $|v_i\rangle$ in the OR, test i_j is $\Pi_{i_j} = |v_{i_j}\rangle\langle v_{i_j}|$, with $|v_{i_j}\rangle$ in the OR, and $\{i_1, \ldots, i_{n(i)}\}$ is the set of tests corresponding to vertices adjacent to i. Note that $1, 0, \ldots, 0 | i, i_1, \ldots, i_{n(i)}$, which belongs to the same equivalence class as $1|i$ (see 1.1.4; both of them are possible realizations of the same event), is a repeatable event with a well-defined probability, even though $i, i_1, \ldots, i_{n(i)}$ need not be compatible tests.

The important point is that S so defined reaches $\vartheta(G)$ when a quantum system is prepared in the quantum state $|\psi\rangle$, and this fact identifies $\vartheta(G)$ as a fundamental physical limit for quantum correlations.

On the other hand, in QT, the set of probabilities that can be assigned to the vertices of G by performing tests on a quantum system is

$$\mathcal{Q}(G) := \left\{ (|\langle\psi|v_i\rangle|^2 : i \in V) : (|v_i\rangle : i \in V) \text{ is an OR of } \overline{G} \text{ and } |\psi\rangle \text{ a handle} \right\}. \tag{1.34}$$

If the quantum system has dimension greater than or equal to D, then $\mathcal{Q}(G)$ is exactly the theta body $\mathrm{TH}(G)$ introduced in Ref. [69] (see Theorem 3.5 in Ref. [69] and Corollary 9.3.22 (c) in Ref. [75]).

In other words, given any graph G, there is always a correlation experiment in which the whole set of quantum probabilities for G can be reached, and $\mathrm{TH}(G)$ is such set of *physical* correlations for G.

Let us note that, according to Refs. [6, 7], and for a given exclusivity graph G, the set-inclusion relationship among the set of quantum correlations $\mathcal{Q}(G)$ (that is, the theta body $\mathrm{TH}(G)$), the set of classical correlations $\mathcal{C}(G)$ (coincident with the stable set polytope or vertex packing polytope, $\mathrm{STAB}(G)$, in Ref. [69]), and the set of correlations obeying the E1 principle, $\mathcal{E}^1(G)$ (which is exactly the fractional stable set polytope or clique-constrained stable set polytope, $\mathrm{QSTAB}(G)$), is given by

$$\mathcal{C}(G) \subseteq \mathcal{Q}(G) \subseteq \mathcal{E}^1(G), \tag{1.35}$$

since $\mathrm{STAB}(G) \subseteq \mathrm{TH}(G) \subseteq \mathrm{QSTAB}(G)$ after Ref. [69]. Such relationship[23] is depicted in Fig. 1.4, which is inspired in another figure taken from Ref. [76]. Note that in Fig. 1.4 the sets refer to a particular exclusivity graph G, whereas in Fig. 1.1 the depicted sets of correlations are general, in the sense that they do not refer to a particular exclusivity graph G, but to every possible correlations of each type: local, quantum, no-signaling or general.

1.4.6 Suggested developments and connections to our work

As the authors point out, Results 1 and 2 in Ref. [7] would allow to design experiments with quantum contextuality on demand by selecting graphs with the desired relationships between

[23] The relation of set-inclusion among these sets may be strict or not, depending on the graph G. A direct example: consider a perfect graph, i.e., a graph which does not contain, as induced subgraph, any cycle or complement of a cycle with an odd number of vertices equal or greater than five. Then, $\mathrm{STAB}(G) = \mathrm{TH}(G)$. In fact, it is proven in Ref. [69] that $\mathrm{STAB}(G) = \mathrm{TH}(G)$ if and only if G is a perfect graph.

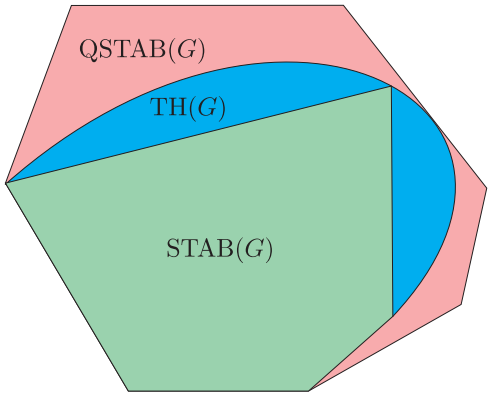

Figure 1.4: Schematic representation of the set-inclusion relationship among the theta body TH(G), which is in general a convex set but not a polytope, and the stable set and fractional stable set polytopes, STAB(G) and QSTAB(G). Note that the set-inclusion relationship among these three sets may or may not be strict, depending on the combinatorial numbers characteristic of the graph G.

$\alpha(G)$, $\vartheta(G)$ and $\alpha^*(G)$, graphs for which a general method to construct NC inequalities is provided.

As we emphasize in Chap. 2, *any* experiment producing quantum contextual correlations can be associated to an exclusivity graph G for which $\alpha(G) < \vartheta(G)$. A graph with this property is called there a *quantum contextual* graph (QCG), whereas one fulfilling $\alpha(G) = \vartheta(G)$ is called a *quantum noncontextual* graph (QNCG). According to Ref. [7], specifically, for every QCG there is a NC inequality with classical limit given by $\alpha(G)$ and quantum violation given by $\vartheta(G)$.

In addition, making use of Results 1 and 2 in Ref. [7], a question such as which are the correlations with maximum quantum contextuality can now be addressed, since it can be related to the question of which graphs have the maximum ratio $\vartheta(G)/\alpha(G)$ for a given number of vertices. Similarly, all possible forms of quantum contextuality can be classified by classifying graphs according to their combinatorial numbers.

We tackle the above-mentioned proposals in Sect. 1.5: a complete classification of QCGs up to 10 vertices is provided, which allows to identify experimental scenarios with correlations on demand by picking out graphs with the required properties, and classify quantum correlations through the study of their graph combinatorial numbers.

On the other hand, for every G such that $\alpha(G) < \vartheta(G) = \alpha^*(G)$, there is a NC inequality in which the maximum quantum violation cannot be higher without violating the E principle (Ref. [7]). In Chap. 3 we refer to quantum correlations achieving $\alpha^*(G)$ as quantum *fully contextual* correlations. Accordingly, we can denominate such a graph as quantum fully contextual graph (QFCG). Finding the simplest QFCGs is possible once a classification of QCGs with respect to their combinatorial numbers is at disposal, by selecting the graphs fulfilling the desired constraints. In Sect. 1.5 we identify the four simplest QFCGs on the basis of our classification.

Moreover, in Chap. 3 we single out the QFCG for which the violation of the associated NC inequality requires a physical system of lower dimension, and describe the experiment testing such NC inequality and revealing experimental fully contextual quantum correlations for the first time.

Finally, Result 2 in Ref. [7] suggests that an important question for understanding quantum correlations is which is the principle that singles out $\mathrm{TH}(G)$ among all possible sets of probabilities that can be assigned to the vertices of G. A way to consider such question is to understand why QT only violates some NC inequalities, and to elucidate what physical principles prevent higher-than-quantum violations. The E principle has recently revealed as one promising candidate to accomplish the goal in Refs. [77, 19, 20, 21]. Our contribution in Ref. [78] to this fundamental problem is the subject of Chap. 2: we prove that QT only violates those NC inequalities whose exclusivity graphs contain, as induced subgraphs, odd cycles of length five or more, and/or their complements. In addition, we show that odd cycles are the exclusivity graphs of a well-known family of NC inequalities and that there is also a family of NC inequalities whose exclusivity graphs are the complements of odd cycles. We characterize the maximum non-contextual and quantum values of these inequalities, and provide evidence supporting the conjecture that the maximum quantum violation of these inequalities is exactly singled out by the E principle.

1.5 Classification of contextual exclusivity graphs

As we have asserted in the previous section, quantum contextuality is experimentally observed through the violation of NC inequalities. For each NC inequality $S(G)$ formulated in terms of a positive linear combination of probabilities of events there is an associated exclusivity graph G whose independence, Lovász and fractional packing numbers provide the limits of correlations in NCHV theories, QT and theories satisfying the E principle, respectively. By virtue of this graph-theoretic approach, the problem of singling out all NC inequalities with a quantum violation becomes equivalent to the problem of identifying all QCGs, i.e., those graphs for which $\alpha(G) < \vartheta(G)$. A classification of QCGs is, therefore, a powerful tool to identify experiments of physical relevance.

We addressed the elaboration of a classification of QCGs according to their combinatorial numbers $\alpha(G)$, $\vartheta(G)$ and $\alpha^*(G)$. For that purpose, we generated all non-isomorphic simple connected graphs with less than 11 vertices using `nauty`, Ref. [79]. There are 11989764 of them. For each of them we calculated $\alpha(G)$ using `Mathematica` (Ref. [80]) and $\vartheta(G)$ using `SeDuMi` (Ref. [81]) and `DSDP` (Refs. [82, 83]). There are 992398 graphs for which $\alpha(G) < \vartheta(G)$. Then, we calculated $\alpha^*(G)$ using `Mathematica` from the clique-vertex incidence matrix of G obtained from the adjacency matrix of G using `MACE` (Refs. [84, 85]), an algorithm for enumerating all maximal cliques.

In addition, we obtained the minimum dimensionality $d(G)$ of the quantum system in which the maximum quantum violation of $S(G)$ occurs, or a lower bound of $d(G)$, by identifying subgraphs in G which are geometrically impossible in a space of lower dimensionality. For example, the simplest impossible graph in dimension $d = 1$ consists of two non-adjacent vertices; in $d = 2$, three vertices, one of them adjacent to the other two. From these two impossible graphs,

one can recursively construct impossible graphs in any dimension d by adding two vertices linked to all vertices of an impossible graph in $d-2$. For example, if a graph contains a square (a 4-cycle), then $d > 3$.[24]

This procedure results in a list containing G, $\alpha(G)$, $\vartheta(G)$, $\alpha^*(G)$ and $d(G)$ [or a lower bound of $d(G)$]. From this list we filtered out those graphs for which $\alpha(G) = \vartheta(G)$, i.e., QNCGs, and kept the remaining graphs (i.e., the QCGs).

In order to organize the resulting information, we also calculated the minimum dimensionality of a classical system reproducing the exclusivity relationships among events in $S(G)$, i.e., the adjacency relationships in G. Such number is given by a property of G known in graph theory as the *intersection number*[25] (Ref. [86]) of the complement of G, $i(\overline{G})$. For that calculation we employed a program based on `nauty`, `very-nauty` (Refs. [87, 88]). Then, we introduced a measure of quantumness, given by

$$\mathcal{Q}(G) = \frac{\vartheta(G) - \alpha(G)}{i(\overline{G})}, \tag{1.36}$$

and a measure of how close the maximun quantum value is from the largest violation allowed by theories satisfying E1, namely,

$$\mathcal{E}(G) = \frac{\alpha^*(G) - \vartheta(G)}{i(\overline{G})}. \tag{1.37}$$

We then ordered the QCGs attending to the following criteria: (i) $n(G) = |V(G)|$, (ii) $\mathcal{Q}(G)$, (iii) (decreasing) $\mathcal{E}(G)$, (iv) $d(G)$, (v) $|E(G)|$ (number of edges of G), (vi) size of the largest clique (subset of pairwise connected vertices), and (vii) number of cliques with the largest size.

1.5.1 Results

An ordered list containing G, $\alpha(G)$, $\vartheta(G)$, and $\alpha^*(G)$ for all graphs with less than 11 vertices for which $\alpha(G) < \vartheta(G)$ is provided in Ref. [8]. In Table 1.1, we present the total number of non-isomorphic simple connected graphs for a number of vertices ranging from 2 to 10; the number of them which are QCGs [$\alpha(G) < \vartheta(G)$], and for the latter, the number of those which are QFCGs [$\alpha(G) < \vartheta(G) = \alpha^*(G)$]. We can extract some conclusions:

On one hand, there are no QCGs with a number of vertices less than 5. In Fig. 1.5 we present a sample with the 37 simplest QCGs, those corresponding to a number of vertices ranging from 5 to 7, along with data corresponding to the values of $\alpha(G)$, $\vartheta(G)$, $d(G)$ or a lower bound of it (in parentheses), and $\alpha^*(G)$, for each graph G. The simplest QCG is the pentagon or 5-cycle, C_5, depicted in red in Fig. 1.5, which is the exclusivity graph corresponding to the Wright and Klyachko-Can-Binicioğlu-Shumovsky NC inequalities in Refs. [49, 74]. A careful inspection of the figure reveals that all the graphs shown in it contain C_5 as induced subgraph, with the exception of two: the heptagon (C_7) and its complement ($\overline{C_7}$), both also depicted in red. This three graphs belong to a well-known family in graph theory: the so-called *odd holes* and *odd*

[24] See 2.4 for an application of this argument to the complements of odd cycles. In brief, the graph F obtained by deleting $\lfloor d/2 \rfloor$ disjoint edges from a d-vertex complete graph K_d is an impossible subgraph in dimension $d-1$.

[25] This number is described in detail on p. 84, in a different context.

antiholes (see p. 65 for a definition, and a brief outline of their interest in graph theory). A subsequent analysis of the QCGs of up to 10 vertices, the scope of our classification, suggests that all QCGs might necessarily contain odd holes and/or odd antiholes as induced subgraphs (Ref. [78]). The deep insight encompassed by this fact is the main thrust of Chap. 2, where we deal with this issue in detail, and give the corresponding proof.

Table 1.1: Number of non-isomorphic simple connected graphs, QCGs and QFCGs with a number of vertices up to 10.

Vertices	Connected graphs	QCGs	QFCGs
< 5	10	0	0
5	21	1	0
6	112	3	0
7	853	33	0
8	11117	498	0
9	261080	16533	0
10	11716571	975330	4

On the other hand, there is no QFCG with less than 10 vertices. The simplest ones are the four 10-vertex graphs depicted in Fig. 1.6. Given that for such graphs $\alpha(G) < \vartheta(G) = \alpha^*(G)$, there is an NC inequality associated to each of them in which the maximum quantum violation cannot be higher without violating the E principle. Achieving such maximum quantum violation would reveal, therefore, fully contextual quantum correlations. Graph (c) in Fig. 1.6, which we shall call S_3, is the graph corresponding to the simplest NC inequality capable of revealing fully contextual quantum correlations, from the viewpoint of the dimensionality of the required quantum system (see Ref. [89]). Graph (d) in Fig. 1.6 is the Johnson graph $J(5, 2)$, which is the complement of the Petersen graph (a well-known graph in the field of graph theory; see Fig. 4.3 (b)). $J(5, 2)$ is the exclusivity graph corresponding to Cabello's twin-inequality in Ref. [90], which is the simplest NC inequality capable of revealing fully contextual quantum correlations, from the viewpoint of the number of experiments (involving yes-no tests) needed. Graphs (a) and (b) are essentially as graph (c) minus one or two edges, and do not outperform (c) nor (d) regarding the number of experiments needed or the dimensionality of the quantum system required. Graph S_3 and its corresponding NC inequality, and the experiment revealing fully contextual quantum correlations on the basis of them, is the main issue of Chap. 3, to which we refer the reader for further details.

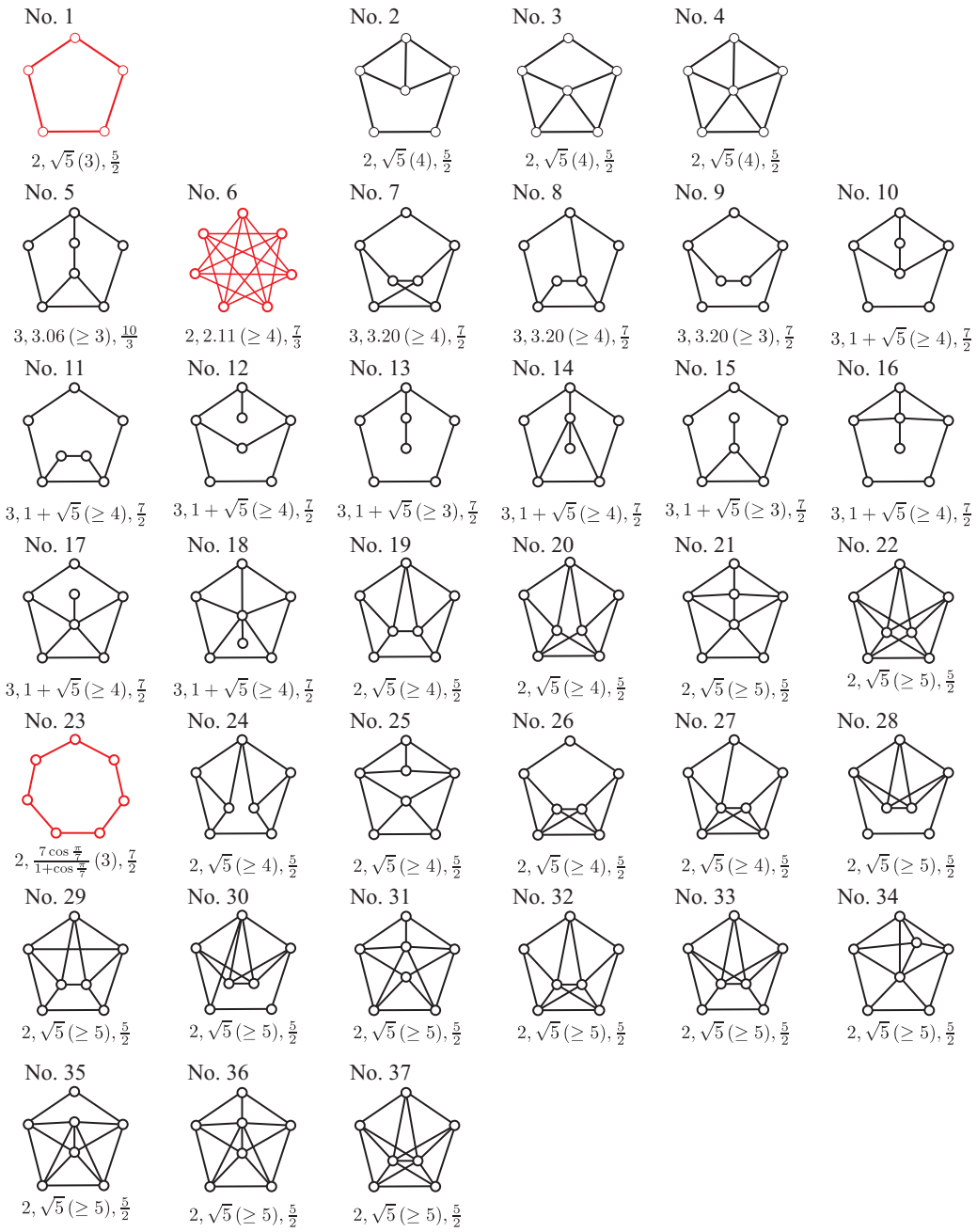

Figure 1.5: Quantum contextual graphs up to 7 vertices. In red, the pentagon or 5-cycle, C_5; the heptagon or 7-cycle, C_7; and the complement of the heptagon, $\overline{C_7}$.

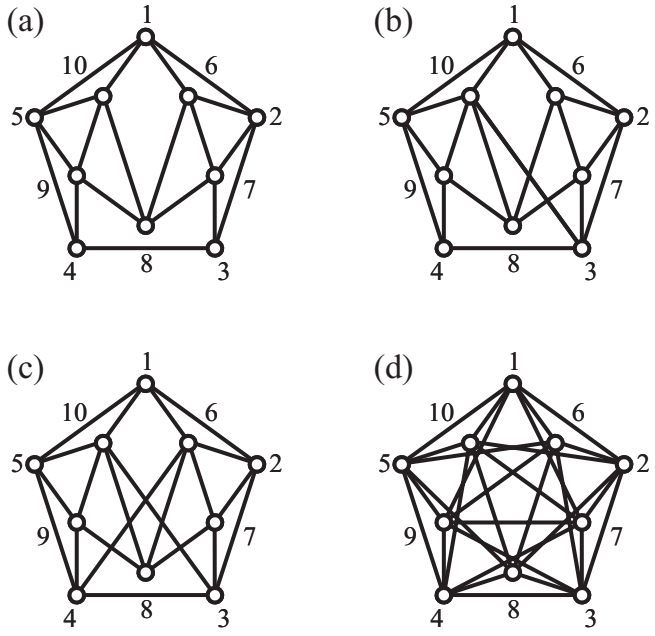

Figure 1.6: The four simplest quantum fully contextual graphs. Graph (c) is S_3 (see main text). Graphs (a) and (b) are the same as (c), minus one or two edges. Graph (d) is the Johnson graph $J(5, 2)$, which is the complement of the Petersen graph.

Chapter 2

Basic exclusivity graphs in quantum correlations

In this chapter we present the results obtained in Ref. [78]. Below we provide a brief summary.

Summary: A fundamental problem is to understand why quantum theory only violates some NC inequalities and identify the physical principles that prevent higher-than-quantum violations. We prove that quantum theory only violates those NC inequalities whose exclusivity graphs contain, as induced subgraphs, odd cycles of length five or more, and/or their complements. In addition, we show that odd cycles are the exclusivity graphs of a well-known family of NC inequalities and that there is also a family of NC inequalities whose exclusivity graphs are the complements of odd cycles. We characterize the maximum non-contextual and quantum values of these inequalities, and provide evidence supporting the conjecture that the maximum quantum violation of these inequalities is exactly singled out by the E principle.

2.1 Introduction

Quantum contextuality[1], namely, the fact that the quantum correlations between the results of compatible measurements cannot be reproduced with NCHV theories (Refs. [17, 29, 30]) is behind a wide spectrum of applications of QT to communication and computation (Refs. [91, 42, 92, 41, 93, 45]). Quantum contextual correlations are experimentally detected through the violation of inequalities satisfied by NCHV models, called NC inequalities (Refs. [94, 74, 95, 96]). A fundamental problem is to understand why QT only violates some NC inequalities and identify the physical principles that prevent higher-than-quantum violations of these inequalities (Refs. [61, 62, 97, 19]).

In this chapter we investigate this problem. We will use, as a main tool throughout the chapter, the exclusivity graph of an NC inequality which was already introduced in Sect. 1.4.2. In Sect. 2.3, we present a necessary condition for the existence of quantum contextual correlations: We prove that QT violates only those NC inequalities whose exclusivity graphs contain, as

[1] See Sect. 1.3 for a accurate definitions of quantum contextuality and NC inequalities.

induced subgraphs, odd cycles on five or more vertices and/or their complements. In Sect. 2.4, we show that a lower bound of the dimension (i.e., of the number of perfectly distinguishable states) of the quantum system that is used to violate an NC inequality can be obtained by identifying induced basic exclusivity subgraphs in the exclusivity graph of the NC inequality.

The result in Sect. 2.3 suggests that NC inequalities whose exclusivity graph is either an odd cycle or its complement are especially important for understanding the way QT violates NC inequalities. In Sect. 2.5, we show that each of these types of exclusivity graphs is connected to a family of NC inequalities and provide the quantum states and measurements leading to the maximum quantum violation. Finally, in Sect. 2.6 we present some results that suggest that the E principle, namely, that the sum of the probabilities of a set of pairwise exclusive events cannot exceed 1, explains the maximum quantum violation of all the NC inequalities discussed in Sect. 2.5.

2.2 The exclusivity graph of a non-contextuality inequality

As we pointed out in some detail in Sect. 1.4.2, the correlations in any NC inequality can be expressed as a linear combination of probabilities of a subset of events of the corresponding experiment. The fact that the sum of probabilities of outcomes of a test is 1 (normalization condition) allows us to express these correlations as a *positive* linear combination S of probabilities of events e_i, that is, $S = \sum_i w_i p(e_i)$, with $w_i > 0$. The exclusivity graph G of the NC inequality S is the one in which the vertices represent the events and adjacent vertices represent mutually exclusive events (Refs. [6, 7]).

The interest of the exclusivity graph G is that the maximum value of S for NCHV theories is exactly given by the independence number of the graph $\alpha(G)$ (which is the maximum number of pairwise nonadjacent vertices in G), while the maximum value in QT is upper bounded (and frequently exactly given) by the Lovász number of the graph $\vartheta(G)$ (Refs. [6, 7]). We refer the reader to Sect. 1.4.4 for definitions and a precise formulation of this fact.

The important point is that *any* experiment producing quantum contextual correlations can be associated to an exclusivity graph G for which $\alpha(G) < \vartheta(G)$. Hereafter, as we previously have done in Sect. 1.4.6, we will refer to a graph with this property as a quantum contextual graph (abbreviated QCG), and to a graph for which $\alpha(G) = \vartheta(G)$ as a quantum non-contextual graph (abbreviated QNCG). We provide a classification of all QCGs up to 10 vertices in Sect. 1.5.

2.3 Basic exclusivity graphs

The following definition is necessary to present out first result: A subgraph H of a graph G is said to be *induced* if, for any pair of vertices i and j of H, ij is an edge of H if and only if ij is an edge of G. For example, a graph G has an induced pentagon if it is possible to remove from G all but five vertices (and their corresponding edges) so that we end up with a pentagon with no additional edges.

Result 1: The exclusivity graph of any NC inequality violated by QT contains, as induced subgraphs, odd cycles on five or more vertices and/or their complements.

This result[2] is based on two fundamental results in graph theory: The strong perfect graph theorem and the (weak) perfect graph theorem. Perfect graphs were introduced in Ref. [98] in connection to the problem of the zero-error capacity of a noisy channel in Ref. [68]: Shannon observed that $\omega(G^{*n}) = \omega(G)^n$ for graphs such that $\omega(G) = \chi(G)$, which made the problem of characterizing the Shannon capacity of such graphs more tractable [G^{*n} is the disjunctive product[3] of n copies of G, $\omega(G)$ is the clique number, and $\chi(G)$ is the chromatic number of G; in general, $\omega(G) \leq \chi(G)$]. Berge defined perfect graphs as those graphs G for which $\omega(H) = \chi(H)$ for each induced subgraph $H \subseteq G$. Berge observed that all odd cycles C_n with $n \geq 5$ (known in graph theory as "odd holes") and their complements $\overline{C_n}$ (known as "odd antiholes") satisfy $\omega(G) < \chi(G)$. From this result, Berge conjectured that a graph G is perfect if and only if G has no odd hole or odd antihole as induced subgraph (strong perfect graph conjecture). This conjecture has been recently proven in Ref. [100], and it is now known as the strong perfect graph theorem. The simplest odd holes and antiholes are illustrated in Fig. 2.1.

The perfect graph conjecture (due also to Berge), which was later proved by Lovász in Ref. [101] and is now known as the (weak) perfect graph theorem, states that if G is a perfect graph, then its complement, $\overline{G}$, is also a perfect graph.

Theorem 1: Let G be the exclusivity graph of an NC inequality. If G is a perfect graph, then G is a QNCG and, as a consequence, the NC inequality is not violated by QT.

Proof: If G is perfect, then $\omega(G) = \chi(G)$. On the other hand, according to the sandwich theorem in Ref. [102], $\omega(G) \leq \vartheta(\overline{G}) \leq \chi(G)$ for any graph G. Hence, G perfect implies $\omega(G) = \vartheta(\overline{G}) = \chi(G)$. Given that $\omega(G) = \alpha(\overline{G})$, we obtain $\alpha(\overline{G}) = \vartheta(\overline{G})$, i.e., if G is a perfect graph, then $\overline{G}$ is a QNCG. Applying now the (weak) perfect graph theorem, if G is perfect, then $\overline{G}$ is also perfect. Therefore, repeating the previous argument the other way around we conclude that G is a QNCG as well: $\alpha(G) = \vartheta(G)$. This finishes the proof. ■

Corollary 1: If G is a QCG, i.e., if G is the exclusivity graph of an NC inequality violated by QT, then G is *not* perfect. Consequently, by the strong perfect graph theorem, G must contain odd holes and/or odd antiholes as induced subgraphs.

This proves Result 1.

Observation 1: A NC inequality not violated by QT may contain an NC inequality violated by QT. This means that, even if the exclusivity graph of the initial NC inequality is not a QCG, the exclusivity graph of the initial NC inequality may have an induced subgraph that is a QCG.

Observation 2: No odd cycle or complement of an odd cycle has an odd cycle or a complement of an odd cycle as an induced subgraph. This suggests that odd cycles and their complements could be used as a basis for a decomposition of any exclusivity graph.

Observation 3: The basic exclusivity graphs necessary for quantum contextuality are the same basic graphs necessary for graph nonperfectness.

[2] One of the conclusions in Sect. 1.5.1, derived on the basis of the classification of QCGs, is directly connected to Result 1.

[3] The disjunctive product of graphs, also known as OR product or co-normal product, is defined as follows: given two graphs $G = (V(G), E(G))$ and $H = (V(H), E(H))$, the OR product $G * H$ is a graph such that (i) the vertex set of $G * H$ is the Cartesian product $W = V(G) \times V(H)$; and (ii) any two distinct vertices $(u, u') \in W$ and $(v, v') \in W$ are adjacent in $G * H$ if and only if u is adjacent to v in G, or u' is adjacent to v' in H. The OR product is the complementary product of the well-known strong (normal or AND) product $\otimes$, and hence their mutual relationship is $G * H = \overline{(\overline{G} \otimes \overline{H})}$. We refer the reader interested in a comprehensive overview about associative products of graphs to Ref. [99].

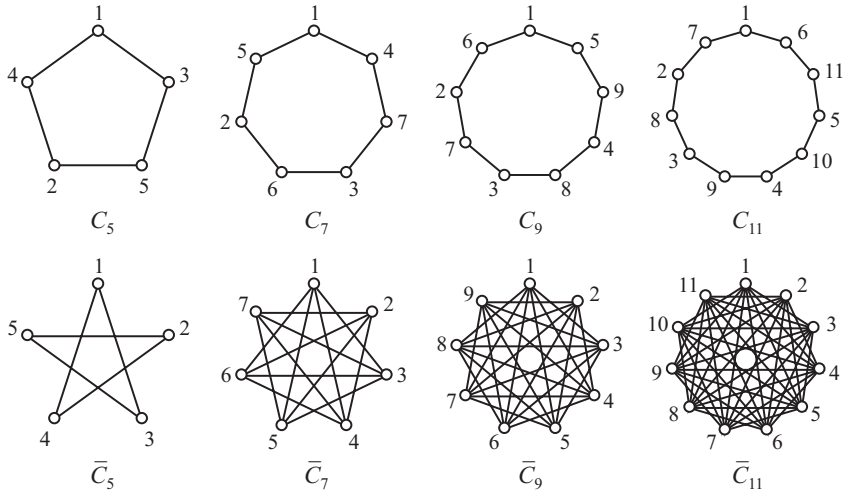

Figure 2.1: C_j denote the odd cycles on j vertices and $\overline{C_j}$ their complements. The figure depicts the cases $j = 5, 7, 9, 11$. Notice that C_5 and $\overline{C_5}$ are isomorphic.

Proof: A graph G is called almost perfect (Refs. [103, 104]) if there exists at least one vertex $v \in V(G)$ such that the graph $G - v$ obtained by deleting v (and its incident edges) is perfect. Trivially, every perfect graph is almost perfect. There are many nonperfect graphs which are almost perfect. The interesting point is that there are nonperfect graphs for which the deletion of *any* vertex gives rise to a perfect graph: A graph G is minimal (or minimally) imperfect if it is not perfect but *every* induced subgraph $H \subset G$ is perfect [i.e., $\omega(G) < \chi(G)$ but $\omega(H) = \chi(H), \forall H \subset G$, H induced]. Note that, as a consequence of the strong perfect graph theorem, any nonperfect graph is either an odd hole or an odd antihole, or must contain such odd holes and/or odd antiholes as induced subgraphs. Hence, the *only* minimal imperfect graphs are the odd holes and odd antiholes. Moreover, given that every induced subgraph $H \subset G_m$ of a minimal imperfect graph G_m is perfect, then the deletion of an arbitrary vertex $v \in V(G_m)$ produces an induced subgraph of G_m which is a perfect graph (Ref. [105]). Therefore, minimal imperfect graphs are not only almost perfect but the only almost-perfect graphs for which almost perfectness does not depend on the vertex choice. That is why odd holes and antiholes are the necessary basic graphs for nonperfectness: Starting from an arbitrary nonperfect graph, and deleting vertex by vertex trying to preserve nonperfectness in the subsequent resulting induced subgraphs, eventually leads to a minimal imperfect graph. Since minimal imperfect graphs are also QCGs and all QCGs are nonperfect (Corollary 1), then minimal imperfect graphs are the simplest ones giving rise to quantum contextuality. ■

2.4 Basic exclusivity graphs and the dimension of the quantum system

A distinguishing feature of the complements of the odd cycles is that their presence as induced subgraphs in an exclusivity graph G provides valuable information about the minimum dimension that a quantum system must have in order to generate events reproducing all the relationships of exclusivity described by G. While any of the relationships of exclusivity in an odd cycle can be reproduced using a quantum three-dimensional system, this is impossible for the relationships of exclusivity described by the complement of an odd cycle with $n \geq 7$ vertices.

Result 2: If an exclusivity graph corresponding to an NC inequality has as an induced subgraph a complement of an odd cycle on $n \geq 5$ vertices, then the quantum dimension of the systems whose events reproduce these exclusivity relationships is, at least, $\lfloor 2n/3 \rfloor$.

Proof: A (faithful) OR of $\overline{G}$ is an assignment of unit vectors $\{|v_j\rangle\}_{j=1}^{n}$ to the vertices of G such that orthogonal vectors are assigned to the vertices (iff) if they are adjacent.[4] Vectors $\{|v_j\rangle\}_{j=1}^{n}$ represent the states of the system after the corresponding events; vectors are orthogonal if (iff) events are exclusive.

Let G be an exclusivity graph containing an odd antihole $\overline{C_n}$ as induced subgraph. To obtain a lower bound of the dimension d of the quantum system producing events whose exclusivity relationships are described exactly by G, we can study the constraints imposed by the presence of $\overline{C_n}$. Note that for any two different vertices $u, v \in \overline{C_n}$, $N(u) \neq N(v)$, where $N(i)$ denotes the neighborhood of vertex i (see Fig. 2.1). This implies that a faithful OR of $\overline{G}$ must assign different vectors to u and v. As a consequence, we can lower bound d by identifying subgraphs in $\overline{C_n}$ which are geometrically impossible in a space of lower dimension, assuming that distinct vertices are assigned distinct vectors. For example, the simplest impossible graph in $d = 1$ consists of two nonadjacent vertices in $\overline{C_n}$; in $d = 2$, three vertices, one of them adjacent to the other two. From these two impossible graphs, one can recursively construct impossible graphs in any d by adding two vertices adjacent to all vertices of an impossible graph in $d - 2$. For example, if $\overline{C_n}$ contains a square, then $d > 3$. In brief, the graph F obtained by deleting $\lfloor d/2 \rfloor$ disjoint edges from a d-vertex complete graph K_d is an impossible subgraph in dimension $d - 1$ of $\overline{C_n}$.

To lower bound d, we must consider three cases: (C1) If $n = 3m, m \in \mathbb{N}$, take the subgraph F induced in $\overline{C_n}$ by vertices $\{1, 2, 4, 5, \ldots, 3i + 1, 3i + 2, \ldots, 3(m - 1) + 1, 3(m - 1) + 2\}$ (see Fig. 2.1). F is isomorphic to K_{2m} minus m disjoint edges and is, therefore, an impossible graph in $d = 2m - 1$. Hence, $\overline{C_n}$ is not faithfully representable in $d = 2m - 1 = \frac{2n}{3} - 1 = \lfloor 2n/3 \rfloor$-1. The same holds true for $G \supseteq \overline{C_n}$. (C2) If $n = 3m + 1, m \in \mathbb{N}$, take the subgraph F induced in $\overline{C_n}$ by vertices $\{1, 2, 4, 5, \ldots, 3i + 1, 3i + 2, \ldots, 3(m - 1) + 1, 3(m - 1) + 2\}$. F is isomorphic to K_{2m} minus m disjoint edges and is, therefore, an impossible graph in $d = 2m - 1$. Hence, $\overline{C_n}$ is not faithfully representable in $d = 2m - 1 = \frac{2n-1}{3} - 1 = \lfloor 2n/3 \rfloor$-1. The same holds true for $G \supseteq \overline{C_n}$. (C3) If $n = 3m + 2, m \in \mathbb{N}$, take the subgraph F induced in $\overline{C_n}$ by vertices $\{1, 2, 4, 5, \ldots, 3i + 1, 3i + 2, \ldots, 3(m - 1) + 1, 3(m - 1) + 2, 3m + 1\}$. F is isomorphic to K_{2m+1} minus m disjoint edges and, therefore, it is an impossible graph in $d = 2m$. Hence, $\overline{C_n}$ is not faithfully representable in $d = 2m = \frac{2(n-2)}{3} = \lfloor 2n/3 \rfloor$-1. The same holds true for $G \supseteq \overline{C_n}$. ■

[4] See definition of orthonormal representation of a graph G on p. 54.

2.5 NC inequalities represented by basic exclusivity graphs

Result 3: For any cycle C_n with n odd ≥ 5, there is an NC inequality such that

$$S(C_n) \overset{\text{NCHV}}{\leq} \alpha(C_n) \overset{\text{Q}}{\leq} \vartheta(C_n), \tag{2.1}$$

where $S(C_n)$ is a sum of probabilities of events matching the relationships of exclusivity represented by C_n, $\overset{\text{Q}}{\leq} \vartheta(C_n)$ indicates that its maximum value in QT is *exactly* $\vartheta(C_n)$, and

$$\alpha(C_n) = \frac{n-1}{2}, \tag{2.2a}$$

$$\vartheta(C_n) = \frac{n\cos\left(\frac{\pi}{n}\right)}{1+\cos\left(\frac{\pi}{n}\right)} \tag{2.2b}$$

are, respectively, the independence number and the Lovász number of C_n.

Proof. By explicit construction. For any n odd ≥ 5, the events in the following sum of probabilities of events:

$$S(C_n) = \sum_{i=1}^{n} P(1,0|i, i+\left[\frac{n}{2}\right]), \tag{2.3}$$

where the sum in each event is taken modulo n, and numerating[5] the vertices of C_n as in Fig. 2.1, have exactly the relationships of exclusivity represented by C_n.

The fact that the maximum value of $S(C_n)$ for NCHV theories is $\alpha(C_n)$ is proven in Ref. [6]. The fact that $\vartheta(C_n)$ is not only an upper bound of the maximum quantum value, but a value that QT actually reaches can be seen by preparing the system in the quantum state

$$\langle\psi| = (1,0,0) \tag{2.4}$$

and measuring the observables represented by

$$j = |v_j\rangle\langle v_j|, \tag{2.5}$$

where

$$\langle v_j| = \left[\cos\phi, \sin\phi\cos\left(\frac{2\pi j}{n}\right), \sin\phi\sin\left(\frac{2\pi j}{n}\right)\right], \tag{2.6}$$

with $j = 1,\ldots,n$, $\cos^2\phi = \frac{\vartheta(C_n)}{n}$. ∎

The vectors (2.6) constitute a Lovász-optimum OR of C_n. An OR is Lovász optimum if there is a unit vector $|\psi\rangle$, called handle, such that $\sum_{j=1}^{n} |\langle v_j|\psi\rangle|^2 = \vartheta(G)$. In our case, the handle is given by Eq. (2.4).

Result 4: For any complement of a cycle $\overline{C_n}$ with n odd ≥ 5, there is an NC inequality such that

$$S(\overline{C_n}) \overset{\text{NCHV}}{\leq} \alpha(\overline{C_n}) \overset{\text{Q}}{\leq} \vartheta(\overline{C_n}), \tag{2.7}$$

[5]Note that we have chosen this labelling of the events in (2.3) and vertices in Fig. 2.1 in order to match the compact expression of the vectors (2.6). Needless to say, other labellings are possible, giving rise to different ways to write the NC inequality (2.3). The same can be said about odd antiholes.

where

$$\alpha(\overline{C_n}) = 2, \tag{2.8a}$$

$$\vartheta(\overline{C_n}) = \frac{1+\cos\left(\frac{\pi}{n}\right)}{\cos\left(\frac{\pi}{n}\right)}. \tag{2.8b}$$

Proof. For $n = 5$, the proof of Result 3 is valid, since C_5 and $\overline{C_5}$ are isomorphic. For any n odd ≥ 7, the events in the following sum of probabilities of events:

$$S(\overline{C_n}) = \sum_{i=1}^{n} P(1, 0, \ldots, 0 | i, i+2, \ldots, i+n-3), \tag{2.9}$$

where the sum in each event is taken modulo n, and numerating the vertices of $\overline{C_n}$ as in Fig. 2.1, have all the relationships of exclusivity represented by $\overline{C_n}$.

The fact that the maximum value of $S(\overline{C_n})$ for NCHV theories is $\alpha(\overline{C_n})$ is proven in Ref. [6]. The fact that $\vartheta(\overline{C_n})$ is not only an upper bound of the maximum quantum value, but a value that QT actually reaches can be seen by preparing the system in the quantum state

$$\langle\psi| = (1, 0, \ldots, 0), \tag{2.10}$$

and measuring the observables represented by

$$j = |v_j\rangle\langle v_j|, \tag{2.11}$$

where the k-th component of $\langle v_j|$, denoted as $v_{j,k}$, with[6] $0 \leq j \leq n-1$ and $0 \leq k \leq n-3$, is given by

$$v_{j,0} = \sqrt{\frac{\vartheta(\overline{C_n})}{n}}, \tag{2.12a}$$

$$v_{j,2m-1} = T_{j,m} \cos\left(R_{j,m}\right), \tag{2.12b}$$

$$v_{j,2m} = T_{j,m} \sin\left(R_{j,m}\right), \tag{2.12c}$$

where $m = 1, 2, \ldots, \frac{n-3}{2}$ and

$$T_{j,m} = (-1)^{j(m+1)} \sqrt{\frac{2\left(\cos\left(\frac{\pi}{n}\right) + (-1)^{m+1} \cos\left[\frac{(m+1)\pi}{n}\right]\right)}{n\cos\left(\frac{\pi}{n}\right)}}, \tag{2.13a}$$

$$R_{j,m} = \frac{j(m+1)\pi}{n}. \tag{2.13b}$$

■

[6] Note that here, for the sake of convenience, we relabel the observables (2.11) in such a way that, for the complements of odd cycles, $j = |v_j\rangle\langle v_j|$ corresponds to vertex $i = j + 1$ in Fig. 2.1.

The vectors defined by Eqs. (2.12) and (2.13) constitute a Lovász-optimum OR[7] of $\overline{C_n}$ with handle given by Eq. (2.10).

Note that, for every NC inequality presented in this section, the compatibility graph of the observables is isomorphic to the exclusivity graph of the events. This follows from the fact that every observable in these NC inequalities is of the form (2.5) and every event is of the type $1, 0, \ldots, 0|i, j, \ldots, z$.

2.6 The exclusivity principle enforces the quantum violation of the NC inequalities represented by basic exclusivity graphs

It has been recently proved that the principle that the sum of probabilities of a set of pairwise exclusive events cannot be higher than 1 (Refs. [17, 6, 49, 18, 19, 65, 107, 77]), i.e., the E principle (see 1.1.6 for details), exactly singles out the maximum quantum value for the NC inequality associated to C_5 (see Ref. [19]). The LO principle in Ref. [65] may be seen as the E principle restricted to Bell scenarios (Ref. [107]). Note, however, that while for a given graph G, there

[7] After some algebraic manipulations, these general expressions for Lovász-optimum ORs of odd antiholes can be expressed in a much more compact way. For instance, taking the graph $\overline{C_7}$, and for the same labeling of the vertices as in Fig. 2.1, and handle $\langle\psi| = (1, 0, 0, 0, 0)$, one can obtain for $k = 1, \ldots, 7$ that

$$|w_k\rangle = \begin{pmatrix} \cos(\phi_1) \\ \sin(\phi_1)\cos(\phi_2)\cos(\phi_3) \\ \sin(\phi_1)\cos(\phi_2)\sin(\phi_3) \\ \sin(\phi_1)\sin(\phi_2)\cos(\phi_4) \\ \sin(\phi_1)\sin(\phi_2)\sin(\phi_4) \end{pmatrix}, \tag{2.14}$$

with

$$\cos(\phi_1) = \sqrt{\frac{1+\cos(\pi/7)}{7\cos(\pi/7)}}, \tag{2.15a}$$

$$\cos(\phi_2) = 2\sin(\pi/7)\sqrt{\frac{2\cos(\pi/7)}{-1+6\cos(\pi/7)}}, \tag{2.15b}$$

$$\phi_3 = \frac{2\pi 2k}{7}, \tag{2.15c}$$

$$\phi_4 = \frac{2\pi k}{7}. \tag{2.15d}$$

Interestingly, this kind of compact expression for the Lovász-optimum OR of $\overline{C_7}$ is related to the fact that this graph is what is known in graph theory as a 2-factorable graph: a *factor* or *spanning subgraph* of a graph G is a subgraph of G with the same vertex set as G. A k-factor of G is a k-regular factor, and a k-factorization partitions the edges of the graph G into disjoint k-factors. Note that a 2-factor is always a spanning cycle (or a collection of disjoint cycles that spans the vertex set of G), so that a 2-factorization is a factorization of G in disjoint cycles. It turns out that $\overline{C_7}$ can be 2-factorized into two disjoint factors isomorphic to C_7, each of which span the entire set of vertices, and such that the two of them collectively exhaust the set of edges. Examining and comparing (2.14) with (2.6), we can interpret that the compact expression for the Lovász-optimum OR of $\overline{C_7}$ in dimension 5 is constructed from two interwoven Lovász-optimum ORs of C_7, each of which spans a subspace of dimension 3. This 2-factorization property is a common feature of odd antiholes, which comes from a necessary and sufficient condition found by Julius Petersen in 1891 (Ref. [106]), according to which, for k integer, any 2k-regular graph is 2-factorable. As a consequence, the same idea applies to odd antiholes of higher orders.

is always an NC inequality for which QT reaches $\vartheta(G)$ (Refs. [6, 7]), this is not true if "NC inequality" is replaced by "Bell inequality", as in Ref. [27] (see 1.4.5).

A natural question, especially important in the light of Result 1, is whether the E principle may single out the maximum quantum value for the NC inequalities associated to C_n and $\overline{C_n}$ for n odd ≥ 7 presented in Sect. 2.5.

Observation 4. "[T]he evidence that the Shannon capacity of odd cycles is extremely close to the value of the Lovász theta function" (Ref. [108]) strongly suggests that the E principle singles out the maximum quantum value for the NC inequalities (2.7). This implies that the E principle also singles out the maximum quantum value for the NC inequalities (2.1). In any case, it is very unlikely that any actual experiment would allow us to distinguish nature's maximum violation (assumed to be given by QT) from the maximum value allowed by the E principle.

Proof. Ref. [6] shows that, for a given exclusivity graph G, the maximum value satisfying the E principle (applied only to one copy of G) for the sum $S(G)$ of probabilities of events whose relationships of exclusivity are represented by G is given by the fractional packing number of G, $\alpha^*(G,\Gamma)$, which is equal to $\max \sum_{i\in V(G)} w_i$, where the maximum is taken over all $0 \leq w_i \leq 1$ and for all cliques (subsets of pairwise linked vertices) $C_j \in \Gamma$, under the restriction $\sum_{i\in C_j} w_i \leq 1$ (Refs. [68, 109]). When Γ is the set of all cliques of G, then $\alpha^*(G,\Gamma)$ is also called the Rosenfeld number $p(G)$ (Ref. [110]). As shown in Ref. [19], for vertex-transitive graphs[8] (such us, e.g., C_n and $\overline{C_n}$), the maximum value of $S(G)$ satisfying the E principle applied to n copies is given by $\sqrt[n]{p(G^{*n})}$, where G is the exclusivity graph of the NC inequality. Recall that the maximum quantum value is given by $\vartheta(G)$. For C_5, $p(C_5) = \frac{5}{2}$ and $\sqrt{p(C_5 * C_5)} = \vartheta(C_5) = \sqrt{5}$, which proves that the E principle applied to two copies of C_5 singles out the maximum quantum value of $S(\overline{C_5})$. The whole process can be summarized in the following expression:

$$S(\overline{C_5}) \overset{\text{NCHV}}{\leq} 2 \overset{\text{Q, E2}}{\leq} \sqrt{5} \overset{\text{E1}}{\leq} \frac{5}{2}, \tag{2.16}$$

where $\overset{\text{NCHV}}{\leq} 2$ indicates that the maximum value for NCHV theories is 2, $\overset{\text{Q, E2}}{\leq} \sqrt{5}$ indicates that the maximum value for QT and for theories satisfying the E principle applied to two copies of C_5 is $\sqrt{5}$, and $\overset{\text{E1}}{\leq} \frac{5}{2}$ indicates that the maximum value for theories satisfying the E principle applied to one copy of C_5 is $\frac{5}{2}$.

For C_7, with $n = 1, 2, 3$, $\sqrt[n]{p(C_7^{*n})} = \frac{7}{2}$. Since $p(C_7) = \frac{7}{2}$, this means that, for C_7, the E principle applied to two or three copies of C_7 does not tell us more than the E principle applied to one copy. However, the E principle applied to four copies of C_7 leads us to a value closer to the maximum quantum one. This follows from Ref. [111], where it is proven that

$$\sqrt[4]{p(C_7^{*4})} \leq \frac{7}{\sqrt[4]{17}} \approx 3.4474. \tag{2.17}$$

The situation is similar for C_n with n odd ≥ 9: the value singled out by the E principle seems to converge to the maximum quantum one as more copies of C_n are taken into account, but there is no clear evidence that this actually happens.

[8] A graph G is vertex transitive if, given *any* two vertices v and w of G, there exists an automorphism $\psi : V(G) \longrightarrow V(G)$ such that $\psi(v) = w$, i.e., every pair of vertices of G is equivalent under some element of its automorphism group.

However, note that odd cycles are sparser than their complements. As a result, when the E principle is applied to multiple copies of complements of odd cycles, the resulting value approaches the maximum quantum one much faster. Consider, for example, $\overline{C_7}$. From Ref. [112], we obtain that

$$p(\overline{C_7}) = \frac{7}{3} > \sqrt{p(\overline{C_7}^{*2})} = \frac{7}{\sqrt{10}} > \sqrt[3]{p(\overline{C_7}^{*3})} = \frac{7}{\sqrt[3]{33}}. \tag{2.18}$$

Therefore,

$$S(\overline{C_7}) \overset{\text{NCHV}}{\leq} 2 \overset{\text{Q}}{\leq} 2.1099 \overset{\text{E3}}{\leq} 2.1824 \overset{\text{E2}}{\leq} 2.2136 \overset{\text{E1}}{\leq} 2.3333. \tag{2.19}$$

For four copies of $\overline{C_7}$, only bounds of $\omega(\overline{C_7}^{*4})$ are known (see Ref. [113]), but it is clear that the value is even closer to the maximum quantum one after considering the fourth copy, since

$$\frac{7}{\sqrt[4]{115}} \approx 2.1376 \leq \sqrt[4]{p(\overline{C_7}^{*4})} \leq \frac{7}{\sqrt[4]{108}} \approx 2.1714. \tag{2.20}$$

For five copies, the best bounds known (Ref. [113]) are also compatible with a value even closer to the maximum quantum one.

The point is that there is strong evidence (Ref. [108]) that the Shannon capacity of odd cycles, $\Theta(C_n)$, is extremely close to their Lovász number, $\vartheta(C_n)$. This is important since

$$\lim_{m\to\infty} \sqrt[m]{p(\overline{C_n}^{*m})} = \frac{n}{\lim_{m\to\infty} \sqrt[m]{\omega(\overline{C_n}^{*m})}} = \frac{n}{\Theta(C_n)} \tag{2.21}$$

(this holds because C_n and $\overline{C_n}$ are vertex transitive), which, if $\Theta(C_n) = \vartheta(C_n)$, would be equal to $\vartheta(\overline{C_n})$, which is exactly the maximum quantum value for $\overline{C_n}$.

If the E principle singles out the maximum quantum value of inequalities (2.7), then it also singles out the maximum quantum value of inequalities (2.1). To see it,[9] consider one experiment testing the inequality (2.7) for a given n, and a completely independent experiment testing the inequality (2.1) for the same n. Notice that the exclusivity graph of the events defined by taking one event of the first inequality and the corresponding event of the second inequality is the complete graph on n vertices, since the exclusivity graphs of the two inequalities are complementary. Therefore, the E principle imposes that the sum of the probabilities of the n events constructed this way cannot exceed 1. Take into account that each of these probabilities is the product of the probability of the event in the first inequality times the probability of the corresponding event in the second inequality, since the corresponding experiments are independent. Assume now that the E principle predicts that the maximum of the first inequality is $\vartheta(\overline{C_n})$ and that the maximum value of the first inequality is reached when all the probabilities are equal. Assuming that the maximum value of the second inequality is also reached when all the probabilities are equal, and recalling that $\vartheta(C_n)\vartheta(\overline{C_n}) = n$, we are led to the conclusion that the maximum value allowed by the E principle for the second inequality cannot be higher than $\vartheta(C_n)$, which is precisely the maximum value in QT. ■

[9] We refer the reader to Ref. [21], in particular Result 3 and its proof, which is directly connected to this assertion and the subsequent argument. In fact it constitutes a generalization: If G is a vertex-transitive graph on n vertices, given the quantum maximum for $\overline{G}$, the E principle singles out the quantum maximum for G.

2.7 Appendix: Basic exclusivity graphs inside the exclusivity graphs of some NC inequalities

Table 2.1 shows the number of induced basic exclusivity graphs inside some NC inequalities and Kochen-Specker (KS) proofs. The absence of induced odd antiholes may explain why the NC inequalities associated to the exclusivity graphs of type (ii) were not pointed out before. To our knowledge, the first time a type (ii) graph with $n \geq 7$ was identified as a QCG is in Ref. [8].

Table 2.1: Number of induced basic exclusivity graphs in some NC inequalities and KS proofs. The column "Graph" gives the standard name in graph theory, "Vertices" indicates its number of vertices, "Dimension" indicates the minimum dimension of the quantum system needed to define events with the corresponding exclusivity relationships.

NC inequality/KS proof	Graph	Vertices	Dimension	C_5	C_7	$\overline{C_7}$	C_9	$\overline{C_9}$
KCBS (Ref. [74])	C_5	5	3	1	0	0	0	0
CHSH (Ref. [46])	$Ci_8(1,4)$	8	4	8	0	0	0	0
S_3 (Refs. [93, 89])		10	4	10	0	0	0	0
KCBS-twin (Ref. [90])	$J(5,2)$	10	6	12	0	0	0	0
Mermin (Ref. [114])	Complement of Shrikhande	16	8	96	0	0	0	0
KS-18 (Refs. [115, 116])		18	4	144	108	0	12	0
YO (Ref. [117]) and its tight version (Ref. [118])		22	3	288	384	0	0	0
KS-24 (Ref. [119])		24	4	576	576	0	192	0
KS-31 (Ref. [24])		31	3	70	184	0	248	0
KS-33 (Ref. [119])		33	3	72	84	0	128	0

Chapter 3

Quantum fully contextual correlations

In this chapter we present the results obtained in Ref. [89]. Below we provide a brief summary.

Summary: Quantum correlations are contextual yet, in general, nothing prevents the existence of even more contextual correlations. We identify and test an NC inequality in which the quantum violation cannot be improved by any hypothetical post-quantum theory, and use it to experimentally obtain correlations in which the fraction of non-contextual correlations is less than 0.06. Our correlations are experimentally generated from the results of sequential compatible tests on a four-state quantum system encoded in the polarization and path of a single photon.

3.1 Introduction

In this chapter we make use of concepts and results already presented in previous sections of this thesis. In particular, we refer the reader to the basic definitions of quantum contextuality and compatibility of tests, and their corresponding mathematical descriptions, which can be found in Sect. 1.3.

As we pointed out in 1.4.6, the application of CSW's graph-theoretic approach in Ref. [7] on the basis of a classification of QCGs would allow to design experiments with quantum contextuality on demand, by selecting graphs with the desired properties. Such classification is provided in Ref. [8] and described in Sect. 1.5.

This chapter presents a remarkable example of this programme: Our goal is to use the graph-theoretic approach in order to identify and perform an experiment with sequential quantum compatible tests, which produces correlations with the largest contextuality allowed under the no-disturbance assumption (1.20), which is assumed to be valid also for post-quantum theories. For this purpose, we first introduce a measure of contextuality of the correlations, the non-contextual content W_{NC}, so that $W_{\mathrm{NC}} = 0$ corresponds to the maximum contextuality. Then, we show how to experimentally obtain testable upper bounds to W_{NC}. Next, we show how graph theory allows us to identify experiments in which the upper bound to W_{NC} predicted by QT

is zero, and apply this method to single out an experiment for which $W_{\rm NC} = 0$. Finally, we perform this experiment and obtain correlations in which $W_{\rm NC} < 0.06$.

3.2 Non-contextual content. Quantum fully contextual correlations

Every correlation among compatible tests [therefore satisfying (1.20)] can be expressed as

$$\begin{aligned} P(a_1,\ldots,a_n|x_1,\ldots,x_n) &= w_{\rm NC}\, P_{\rm NC}(a_1,\ldots,a_n|x_1,\ldots,x_n) \\ &+ (1-w_{\rm NC})\, P_{\rm C}(a_1,\ldots,a_n|x_1,\ldots,x_n), \end{aligned} \tag{3.1}$$

where $0 \leq w_{\rm NC} \leq 1$, and $P_{\rm NC}(a_1,\ldots,a_n|x_1,\ldots,x_n)$ can be expressed as (1.21), whereas $P_{\rm C}(a_1,\ldots,a_n|x_1,\ldots,x_n)$ satisfies (1.20) but cannot be expressed as (1.21). We define the *non-contextual content* $W_{\rm NC}$ of the correlations as the maximum value of $w_{\rm NC}$ over all possible decompositions as (3.1), i.e.,

$$W_{\rm NC} \equiv \max_{\{P_{\rm NC},P_{\rm C}\}} w_{\rm NC}. \tag{3.2}$$

This definition is parallel to the definition of local content introduced in Ref. [120]. In fact, for correlations generated through space-like separated tests, the non-contextual content equals the local content.

$\Omega_{\rm NC}$, $\Omega_{\rm Q}$, and $\Omega_{\rm C}$ will denote, respectively, the maximum value of S [see (1.22)] for non-contextual correlations [i.e., which can be expressed as (1.21)], quantum correlations, and correlations satisfying (1.20). Now consider correlations satisfying (1.20) and saturating $\Omega_{\rm Q}$. Then, given a decomposition of such correlations as (3.1), with $w_{\rm NC} = W_{\rm NC}$, $\Omega_{\rm Q}$ can be expressed as

$$\begin{aligned} \Omega_{\rm Q} &= \sum T_{a_1,\ldots,a_n,x_1,\ldots,x_n}[W_{\rm NC}\, P_{\rm NC}(a_1,\ldots,a_n|x_1,\ldots,x_n) \\ &+ (1-W_{\rm NC})\, P_{\rm C}(a_1,\ldots,a_n|x_1,\ldots,x_n)] \\ &= W_{\rm NC} \sum T_{a_1,\ldots,a_n,x_1,\ldots,x_n} P_{\rm NC}(a_1,\ldots,a_n|x_1,\ldots,x_n) \\ &+ (1-W_{\rm NC}) \sum T_{a_1,\ldots,a_n,x_1,\ldots,x_n} P_{\rm C}(a_1,\ldots,a_n|x_1,\ldots,x_n). \end{aligned} \tag{3.3}$$

The first sum can be expressed in a non-contextual form, so it is upper bounded by $\Omega_{\rm NC}$. The second sum cannot be expressed in a non-contextual form, so it can only be upper bounded by $\Omega_{\rm C}$. Hence, $\Omega_{\rm Q} \leq W_{\rm NC}\,\Omega_{\rm NC} + (1-W_{\rm NC})\,\Omega_{\rm C}$, and, taking into account that $\Omega_{\rm NC} \leq \Omega_{\rm Q} \leq \Omega_{\rm C}$, then

$$W_{\rm NC} \leq \frac{\Omega_{\rm C}-\Omega_{\rm Q}}{\Omega_{\rm C}-\Omega_{\rm NC}}. \tag{3.4}$$

Any experimental violation $S_{\rm exp}$ of a NC inequality indicates that $\Omega_{\rm C} > \Omega_{\rm NC}$ and, therefore, provides an upper bound on $W_{\rm NC}$, namely $W_{\rm NC} \leq (\Omega_{\rm C} - S_{\rm exp})/(\Omega_{\rm C} - \Omega_{\rm NC})$. Assuming that the maximum $S_{\rm exp}$ in an ideal experiment is given by $\Omega_{\rm Q}$, to observe correlations with zero non-contextual content, here called *quantum fully contextual correlations*, one has to test a NC inequality such that its maximum quantum violation equals its maximum possible violation under the assumption (1.20), i.e., an inequality for which $\Omega_{\rm NC} < \Omega_{\rm Q} = \Omega_{\rm C}$.

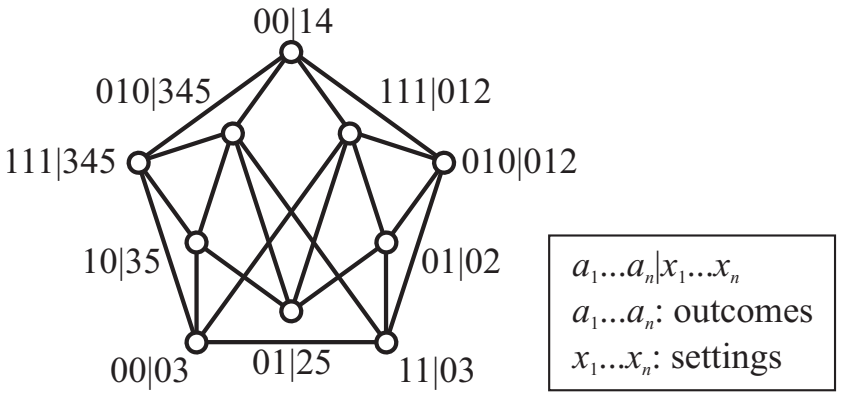

Figure 3.1: Exclusivity graph S_3 corresponding to the NC inequality (3.5). Vertices represent propositions. For example, 01|25 means "result 0 is obtained when test 2 is performed, and result 1 is obtained when test 5 is performed". Edges link propositions that cannot be simultaneously true. For example, 01|25 and 01|02 are linked, since in the first proposition the result of test 2 is 0, while in the second proposition the result of test 2 is 1.

However, even if $\Omega_{\mathrm{Q}} = \Omega_{\mathrm{C}}$, inherent imperfections of actual experiments will prevent the observation of $W_{\mathrm{NC}} = 0$. In general, the more complex the experiment to produce the required quantum correlations is, the higher the probability that experimental imperfections lead to a higher upper bound for the non-contextual content. Therefore, the task is to identify the simplest NC inequality violated by QT and such that $\Omega_{\mathrm{Q}} = \Omega_{\mathrm{C}}$.

3.3 Graph approach

Let us recall that, according to Refs. [6, 7], for any graph G there is a NC inequality[1] for which Ω_{NC}, Ω_{Q}, and Ω_{C} are given, respectively, by the independence number $\alpha(G)$, the Lovász number $\vartheta(G)$, and the fractional packing number $\alpha^*(G)$ of the graph. Therefore, the problem of identifying the simplest NC inequality violated by QT and such that $\Omega_{\mathrm{Q}} = \Omega_{\mathrm{C}}$ (and consequently, the simplest NC inequality experiment capable of revealing quantum fully contextual correlations), is equivalent to the problem of singling out the simplest QCG for which $\alpha(G) < \vartheta(G) = \alpha^*(G)$. We refer to a graph with this property as a QFCG.

[1] Needless to say, following Sect. 1.4.2, and in the spirit of CSW's graph theoretic approach, by NC inequality we refer to a positive linear combination of probabilities of events, and by graph we refer to the corresponding exclusivity graph.

3.3.1 Quantum fully contextual exclusivity graphs

For the purpose of identifying QFCGs, we generated all non-isomorphic graphs with less than 11 vertices using `nauty` (Ref. [79]). There are 11989764 of them. For each of them we calculated $\alpha(G)$ using `Mathematica` (Ref. [80]) and $\vartheta(G)$ using `SeDuMi` (Ref. [81]) and `DSDP` (Refs. [82, 83]). There are 992398 graphs for which $\alpha(G) < \vartheta(G)$. Then, we calculated $\alpha^*(G)$ using `Mathematica` from the clique-vertex incidence matrix of G obtained from the adjacency matrix of G using `MACE` (Refs. [84, 85]), an algorithm for enumerating all maximal cliques. A list containing G, $\alpha(G)$, $\vartheta(G)$, and $\alpha^*(G)$ for all graphs with less than 11 vertices for which $\alpha(G) < \vartheta(G)$ is provided in Ref. [8].

As we already have commented in Sect. 1.5.1, there are only four graphs with less than 11 vertices for which $\alpha(G) < \vartheta(G) = \alpha^*(G)$; all of them have 10 vertices, and they are depicted in Fig. 1.6. Moreover, the minimum dimension of the quantum system needed for the maximum quantum violation is given by the minimum dimension of the orthogonal representation of the complement of the graph leading to $\vartheta(G)$. Using this, it can be shown that the maximum quantum violation of NC inequalities associated to three of the aforementioned QFCGs requires quantum systems of dimension higher than four, while only the complement of the graph (a) in Fig. 1.6 admits an orthogonal representation in dimension four. For the sake of convenience, we show this graph in Fig. 3.1. We will denote this graph by S_3.

The inequality associated to the graph S_3 is constructed by looking for propositions involving compatible tests, such that each vertex represents one proposition in the inequality and the edges only link propositions that cannot be simultaneously true. Then, the inequality is simply given by the sum of all the probabilities of the propositions represented in the graph.

For the graph S_3, it can be easily seen that the following NC inequality is in one-to-one correspondence with the graph:

$$\begin{aligned} S \equiv & P(010|012) + P(111|012) + P(01|02) + P(00|03) \\ & + P(11|03) + P(00|14) + P(01|25) + P(010|345) \\ & + P(111|345) + P(10|35) \overset{\text{NC}}{\leq} 3, \end{aligned} \tag{3.5}$$

where $P(10|35)$ is the probability of obtaining result 1 when test 3 is performed and result 0 when test 5 is performed. In this case, the coefficients $T_{a_1,\ldots,a_n,x_1,\ldots,x_n}$ in (1.22) are all 1. The non-contextual bound, $\Omega_{\text{NC}} = 3$, can be obtained from the independence number of the graph S_3. The maximum quantum violation of inequality (3.5) and its maximum possible violation under the assumption (1.20) can be obtained from the Lovász and the fractional packing numbers of the graph S_3, respectively. This gives

$$\Omega_{\text{Q}} = \Omega_{\text{C}} = 3.5. \tag{3.6}$$

The maximum quantum violation can be achieved by preparing a four-state quantum system in the state

$$|\psi\rangle = \frac{1}{\sqrt{2}} \left(|0\rangle + |3\rangle \right), \tag{3.7}$$

where $\langle 0| = (1,0,0,0)$, $\langle 1| = (0,1,0,0)$, $\langle 2| = (0,0,1,0)$, and $\langle 3| = (0,0,0,1)$, and with the tests

represented by the following tensor products of Pauli matrices σ_i and the 2×2 identity matrix $\mathbb{1}$:

$$\begin{aligned} 0 &= \sigma_x \otimes \mathbb{1}, \qquad 1 = \mathbb{1} \otimes \sigma_z, \qquad 2 = \sigma_x \otimes \sigma_z, \\ 3 &= \mathbb{1} \otimes \sigma_x, \qquad 4 = \sigma_z \otimes \mathbb{1}, \qquad 5 = \sigma_z \otimes \sigma_x. \end{aligned} \tag{3.8}$$

The results 0 and 1 correspond to the eigenvalues -1 and $+1$, respectively, of the operators in (3.8). Notice that every probability in (3.5) includes only pairs or trios of mutually compatible tests.

3.4 Experimental quantum fully contextual correlations

The experiment testing the NC inequality (3.5) required two-test sequences [for instance, to obtain $P(00|14)$], and three-test sequences [for instance, to obtain $P(010|012)$]. We built six devices for the six dichotomic tests defined in (3.8). The sequential tests were performed using cascade setups (Ref. [36]) like the one shown in Fig. 3.2. We tested inequality (3.5) using the spatial path and polarization of a single photon carrying a four-state quantum system with the following encoding:

$$|0\rangle = |t, H\rangle, \quad |1\rangle = |t, V\rangle, \quad |2\rangle = |r, H\rangle, \quad |3\rangle = |r, V\rangle, \tag{3.9}$$

where t, r, H, and V denote the transmitted path, reflected path, horizontal, and vertical polarization of the photon, respectively.

The cascade setup used to implement two sequential tests on a single photon consists of three parts: state preparation, testing devices, and detectors. The preparation of the polarization-spatial path-encoded single photon state $|\psi\rangle$ is achieved using a source of H-polarized single photons. This single-photon source consists on an attenuated stabilized narrow bandwidth diode laser emitting at the wavelength of 780 nm. This laser offers a long coherence length. The two-photon coincidences were set to a negligible level by attenuating the laser to a mean photon number of 0.06 per time coincidence window. This source is followed by a half-wave plate (HWP) set at 22.5° and a polarizing beam splitter (PBS), allowing the photon to be distributed with equal probability between the two paths t and r with the right polarization H and V, respectively (see Fig. 3.2).

Then, the photon in the two paths enters the device for testing x_1 through the device's input and follows one of the two possible outputs, which correspond to the values $+1$ and -1. After each of the two outputs we placed a device for testing x_2. We used two identical devices for testing x_2. Finally, we placed a single-photon detector (D) at the output of the two devices x_2. The same idea is used for sequences of three tests x_1, x_2, and x_3, by adding four devices for measuring x_3 and using eight single photon detectors.

Devices for measuring the six tests defined in (3.8) are given in Fig. 3.3. Measurements 1 and 3 are standard polarization measurements using a PBS and a HWP which map the polarization eigenstate of the operator to $|t, H\rangle$ and $|r, V\rangle$. The mapping to the eigenstates of test 0, namely $(|t\rangle \pm |r\rangle)/\sqrt{2}$, was accomplished by interfering the two paths in a 50/50 beam splitter (BS). A wedge (W) is placed in one of the paths to set the phase between both paths (see Fig. 3.3). Tests 2 and 5 are represented by the tensor product of a spatial path and a polarization

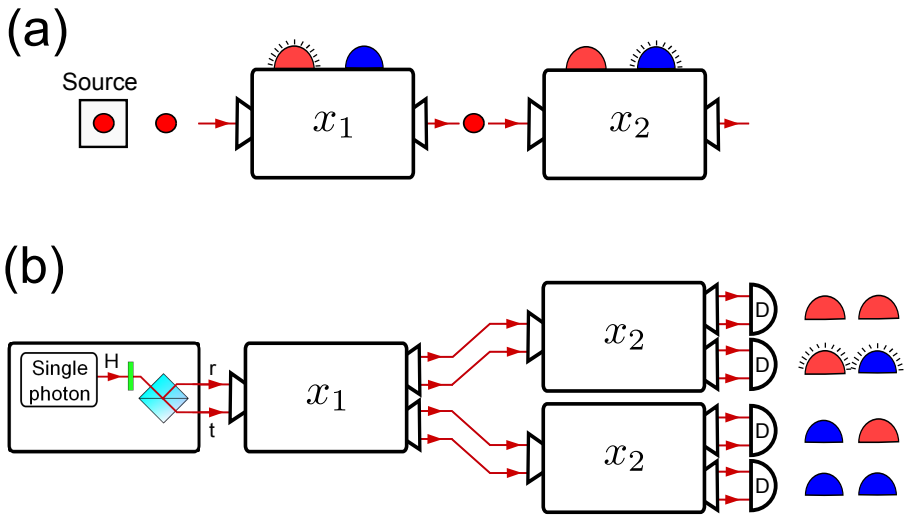

Figure 3.2: (a) Scheme for sequential tests of x_1 and x_2. The two possible results of each test are assigned the values $+1$ and -1, and are represented by whichever lamp is flashing. (b) Cascade setup used to implement two sequential tests on a single photon. It consists of three parts: state preparation, testing devices, and detectors. The preparation part produces the polarization-spatial path-encoded single photon state $|\psi\rangle$. The two outputs of the device for testing x_1 correspond to the two possible results. After each of these two outputs we placed a device for testing x_2. Single photon detectors are placed at each of the four outputs of the two devices x_2 (see the main text for details).

operator so they have a four-dimensional eigenspace. However, since the tests need to be rowwise and columnwise compatible, only their common eigenstates can be used for distinguishing the eigenvalues. Measurement 4 requires us only to distinguish between paths t and r. We needed to recreate the eigenstates of the performed tests after each mapping and before entering the next test, since our single-test devices map eigenstates to a fixed spatial path and polarization.

All interferometers in the experimental setup were based on a displaced Sagnac configuration. The stability of these interferometers is very high. We obtained visibilities over 99% for phase insensitive interferometers, and ranging between 90% and 95% for phase sensitive interferometers. We used silicon avalanche photodiodes calibrated to have the same detection efficiency for single-photon detection. All single counts were registered using an eight-channel coincidence logic with a time window of 1.7 ns. The raw detection events were gathered in a 10-second time period for each of the six experimental configurations.

The experimental results are presented in Table 3.1. The errors in the results were deduced from the standard deviation of 50 samples in the 10-second time period. The main sources of systematic errors were the small imperfections in the interferometers and in the overlapping of the light modes and the polarization components. These are the causes of the deviation of the experimental results from the ideal case observed in Table 3.1. The fact that some of the experimental results exceeded the corresponding ideal predictions was due to the lack of

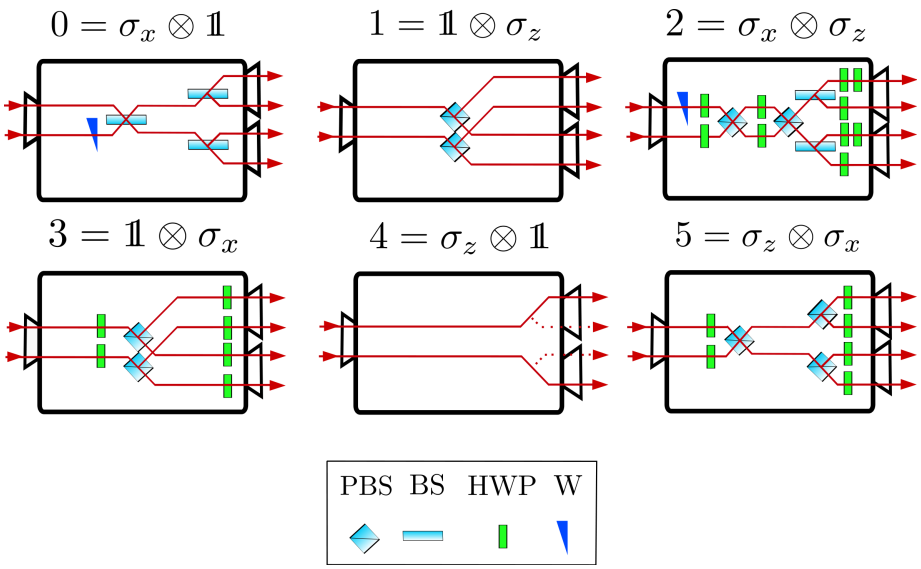

Figure 3.3: Devices for measuring the six tests defined in (3.8). The technique used consists in mapping the eigenstates of the operator to the two states $|t, \phi\rangle$ and $|r, \phi\rangle$, where ϕ is a polarization state (see the main text for details).

Table 3.1: Experimental results for inequality (3.5). The column "Ideal" refers to the predictions of QT for an ideal experiment.

Probability	Experimental result	Ideal
$P(010\|012)$	0.24091 ± 0.00021	0.25
$P(111\|012)$	0.30187 ± 0.00020	0.25
$P(01\|02)$	0.28057 ± 0.00020	0.25
$P(00\|03)$	0.50375 ± 0.00014	0.5
$P(11\|03)$	0.47976 ± 0.00014	0.5
$P(00\|14)$	0.47511 ± 0.00034	0.5
$P(01\|25)$	0.43765 ± 0.00015	0.5
$P(010\|345)$	0.24296 ± 0.00051	0.25
$P(111\|345)$	0.25704 ± 0.00052	0.25
$P(10\|35)$	0.24751 ± 0.00035	0.25
Ω	3.4671 ± 0.0010	3.5

perfect compatibility between the sequential tests caused by the non-perfect visibilities of the interferometers. Ref. [32] explains how to deal with this loophole.

From the results in Table 3.1, we can establish the following experimental upper bound to

the non-contextual content of the correlations:

$$W_{\mathrm{NC}} \leq 0.0658 \pm 0.0019. \tag{3.10}$$

This is the lowest experimental bound on the non-contextual content ever reported in any Bell or NC inequalities experiment. The previous lowest experimental upper bound on the non-contextual (local) content was 0.218 ± 0.014 (see Ref. [121]).

As in most experiments of Bell and NC inequalities with photons, we assumed that the detected photons were an unbiased sample of the prepared photons. This assumption is necessary, since the detection efficiency, without taking into account the losses in the setup, was 0.50 (a value obtained considering that the detection efficiency of the single-photon detectors was 55% and the efficiency of the fiber coupling was 90%). Future experiments using heralded sources and single-photon detectors of very high efficiency (Refs. [122, 123]) may close this loophole. Our experiment was intended to be a proof-of-principle experiment to illustrate the power of the graph approach in Ref. [6] to single out experiments with properties on demand (in our case, $\Omega_{\mathrm{NC}} < \Omega_{\mathrm{Q}} = \Omega_{\mathrm{C}}$), and to experimentally observe fully contextual correlations.

Chapter 4

Quantum social networks

In this chapter we present the results obtained in Ref. [124]. Below we provide a brief summary.

Summary:

We introduce a physical approach to social networks (SNs) in which each actor is characterized by a yes-no test on a physical system. This allows us to consider SNs beyond those originated by interactions based on pre-existing properties, as in a classical SN (CSN). As an example of SNs beyond CSNs, we introduce quantum SNs (QSNs) in which actor i is characterized by a test of whether or not the system is in a quantum state $|\psi_i\rangle$. We show that QSNs outperform CSNs for a certain task and some graphs. We identify the simplest of these graphs and show that graphs in which QSNs outperform CSNs are increasingly frequent as the number of vertices increases. We also discuss more general SNs and identify the simplest graphs in which QSNs cannot be outperformed.

We start this chapter with a short preamble intended to explain its apparently dissimilar goal when compared with the previous ones.

At first glance, the title does not seem to have any relation with either quantum correlations or exclusivity graphs, but this impression is far from being true: An appealing approach in the quest for properties singling out QT from the landscape of general probabilistic theories contemplates communication and computational tasks, in which not only does QT outperform classical theories, but also in some cases cannot be improved by using hypothetical post-quantum theories. Here, as in previous chapters, we consider post-quantum theories with the only requirement that they cannot assign a value larger than 1 to the sum of probabilities of mutually exclusive possibilities, i.e., theories which fulfill the E principle.[1] As a consequence, the class of tasks we are interested in consists of those requiring one to maximize a sum of probabilities of propositions tested on a physical system. There are many examples of tasks belonging to such class, ranging from some communication complexity tasks to all NC and Bell inequalities (Refs. [125, 95, 33, 36, 93, 116]). The one we present in this chapter (the maximization of certain average probability) also belongs to this class. Remarkably, for such class of tasks, CSW's

[1] See Sect. 1.1.6.

graph-theoretic approach is a natural framework, through the identification of possibilities (or events) with vertices of a graph, and mutual exclusivity relationships between pairs of events with edges.

The novel point is that we have made an effort to present this task and the corresponding classical, quantum and post-quantum yields in an attractive way that suggests potential practical applications, maybe even in daily life: for that purpose, we have built a bridge to another discipline, social sciences, in which graph theory provides a major tool in the analysis, in particular in the field of SNs. A final remark: it is important to draw the reader's attention to the fact that, for that reason, in this chapter the adjacency relationships among the vertices of the graphs are *reversed* with respect to foregoing chapters since we must account for usual (classical) SNs, where links are established on the basis of coincident properties of those who interact, and this feature must be preserved when one tries to generalize the concept of SN to give rise to a quantum or post-quantum counterpart.

4.1 Introduction

Social networks (SNs) are a traditional subject of study in social sciences (Refs. [126, 127, 128]) and may be tackled from many perspectives, including complexity and dynamics (Refs. [129, 130, 131]). Recently, they have attracted much attention after their tremendous growth through the internet. A SN is a set of people, "actors", with a pattern of interactions between them. In principle, there is no restriction on the nature of these interactions. In practice, in actual SNs, these interactions are based on relationships or mutual acquaintances (common interests, friendship, kinship,etc). However, to our knowledge, SNs have never been discussed on the basis of general interactions which can give rise to them. This is precisely the aim of this work.

A first observation is that, while a SN is typically described by a graph in which vertices represent actors and edges represent the result of their mutual interactions, the graph does not capture the nature of the interactions or explain why actor i is linked or not to other actors. From this perspective, the graph gives an incomplete description.

In order to account for this, we will consider the following, more general, scenario. We represent each actor i by a yes-no test T_i on a physical system S initially prepared in a state ρ and with possible outcomes 1 (yes) or 0 (no). Of course, these tests must satisfy some rules so that actual SNs naturally fit within them. More importantly, these rules must allow us to consider SNs beyond classical SNs (CSNs), defined as those in which the links between actors are determined by pre-existing properties of the actors, such as, e.g., their enthusiasm for jazz.

First, let us see how a CSN can be characterized in terms of yes-no tests T_i. In any CSN, it is always possible to identify a minimum set of labels such as "jazz" that describes the presence or absence of a link between any two actors; each actor's links are described by the value "yes" or "no" for each of these labels. An example is shown in Fig. 4.1. The size of that minimum set of labels coincides with a property of the underlying graph G, known in graph theory as its intersection number[2] (Ref. [86]), $i(G)$. For example, for the CSN shown in Fig. 4.1, the seven

[2]The intersection number of a graph G is the minimum cardinality of a set $\mathcal{X}$ such that G is the intersection graph of a family $\mathcal{F}$ of subsets of $\mathcal{X}$, that is, the graph whose vertices represent the sets in $\mathcal{F}$, with two distinct

labels which describe the network cannot be reduced to a smaller number since for the underlying graph $i(G) = 7$. Suppose each actor has the complete list of labels with their corresponding value "yes" or "no" as in Fig. 4.1. The input physical system S can be a card, and its state ρ is what is written on it, that is, the name of one of the labels. For instance, for the CSN in Fig. 4.1, the state ρ may be "jazz". Then, the outcome of T_i is 1 if actor i has in its list of labels "yes" for jazz, and 0 if it has "no" for jazz. The initial state of the card does not change after the test.

In this characterization of a SN, tests T_i naturally fulfil the following rules. (i) Two actors i and j are linked if and only if there exists some state ρ for which the results of T_i and T_j are both 1, which simply means that i and j share the pre-existing property described by the label in ρ. (ii) If a test T_i is repeated on the same state ρ, it will always give the same result, which simply means that the actor's label does not change under the execution of the test. (iii) For any ρ, the order of the tests is irrelevant, which reflects the symmetry of the interaction.

Note that, as a consequence of rule (i), if for a given ρ the outcome of T_i is 1, then a test T_j in any j which is not linked to i will never give the outcome 1. This means that, for any ρ and any set I of pairwise non-linked actors, the sum of the outputs of the tests T_i over all actors in I is upper bounded by 1. Moreover, this results in a restriction on the possible states ρ. For instance, in the previous example, the state "jazz or Oxford" is not allowed. For such a state, the tests T_i and T_j corresponding to two non-linked actors i and j for which the values of the labels "jazz" and "Oxford" are, respectively, "jazz: yes; Oxford: no" and "jazz: no; Oxford: yes", would give both the outcome 1, in contradiction with rule (i).

Let us consider now more general SNs (GSNs). We denote by $P_\rho(a, b|T_i, T_j)$ the joint probability of obtaining outcome $a \in \{0, 1\}$ when performing T_i on the system S initially prepared in the state ρ, and outcome $b \in \{0, 1\}$ when performing T_j on S in the state ρ_i resulting from the previous test T_i. The tests must obey the following rules, which generalize (i)–(iii): (I) $P_\rho(1, 1|T_i, T_j)$ determines the linkage between actors i and j; they are linked if and only if there exists some ρ such that $P_\rho(1, 1|T_i, T_j) > 0$. (II) For any ρ, $P_\rho(a, a|T_i, T_i) = P_\rho(a|T_i)$, i.e., when T_i is repeatedly performed on S initially in the state ρ, it always yields the same result. (III) For any ρ, the order of the tests is irrelevant: $P_\rho(a, b|T_i, T_j) = P_\rho(b, a|T_j, T_i)$.

Note that in a CSN the probabilities $P_\rho(a|T_i)$ can take only the values 0 or 1, whereas in a GSN these probabilities can take any values compatible with rules (I)–(III). Moreover, here we will assume that the state ρ may change according to the results of the tests T_i.

There is a simple task which highlights the difference between a GSN and a CSN described by the same graph G: the average probability $\mathcal{T}$ that, for an actor i chosen at random, the test T_i yields the outcome 1. The interesting point is that $\mathcal{T}$ *is upper bounded differently depending on the nature of the interactions defining the SN*. For the CSN, let us suppose that the card is

vertices linked by an edge if and only if the corresponding sets have a non-empty intersection. Let us note that this number coincides with the edge clique cover number, usually denoted as $\theta'(G)$ or $\theta_E(G)$, which has a direct graphical interpretation, based on its definition: Let $V(G)$ and $E(G)$ be the sets of vertices and edges of G, respectively. Let $C \subseteq V(G)$ be a clique, and $e = (i, j) \in E(G)$ an edge. It is said that C covers e if and only if $i, j \in C$. An edge clique cover (ECC) of G is a collection $\mathcal{C} = \{C_1, \ldots, C_N\}$ of cliques of G such that for every edge $e \in E(G)$ there is at least one clique $C_e \in \mathcal{C}$ that covers e. It is said that $\mathcal{C}$ is optimal if there is no other ECC of G, say $\mathcal{C}'$, such that $|\mathcal{C}'| < |\mathcal{C}|$. The number of cliques in an optimal ECC is the ECC number $\theta_E(G)$ of G. This number has previously appeared in this thesis on p. 59, regarding the classification of quantum contextual graphs (QCGs).

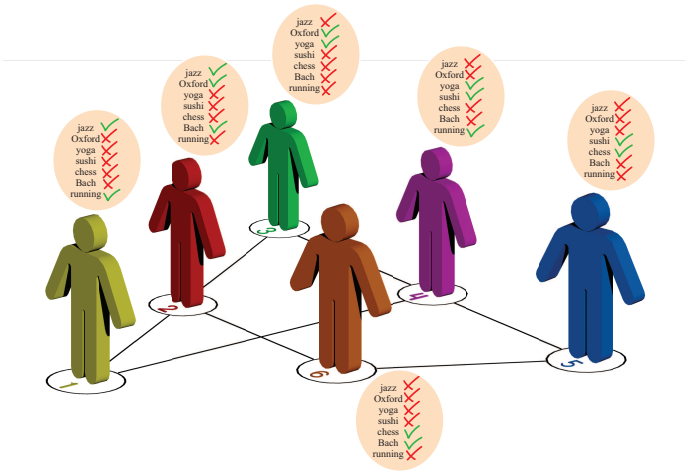

Figure 4.1: A CSN. Each actor is represented by a vertex of a graph and each link by an edge. The characteristic of a CSN is that links can be explained on the basis of pre-existing properties of the actors such as whether or not they are jazz enthusiasts, attended Oxford University, practice yoga, like sushi, will participate in a chess tournament, love the music of J. S. Bach or run four times a week.

in the state ρ (e.g., jazz). Then, for an actor i chosen at random, $\mathcal{T} = \frac{1}{n}\sum_{i=1}^{n} P_\rho(1|T_i)$, where n is the number of actors. The maximum value of $\mathcal{T}$ over all possible states ρ is the maximum number of actors sharing the value "yes" for a pre-existing property, divided by the number of actors. This corresponds to $\frac{\omega(G)}{n}$, where $\omega(G)$ is the clique number (Ref. [86]) of G, i.e. the number of vertices in the largest clique. Given a graph, a clique is a subset of vertices such that every pair is linked by an edge. The term "clique" comes from the social sciences, where social cliques are groups of people all of whom know each other (Ref. [132]). In the example of Fig. 4.1, the value of the clique number for the graph is $\omega(G) = 2$. As a consequence, for any CSN represented by that graph, the maximum of $\mathcal{T}$ is $\frac{\omega(G)}{n} = \frac{1}{3}$.

However, for a GSN described by a graph G, the maximum value for $\mathcal{T}$ compatible with rules (I)–(III) is $\frac{\alpha^*(\overline{G})}{n}$, where $\overline{G}$ denotes the complement of G, which is the graph $\overline{G}$ on the same vertices such that two vertices of $\overline{G}$ are adjacent if and only if they are not adjacent in G, and $\alpha^*(\overline{G})$ is the so-called fractional packing number (Ref. [109]) of $\overline{G}$, defined as $\max \sum_{i\in V} w_i$, where the maximum is taken for all $0 \leq w_i \leq 1$ and for all cliques c_j of $\overline{G}$, under the restriction[3] $\sum_{i\in c_j} w_i \leq 1$. In the example of Fig. 4.1, $\alpha^*(\overline{G}) = \frac{5}{2}$. Hence, the maximum of $\mathcal{T}$ satisfying rules (I)–(III) is $\frac{5}{12} > \frac{1}{3}$, attainable for instance by taking $P_\rho(1|T_i) = \frac{1}{4}$ for $i = 1, 3$ and $P_\rho(1|T_j) = \frac{1}{2}$ for $j = 2, 4, 5, 6$.

Note that the maximum value of $\mathcal{T}$ does not change when the outcome 1 is not deterministic, as in a CSN, but occurs with certain probability. In this sense, such "randomized" SNs do not perform better than CSNs.

The interesting point is that, since there are graphs for which $\omega(G) < \alpha^*(\overline{G})$, then there

[3] As we said on p. 54, this restriction accounts for the E principle.

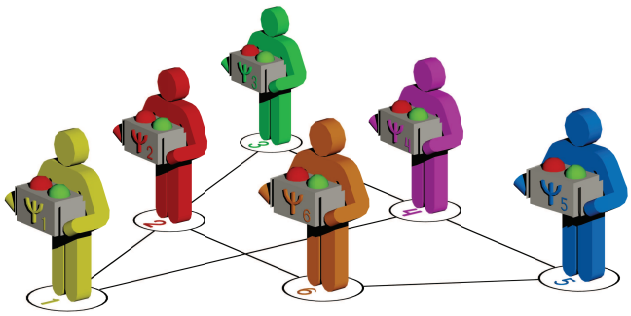

Figure 4.2: A QSN can be visualized as a CSN in which each actor i has a device to measure a quantum state $|\psi_i\rangle$.

should exist SNs in which $\mathcal{T}$ goes beyond the maximum value for CSNs.

4.2 Quantum social networks

We shall introduce now a natural SN for which $\mathcal{T}$ may be larger than the maximum for any CSN represented by the same graph. A quantum SN (QSN) is defined as a SN in which each actor i is associated with a quantum state $|\psi_i\rangle$. The states are chosen to reflect the graph of the network in the following sense: Non-adjacent (adjacent) vertices in the graph correspond to orthogonal (non-orthogonal) states.[4] It is always possible to associate quantum states to the actors of any network fulfilling the orthogonality relationships imposed by its graph (Ref. [133]). Reciprocally, any set of quantum states defines a QSN.

A QSN can be constructed from a CSN by assigning to actor i a device to test the quantum state $|\psi_i\rangle$, as illustrated in Fig. 4.2. The characterization of the QSN in terms of yes-no tests T_i satisfying rules (I)–(III) is as follows. Each device receives a system S in a quantum state ρ as input, and gives as output either the state $|\psi_i\rangle$ and the outcome 1, or a state orthogonal to $|\psi_i\rangle$ and the outcome 0. These tests are measurements represented in quantum mechanics by rank-1 projectors. Note that projective measurements are the simplest repeatable measurements in quantum mechanics [in agreement with rule (II)], whereas general measurements represented by POVMs are not repeatable.

In a QSN, $\mathcal{T}$ may be larger than the maximum for any CSN represented by the same graph. If each and every actor is provided with the same input state $|\Psi\rangle$, according to quantum mechanics the probability of getting the outcome 1 when performing T_i for a randomly chosen i is now $\mathcal{T} = \frac{1}{n}\sum_{i=1}^{n} |\langle\Psi|\psi_i\rangle|^2$. Given G, the quantity $\frac{1}{n}\max\sum_{i=1}^{n} |\langle\Psi|\psi_i\rangle|^2$, where the maximum is taken over all quantum vectors $|\Psi\rangle$ and $|\psi_i\rangle$ and all dimensions, gives the maximum value of $\mathcal{T}$ for any QSN. This number is equal to $\frac{\vartheta(\overline{G})}{n}$, where $\vartheta(\overline{G})$ is the Lovász number (Ref. [71]) of $\overline{G}$, which can be computed to arbitrary precision by semi-definite programming in polynomial time

[4] This assignment corresponds to a faithful orthogonal representation of the graph G of the network. See definitions on pp. 54 and 67.

(see the Appendix, 4.5).

The Lovász number was introduced as an upper bound of the Shannon capacity of a graph (Ref. [68]), and it is sandwiched between the clique number $\omega(G)$ and the chromatic number $\chi(G)$ of a graph (Ref. [102]): $\omega(G) \leq \vartheta(\overline{G}) \leq \chi(G)$. The interesting point is that, for those graphs such that $\vartheta(\overline{G}) > \omega(G)$, QSNs outperform CSNs.

On the other hand, $\vartheta(\overline{G})$ is upper bounded by the fractional packing number $\alpha^*(\overline{G})$, as was shown by Lovász in Ref. [71]. In a nutshell, $\mathcal{T}$ and its three upper bounds fulfil $\mathcal{T} \overset{\text{CSN}}{\leq} \frac{\omega(G)}{n} \overset{\text{QSN}}{\leq} \frac{\vartheta(\overline{G})}{n} \overset{\text{GSN}}{\leq} \frac{\alpha^*(\overline{G})}{n}$. For example, for the SNs in Figs. 4.1 and 4.2, one has $\mathcal{T} \overset{\text{CSN}}{\leq} \frac{1}{3} \overset{\text{QSN}}{\leq} \frac{\sqrt{5}}{6} \overset{\text{GSN}}{\leq} \frac{5}{12}$.

These numbers, $\omega(G)$ [which is equal to the independence number $\alpha(\overline{G})$ of the complement graph], $\vartheta(\overline{G})$ and $\alpha^*(\overline{G})$ have previously appeared in quantum information, in the discussion of the quantum channel version of Shannon's zero-error capacity problem in Refs. [134, 43], and in foundations of quantum mechanics, in the discussion of NC inequalities, in Ref. [6].

We generated all non-isomorphic connected graphs with less than 11 vertices (more than 11×10^6 graphs) and singled out those for which $\vartheta(\overline{G}) > \omega(G)$ (as explained in the Appendix, 4.5). The graph with less number of vertices such that $\vartheta(\overline{G}) > \omega(G)$ is the pentagon, for which $\omega(G) = 2$ and $\vartheta(\overline{G}) = \sqrt{5}$, which can be attained using a quantum system of dimension $d = 3$ [see Fig. 4.3 (a)]. The second simplest graph for which $\vartheta(\overline{G}) > \omega(G)$ is the one in Figs. 4.1 and 4.2. For a given number of vertices, the number of graphs such that the maximum of $\mathcal{T}$ for QSNs is larger than for CSNs rapidly increases. The complete list of these graphs with less than 11 vertices is provided in the Appendix, 4.5.

Interestingly, the probability that the graph of an arbitrary network with a large number of actors contains induced graphs in which a QSN outperforms a CSN is almost identity. This follows from a result in graph theory according to which an arbitrarily large graph contains with almost certainty an induced copy of every graph (Ref. [70]).[5] A graph H is said to contain an induced copy of G when G is a subgraph of H obtained by removing some of the vertices and all the edges incident to these vertices.

Moreover, a stronger result can be proven. The probability that QSNs outperform CSNs for an arbitrarily large graph is almost identity. This follows from the observation in Ref. [135] that, while for an n-vertex random graph with edges generated with probability 1/2 the value of $\omega(G)$ is almost surely (Ref. [136]) roughly $2\log_2 n$, the value of $\vartheta(G)$ is almost surely $o(\sqrt{n})$ (Ref. [137]).

Once one has identified a graph for which $\vartheta(\overline{G}) > \omega(G)$, one can compute the quantum states $|\Psi\rangle$ and $|\psi_i\rangle$ of minimum dimensionality d_Q providing the optimal quantum solution, the one that maximizes $\mathcal{T}$. For the simplest graph with quantum advantage these states are in Fig. 4.3 (a). The state $|\Psi\rangle$ is the initial state of S needed to obtain the maximum quantum advantage.

4.3 Social networks with no-better-than-quantum advantage

Remarkably, there are graphs for which QSNs outperform CSNs but no GSN outperforms the best QSN: those satisfying $\omega(G) < \vartheta(\overline{G}) = \alpha^*(\overline{G})$. To single out such graphs is particularly interesting because they would allow us to construct the best GSN in a simple way.

[5] Ibid., proposition 11.3.1.

We identified all the graphs with less than 11 vertices with $\omega(G) < \vartheta(\overline{G}) = \alpha^*(\overline{G})$. There are only four of them. The simplest one is in Fig. 4.3 (b). Its quantum realization requires a quantum system of dimension $d = 6$ (e.g., a qubit-qutrit system) and $\omega(G) = 2$ and $\vartheta(\overline{G}) = \frac{5}{2}$. The second simplest graph contains the first one, and it is shown in Fig. 4.3 (c). It only requires a quantum system of dimension $d = 4$; for this graph $\omega(G) = 3$ and $\vartheta(\overline{G}) = \frac{7}{2}$. The other two graphs are the one in Fig. 4.3 (c) with one or two extra edges.

In all the graphs we have explored so far, the quantum advantage requires the preparation of S in a specific quantum state $|\Psi\rangle$. However, as the complexity of the network increases this requirement becomes unnecessary. This is due to the fact that there are graphs for which the quantum advantage is independent of $|\Psi\rangle$; thus any quantum state (pure or mixed, including maximally mixed) can be used as initial state for the tests T_i.

As proven in the Appendix (4.5), any set of quantum states $|\psi_i\rangle$ belonging to the class of the so-called KS sets (see Refs. [30, 24]) defines a QSN in which the quantum advantage is independent of the state $|\Psi\rangle$. The graph corresponding to the SN associated to the simplest KS set (Ref. [115]) is illustrated in Fig. 4.3 (d). It has $\omega(G) = 4$ and $\vartheta(\overline{G}) = \frac{9}{2}$, requires a quantum system of dimension $d = 4$, and no GSN can outperform it. Methods to generate KS sets (Refs. [138, 139, 140, 141]) can be used to obtain QSNs with all these features.

4.4 Final remarks

Any actual SN through the internet, like Facebook or Twitter, is complex enough to potentially benefit from assigning quantum tests to the actors. An example is the following: suppose that a company wants to sell a product to as many Facebook users as possible. Under the (correct) assumption that Facebook is a CSN, the optimal strategy would be to identify the biggest subgroup of mutually linked actors, single out their common interest, and then design a commercial targeting this common interest. However, if Facebook were a QSN with exactly the same links as the actual Facebook, then the company would have a larger positive feedback by linking its commercial to the results of the quantum tests.

As in a CSN, the vertices of a QSN can be organized in communities or clusters, with many edges joining vertices of the same cluster and comparatively few edges joining vertices of different clusters. Given a graph G, community detection might be simpler if the graph represents a QSN rather than a CSN. The reason is that a QSN with a given G requires a (quantum) physical system of dimension (i.e., number of perfectly distinguishable states) $d_Q = \xi(\overline{G})$, with $\xi(\overline{G})$ the orthogonal rank of the complement of G, defined as the minimum d such that there exists an orthogonal representation of G in d dimensions (i.e., a function mapping non-adjacent vertices in G to orthogonal vectors in $\mathcal{C}^d$). However, building a CSN requires a physical system of dimension $d_C = i(G)$ (e.g., for the graph G in Fig. 4.1, there are $i(G) = 7$ distinguishable states ρ: jazz,..., running). We have $d_Q \leq d_C$ and, in most cases, $d_Q < d_C$. As an example, while for the graphs in Fig. 4.3 (a)–(d), d_C is $5, 15, 10$ and 18; d_Q is $3, 6, 4$ and 4, respectively. Once a community is detected, the study of its induced subgraph will tell us whether or not it has a quantum advantage. Note that QSNs with no global quantum advantage can contain induced subgraphs (e.g., representing communities) with quantum advantage.

On the experimental side, constructing a simple QSN with advantage over its classical coun-

terpart is within actual experimental capabilities. The simplest example is a pentagon in which each actor has a device for testing the appropriate quantum state.

4.5 Appendix

We explain how we obtained all graphs G with less than 11 vertices for which $\vartheta(\overline{G}) > \omega(G)$. We also prove that a set of quantum states belonging to the class of KS sets defines a QSN in which the quantum advantage is independent of the state.

4.5.1 Finding graphs in which QSNs can outperform CSNs

To obtain all SNs with less than 11 actors in which the assignment of quantum states can outperform the corresponding CSNs, we generated all non-isomorphic connected graphs using `nauty` (Ref. [79]), and then we calculated $\omega(G)$ (using `Mathematica`, Ref. [80]), $\vartheta(\overline{G})$ (using `SeDuMi`, Ref. [81], and also `DSDP`, Refs. [82, 83]) and $\alpha^*(\overline{G})$ (using `Mathematica` from the clique-vertex incidence matrix of $\overline{G}$, obtained from the adjacency matrix of $\overline{G}$ calculated using `MACE`, Refs. [84, 85], for enumerating all maximal cliques). In addition, we obtained the minimum dimensionality $\xi(\overline{G})$ of the quantum system in which the maximum quantum versus classical advantage occurs, or a lower bound of $\xi(\overline{G})$, by identifying subgraphs in $\overline{G}$ which are geometrically impossible in a space of lower dimensionality. For example, the simplest impossible graph in dimension $d = 1$ consists of two non-linked (non-orthogonal) vertices in $\overline{G}$; in $d = 2$, three vertices, one of them linked to the other two. From these two impossible graphs, one can recursively construct impossible graphs in any dimension d by adding two vertices linked to all vertices of an impossible graph in $d - 2$. For example, if $\overline{G}$ contains a square, then $\xi(\overline{G}) > 3$. Finally, we have calculated the minimum dimensionality $i(G)$ needed for a CSN by using a program based on `nauty`, `very-nauty` (Ref. [87] and Ref. [88]).

Table 4.1 contains the number of non-isomorphic graphs with a given number of vertices, up to 10 vertices; the number of them in which QSNs outperform CSNs, and for the latter, the number of those for which no GSN outperforms the best QSN. All non-isomorphic graphs with less than 11 vertices (around 10^6) in which QSNs outperform CSNs are presented in Ref. [142].

Table 4.1: Number of non-isomorphic graphs with vertices ranging from 5 to 10 corresponding to SNs in which the assignment of quantum states to the actors provides advantage, and number of them in which the advantage cannot be improved by GSNs.

Vertices	Graphs	With quantum advantage	With no-better-than-quantum advantage
5	21	1	0
6	112	2	0
7	853	28	0
8	11117	456	0
9	261080	15951	0
10	11716571	957639	4

4.5.2 State-independent QSNs

A KS set in dimension d (Ref. [30]) is a set of rays S in the d-dimensional complex space such that there is no function $f : S \to \{0, 1\}$ satisfying that for all orthonormal bases $b \subseteq S$, $\sum_{u \in b} f(u) = 1$.

Proposition: For any KS set in dimension d represented by a graph G, $\omega(G) < \vartheta(\overline{G})$ for any initial state in dimension d.

Proof: For an n-ray KS set in dimension d, $\vartheta(\overline{G}) = \frac{n}{d}$, since $\vartheta(\overline{G})$ is the same for any initial state, including the maximally mixed state $\rho = \frac{1}{d}\mathbb{1}$ (where $\mathbb{1}$ represents the identity matrix). $\omega(G)$ cannot reach this number since, by definition of KS set in dimension d, there is no way to assign 0 or 1 to their elements in such a way that, for every clique of size d in the complement graph $\overline{G}$, which corresponds to a basis $b \subseteq S$, $d - 1$ elements are 0 and one is 1. This means that the best possible assignment respecting that two non-adjacent vertices in G cannot be both 1 includes at least one clique C in $\overline{G}$ for which 0 is assigned to the d elements. The KS set can be expanded so that every vector belongs to a clique of size d in $\overline{G}$, and the assignments can be replicated an integer number m such that $m\omega(G)$ and $m\vartheta(\overline{G})$ can be expressed as a sum of elements grouped in cliques. The contribution of each clique is either 0 or 1. In $m\vartheta(\overline{G})$ all cliques's contribution is 1, whereas in $m\omega(G)$ the contribution of the clique C in which the assignment fails is 0. ■

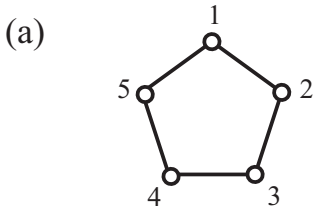

$$\langle\psi_k| = (\cos\theta, \sin\theta\cos\phi_k, \sin\theta\sin\phi_k)$$
$$k = 1, \ldots, 5$$
$$\cos\theta = \frac{1}{\sqrt[4]{5}}, \phi_k = \frac{2\pi k}{5}$$

$$\langle\Psi| = (1, 0, 0)$$

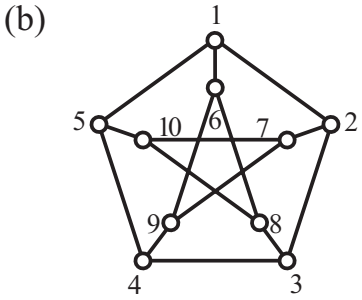

$$\langle\psi_1| = (1, 0, 0, 0, 0, 0)$$
$$\langle\psi_2| = 12^{-1/2}(\sqrt{3}, 0, 0, -1, 2, 2)$$
$$\langle\psi_3| = 2^{-1}(0, -1, 0, 0, 0, \sqrt{3})$$
$$\langle\psi_4| = (0, 1, 0, 0, 0, 0)$$
$$\langle\psi_5| = 12^{-1/2}(\sqrt{3}, -\sqrt{3}, \sqrt{3}, -1, -1, -1)$$
$$\langle\psi_6| = 2^{-1}(1, 0, 0, \sqrt{3}, 0, 0)$$
$$\langle\psi_7| = 2^{-1}(0, 0, 1, 0, \sqrt{3}, 0)$$
$$\langle\psi_8| = 12^{-1/2}(0, 0, \sqrt{3}, 2, -1, 2)$$
$$\langle\psi_9| = 12^{-1/2}(0, -\sqrt{3}, 0, 2, 2, -1)$$
$$\langle\psi_{10}| = (0, 0, 1, 0, 0, 0)$$

$$\langle\Psi| = 12^{-1/2}(\sqrt{3}, -\sqrt{3}, \sqrt{3}, 1, 1, 1)$$

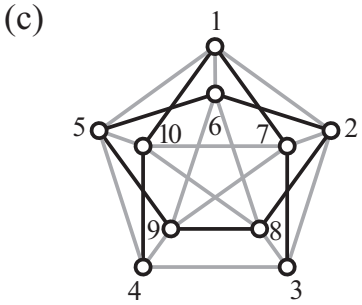

$$\langle\psi_1| = 2^{-1/2}(0, 0, 1, 1)$$
$$\langle\psi_2| = 2^{-1/2}(1, 0, 0, -1)$$
$$\langle\psi_3| = 2^{-1}(1, -1, 1, -1)$$
$$\langle\psi_4| = 2^{-1}(1, 1, -1, 1)$$
$$\langle\psi_5| = 2^{-1/2}(1, 0, 0, 1)$$
$$\langle\psi_6| = 2^{-1/2}(0, 1, 0, -1)$$
$$\langle\psi_7| = 2^{-1}(-1, 1, 1, 1)$$
$$\langle\psi_8| = 2^{-1}(1, 1, 1, -1)$$
$$\langle\psi_9| = 2^{-1}(1, -1, -1, 1)$$
$$\langle\psi_{10}| = 2^{-1}(1, 1, 1, 1)$$

$$\langle\Psi| = (0, 0, 0, 1)$$

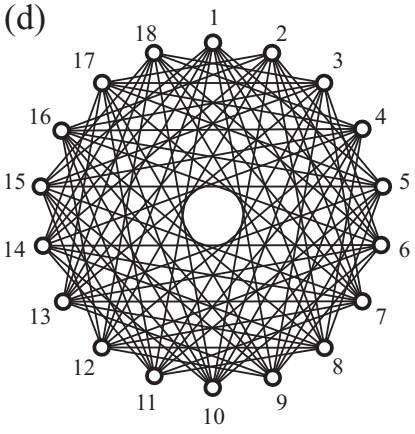

$$\langle\psi_1| = (1, 0, 0, 0)$$
$$\langle\psi_2| = (0, 1, 0, 0)$$
$$\langle\psi_3| = 2^{-1/2}(0, 0, 1, 1)$$
$$\langle\psi_4| = 2^{-1/2}(0, 0, 1, -1)$$
$$\langle\psi_5| = 2^{-1/2}(1, -1, 0, 0)$$
$$\langle\psi_6| = 2^{-1}(1, 1, -1, -1)$$
$$\langle\psi_7| = 2^{-1}(1, 1, 1, 1)$$
$$\langle\psi_8| = 2^{-1}(1, -1, 1, -1)$$
$$\langle\psi_9| = 2^{-1/2}(1, 0, -1, 0)$$
$$\langle\psi_{10}| = 2^{-1/2}(0, 1, 0, -1)$$
$$\langle\psi_{11}| = 2^{-1/2}(1, 0, 1, 0)$$
$$\langle\psi_{12}| = 2^{-1}(1, 1, -1, 1)$$
$$\langle\psi_{13}| = 2^{-1}(-1, 1, 1, 1,)$$
$$\langle\psi_{14}| = 2^{-1}(1, 1, 1, -1)$$
$$\langle\psi_{15}| = 2^{-1/2}(1, 0, 0, 1)$$
$$\langle\psi_{16}| = 2^{-1/2}(0, 1, -1, 0)$$
$$\langle\psi_{17}| = 2^{-1/2}(0, 1, 1, 0)$$
$$\langle\psi_{18}| = (0, 0, 0, 1)$$

Figure 4.3: Graphs for which QSNs can outperform CSNs. The right side displays the quantum states $|\psi_i\rangle$ and $|\Psi\rangle$ needed for the maximum quantum advantage using a quantum system of the smallest dimension. (a) is the simplest graph for which QSNs can outperform CSNs. (b) and (c) are the simplest graphs for which QSNs cannot be improved. Graph (c) has the same edges as graph (b) plus extra ones. (d) is the simplest known graph in which the quantum advantage is independent of $|\Psi\rangle$.

Part II

Graph states: Classification and optimal preparation

Chapter 5

Introduction: Stabilizer formalism and graph states

The purpose of this chapter is to provide the main definitions and minimum necessary theoretical background that pave the way for discussing the results of the second part of this thesis. The chapter is organized in two sections:

Sect. 5.1 is devoted to introducing the stabilizer formalism. We present, in a rather self-contained and compact fashion, some basic concepts and definitions along with the notation and techniques that will be used in the subsequent chapters. We put special emphasis on the concepts of stabilizer and generator, that will be profusely used later, and also in the important role of the operations belonging to the Clifford group, which will be useful when dealing with graph states and their entanglement properties.

Sect. 5.2 focuses the attention on graph states, a particular instance of stabilizer states which constitute the subject of study in this part of our research. After giving the definition and a condensed list of possible applications, we deal with graph states as a "theoretical laboratory" for multipartite entanglement, and describe some relevant results previously obtained by other authors in relation to the general problem of the classification of entanglement in pure quantum states, which provide the conceptual scenario for our contributions. We will finish the exposition with a succinct outline of the classification of graph states of up to 7 qubits in classes of equivalence under local Clifford operations carried out by our predecessors Hein, Eisert and Briegel in Ref. [9], which can be considered the starting point of our work on graph states.

5.1 Stabilizer formalism

Graph states constitute a family of multipartite pure entangled states belonging to the broader family of the so-called stabilizer states. The concept of *stabilizer* is a key issue in order to study graph states and present some of our results: this is the main reason why we will dedicate this section to briefly introduce the basics of the stabilizer formalism.

Representing quantum states as linear combinations of basis states can quickly become prolix and even useless for certain problems as the dimension (or the number of subsystems) of the

system increases.[1] As an alternative, we could constrain ourselves to studying certain types of quantum states. An obvious possibility is to limit ourselves to those states that can be written as a linear combination of an upper bounded number of basis vectors, but such restriction would lead us to put aside most quantum states and therefore to miss many of the interesting features of quantum mechanics.

Another more fruitful possibility consists in considering "theoretical laboratories",[2] i.e., specific sets or families of quantum states which capture essential features of the problem we are interested in, but which are nevertheless relatively easier to understand in their properties — without bounding the dimension of the system—, due to the fact that they admit an economical description, much more compact than that of the state vector. Among those theoretical laboratories, stabilizer states (and the associated stabilizer formalism) constitute a conspicuous example. Another one, to which we will devote further analysis in the next chapters, is the set of graph states, a proper subset of the set of stabilizer states. We develop this issue in some more detail in Sect. 5.2.2, where we discuss graph states as a theoretical laboratory for the study of multipartite entanglement.

The stabilizer formalism has proved useful in many applications: for instance, in measurement-based quantum computation (Refs. [144, 145]), in quantum error correction (Ref. [146]), or in quantum secret sharing (Ref. [147]). And also in fundamental problems, such as the study of quantum entanglement (Refs. [148, 149]), or the stabilizer-state violation of local realism (Ref. [150]). The idea that underlies the stabilizer formalism is that many quantum states can be more easily described through the operators that stabilize[3] them than by the usual state vector description. A pivotal aspect of the stabilizer formalism is the clever use of elements of group theory: in particular, it focuses the attention on a specific class of unitary operators which has the structure of a group, the so-called *Pauli group*, which can be considered as a multi-qubit

[1] For instance, if we had to carry out the analysis, characterization and classification of the multipartite quantum entanglement, we would find that the number of entanglement classes of equivalence for pure multipartite states grows very rapidly as a direct consequence of the exponential increase in the dimension of the corresponding Hilbert space.

[2] This denomination —an apparent oxymoron— is used, v.g., in Ref. [143], regarding the systematic study of multi-particle entanglement.

[3] See Sect. 5.1.2 for the definition.

extension of the Pauli matrices[4] for single qubits.

5.1.1 The Pauli group

The Pauli group $\mathcal{P}_n$ on n qubits consists of all 4×4^n n-fold tensor products of the form $M = \alpha_M M_1 \bigotimes \cdots \bigotimes M_n$, where $\alpha_M \in \{\pm 1, \pm \imath\}$ is an overall phase factor and M_i is either the 2×2 identity matrix $\sigma_0 = \mathbb{1}$ or one of the Pauli matrices $X = \sigma_x$, $Y = \sigma_y$, and $Z = \sigma_z$. In compact notation, following Ref. [151], $\mathcal{P}_n = \{\pm 1, \pm i\} \times \{\mathbb{1}, X, Y, Z\}^{\otimes n}$.

As an example, $\mathcal{P}_1$, which is the Pauli group on one qubit, is the 16-element set[5]

$$\mathcal{P}_1 \equiv \{\pm I, \pm iI, \pm X, \pm iX, \pm Y, \pm iY, \pm Z, \pm iZ\}. \tag{5.11}$$

Another example: the operator $X \otimes iI \otimes -Z \otimes iY \otimes -iI \otimes Z \otimes Y$ is an element of $\mathcal{P}_7$ (which involves $4 \times 4^7 = 65536$ elements). Note that one can merge all the phases affecting each one-qubit tensor factor into an unique overall phase, and write $-iX \otimes I \otimes Z \otimes Y \otimes I \otimes Z \otimes Y$. And one can even opt for a more compact notation, like $-iX_1Z_3Y_4Z_6Y_7$: here, each subindex refers to the qubit onto which the Pauli operator is acting; both identity operators and tensor product symbols $\otimes$ are unstated.

Let us recall some basic ideas of group theory. Given that $\mathcal{P}_n$ is a group, then it is a set of elements endowed with an associative multiplication operation, satisfying the following properties:

1. $\mathcal{P}_n$ contains the identity operator, $\mathbb{1} \otimes \cdots \otimes \mathbb{1} = \mathbb{1}^{\otimes n}$.

[4] Recall that the Pauli matrices can be expressed in the computational basis $\{|0\rangle, |1\rangle\}$ as:

$$X = \sigma_x = \begin{pmatrix} 0 & 1 \\ 1 & 0 \end{pmatrix};\ Y = \sigma_y = \begin{pmatrix} 0 & -i \\ i & 0 \end{pmatrix};\ Z = \sigma_z = \begin{pmatrix} 1 & 0 \\ 0 & -1 \end{pmatrix};\ \mathbb{1} = \sigma_0 = \begin{pmatrix} 1 & 0 \\ 0 & 1 \end{pmatrix}. \tag{5.1}$$

The action of the Pauli operators on the states of the computational basis is

$$X|0\rangle = |1\rangle, \tag{5.2}$$
$$X|1\rangle = |0\rangle, \tag{5.3}$$

$$Y|0\rangle = i|1\rangle, \tag{5.4}$$
$$Y|1\rangle = -i|0\rangle, \tag{5.5}$$

$$Z|0\rangle = |0\rangle, \tag{5.6}$$
$$Z|1\rangle = -|1\rangle. \tag{5.7}$$

As a consequence, Pauli's matrices can be alternatively expressed in Dirac's notation as:

$$X = |0\rangle\langle 1| + |1\rangle\langle 0|, \tag{5.8}$$
$$Y = -i|0\rangle\langle 1| + i|1\rangle\langle 0|, \tag{5.9}$$
$$Z = |0\rangle\langle 0| - |1\rangle\langle 1|. \tag{5.10}$$

[5] This set has algebraic structure of group under the operation of matrix multiplication: factors $\pm 1, \pm i$ are necessary to guarantee closure under such operation.

2. Closure property, i.e., the product of any two elements of $\mathcal{P}_n$ must also be an element of $\mathcal{P}_n$. Multiplying $g = g_1 \otimes \cdots \otimes g_n \in \mathcal{P}_n$ and $h = h_1 \otimes \cdots \otimes h_n \in \mathcal{P}_n$, gives $gh = g_1 h_1 \otimes \cdots \otimes g_n h_n$, which also belongs to $\mathcal{P}_n$ (each single-qubit factor $g_j h_j$ is a Pauli matrix affected by a coefficient ± 1 ó $\pm i$).

3. For each element in $\mathcal{P}_n$ there is an inverse within $\mathcal{P}_n$: given $g = g_1 \otimes \cdots \otimes g_n \in \mathcal{P}_n$, the operator $g^\dagger = g_1^\dagger \otimes \cdots \otimes g_n^\dagger$ also belongs to $\mathcal{P}_n$ (recall that Pauli matrices are Hermitian, $X = X^\dagger$, $Y = Y^\dagger$, $Z = Z^\dagger$, $\mathbb{1} = \mathbb{1}^\dagger$). Furthermore, $gg^\dagger = g_1 g_1^\dagger \otimes \cdots \otimes g_n g_n^\dagger = \mathbb{1}^{\otimes n}$, implying that $g^\dagger$ is the inverse of g.

The previous properties are satisfied by *any* group, regardless of its nature. The following ones are specific of the elements of the Pauli group (Ref. [150]):

- Given that Pauli matrices (except for $\mathbb{1}$) are traceless, the elements of $\mathcal{P}_n$ are also traceless operators (with the exception of $\{\pm 1, \pm i\} \times \mathbb{1}^{\otimes n}$).

- Pauli matrices are unitary, and as a consequence the same is true for the elements of $\mathcal{P}_n$.

- The elements of $\mathcal{P}_n$ whose overall phases are ± 1 are Hermitian, unlike those with overall phases $\pm i$, which are anti Hermitian. Hence, we can partition $\mathcal{P}_n$ in two subsets: the first one consists of all the Hermitian elements $g \in \mathcal{P}_n$. These elements fulfill $g^2 = \mathbb{1}^{\otimes n}$, and consequently their eigenvalues are ± 1; the second subset consists of all the anti Hermitian elements $h \in \mathcal{P}_n$, which satisfy $h^2 = -\mathbb{1}^{\otimes n}$, and therefore have eigenvalues $\pm i$.

- Any two elements belonging to $\mathcal{P}_n$ either commute or anticommute. This property is trivial for $\mathcal{P}_1$. Following literally Ref. [150], we can extend it to $\mathcal{P}_n$ by defining a function $f(g_j, h_j)$ of $g_j, h_j \in \mathcal{P}_1$, such that

$$f(g_j, h_j) = \begin{cases} 0 & \text{if } g_j \text{ and } h_j \text{ conmmute,} \\ 1 & \text{if } g_j \text{ and } h_j \text{ anticonmmute.} \end{cases} \tag{5.12}$$

  Note that $g_j h_j = (-1)^{f(g_j,h_j)} h_j g_j$. Taking now two elements $g = g_1 \otimes \cdots \otimes g_n$ and $h = h_1 \otimes \cdots \otimes h_n$ in $\mathcal{P}_n$, and evaluating their commutator and anti-commutator, we obtain

$$[g, h] = gh - hg = hg\ ((-1)^{\sum_{j=1}^n f(g_j,h_j)} - 1), \tag{5.13}$$

$$\{g, h\} = gh + hg = hg\ ((-1)^{\sum_{j=1}^n f(g_j,h_j)} + 1). \tag{5.14}$$

  Obviously, g and h either commute or anticommute, depending on the number of pairs of one-qubit tensor factors (g_j, h_j) which anticommute. The necessary and sufficient condition for $g, h \in \mathcal{P}_n$ to commute is that $\sum_{j=1}^n f(g_j, h_j)$ is an *even* number, which implies that these elements of $\mathcal{P}_n$ *must have an even number of elements of* $\mathcal{P}_1$ *that anticommute.*

According to group theory, for any group G (v.g., $\mathcal{P}_n$) there exists a subset of elements that *generates* the entire group. Assuming that the group operation is a multiplication (in case of additive groups the definition is similar), we say that a subset $\gamma_G = \{g_1, \ldots, g_l\} \subseteq G$ generates G if any element of G can be written as a product of elements of γ_G. The notation $G = \langle g_1, \ldots, g_l \rangle$

(or $G = \langle \gamma_G \rangle$) is commonly used to describe this fact. The set γ_G is called a *generating set* or *generator* of the group G. Note that the generating set of a group is not necessarily unique. Furthermore, one can always choose a generating set γ_G in such a way that all its elements are independent, in the sense that no element of γ_G is the product of other elements of γ_G.[6] As a consequence, removing dependent elements from a generating set γ_G does not alter its capacity to generate the group G, unlike the elimination of any operator g_i from an independent generating set: this would result in a decrease of the size of the (new) generated group.

5.1.2 Stabilized states and stabilizing operators

The key definition on which the stabilizer formalism is based is the following: we say that a state $|\psi\rangle$ is *stabilized* by some operator A if $|\psi\rangle$ is an eigenstate of A with eigenvalue $+1$, i.e., $A|\psi\rangle = |\psi\rangle$. The operator A is a *stabilizing operator* of $|\psi\rangle$. For instance, the state $|+\rangle = \frac{1}{\sqrt{2}}(|0\rangle + |1\rangle)$ is the eigenvector of the Pauli operator X with eigenvalue $+1$, $X|+\rangle = |+\rangle$, and consequently it is a state (in fact, the only one) stabilized by X.

We can easily extend this concept to states of higher dimension: if we consider an operator given by the tensor product of two Pauli matrices, then, we find that there are two linearly independent states stabilized by such an operator. For example (Ref. [150]), given the operator $X \otimes X = X_1 X_2$, we see that it stabilizes both the state $|\Phi^+\rangle = \frac{1}{\sqrt{2}}(|00\rangle + |11\rangle)$ and the state $|\Psi^+\rangle = \frac{1}{\sqrt{2}}(|10\rangle + |01\rangle)$, i.e., $X_1X_2|\Phi^+\rangle = |\Phi^+\rangle$, and $X_1X_2|\Psi^+\rangle = |\Psi^+\rangle$.

As we will see later, the denomination *stabilizer states* on n qubits comes from the fact that such kind of states are stabilized by n-fold tensor products of Pauli matrices. But there are certain subtle aspects in this generalization that must be clarified:

Recall that we have stated above, on p. 98, that $\mathcal{P}_n$ splits into two subsets: first, the subset of Hermitian elements $g \in \mathcal{P}_n$, whose overall phases are ± 1, which satisfy $g^2 = \mathbb{1}^{\otimes n}$, and have eigenvalues ± 1. And second, the subset of anti-Hermitian elements $h \in \mathcal{P}_n$, whose overall phases are $\pm i$, which satisfy $h^2 = -\mathbb{1}^{\otimes n}$, and have eigenvalues $\pm i$. According to the definitions of stabilized state and stabilizing operator previously given, the eigenvalue of the stabilizing operator A corresponding to the stabilized state $|\psi\rangle$ must necessarily be equal to $+1$. As a consequence, the anti-Hermitian elements of $\mathcal{P}_n$ cannot be stabilizing operators of any state. Therefore, the anti-Hermitian half of the Pauli group $\mathcal{P}_n$ is discarded from the stabilizer formalism.[7]

Moreover, there is another operator belonging to the Pauli group $\mathcal{P}_n$ that is also out of the stabilizer formalism: the operator $-\mathbb{1}^{\otimes n}$. Here is the reason: if we suppose that this operator stabilizes some state $|\psi\rangle$, then it must fulfill $-\mathbb{1}^{\otimes n}|\psi\rangle = |\psi\rangle = -|\psi\rangle$, which results in $|\psi\rangle = 0$. This rules $-\mathbb{1}^{\otimes n}$ out as stabilizing operator for any meaningful state.

According to Ref. [150], let $g \in \mathcal{P}_n$ be a Hermitian element, and let us consider the operator given by $P_g = \frac{1}{2}(\mathbb{1}^{\otimes n} + g)$, where $\mathbb{1}^{\otimes n}$ is the identity operator in $\mathcal{P}_n$. Such operator P_g has the

[6] Or more precisely: given certain coefficients $a_i \in \{0, 1\}$, no product of the form $g_1^{a_1} \cdots g_k^{a_k}$ will be equal to the identity, unless $a_i = 0, \forall i$.

[7] Alternatively, on a more fundamental level, we demand that stabilizing operators are observables, and hence Hermitian.

following property:

$$\left(\frac{1}{2}(\mathbb{1}^{\otimes n}+g)\right)^2=\frac{1}{4}(\mathbb{1}^{\otimes n}+2g+g^2)=\frac{1}{4}(\mathbb{1}^{\otimes n}+2g+\mathbb{1}^{\otimes n})=\frac{1}{2}(\mathbb{1}^{\otimes n}+g), \tag{5.15}$$

that is, $P_g = P_g^2$, which implies that P_g is a projection operator. It is easy to check that $\frac{1}{2}(\mathbb{1}^{\otimes n}+g)|\psi\rangle = |\psi\rangle$ for those states $|\psi\rangle$ stabilized by g, and $\frac{1}{2}(\mathbb{1}^{\otimes n}+g)|\phi\rangle = 0$ for the other eigenvectors of g (those corresponding to the eigenvalue -1). From these features we conclude that $P_g = \frac{1}{2}(\mathbb{1}^{\otimes n}+g)$ is the *projection operator onto the states stabilized by* g. These states constitute a Hilbert subspace whose dimension, d_g can be calculated from the trace of the projection operator P_g,

$$d_g=\mathrm{tr}\left[\frac{1}{2}(\mathbb{1}^{\otimes n}+g)\right]=\frac{1}{2}\mathrm{tr}(\mathbb{1}^{\otimes n})=2^{n-1}, \tag{5.16}$$

where we have used the traceless property $\mathrm{tr}(g) = 0$ fulfilled by any operator of $\mathcal{P}_n$. Therefore, any Hermitian operator of the Pauli group $\mathcal{P}_n$ stabilizes exactly 2^{n-1} linearly independent states.[8]

Let us see now what happens when we consider states stabilized by several Pauli operators. For instance, let us take those states stabilized by the operator X_1X_2. In addition, let us impose the condition that they are stabilized by $Z\otimes Z = Z_1Z_2$. Then, the *only* state out of the two $(|\Phi^+\rangle, |\Psi^+\rangle)$ initially stabilized by X_1X_2 which is also stabilized by Z_1Z_2 is $|\Phi^+\rangle = \frac{1}{\sqrt{2}}(|00\rangle + |11\rangle)$.

We observe a reduction in the dimension of the Hilbert subspace of stabilized states. In order to generalize this example, let $g, h \in \mathcal{P}_n$ be two different Hermitian elements of the Pauli group of order n such that they *commute*: then, g and h will have common eigenvectors. To determine the number of linearly independent states stabilized by both operators at the same time, we can resort to the corresponding projection operators P_g and P_h onto the subspaces stabilized by g and h. The intersection of both subspaces is described by P_gP_h, and its dimension, $d_{(g,h)}$, coincides with the trace of P_gP_h, namely,

$$d_{(g,h)}=\mathrm{tr}\left[\frac{1}{2}(\mathbb{1}^{\otimes n}+g)\frac{1}{2}(\mathbb{1}^{\otimes n}+h)\right]=\mathrm{tr}\left[\frac{1}{4}(\mathbb{1}^{\otimes n}+g+h+gh)\right]=2^{n-2}. \tag{5.17}$$

Again, we have used the traceless property for Pauli operators, $\mathrm{tr}(g) = \mathrm{tr}(h) = 0$, and the fact that $\mathrm{tr}(gh) = 0$ since $gh \in \mathcal{P}_n$, and $g \neq h$, by hypothesis. The obvious conclusion is the following: the number of linearly independent states stabilized both by g and by h is 2^{n-2}, and hence *the dimension of the stabilized subspace is reduced by half with respect to the initial* d_g *because of the introduction of a new commuting stabilizing operator* h. The repetition of such projection argument leads us to state that

1. a set of k mutually independent[9] and commuting n-fold operators of $\mathcal{P}_n$ jointly stabilizes 2^{n-k} linearly independent states, and

[8] For instance, the operator $X\otimes X \in \mathcal{P}_2$ stabilizes two linearly independent states, namely, $|\Phi^+\rangle$ and $|\Psi^+\rangle$.

[9] Recall footnote 6 on p. 99. The independence property means that no operator can be written as a product of other operators, up to a sign, and this is equivalent to products of operators being traceless (Ref. [150]).

2. for each new addition of an independent and commuting operator belonging to $\mathcal{P}_n$ to such set, the dimension of the common stabilized subspace is cut in half.

Another remarkable issue is the following: if a given set of elements of the Pauli group $\mathcal{P}_n$ jointly stabilizes a common subspace, then such set constitutes a *subgroup*[10] in $\mathcal{P}_n$. This follows from three facts: (i) In case that two given Hermitian operators $g, h \in \mathcal{P}_n$ stabilize a certain state $|\psi\rangle$, then their product $gh \in \mathcal{P}_n$ also stabilizes the same state, i.e., $g|\psi\rangle = |\psi\rangle$, $h|\psi\rangle = |\psi\rangle \Rightarrow gh|\psi\rangle = |\psi\rangle$. (ii) The identity operator $\mathbb{1}^{\otimes n}$ stabilizes all states. (iii) The Hermitian elements of $\mathcal{P}_n$ are their own inverses (and trivially, they stabilize the same states).

5.1.3 Stabilizers and stabilizer states

Now we can proceed to define on a sound basis the concepts of *stabilizer* and *stabilizer state*, along with a summary of key ideas, some of them already presented:

- As we have said before, given a set of $k(\leq n)$ mutually independent and commuting[11] operators $\{g_1, \ldots, g_k\}$ of the Pauli group $\mathcal{P}_n$, this set stabilizes a total amount of 2^{n-k} linearly independent states, which collectively constitute a basis of the common vector space stabilized by the k operators. Let us denote such stabilized vector space as $V_{\mathcal{S}}$.

- Any other operator h which is obtained by multiplying in all possible ways the k operators g_i among one another (there are 2^k ways to do that) stabilizes $V_{\mathcal{S}}$ as well. Moreover, the identity operator $\mathbb{1}^{\otimes n}$, and the corresponding inverse operators of the g_i (themselves) also stabilize $V_{\mathcal{S}}$. Therefore, the set of all the n-fold Pauli operators that together stabilize the vector space $V_{\mathcal{S}}$ has the structure of a group. In particular, it is a subgroup of the Pauli group $\mathcal{P}_n$, the so-called *stabilizer group* of $V_{\mathcal{S}}$, or simply *stabilizer* of $V_{\mathcal{S}}$, denoted by $\mathcal{S}$.

- Therefore, a stabilizer $\mathcal{S} \subseteq \mathcal{P}_n$, is defined as an Abelian subgroup of $\mathcal{P}_n$ which does not contain the operator $-\mathbb{1}^{\otimes n}$ (Ref. [152]). A stabilizer consists of 2^k n-qubit Pauli operators, $s_i, i = 1, \ldots, 2^k$, mutually commuting, and all of them Hermitian (with overall phases ± 1). Hence, we can write $s_i = \alpha_i M_1^{(i)} \otimes \cdots \otimes M_n^{(i)} \in \mathcal{P}_n$, $i = 1, \ldots, 2^k$, for some $k \leq n$, where α_i is an overall phase factor, and $M_j^{(i)}$ stands for one of the four one-qubit Pauli operators $\{\mathbb{1}, X, Y, Z\}$ acting on qubit j. The operators s_i are called *stabilizing operators*.

- The set of k independent operators $\{g_1, \ldots, g_k\}$ which under multiplication generates the group $\mathcal{S}$ is the *generating set* or *generator* of the stabilizer $\mathcal{S}$. We will denote it by $\gamma_{\mathcal{S}} = \{g_1, \ldots, g_k\}$. Following the notation previously introduced on p. 98, we have $\mathcal{S} = \langle \gamma_{\mathcal{S}} \rangle$. Each operator g_i is a *generating operator*. The number of generating operators is the cardinality of the generator, $|\gamma_{\mathcal{S}}| = k$.

- A stabilizer $\mathcal{S}$ is completely specified by its generator $\gamma_{\mathcal{S}}$. Nevertheless, the generator is not unique: note that given two generating operators $g_i, g_j \in \gamma_{\mathcal{S}}$, $g_i \neq g_j$, we can always substitute any of them by their product $h = g_i g_j$, and the new set $\tilde{\gamma}_{\mathcal{S}}$ obtained is a generator of $\mathcal{S}$ as well.

[10] A subgroup is a subset of group elements that by themselves constitute a group. Consequently, a subgroup satisfies the group properties on p. 97.

[11] So that they can be diagonalized simultaneously and, therefore, share a common set of eigenvectors.

- If the cardinality of the generator is $|\gamma_{\mathcal{S}}| = k$, then the cardinality of the corresponding stabilizer is $|\mathcal{S}| = 2^k$, and the dimension of the stabilized vector space is $\dim V_{\mathcal{S}} = 2^{n-k} = 2^{n-|\gamma_{\mathcal{S}}|}$. Therefore, the generator provides and economical way to describe not only the stabilizer $\mathcal{S}$, but also the stabilized vector space $V_{\mathcal{S}}$ (much more compact than the usual vector state description), which is one of the main advantages of the stabilizer formalism.[12]

- The case where the number of generating operators, k, equals the number of qubits, n, is special: if $|\gamma_{\mathcal{S}}| = n$, then $|\mathcal{S}| = 2^n$, and the dimension of the vector space stabilized by $\mathcal{S}$ is $\dim V_{\mathcal{S}} = 2^0 = 1$. As a consequence, for the set of 2^n stabilizing operators $s_i \in \mathcal{S}$, there exists an unique common n-qubit eigenstate $|\psi\rangle$ with eigenvalue $+1$, hence fulfilling $s_i|\psi\rangle = |\psi\rangle, \forall i$. Such state $|\psi\rangle$ is called a *stabilizer state*,[13] since it is the only state stabilized by each and every stabilizing operator $s_i \in \mathcal{S}$. Alternatively, we define a stabilizer state on n qubits as the simultaneous $+1$ eigenstate of n independent, commuting elements of the Pauli group $\mathcal{P}_n$.

5.1.4 Unitary operations and stabilizer formalism

For our purposes, it is also useful to make a brief review about the effect of unitary operations on the stabilizer, and the associated dynamics of the stabilized vector subspaces inside the larger Hilbert space in which they are immersed.

Let $V_{\mathcal{S}}$ be the space of states stabilized by a stabilizer $\mathcal{S}$. Suppose that we apply an arbitrary unitary operation U (i.e., an U such that $U^\dagger U = UU^\dagger = \mathbb{1}$) on $V_{\mathcal{S}}$, so that the stabilized states "evolve" under U. Let $|\psi\rangle \in V_{\mathcal{S}}$ be any of such states, and $s_i \in \mathcal{S}$ any stabilizing operator.

[12] An example will suffice: take the following generator

$$\gamma(\mathcal{S}) \equiv \begin{cases} g_1 & X & Z & Z & X & \mathbb{1} \\ g_2 & \mathbb{1} & X & Z & Z & X \\ g_3 & X & \mathbb{1} & X & Z & Z \\ g_4 & Z & X & \mathbb{1} & X & Z. \end{cases} \tag{5.18}$$

This 4 generating operators completely specify the corresponding $2^4 = 16$ operators of the stabilizer $\mathcal{S}$, and consequently the stabilized vector space $V_{\mathcal{S}}$, whose dimension is $\dim V_{\mathcal{S}} = 2$. A basis of $V_{\mathcal{S}}$ is, for instance,

$$\begin{aligned} |\psi_1\rangle = \frac{1}{4}(&|00000\rangle + |10010\rangle + |01001\rangle + |10100\rangle + |01010\rangle - |11011\rangle - |00110\rangle - |11000\rangle \\ &-|11101\rangle - |00011\rangle - |11110\rangle - |01111\rangle - |10001\rangle - |01100\rangle - |10111\rangle + |00101\rangle), \end{aligned} \tag{5.19}$$

$$\begin{aligned} |\psi_2\rangle = \frac{1}{4}(&|11111\rangle + |01101\rangle + |10110\rangle + |01011\rangle + |10101\rangle - |00100\rangle - |11001\rangle - |00111\rangle \\ &-|00010\rangle - |11100\rangle - |00001\rangle - |10000\rangle - |01110\rangle - |10011\rangle - |01000\rangle + |11010\rangle). \end{aligned} \tag{5.20}$$

[13] We illustrate this point with a simple example taken from Ref. [150]: the state $|\Phi^-\rangle = \frac{1}{\sqrt{2}}(|00\rangle - |11\rangle)$ is the only state stabilized both by $-X_1X_2$ and by Z_1Z_2. These two operators commute, since there is an even number one-qubit tensor factors that anticommute [see eq. (5.13)]. On the other hand, the two operators are independent, and therefore, they constitute a generator $\gamma_{\mathcal{S}}$ of certain stabilizer $\mathcal{S}$. Since the cardinality of this generator equals 2, then the number of operators in the stabilizer is equal to $2^2 = 4$, namely: $\mathcal{S} = \{\mathbb{1} \otimes \mathbb{1}, -X \otimes X, Y \otimes Y, Z \otimes Z\}$. The dimension of the stabilized vector space $V_{\mathcal{S}}$ is equal to $\dim V_{\mathcal{S}} = 2^{2-2} = 1$. Therefore, there is a unique state which is stabilized by $\mathcal{S}$, the aforementioned $|\Phi^-\rangle = \frac{1}{\sqrt{2}}(|00\rangle - |11\rangle)$, which is a stabilizer state.

Given that, by definition, $s_i|\psi\rangle = |\psi\rangle$, then

$$U|\psi\rangle = Us_i|\psi\rangle = Us_iU^\dagger U|\psi\rangle. \tag{5.21}$$

According to Eq. (5.21), the transformed state under the action of U, namely $U|\psi\rangle$, is stabilized by the operator $Us_iU^\dagger$. We can extend this result to the entire initial subspace $V_\mathcal{S}$, and conclude that the new transformed vector space $UV_\mathcal{S}$ is stabilized by the group $U\mathcal{S}U^\dagger \equiv \{Us_iU^\dagger \mid s_i \in \mathcal{S}\}$. In other words, *we can follow the unitary dynamics of the stabilized states through the corresponding transformation undergone by the stabilizer.*

In addition, if $\gamma_\mathcal{S} = \{g_1, \ldots, g_k\}$ is the generator of $\mathcal{S}$, then $U\mathcal{S}U^\dagger = \langle Ug_1U^\dagger, \ldots, Ug_kU^\dagger\rangle$. That is, to account for the change that U induces on the stabilizer $\mathcal{S}$ *it suffices to see how* U *affects the generator* $\gamma_\mathcal{S}$.

As an easy but useful example, let us discuss concisely the case of the one-qubit Hadamard gate H, which can be expressed in the computational basis in matrix form as

$$H = \frac{1}{\sqrt{2}}\begin{pmatrix} 1 & 1 \\ 1 & -1 \end{pmatrix}, \tag{5.22}$$

or in Dirac's notation as $H = \frac{1}{\sqrt{2}}(|0\rangle\langle 0| + |0\rangle\langle 1| + |1\rangle\langle 0| - |1\rangle\langle 1|)$. The Hadamard gate is a unitary operation ($H^\dagger = H^{-1}$), to which we can apply what we have said before. A well-known result reflects the way Pauli operators are transformed under the action of H, namely

$$HXH^\dagger = Z;\ HYH^\dagger = -Y;\ HZH^\dagger = X;\ H\mathbb{1}H^\dagger = \mathbb{1}. \tag{5.23}$$

Consequently, if H is applied on a quantum state stabilized by the operator Z (i.e., the state $|0\rangle$) then the resulting state (i.e., $|+\rangle$) is stabilized by the transformed stabilizing operator, which is precisely X, as expected. This —apparently naive— result entails one of the main advantages of the stabilizer formalism, which is evidenced when we apply the same idea to n qubits: let us take the n-qubit state whose stabilizer is $\mathcal{S} = \langle Z_1, Z_2, \ldots, Z_n\rangle$. Such state, on the basis of the one-qubit case that we have just discussed, is $|0\rangle^{\otimes n}$. If we apply now the Hadamard operation onto each of the n qubits, i.e., $H^{\otimes n}$, then the stabilizer of the resulting state after the transformation is $\mathcal{S}' = \langle X_1, X_2, \ldots, X_n\rangle$, so that the state is $|+\rangle^{\otimes n}$. The key point is the remarkable economy of such description: the resulting vector state, in its usual expression, requires 2^n complex amplitudes to be specified, whereas the alternative description based on the generator is *linear* with n (there are n generating operators, which by themselves completely specify the stabilizer, and therefore the stabilized state). This is the main thrust of the stabilizer formalism, as we pointed out at the beginning of this chapter, and also on p. 102.

Of course, the same ideas come into play for other one-qubit unitary operations, like the phase gate $S = Ph(\frac{\pi}{2}) = |0\rangle\langle 0| + i|1\rangle\langle 1|$, in matrix form

$$S = \begin{pmatrix} 1 & 0 \\ 0 & i \end{pmatrix}, \tag{5.24}$$

or for unitary operations involving more than one qubit, like for instance the 2-qubit controlled-NOT (C-NOT, XOR or ${}^CX$) gate,

$${}^CX = |0\rangle\langle 0| \otimes \mathbb{1} + |1\rangle\langle 1| \otimes X = |00\rangle\langle 00| + |01\rangle\langle 01| + |10\rangle\langle 11| + |11\rangle\langle 10|, \tag{5.25}$$

or in matrix form

$$ {}^{C}X = \begin{pmatrix} \mathbb{1} & 0 \\ 0 & X \end{pmatrix} = \begin{pmatrix} 1 & 0 & 0 & 0 \\ 0 & 1 & 0 & 0 \\ 0 & 0 & 0 & 1 \\ 0 & 0 & 1 & 0 \end{pmatrix}, \tag{5.26} $$

which, as it is well-known, in combination with the Hadamard gate can be used to create entanglement (Ref. [152]). The fact that the action of these three gates can be described within the stabilizer formalism is interesting since any unitary operation taking elements of $\mathcal{P}_n$ to elements of $\mathcal{P}_n$ under conjugation can be composed from the Hadamard, C-NOT and phase gates. We refer the interested reader to Ref. [152], Sect. 10.5.2, for further details.

The Clifford group

We must remark that given some n-qubit stabilizer state $|\psi\rangle$ and an arbitrary unitary operator U, the resulting state $U|\psi\rangle$ after the action of U *is not*, in general, a "Pauli-type" stabilizer state, meaning that the transformed stabilizer under conjugation by U, i.e., $U\mathcal{S}U^\dagger = \langle Ug_1U^\dagger, \ldots, Ug_kU^\dagger\rangle$, need not be a subgroup of the Pauli group $\mathcal{P}_n$.[14] Noticing this fact makes particularly interesting (and important) to consider those unitary operations that map elements of the Pauli group $\mathcal{P}_n$ to elements *also* belonging to $\mathcal{P}_n$ under conjugation, and hence, such that they apply a "Pauli-type" stabilizer state onto another stabilizer state of the same type. The set of operations which verify this condition is a group, known as the *Clifford group*, $\mathcal{C}_n$. Unitary operations belonging to the Clifford group are usually called Clifford elements, Clifford operations or Clifford unitaries. According to a well-known definition in group theory, those operations that map a group G onto itself under conjugation constitute the so-called *normalizer* of the group, $N(G)$. Therefore, the Clifford group is the *normalizer of the Pauli group*, i.e.,

$$ \mathcal{C}_n = N(\mathcal{P}_n) = \{U \mid U\mathcal{P}_nU^\dagger = \mathcal{P}_n\}. \tag{5.27} $$

The normalizer of the one-qubit Pauli group, $N(\mathcal{P}_1)$, is the one-qubit Clifford group, $\mathcal{C}_1$, whose elements are the one-qubit Clifford operations. It is straightforward to check that the Pauli matrices themselves belong to $\mathcal{C}_1$: if g and h are two arbitrary Pauli matrices, then the transformation of h under conjugation with respect to g fulfills $ghg^\dagger = \pm\, hgg^\dagger = \pm\, h$, given that g and h either commute or anticommute.

The so-called *local* Clifford (LC) group on n qubits, $\mathcal{C}_1^n$, is the n-fold tensor product of the one-qubit Clifford group $\mathcal{C}_1$ with itself. The elements of $\mathcal{C}_1^n$ are the LC operators, of the form $U = \bigotimes_{i=1}^n U_i$, where $U_i \in \mathcal{C}_1$.

About the generating set of the one-qubit Clifford group $\mathcal{C}_1$, it is shown in Refs. [146, 153, 151] that, disregarding overall phases, $\mathcal{C}_1$ is a finite group with 24 elements, all of them obtainable as a product of operators chosen from the set $\{H, S\}$, i.e., the Hadamard and phase unitary

[14] Recall that, according to the definition on p. 99, if certain quantum state $|\psi\rangle$ is an eigenstate with eigenvalue $+1$ of some operator A, i. e., $A|\psi\rangle = |\psi\rangle$, then $|\psi\rangle$ is stabilized by A, and A is a stabilizing operator for $|\psi\rangle$. Note that nothing in this definition imposes A to be an operator of the Pauli group.

operations, which also belong to the one-qubit Clifford group.[15] In compact notation:

$$N(\mathcal{P}_1) = \langle H, S \rangle. \tag{5.29}$$

With respect to the Clifford group $\mathcal{C}_n$, the corresponding generator consists of the unitary one-qubit operations H and S, along with an additional unitary operator (Refs. [146, 153, 151]): although there is some freedom for this choice, the most usual option is the C-NOT gate or, alternatively (and better for our purposes), the controlled-Z gate[16] ${}^{C}Z$, defined as

$${}^{C}Z = |0\rangle\langle 0| \otimes \mathbb{1} + |1\rangle\langle 1| \otimes Z = |00\rangle\langle 00| + |01\rangle\langle 01| + |10\rangle\langle 10| - |11\rangle\langle 11|, \tag{5.30}$$

or in matrix form

$${}^{C}Z = \begin{pmatrix} \mathbb{1} & 0 \\ 0 & Z \end{pmatrix} = \begin{pmatrix} 1 & 0 & 0 & 0 \\ 0 & 1 & 0 & 0 \\ 0 & 0 & 1 & 0 \\ 0 & 0 & 0 & -1 \end{pmatrix}. \tag{5.31}$$

Note that one can define two-qubit general controlled unitary operations ${}^{C}U = |0\rangle\langle 0| \otimes \mathbb{1} + |1\rangle\langle 1| \otimes U$ (of which ${}^{C}Z$ and ${}^{C}X$ are two remarkable instances): one of the qubits onto which ${}^{C}U$ acts is the so-called *control* qubit, and the other is the *target* qubit. If the control qubit is in the state $|0\rangle$, $\mathbb{1}$ is applied to the target qubit. Only when the control qubit is in the state $|1\rangle$ is the U operation applied to the target qubit. In general, the action of a general controlled unitary operation is *not* symmetric under exchange of the dichotomic character control/target between the qubits. That is the case for ${}^{C}X$. On the contrary, ${}^{C}Z$ has the little advantage of being symmetric under control/target exchange, and that is the reason why some authors (Refs. [153, 154, 155, 150], and we among them) prefer it. Anyway, we can write

$$\mathcal{C}_n = N(\mathcal{P}_n) = \langle H, S, {}^{C}X \rangle = \langle H, S, {}^{C}Z \rangle. \tag{5.32}$$

5.1.5 Measurements in the stabilizer formalism

Although not fundamental for the purposes of this thesis (in a first reading it may be skipped), for the sake of completeness we will devote a few lines in this subsection to the description of measurements in the stabilizer formalism. We will follow Refs. [152, 150], where we refer the interested reader for further details. The main motivation is that any quantum operation (think, for instance, in applications such as measurement-based quantum computation, or a quantum error correction) may be thought of as a unitary operation followed by a projective measurement whose outcome is ignored (Ref. [24]). Focussing on measurements, we will consider those that are in a certain sense "natural" in the context of the stabilizer formalism.

[15] Such belonging to $\mathcal{C}_1$ is trivial, given the way H transforms the Pauli matrices under conjugation in Eqs. (5.23), and since

$$SXS^\dagger = Y;\ SYS^\dagger = -X;\ SZS^\dagger = Z;\ S\mathbb{1}S^\dagger = \mathbb{1}. \tag{5.28}$$

[16] It is straighforward to check that ${}^{C}X = (\mathbb{1} \otimes H)\,{}^{C}Z\,(\mathbb{1} \otimes H)$, which in the end means that it is possible to reproduce the action of a C-NOT gate by combining one ${}^{C}Z$ gate and two Hadamard gates on the target qubit. This accounts for the freedom of choice aforementioned.

Let $|\psi\rangle$ be a n-qubit stabilizer state, whose stabilizer $\mathcal{S}$ is generated by $\gamma_{\mathcal{S}} = \{g_1, \ldots, g_n\}$. This implies that $\dim V_{\mathcal{S}} = 1$. Let us suppose that we make a measurement of certain observable represented by a Hermitian operator M. To exploit the power of the stabilizer formalism, we would like the post-measurement state to be a stabilizer state as well. In order to satisfy such requirement, and given that according to QT the post-measurement state is an eigenstate of M, then M must be a Hermitian tensor product of Pauli matrices, i.e., a Hermitian element (overall phase ± 1) of the Pauli group $\mathcal{P}_n$, namely

$$M = \alpha_M M_1 \otimes \ldots \otimes M_n, \tag{5.33}$$

where α_M is an overall phase and each M_j is one of the Pauli matrices $\{\mathbb{1}, X, Y, Z\}$ acting on qubit j. A measurement of such an operator M is sometimes called a *Pauli measurement*.

For the sake of simplicity, let us assume that $M \in \mathcal{P}_n$ with $\alpha_M = +1$ (if $\alpha_M = -1$, the discussion is almost the same except for a exchange in the probabilities of the two outcomes). Let the state of the physical system of n qubits be the stabilizer state $|\psi\rangle$, and suppose we carry out a measurement of M. We are interested in the transformation (if any) undergone by the stabilizer $\mathcal{S}$. There are two possibilities:

- M commutes with *all* the generating operators $\{g_1, \ldots, g_n\}$ of $\mathcal{S}$.

  Then, either M or $-M$ is an element of $\mathcal{S}$: taking any $g_j \in \gamma_{\mathcal{S}}$, we have

  $$g_j M|\psi\rangle = M g_j|\psi\rangle = M|\psi\rangle, \ \forall g_j \ ; \ j = 1, \ldots, n. \tag{5.34}$$

  That is, $M|\psi\rangle \in V_{\mathcal{S}}$. Since $\dim V_{\mathcal{S}} = 1$, $M|\psi\rangle$ must be a multiple of $|\psi\rangle$. On the other hand $M \in \mathcal{P}_n$, and thus $M^2 = \mathbb{1}^{\otimes n}$, which leads to $M|\psi\rangle = \pm\,|\psi\rangle$. I.e, either M or $-M$ belongs to $\mathcal{S}$. Let us assume that $M \in \mathcal{S}$ (otherwise the discussion is similar): then $M|\psi\rangle = |\psi\rangle$, and hence $|\psi\rangle$ is an eigenstate of M with eigenvalue $+1$: *the measurement outcome is* $+1$ *with probability one, whereas the measurement does not alter the state, and the stabilizer remains invariant.*

- M anticommutes with *at least one* of the generating operators $\{g_1, \ldots, g_n\}$ of $\mathcal{S}$.

  Without loss of generality we can assume that M anticommutes only with certain $g \in \gamma_{\mathcal{S}}$, and commutes with the rest.[17] Then, since $M^2 = \mathbb{1}^{\otimes n}$ (because $M \in \mathcal{P}_n$) its eigenvalues are ± 1. Now we can write the projection operator corresponding to the outcomes ± 1 of the measurement of M as $\Pi_M^{(\pm)} = \frac{1}{2}(\mathbb{1}^{\otimes n} \pm M)$, and subsequently apply the rules of quantum mechanics in order to calculate the probabilities $p(\pm 1)$ of such outcomes, obtaining

  $$p(+1) = \mathrm{tr}\left(\frac{\mathbb{1}^{\otimes n} + M}{2}|\psi\rangle\langle\psi|\right), \tag{5.36}$$

  $$p(-1) = \mathrm{tr}\left(\frac{\mathbb{1}^{\otimes n} - M}{2}|\psi\rangle\langle\psi|\right). \tag{5.37}$$

[17] If, for instance, M anticommuted with another generating operator different from g, say g_i, we would have

$$M g g_i = -g M g_i = g g_i M, \tag{5.35}$$

and therefore M would commute with gg_i. Recall that, according to one of the key properties of a stabilizer $\mathcal{S}$ listed on p. 101, the substitution of an element g_i of the generator $\gamma_{\mathcal{S}}$ by the product $g_i g$ with another element g produces a new generator $\tilde{\gamma}_{\mathcal{S}}$ *of the same stabilizer* $\mathcal{S}$. Proceeding with such substitutions, we arrive at the desired case in which M anticommutes only with $g \in \gamma_{\mathcal{S}}$.

Using the fact that $g|\psi\rangle = |\psi\rangle$, and also that $Mg = -gM$:

$$p(+1) = \mathrm{tr}\left(\frac{\mathbb{1}^{\otimes n} + M}{2} g|\psi\rangle\langle\psi|\right) = \mathrm{tr}\left(g\frac{\mathbb{1}^{\otimes n} - M}{2}|\psi\rangle\langle\psi|\right). \tag{5.38}$$

The trace is invariant under cyclic permutation of a product of operators. On the other hand, g is a Hermitian operator, i.e., $g = g^\dagger$. Since $g|\psi\rangle = |\psi\rangle$, then $\langle\psi|g = \langle\psi|g^\dagger = \langle\psi|$. Substituting in Eq. (5.38) and operating:

$$p(+1) = \mathrm{tr}\left(g\frac{\mathbb{1}^{\otimes n} - M}{2}|\psi\rangle\langle\psi|\right) = \mathrm{tr}\left(\frac{\mathbb{1}^{\otimes n} - M}{2}|\psi\rangle\langle\psi|g\right) \tag{5.39}$$

$$= \mathrm{tr}\left(\frac{\mathbb{1}^{\otimes n} - M}{2}|\psi\rangle\langle\psi|g^\dagger\right) = \mathrm{tr}\left(\frac{\mathbb{1}^{\otimes n} - M}{2}|\psi\rangle\langle\psi|\right) = p(-1). \tag{5.40}$$

And given that $p(+1) + p(-1) = 1$, we conclude that $p(+1) = p(-1) = 1/2$.

If the result of measuring M is $+1$ (this will happen with probability $1/2$), then the state of the system after the measurement, following the rules of quantum mechanics, will be

$$|\psi^{(+)}\rangle = \frac{\Pi_M^{(+)}|\psi\rangle}{\sqrt{p(+1)}} = \frac{1}{\sqrt{2}}(\mathbb{1}^{\otimes n} + M)|\psi\rangle. \tag{5.41}$$

Notice that the stabilizer of this state, say $\tilde{\mathcal{S}}$, has a generator obtained from $\gamma_{\mathcal{S}} = \{g_1, \ldots, g_n\}$, substituting g —which anticommutes with M— by M itself. In a similar way, if the result of measuring M is -1, the stabilizer $\tilde{\mathcal{S}}$ of the post-measurement state will have a generator obtained from $\gamma_{\mathcal{S}}$ substituting g by $-M$.

In a nutshell, using the stabilizer formalism, the description of the action of measuring a Hermitian operator $M \in \mathcal{P}_n$ (a Pauli measurement) on a stabilizer state $|\psi\rangle$ with stabilizer $\mathcal{S}$ is the following:

1. Find a generator $\gamma_{\mathcal{S}}$ of $\mathcal{S}$ such that *at most one* generating operator anticommutes with M.

2. If all the generating operators of $\gamma_{\mathcal{S}}$ commute with M, then the result of the measurement of M ($+1$ or -1) will occur with probability one, and both the state $|\psi\rangle$ and the stabilizer $\mathcal{S}$ will be left invariant.

3. If one generating operator g anticommutes with M, then the state after the measurement of M will have a new stabilizer $\tilde{\mathcal{S}}$ whose generator is obtained from $\gamma_{\mathcal{S}}$, replacing g by $\pm M$. The outcomes of the measurement (± 1) will occur at random.

In any case, the post-measurement state after a Pauli measurement is carried out on a stabilizer state is also a stabilizer state.

At this point, we finish our review of the basics of the stabilizer formalism. For additional issues like the representation of an n-fold tensor product of Pauli matrices as a $2n$-dimensional binary vector, and the application of this alternative formalism to algebraically describe stabilizer states, we refer the interested reader to Ref. [150]. It might also be very instructive, in order to capture the advantages of the stabilizer formalism, to see how it is applied in the context of quantum codes and quantum error correction. A very suitable approach can be found in Ref. [152] (the entire Chap. 10, and more specifically Sect. 10.5.5).

5.2 Graph states

Graph states (see Refs. [9, 11]) are a type of n-qubit pure states that play several fundamental roles in quantum information theory. In quantum error-correction, the stabilizer codes which protect quantum systems from errors (Ref. [156]) can be realized as graph codes (Refs. [157, 158]). In measurement-based (or one-way) quantum computation (Ref. [144]), graph states are the initial resources consumed during the computation. Moreover, some graph states are universal resources for quantum computation (Ref. [145]). In quantum simulation, graph states allow us to demonstrate fractional braiding statistics of anyons in an exactly solvable spin model (Ref. [159]). Graph states have been used in multipartite purification schemes (Ref. [160]). The Clifford group has been used for entanglement distillation protocols (Ref. [161]). Graph states naturally lead to Greenberger-Horne-Zeilinger (GHZ) or all-versus-nothing proofs of Bell's theorem (Refs. [162, 163, 164, 165, 166, 167]), which can be converted into Bell inequalities which are maximally violated by graph states (Refs. [114, 168, 169, 170, 171, 172]). Some specific graph states are essential for several quantum communication protocols, including entanglement-based quantum key distribution (Ref. [91]), teleportation (Ref. [173]), reduction of communication complexity (Ref. [174]), and secret sharing (Refs. [175, 176]).

In addition to all these applications, graph states also play a fundamental role in the theory of entanglement. For $n \geq 4$ qubits, there is an infinite amount of different, inequivalent classes of n-qubit pure entangled states. The graph state formalism is a useful abstraction which permits a detailed (although not exhaustive) classification of n-qubit entanglement of $n \geq 4$ qubits. Precisely, we will devote the following chapters, where we present the main results of the second part of this thesis, to going more deeply into this topic.

For all these reasons, a significant experimental effort is devoted to the creation and testing of graph states of an increasing number of qubits. On one hand, there are experiments of n-qubit n-photon graph states up to $n = 6$ (Refs. [177, 178, 179, 180, 181]). On the other hand, the combination of two techniques, hyper-entanglement (i.e., entanglement in several degrees of freedom, like polarization and linear momentum) in Refs. [182, 183, 184, 185, 186, 187, 188] and the sources of 4, 5, and 6-photon entanglement using parametric down-conversion in Refs. [189, 190, 191, 192, 193, 178, 194] allows us to create 6-qubit 4-photon graph states (Refs. [195, 196]), 8-qubit 4-photon graph states (Ref. [195]), and even 10-qubit 5-photon graph states (Ref. [195]). The use of 4-photon sources for preparing 8-qubit graph states is particularly suitable due to the high visibility of the resulting states. Finally, if we restrict ourselves to GHZ states (which can be considered a specific class of graph states), it has been reported in Ref. [197] the creation of GHZ states with up to 14 qubits using a string of trapped $^{40}Ca^{+}$ ions, where each ion represents a qubit.[18]

As we have already pointed out at the beginning of this chapter, graph states constitute a special family of stabilizer states, and henceforth we can apply to graph states all the ideas presented in the previous sections.

[18] This is, to our knowledge, the current best achievement.

5.2.1 Definitions

Summarizing the essentials of Sect. 5.1.3, recall that the stabilizing operators s_i of a given stabilizer $\mathcal{S}$ commute, so that they can be diagonalized simultaneously and, therefore, share a common set of eigenvectors that constitute a basis of the vector space $V_{\mathcal{S}}$ stabilized by $\mathcal{S}$. The vector space $V_{\mathcal{S}}$ is of dimension 2^{n-k} when the cardinality of the generator $\gamma_{\mathcal{S}}$ is $|\gamma_{\mathcal{S}}| = k$. As a consequence, if $|\gamma_{\mathcal{S}}| = n$ (and therefore $|\mathcal{S}| = 2^n$), then there exists a *unique* common eigenstate $|\psi\rangle$ on n qubits with eigenvalue 1, such that $s_i|\psi\rangle = |\psi\rangle$ for every stabilizing operator $s_i \in \mathcal{S}$. Such a state $|\psi\rangle$ is called a stabilizer state because it is the only state that is stabilized (or fixed) by every operator of the stabilizer $\mathcal{S}$.

Given that an n-qubit graph state $|G\rangle$ is a specific instance of stabilizer state, the generator of $|G\rangle$ consists of $k = n$ generating operators, which provide a compact mathematical characterization of $|G\rangle$, as we will remark below.

A n-qubit *graph state* $|G\rangle$ is a pure entangled state associated to a graph $G(V, E)$ consisting of a set of n vertices $V = \{1, \ldots, n\}$ and a set of edges E connecting pairs of vertices, $E \subset V \times V$ (Refs. [9, 11]). Each vertex represents a qubit. An edge $(i, j) \in E$ represents an Ising-type interaction between qubits i and j. The graph G provides both a blueprint for preparing $|G\rangle$ and a mathematical characterization of $|G\rangle$ on the basis of the stabilizer formalism:[19]

(I) The recipe for preparing the state $|G\rangle$ is the following (see Figs. 5.1 and 5.2): first prepare each qubit in the state $|+\rangle = \frac{1}{\sqrt{2}}(|0\rangle + |1\rangle)$, i.e., the initial n-qubit state will be $|\psi_0\rangle = \bigotimes_{i\in V} |+\rangle_i$. Then, for each edge $(i, j) \in E$ connecting two qubits i and j, apply a controlled-Z gate between these qubits, i.e., the unitary transformation ${}^{C}Z = |00\rangle\langle 00| + |01\rangle\langle 01| + |10\rangle\langle 10| - |11\rangle\langle 11|$. According to this,

$$|G\rangle = \prod_{(i,j)\in E} {}^{C}Z_{ij}|+\rangle^{\otimes n}, \tag{5.42}$$

where ${}^{C}Z_{ij}$ stands for a controlled-Z operation between qubits i and j.

(II) The alternative mathematical characterization of $|G\rangle$, which exploits the stabilizer formalism, is the following: the graph state $|G\rangle$ associated to the graph G is the unique n-qubit state which fulfills

$$g_i|G\rangle = |G\rangle, \quad \text{for} \quad i = 1, \ldots, n, \tag{5.43}$$

where g_i are the generating operators of the stabilizer group of the state, defined as the set $\{s_j\}_{j=1}^{2^n}$ of all products of the generating operators. Specifically, g_i is the generating operator associated to the vertex i, defined by

$$g_i := X_i \bigotimes_{j\in\mathcal{N}(i)} Z_j, \tag{5.44}$$

[19] We must emphasize that graphs associated to graph states are *simple, connected and undirected graphs without weights*, that is, graphs G with the following properties: (1) all the vertices in G are of the same type (all of them represented by the same symbol); (2) vertices are not connected to themselves (i.e., graphs without loops); (3) there are no multiple edges between the same set of vertices; (4) any two vertices i and j are connected by a path in G; (5) there is no weight assignment to the vertices; and (6) edges have no inherent direction. Note that it is also possible to associate a graph to any stabilizer state, but in that case one should consider different types of nodes or vertices (solid and hollow, and even with signs), and also loops, along with some linkage restrictions. For details, refer to Ref. [150], Sect. 2.3.

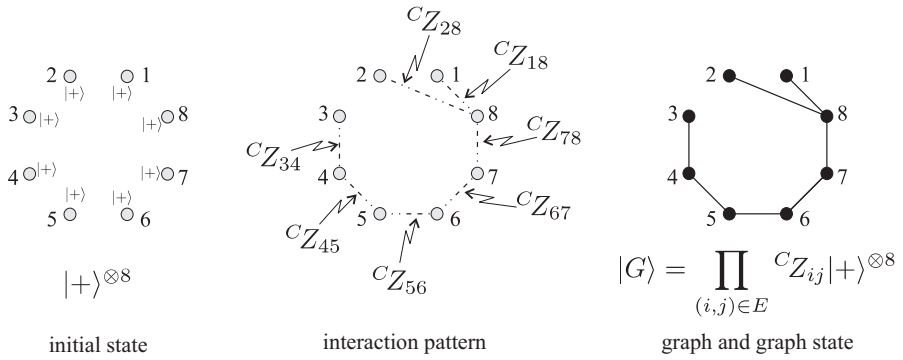

Figure 5.1: Recipe for preparing a 8-qubit graph state, starting from a "blank" state $|+\rangle^{\otimes 8}$ corresponding to a 8-vertex empty graph, and applying a sequence of controlled-Z gates.

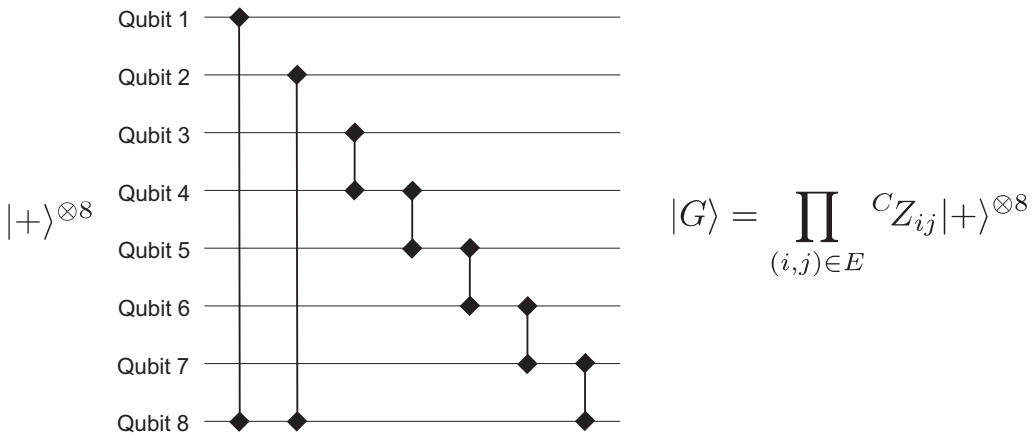

Figure 5.2: A circuit of preparation for the 8-qubit graph state corresponding to Fig. 5.1, using controlled-Z gates. In the circuit, a qubit (vertex of the graph) is represented by a horizontal wire, and a controlled-Z gate (edge in the graph) by a vertical segment with diamond-shaped ends connecting the qubits involved in the operation. Such ends are identical, since controlled-Z gates are symmetric under exchange between control/target qubits.

where $\mathcal{N}(i)$ is the neighborhood of the vertex i, i.e., the set of those vertices which are connected to i, and X_i (Z_i) denotes the Pauli matrix σ_x (σ_z) acting on the ith qubit.[20]

The equivalence between the two ways, (I) and (II), to account for a graph state follows from the next reasoning:[21] the initial state, namely, $|\psi_0\rangle = |+\rangle^{\otimes n}$, is a stabilizer state whose generating n-qubit operators belong to the Pauli group $\mathcal{P}_n$ and are of the form $g_i^{(0)} = X_i$, for $i = 1, \ldots, n$. The two-qubit operator ${}^{C}Z_{ij}$ is Hermitian (i.e., ${}^{C}Z_{ij} = {}^{C}Z_{ij}^{\dagger}$), it is symmetric under exchange of control/target qubits, and belongs to the Clifford group $\mathcal{C}_n$ (see Sect. 5.1.4), so that it maps $\mathcal{P}_n$ onto itself. As a consequence, the resulting state after the application of a sequence of controlled-Z gates is also a stabilizer state (in the strict sense of the term, i.e., it is stabilized by a subgroup of the Pauli group). It is easy to check that, given $|\psi_0\rangle = |+\rangle^{\otimes n}$, if one applies a controlled-Z gate ${}^{C}Z_{ij}$ between qubits i and j (corresponding to an edge $(i, j) \in E$ of the graph G), then it will transform the generating operators $g_i^{(0)} = X_i$ and $g_j^{(0)} = X_j$ under conjugation in such a way that

$$ {}^{C}Z_{ij}\, X_i\, {}^{C}Z_{ij} = X_i Z_j, \tag{5.46} $$

and

$$ {}^{C}Z_{ij}\, X_j\, {}^{C}Z_{ij} = Z_i X_j, \tag{5.47} $$

and will leave the other $g_{k\neq\{i,j\}}^{(0)}$ invariant. The reiterated application of this argument to the sequence of controlled-Z gates following the blueprint provided by the set of edges of G eventually leads to a final state, the graph state $|G\rangle$, which is a stabilizer state with the n generators given by Eq. (5.44), as required.

5.2.2 Graph states as a "theoretical laboratory" for multipartite entanglement

Graph states, as we have mentioned in the introduction to Sect. 5.2, play several fundamental roles in the field of quantum information, not only from a theoretical point of view, but also in the realm of applications. There is another field in which graph states, the stabilizer formalism on which they are based, and the powerful aid provided by selected elements of graph theory, have proved to be very valuable tools to gain an insight: the theory of entanglement. The study

[20] A simple example is the 3-qubit linear cluster state $|\mathrm{LC}_3\rangle$, whose associated graph is the 3-vertex linear cluster LC_3, consisting of three vertices $\{1, 2, 3\}$, one of them (say vertex 2) linked to the other two. With such labeling, the stabilizer of $|\mathrm{LC}_3\rangle$ is the following set of $2^3 = 8$ 3-qubit Pauli operators:

$$ \mathcal{S}(|\mathrm{LC}_3\rangle) = \left\{ \begin{array}{lllllll} s_1 = & g_1 & = & & X_1 & Z_2 & \mathbb{1}_3 \\ s_2 = & g_2 & = & & Z_1 & X_2 & Z_3 \\ s_3 = & g_3 & = & & \mathbb{1}_1 & Z_2 & X_3 \\ s_4 = & g_1 g_2 & = & & Y_1 & Y_2 & Z_3 \\ s_5 = & g_1 g_3 & = & & X_1 & \mathbb{1}_2 & X_3 \\ s_6 = & g_2 g_3 & = & & Z_1 & Y_2 & Y_3 \\ s_7 = & g_1 g_2 g_3 & = & - & Y_1 & X_2 & Y_3 \\ s_8 = & g_j g_j & = & & \mathbb{1}_1 & \mathbb{1}_2 & \mathbb{1}_3, \end{array} \right. \tag{5.45} $$

where the first three of them are the generating operators given by Eq. (5.44).

[21] For the sake of compactness along the argument, the Pauli identity operators acting on qubits not expressly mentioned remain unstated. For instance, X_i will refer to a n-fold tensor product with σ_x acting on qubit i, and identity operators on the other qubits.

and characterization of graph states from the viewpoint of their entanglement properties is, among other things, a direct consequence of the great interest they have raised as a result of the multiple applications and tasks in which they are useful. Nevertheless, at a more fundamental level, the set of graph states constitutes an exceptional "theoretical laboratory" for the study of multipartite entanglement by itself. On one hand, the stabilizer formalism entails a more economical description of graph states (linear in the number of qubits), which allows to set aside the vector state representation: the latter, in case of an n-qubit state, would imply to give account of 2^n complex amplitudes in general, and this is the reason why the analysis of entanglement on the basis of the vector representation becomes unfeasible in practice for a relatively small number of qubits. On the other hand, any graph state has a natural graphical counterpart, in the form of a simple, connected, undirected and unweighted graph, completely determined by its adjacency matrix: this enables us to resort to a plethora of well-known tools and results from graph theory in order to go in depth about the characterization of entanglement, whose treatment becomes more transparent, and computationally more manageable.

Due to the fact that most of the main results of the second part of this thesis deal with this topic, we give below a brief panoramic review of some important results previously obtained by other authors, which constitute the framework for our contributions.

Summary of previous results about classification of multipartite entanglement

1. Two pure states $|\psi\rangle$ and $|\phi\rangle$ are equivalent under local operations assisted by classical communication (LOCC), i.e., they can be obtained with certainty from each other by means of LOCC, if and only if they are equivalent under local unitary (LU) operations (Refs. [198, 199]). Therefore, LOCC equivalence equals LU equivalence:

$$|\psi\rangle \overset{LOCC}{\longmapsto} |\phi\rangle \Leftrightarrow |\psi\rangle \overset{LU}{\longmapsto} |\phi\rangle. \tag{5.48}$$

   However, as it is pointed out in Ref. [200], and already for bipartite systems, two states $|\psi\rangle$ and $|\phi\rangle$ are typically not related by LU operations, and one needs continuous parameters to label all equivalence classes: there are infinitely many of them (Refs. [201, 202]). As a consequence, in order to carry out a simpler classification of pure states in terms of entanglement, the relation of equivalence between states must be based on another kind of conversion between them, different from LOCC. A possibility (Ref. [198]) is to consider the conversion of the states through stochastic local operations and classical communication (SLOCC) instead of LOCC: this means using LOCC but without imposing that the conversion between states has to be attained with certainty. Therefore, it suffices a nonzero probability of success for the transformation under LOCC in order to consider that two states are equivalent.

2. LU operations are a particular instance of SLOCC. Therefore, those states that are equivalent under LU are also equivalent under SLOCC (the converse is not necessarily true). A classification under SLOCC is a coarse graining of the one based on LU:

$$|\psi\rangle \overset{LU}{\longmapsto} |\phi\rangle \Rightarrow |\psi\rangle \overset{SLOCC}{\longmapsto} |\phi\rangle. \tag{5.49}$$

We will say that two quantum states *have the same entanglement if they are SLOCC equivalent*. With this relation of equivalence, several authors have carried out the corresponding classification of n-partite quantum states according to their entanglement properties. The simplest situation implies assuming one qubit per party; unfortunately, for n-qubit systems the situation becomes involved very soon, for a small number of qubits. In a nutshell:

- For $n = 2$ there are essentially two classes of equivalence: one of them includes all product states (unentangled). The other one includes all pure entangled states, since any of them can be converted into the Einstein-Podolski-Rosen (EPR) state $|\Phi^+\rangle = \frac{1}{\sqrt{2}}(|00\rangle + |11\rangle)$ through SLOCC (Refs. [200, 203]).
- For $n = 3$ there are six classes of equivalence under SLOCC (Ref. [200]). One of them corresponds to fully separable (therefore unentangled) states, the $A - B - C$-class. A possible representative state of such class is the state $|\psi_{A-B-C}\rangle = |000\rangle$. Three of them correspond to bi-separable states (one class for each bipartition $A-BC$, $B-AC$, $C - AB$), in which the state of the two-qubit part is entangled. As an example, a possible representative state of the $A - BC$-class is $|\psi_{A-BC}\rangle = \frac{1}{\sqrt{2}}|0\rangle(|00\rangle + |11\rangle)$. Finally, two of them correspond to genuinely tripartite entangled states: the GHZ-class, whose representative state is the 3-qubit GHZ state $|GHZ\rangle = \frac{1}{\sqrt{2}}(|000\rangle + |111\rangle)$, and the W-class, whose representative state is the 3-qubit W state $|W\rangle = \frac{1}{\sqrt{3}}(|100\rangle + |010\rangle + |001\rangle)$.
- For $n \geq 4$ the number of classes of equivalence under SLOCC becomes infinite: as it is shown in Ref. [200], the reason is that the number of parameters of a state which the parties can modify acting locally through SLOCC grows linearly with n, whereas the number of parameters required to specify the state grows exponentially with n. Nevertheless, in the case $n = 4$, the uncountable set of classes can be grouped into nine continuous families, whose representatives can be found in Ref. [204]. A similar treatment to extend the SLOCC classification for states of more than four qubits, or for multipartite systems of qudits of dimension $d > 2$, remains unknown to our knowledge.

3. The exponential growth of the complexity of the problem of classifying pure quantum states according to SLOCC equivalence has led to postpone such attempt for arbitrary states, and to focus the attention on specific families of quantum states ("theoretical laboratories") describable with a relatively small number of parameters when compared with the general problem, but whose more economical description nevertheless captures essential features of the problem of classifying entanglement, in the hope that this strategy makes it possible to gain some insight about the general problem. As we said at the beginning of this section, stabilizer states and graph states constitute appropriate "theoretical laboratories" for such purpose. Any graph state is describable through a simple, connected, undirected and unweighted graph. Recall that graph states belong to the broader family of stabilizer states: as we mentioned in footnote 19 on p. 109, it is also possible to associate a more complicated kind of graph to any stabilizer state. Interestingly, *any stabilizer state* $|S\rangle$ *is*

equivalent under local operations belonging to the LC group[22] (i.e., unitary operations which map the Pauli group onto itself under conjugation) *to some —generally non-unique— graph state* $|G\rangle$ (Ref. [158]). Consequently, we can restrict our analysis to graph states, since the corresponding entanglement classification will account for stabilizer states up to LC operations.

4. Every two graph states which are equivalent under SLOCC are also equivalent under LU operations (Ref. [205]). Recall that according to Eq. (5.49), and for any pair of arbitrary pure states, LU equivalence implies SLOCC equivalence. The converse is not true in general, but it is fulfilled by graph states. Hence, given two different graph states $|G\rangle$ and $|G'\rangle$,

$$|G\rangle \overset{SLOCC}{\longmapsto} |G'\rangle \iff |G\rangle \overset{LU}{\longmapsto} |G'\rangle. \tag{5.50}$$

   In other words, *for graph states* SLOCC equivalence and LU equivalence are coincident notions, which means that the classification of graph states according to entanglement can be based on LU equivalence. We can conclude that two n-qubit graph states $|G\rangle$ and $|G'\rangle$ will have the same degree of n-partite entanglement if and only if there exist n unitary transformations U_i on individual qubits such that $|G'\rangle = \bigotimes_{i=1}^{n} U_i|G\rangle$.

5. In case that the aforementioned one-qubit unitary transformations U_i belong to the one-qubit Clifford group $\mathcal{C}_1$ (equivalently, in case that $U = \bigotimes_{i=1}^{n} U_i$ belongs to the LC group $\mathcal{C}_1^n$; see p. 104 for details), we say that the two graph states $|G\rangle$ and $|G'\rangle$ are equivalent under LC transformations, or LC equivalent, in brief. In relation to this, there is an important conjecture, usually referred to as "LU⇔LC", that poses the question whether LU equivalence and LC equivalence coincide for graph states. Note that, trivially, LC equivalence implies LU equivalence, since LC operations constitute a subset of LU operations. The strong implication, hence, is the converse, LU⇒LC. The triple coincidence of SLOCC, LU and LC equivalence for graph states would make the task of checking whether two given graph states are locally equivalent much more efficient, because it would be based on LC equivalence, yielding an additional advantage: a description of such local equivalence of graph states in purely graph theoretic terms would be possible thanks to the local complementation rule, that we describe later in item 6 on this list of results.

   Unfortunately, the LU⇔LC conjecture is proven false in Ref. [206], where Ji *et al.* offer explicit counterexamples of the conjecture. The smallest counterexample Ji *et al.* have found corresponds to two 27-qubit graph states whose corresponding graphs are the same except for only one edge, and such that they are LU equivalent but not LC equivalent.[23] The same algorithm employed for this finding has generated other counterexamples with 35 qubits. Although not proven, Ji *et al.* in fact "[...] believe that 27 is the smallest possible size of counterexamples of LU⇔LC."

   Nevertheless, the LU⇔LC conjecture is true for several classes of n qubit graph states: on one hand, numerical results show that LC equivalence coincides with local unitary

[22] See details about the Clifford group on p. 104.

[23] In fact, they conclude that two LU-equivalent graph states which are not LC equivalent always have associated graphs that differ only in one edge.

equivalence for qubit graph states associated with connected graphs up to $n = 7$ vertices (see Refs. [9, 11]). On the other hand, LU⇔LC also works for graph states whose stabilizers satisfy certain conditions[24] (Ref. [207]). Moreover, going beyond Ref. [207], the class of stabilizer states for which LU⇔LC is broadened to include all stabilizer states represented by graphs with cycles of length neither 3 nor 4 in Ref. [208].

We must emphasize that in the second part of this thesis the following assumption is made: deciding whether or not two graph states of $n < 27$ qubits have the same entanglement is equivalent to deciding whether or not they are LC equivalent. In other words, we assume that the LU⇔LC conjecture is true for graph states of up to $n = 26$ qubits, a number of qubits beyond $n = 8$ (the one corresponding to the classification we present in Chap. 6) or $n = 12$ (corresponding to the extended classification we provide in Chap. 8).[25]

6. According to Ref. [10], it is possible to translate the action of LC operations on graph states into transformations on their associated graphs, i.e., to provide transformation rules, stated in purely graph theoretical terms, which completely characterize the evolution of graph states under LC operations. There is essentially one basic rule, known as *local complementation* (abbreviated in this thesis[26] as LC*) and described below, the successive application of which on a graph G generates the complete equivalence class of the corresponding graph state $|G\rangle$ under local unitary operations within the Clifford group: such LC equivalence class of a graph state $|G\rangle$ is usually referred to as the *LC orbit* of $|G\rangle$ (or simply, *orbit*).

   Let us note that we can also conform this language of classes of equivalence to the effect of LC* on the associated graph G: we can say that two graphs G and G' are LC* equivalent if it is possible to transform one in the other by means of a sequence of LC* operations. As a consequence, LC* splits the set of graphs into LC* classes of equivalence: all those graphs that can be obtained through reiterative application of LC* on a given graph G constitute the so-called *(LC*) orbit* of G. In principle, one can choose any of the graphs of a given orbit as the *representative* of such orbit. The choice of a certain graph as representative may be based on different criteria. As we will see later, we will adopt in our work one in particular, which entails a clear physical meaning.

   Local complementation on a vertex i of a graph G acts as follows: one picks out the vertex i and inverts (complements) the neighborhood $\mathcal{N}(i)$ of i; i.e., vertices in the neighborhood which were connected become disconnected and vice versa. Mathematically, denoting an

[24] According to Ref. [207], this conditions concern a subgroup $\mathcal{M}(|G\rangle)$ in the stabilizer $\mathcal{S}$ of a graph state $|G\rangle$: $\mathcal{M}(|G\rangle)$ is generated by the so-called *minimal elements*, i.e., the operators of $\mathcal{S}$ with *minimal support* (see Sect. 7.2.1 for the concept of support). The conditions refer to the fact that the three Pauli operators X, Y and Z must appear in each and every qubit throughout the operators in $\mathcal{M}(|G\rangle)$. If $\mathcal{M}(|G\rangle)$ fulfills this conditions and $|G\rangle \overset{LU}{\longmapsto} |G'\rangle$, then $|G\rangle \overset{LC}{\longmapsto} |G'\rangle$.

[25] We suppose that Ji *et al.*'s algorithm (Ref. [206]) would have detected counterexamples of such a relatively small size, in case there were any.

[26] We prefer to use the abbreviation LC* in order to avoid confusion: nevertheless, it is usual to abbreviate local complementation by LC as well, since in the end it is, so to say, the graphical counterpart of LC operations on graph states, expecting that the meaning of the acronym LC will be clear from the context of the discussion: "local Clifford" when applied to graph states, "local complementation" when referred to graphs.

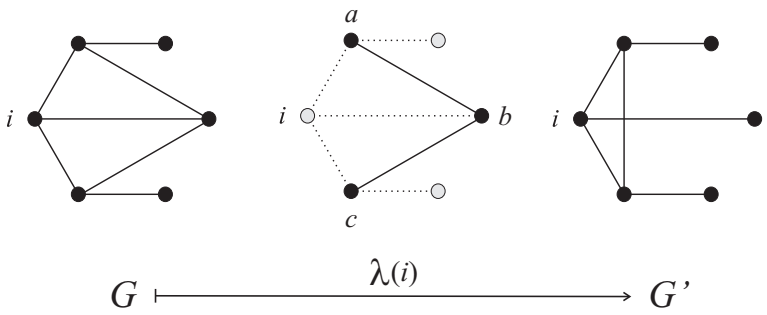

Figure 5.3: Local complementation $\lambda(i)$ on vertex i of the graph G on the left. The neighborhood of i (highlighted in the graph in the center), whose adjacency relationship is inverted (complemented) by $\lambda(i)$, is the set of vertices $\mathcal{N}(i) = \{a, b, c\}$. The rest of the edges of G (dashed lines) remains unaltered. The resulting LC*-equivalent graph G' is on the right.

LC* on vertex i by $\lambda(i)$,

$$G = (V, E) \overset{\lambda(i)}{\longmapsto} G' = (V, E\Delta K_{\mathcal{N}(i)}), \tag{5.51}$$

where Δ stands for the symmetric difference between sets of edges,[27] and $K_{\mathcal{N}(i)}$ is the set of edges of the complete graph over the vertices of $\mathcal{N}(i)$. An example is depicted in Fig. 5.3.

The action of LC* on vertex i of a graph G can be described in the stabilizer formalism. On the stabilizer[28] of $|G\rangle$, LC* on the qubit i induces the map $Y^{(i)} \mapsto Z^{(i)}, Z^{(i)} \mapsto -Y^{(i)}$ on the qubit i, and the map $X^{(j)} \mapsto -Y^{(j)}, Y^{(j)} \mapsto X^{(j)}$ on the qubits $j \in \mathcal{N}(i)$, following Ref. [11]. On the generator, LC* on the qubit i maps the generating operators g_j^{old} with $j \in \mathcal{N}(i)$ to $g_j^{\text{new}} g_i^{\text{new}}$.

Summarizing, we can say that two graph states $|G\rangle$ and $|G'\rangle$ have the same degree of entanglement (and hence, belong to the same LC equivalence class —or LU equivalence class— or orbit) if there exists a sequence Λ of LC* operations transforming the graphs G and G' between each other (i.e., if G and G' belong to the same orbit),

$$|G\rangle \equiv_{LC} |G'\rangle \Longleftrightarrow G \overset{\Lambda}{\longleftrightarrow} G'. \tag{5.53}$$

[27] Given to sets of edges $E \subset V \times V$ and $F \subset V \times V$ connecting vertices of the set V, $E\Delta F$ is the *symmetric difference* between E and F, defined as

$$E\Delta F = (E \cup F) - (E \cap F). \tag{5.52}$$

[28] For the sake of economy, we use the same labels interchangeably both for qubits and for vertices: in a mild abuse of terminology, the "neighborhood of qubit i" must be understood as the set of qubits j whose associated vertices —also labeled by j— belong to the neighborhood of vertex i.

Previous progress on the classification of graph states according to entanglement

The list of results of other authors that we have just revisited constitute the conceptual framework in which we develop our contributions, collected in the next chapters. In order to complete this review, we must briefly discuss another result of importance for us, since it is the starting point of our research on graph states.

The classification and study of the entanglement properties of graph states have been achieved, up to 7 qubits, by Hein, Eisert, and Briegel (HEB, hereafter) in Ref. [9] (see also Ref. [11]). This classification has been useful to identify new two-observer all-versus-nothing proofs (Ref. [167]), new Bell inequalities (Refs. [171, 172]), and has stimulated the preparation of several graph states (Ref. [195]). In our work, we have extended HEB's classification up to 8 qubits in Ref. [13] (see Chap. 6), and subsequently up to 12 qubits in Ref. [209] (see Chap. 8).

The number of orbits under local complementation for simple, connected, non-isomorphic[29] n-vertex graphs grows very rapidly with the number of vertices, as it is shown in Table 5.1, where data have been taken from Ref. [210] (also available in Ref. [11], p. 55). According to that table, the total number of LC* orbits for graphs with a number of vertices ranging from 2 to 7 is 45, and this number coincides with the number of LC equivalence classes for graph states of up to 7 qubits analyzed by HEB from the perspective of their entanglement properties in Ref. [9].

Table 5.1: Number of LC* orbits for simple, connected, non-isomorphic graphs, as a function of the number of vertices.

Number of vertices	Number of LC* orbits
1	1
2	1
3	1
4	2
5	4
6	11
7	26
8	101
9	440
10	3132
11	40457
12	1274068

In a nutshell, the 45 LC classes of graph states are ordered according to the following criteria: (a) number of qubits, (b) minimum number of controlled-Z gates needed for the preparation,

[29] Graph isomorphism (i.e., a permutation of the vertices that map neighbored vertices onto neighbored vertices) physically comes up to an exchange of particles. If we focus on examining the question of how the entanglement in a graph state is related to the topology of its underlying graph, graph isomorphic situations are essentially the same. Of course, if we excluded graph isomorphisms, as we would do, e.g., if we were interested in quantum communication scenarios where the labeling of the qubits and their "local environment" is relevant, the number of inequivalent classes of graph states would be considerably larger.

(c) the Schmidt measure, and (d) the rank indexes (they are calculated and tabulated, for each LC class, in Ref. [9], table II). For the definitions and details we refer the reader to Sect. 6.2. The ordering criteria (c) and (d) refer to entanglement measures[30] which are invariant under LC transformations and quantify the entanglement of graph states belonging to each LC orbit. In principle, they should also allow to label and discriminate unambiguously between any pair of different LC orbits.[31]

Finally, HEB provide a list of simple representatives of each equivalence class, although they do not specify accurately the criterion of simplicity followed for their particular choice. In Fig. 5.4, we show for illustrative purposes the simple representative graphs of the 45 LC orbits of graph states, as they appear in Ref. [9].

We end this introductory chapter with this succinct outline of HEB's classification of graph states up to 7 qubits. Now we are ready to address the three main problems of our research on graph states:

(i) The extension of the classification of graph states in LC equivalence classes up to 8 qubits (Chap. 6).

(ii) The quest for a compact set of LC invariants capable of labeling and distinguishing unambiguously between any pair of LC orbits of graph states of up to 8 qubits (Chap. 7).

(iii) The formulation of an optimal preparation procedure of graph states on the basis of the preparation depth and the LC equivalence classes; and the extension of the LC classification up to 12 qubits, along with a critical discussion about the effectiveness of the previous compact set of invariants as LC orbit-discriminating quantities (Chap. 8).

Moreover we present, as closing contribution, a practical application of graph states to quantum information theory, namely, to the field of communication complexity: we provide an entanglement-assisted experimental protocol of reduction of communication complexity. In that protocol, the participants share an entangled state which is precisely a graph state, the 3-qubit or 4-qubit GHZ state, respectively, whose associated graphs are the complete graphs K_3 or K_4, belonging to the LC classes of graph states Nos. 2 and 3 in Refs. [9, 11]. This protocol is an example to additionally motivate the usefulness and importance of graph states in quantum information theory (Chap. 9).

[30] Other entanglement measures to specifically quantify entanglement in pure graph states have been considered afterwards in the scientific literature. For instance, distance-like measurements as the relative entropy of entanglement or the geometric measure are analyzed for graph states in Ref. [211]. Geometric measure and the calculation of the closest product states are evaluated in Ref. [212] for up to 8 qubits, and in Ref. [213] for 9, 10 and 11 qubits, giving rise to another ordering of the LC orbits.

[31] We see later, in Chap. 6, that the latter —unambiguous discrimination among LC classes— is not the case; we provide a solution up to 8 qubits in Chap. 7, whose degree of validity up to 12 qubits is discussed in Chap. 8.

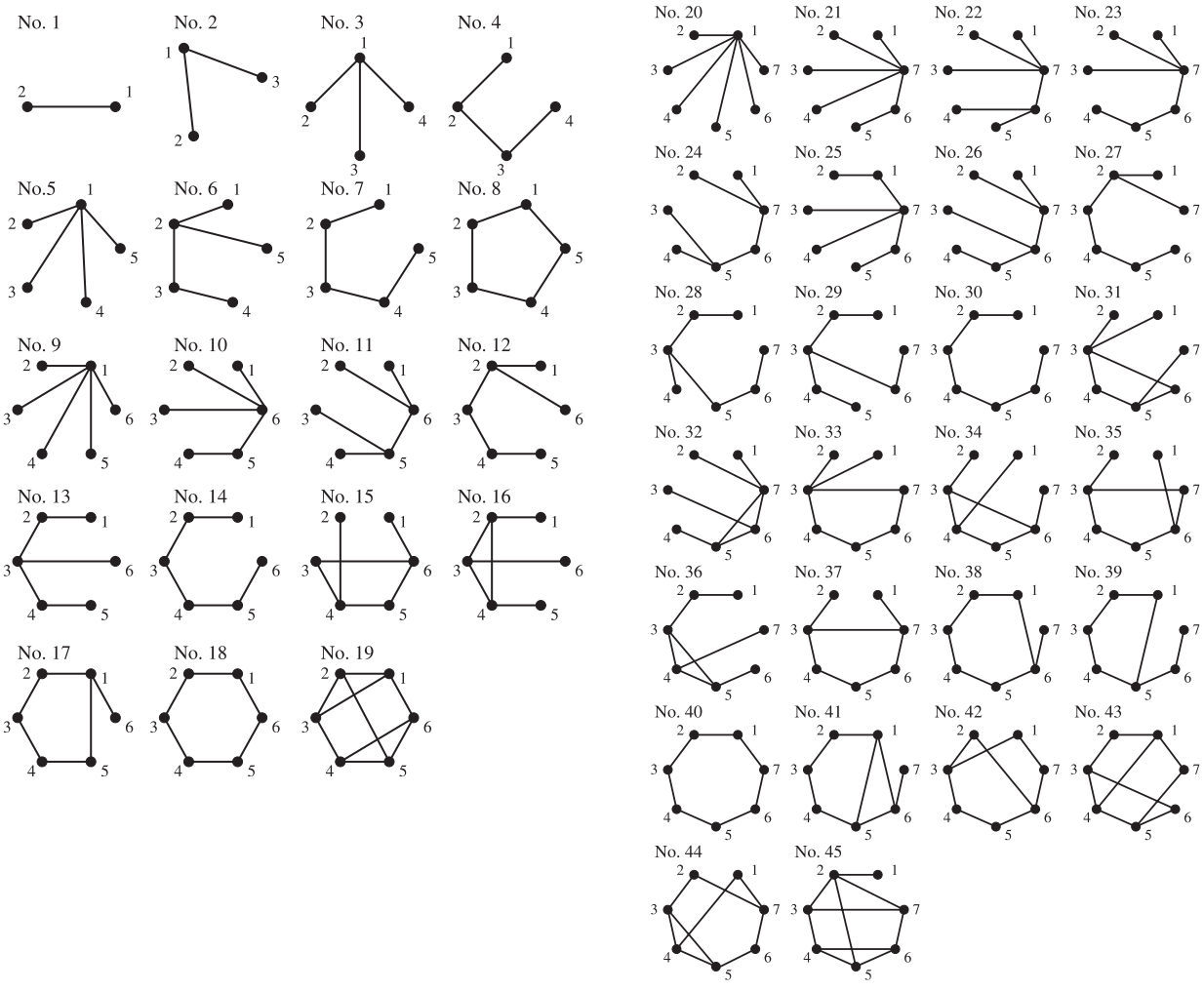

Figure 5.4: List of representative graphs with up to 7 vertices that are not equivalent under local complementation and graph isomorphism, corresponding to the 45 LC equivalence classes of graph states of up to 7 qubits. Figure reproduced from Hein *et al.* (Ref. [9]).

Chapter 6

Entanglement in eight-qubit graph states

In this chapter we present the results obtained in Ref. [13]. Below we provide a brief summary.

Summary:

Any 8-qubit graph state belongs to one of the 101 equivalence classes under local unitary operations within the Clifford group. For each of these classes we obtain a representative which requires the minimum number of controlled-Z gates for its preparation, and calculate the Schmidt measure for the 8-partite split, and the Schmidt ranks for all bipartite splits. This results into an extension to 8 qubits of the classification of graph states proposed by Hein, Eisert, and Briegel [Phys. Rev. A **69**, 062311 (2004)].

6.1 Introduction

As we have discussed in Chap. 5, the classification and study of the entanglement properties of graph states have been achieved, up to 7 qubits, by HEB in Refs. [9, 11]. The main purpose of this chapter is to extend such classification to 8-qubit graph states.

Recall that up to 7 qubits there are 45 orbits, i.e., classes of graph states that are not equivalent under one-qubit unitary transformations. With 8 qubits, there are 101 new classes of equivalence (see Table 5.1). For a small n, the number of orbits has been well known for a long time (see, e.g., Ref. [210]).[1] The purpose here is to classify them according to several relevant physical properties for quantum information theory.

Needless to say, the main object of study in this chapter is the *graph state*. We refer the reader to Sect. 5.2.1 for the definition of graph state, both as a recipe for its preparation and as an algebraic description on the basis of the stabilizer formalism. Many of the most relevant applications of graph states in the field of quantum information, along with a summary of the

[1] There are 995 non-isomorphic connected graphs distributed among the 45 orbits up to 7 vertices, and 11117 for the 101 orbits of 8 vertices (Ref. [210]). Note that in this chapter we are only interested in graph states associated to connected graphs. In quantum codes, connected graphs correspond to indecomposable quantum codes (i.e., those that cannot be expressed as the direct sum of two smaller codes).

experimental efforts devoted to the creation and testing of graph states of an increasing number of qubits can be found in Sect. 5.2, p. 108.

For the purposes of this chapter, the key is *local complementation*, a simple transformation which leaves the entanglement properties of graph states invariant. Summarizing what we have discussed in the previous chapter, let us recall that two n-qubit states, $|\phi\rangle$ and $|\psi\rangle$ have the same n-partite entanglement if and only if there are n one-qubit unitary transformations U_i, such that $|\phi\rangle = \bigotimes_{i=1}^{n} U_i|\psi\rangle$. If these one-qubit unitary transformations belong to the one-qubit Clifford group,[2] then both states are said to be LC equivalent. Van den Nest, Dehaene, and De Moor (VDD, hereafter) found that the successive application of a transformation with a simple graphical description is sufficient to generate the complete equivalence class of graph states under local unitary operations within the Clifford group (the so-called *orbit*, see Ref. [10]). This simple transformation is local complementation, by means of which one can generate the orbits of all LC-inequivalent n-qubit graph states; in particular, the 101 orbits corresponding to 8-qubit graph states, whose classification is the goal of this chapter.

The definition of local complementation —which is our main classifying tool— and the graphical description of its action on a given graph have been introduced in Sect. 5.2.2, item 6 on p. 115, where we refer the reader.

To establish an order between the equivalence classes we will use the criteria proposed in Refs. [9, 11]. These criteria are introduced in Sect. 6.2. In Sect. 6.3 we present our results. In Sect. 6.4 we present the conclusions and point out some pending problems.

6.2 Criteria for the classification

Following HEB, the criteria for ordering the classes are: (a) number of qubits, (b) minimum number of controlled-Z gates needed for the preparation, (c) the Schmidt measure, and (d) the rank indexes. For instance, class No. 1 is the only one containing two-qubit graph states, class No. 2 is the only one containing three-qubit graph states (Refs. [9, 11]). Classes No. 3 and No. 4 both have $n = 4$ qubits and require a minimum of $|E|$=3 controlled-Z gates. However, class No. 3 has Schmidt measure $E_S = 1$, while class No. 4 has $E_S = 2$.

6.2.1 Minimum number of controlled-Z gates for the preparation

Different members of the same LC class require a different number of controlled-Z gates for their preparation starting from the state $|+\rangle = (|0\rangle + |1\rangle)/\sqrt{2}$ for each qubit. The first criterion for our classification is the minimum number of controlled-Z gates required for preparing one graph state *within the LC class*. This corresponds to the number of edges of the graph with the minimum number of edges within the LC* class, $|E|$. We will provide a representative graph with the minimum number of edges for each LC class of graph states.

[2] As a reminder, the one-qubit Clifford group $\mathcal{C}_1$ is generated by the Hadamard gate $H = (|0\rangle\langle 0| + |0\rangle\langle 1| + |1\rangle\langle 0| - |1\rangle\langle 1|)/\sqrt{2}$ and the phase gate $S = |0\rangle\langle 0| + i|1\rangle\langle 1|$.

6.2.2 Schmidt measure

The *Schmidt measure* was introduced by Eisert and Briegel as a tool for quantifying the genuine multipartite entanglement of quantum systems in Ref. [214] (see also Ref. [215]). Any state vector $|\psi\rangle \in \mathcal{H}^{(1)} \otimes \ldots \otimes \mathcal{H}^{(N)}$ of a composite quantum system with N components can be represented as

$$|\psi\rangle = \sum_{i=1}^{R} \xi_i |\psi_i^{(1)}\rangle \otimes \cdots \otimes |\psi_i^{(N)}\rangle, \tag{6.1}$$

where $\xi_i \in \mathbb{C}$ for $i = 1, \ldots, R$, and $|\psi_i^{(j)}\rangle \in \mathcal{H}^{(j)}$, for $j = 1, \ldots, N$. The Schmidt measure associated with a state vector $|\psi\rangle$ is then defined as

$$E_S(|\psi\rangle) = \log_2(r), \tag{6.2}$$

where r is the minimal number R of terms in the sum of Eq. (6.1) over all linear decompositions into product states. In case of a two-component system ($N = 2$), the minimal number of product terms r is given by the *Schmidt rank* of the state $|\psi\rangle$. Hence, the Schmidt measure could be considered a generalization of the Schmidt rank to multipartite quantum systems [see Eq. (6.7) below]. The Schmidt measure can be extended to mixed states by means of a convex roof extension. In this chapter, however, we will deal only with pure states.

Given a graph $G = (V, E)$, a *partition* of V is any tuple $(A_1, \ldots, A_M)$ of disjoint subsets $A_i \subset V$, with $\bigcup_{i=1}^{M} A_i = V$. In case $M = 2$, we refer to the partition as a *bipartition*, and denote it (A, B). We will write

$$(A_1, \ldots, A_N) \leq (B_1, \ldots, B_M), \tag{6.3}$$

if $(A_1, \ldots, A_N)$ is a *finer partition* than $(B_1, \ldots, B_M)$, which means that every A_i is contained in some B_j. The latter is then a *coarser partition* than the former. For any graph $G = (V, E)$, the partitioning where $(A_1, \ldots, A_M) = V$ such that $|A_i| = 1$, for every $i = 1, \ldots, M$, is referred to as the *finest partition*.

We must point out that E_S is nonincreasing under a coarse graining of the partitioning: If two components are merged in order to form a new component, then the Schmidt measure can only decrease. If we denote the Schmidt measure of a state vector $|\psi\rangle$ evaluated with respect to a partitioning $(A_1, \ldots, A_N)$ as $E_S^{(A_1,\ldots,A_N)}(|\psi\rangle)$, meaning that the respective Hilbert spaces are those of the grains of the partitioning, then the nonincreasing property of E_S can be expressed as

$$E_S^{(A_1,\ldots,A_N)}(|\psi\rangle) \geq E_S^{(B_1,\ldots,B_M)}(|\psi\rangle), \tag{6.4}$$

if $(A_1, \ldots, A_N) \leq (B_1, \ldots, B_M)$.

Let (A, B) be a bipartition (i.e., $A \cup B = V; A \cap B = \emptyset$) of a graph $G = (V, E)$, with $V = \{1, \ldots, N\}$, and let us denote the adjacency matrix of the graph by Γ, i.e., the symmetric matrix with elements

$$\Gamma_{ij} = \begin{cases} 1, & \text{if } (i, j) \in E, \\ 0, & \text{otherwise.} \end{cases} \tag{6.5}$$

When we are dealing with a bipartition, it is useful to label the vertices of the graph so that $A = \{1, \ldots, p\}$, $B = \{p + 1, \ldots, N\}$. Then, we can decompose the adjacency matrix Γ into

submatrices Γ_A, Γ_B (that represent edges within A and edges within B), and Γ_{AB} (the $|A| \times |B|$ off-diagonal submatrix of the adjacency matrix Γ that represents those edges between A and B),

$$\begin{pmatrix} \Gamma_A & \Gamma_{AB} \\ \Gamma_{AB}^T & \Gamma_B \end{pmatrix} = \Gamma. \tag{6.6}$$

The Schmidt rank $SR_A(G)$ of a graph state $|G\rangle$ represented by the graph $G = (V, E)$, with respect to the bipartition (A, B), is given by the binary rank [i.e., the rank over $GF(2)$] of the submatrix Γ_{AB},

$$SR_A(G) = \text{rank}_{\mathcal{F}_2}(\Gamma_{AB}). \tag{6.7}$$

It follows straightforwardly from the definition that $SR_A(G) = SR_B(G)$, because the different bipartitions are fixed by choosing the smaller part, say A, of the bipartition (A, B), which gives 2^{N-1} bipartitions.

6.2.3 Rank indexes

While calculating the Schmidt rank with respect to all possible bipartitions of a given graph, let us count how many times a certain rank occurs in all the bipartite splits, and then classify this information according to the number of vertices in A, the smaller part of the split under consideration. There is a compact way to express this information, the so-called *rank indexes* (Refs. [9, 11]). The rank index for all the bipartite splits with p vertices in the smaller part A is given by the p-tuple

$$RI_p = (\nu_p^p, \ldots, \nu_1^p) = [\nu_j^p]_{j=p}^1, \tag{6.8}$$

where ν_j^p is the number of times in which $SR_A(G) = j$, with $|A| = p$, occurs.

6.3 Procedures and results

The main results of the chapter are summarized in Fig. 6.2 and Table 6.1. In the following, we provide details on the calculations leading to these results.

6.3.1 Orbits under local complementation

We have generated all LC* orbits for $n = 8$ and calculated the number of non-isomorphic graphs in each LC* orbit, denoted by $|LC|$. These numbers are counted up to isomorphism.

In addition, for each orbit, we have calculated a representative with the minimum number of edges $|E|$. As representative, we have chosen the one (or one of those) with the minimum number of edges and the minimum maximum degree (i.e., number of edges incident with a vertex). This means that the graph state associated to this graph requires the minimum number of controlled-Z gates for its preparation, and the minimum preparation depth[3] (i.e., its preparation requires

[3]This particular choice paves the way for Chapter 8, where we show how to prepare any graph state of up to 12 qubits with the minimum number of controlled-Z gates and the minimum preparation depth by means of one-qubit and controlled-Z gates. We refer the reader to that chapter for the definition of preparation depth and its implications.

a minimum number of steps; see Ref. [216]). All the representatives of each of the 101 orbits are illustrated in Fig. 6.2. $|LC|$ and $|E|$ are in Table 6.1.

6.3.2 Bounds to the Schmidt measure

It is a well-known fact that for any measure of multiparticle entanglement proposed so far, including the Schmidt measure E_S, the computation is exceedingly difficult for general states. In order to determine E_S, one has to show that a given decomposition in Eq. (6.1) with R terms is minimal. For a general state, the minimization problem involved can be a very difficult problem of numerical analysis, which scales exponentially in the number of parties N as well as in the degree of entanglement of the state itself. Nevertheless, this task becomes feasible if we restrict our attention to graph states. HEB established several upper and lower bounds for the Schmidt measure in graph theoretical terms in Refs. [9, 11]. These bounds make possible to determine the Schmidt measure for a large number of graphs of practical importance, because in many cases the bounds proposed are easily computable and, remarkably, the upper and lower bounds frequently coincide.

Pauli persistency and size of the minimal vertex cover

For any graph state $|G\rangle$, upper bounds for its Schmidt measure $E_S(|G\rangle)$ are the *Pauli persistency* $PP(G)$ and the *size of the minimal vertex cover* $VC(G)$,

$$E_S(|G\rangle) \leq PP(G) \leq VC(G). \tag{6.9}$$

The Pauli persistency is the minimal number of local Pauli measurements necessary to disentangle a graph state. Concerning this question, HEB described graphical transformation rules when local Pauli measurements are applied (Refs. [9, 11]).

A vertex cover is a concept from graph theory: It is any subset $V' \subseteq V$ of vertices in a graph G to which *any* edge of G is incident (see Fig. 6.1). Therefore, the minimal vertex cover of a graph is the smallest one, whose size[4] is denoted by $VC(G)$. According to the graphical rules for the Pauli measurements, since each σ_z measurement simply deletes all edges incident to a vertex, the size of the minimal vertex cover would equal the Pauli persistency, provided that we restrict the Pauli measurements to σ_z measurements. Nevertheless, in graphs with many edges, i.e., very connected, a proper combination of σ_x, σ_y, and σ_z measurements could provide a more efficient disentangling sequence, giving a better upper bound $PP(G)$ for the Schmidt measure. See Refs. [9, 11] for details.

Maximal Schmidt rank

For any graph state $|G\rangle$, a lower bound for the Schmidt measure $E_S(|G\rangle)$ is the *maximal Schmidt rank*,

$$SR_{\max}(G) \leq E_S(|G\rangle). \tag{6.10}$$

[4]The size of a minimal vertex cover in a graph G is also known as the *vertex cover number* of G, denoted sometimes as $\tau(G)$ or $\beta(G)$. Interestingly, there is a relation between the vertex cover number $\tau(G)$ and the independence number $\alpha(G)$ (another combinatorial number profusely used in the first part of this thesis), namely, $\alpha(G) + \tau(G) = |G|$, where $|G|$ is the number of vertices of the graph G.

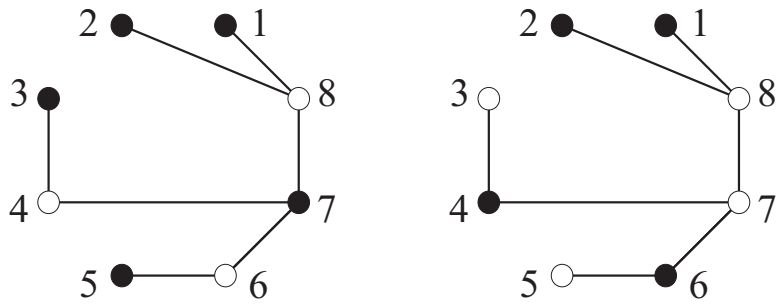

Figure 6.1: The set of vertices 4, 6, and 8 is the minimal vertex cover of the graph (left). The set of vertices 3, 5, 7, and 8, is a vertex cover of the graph, but is not minimal, it has size 4 (right).

While calculating the Schmidt rank with respect to all possible bipartitions of a given graph $G = (V, E)$, if one maximizes the Schmidt rank over all bipartitions (A, B) of the graph, and takes into account the nonincreasing property of $E_S|(G)\rangle$ [see Eq. (6.4)], then one obtains a lower bound for the Schmidt measure with respect to the finest partitioning. This lower bound is the maximal Schmidt rank,

$$SR_{\max}(G) := \max_{A \subseteq V} SR_A(G). \tag{6.11}$$

According to the definition of Schmidt rank, the maximal Schmidt rank for any state is, at most, $\lfloor \frac{N}{2} \rfloor$, i.e., the largest integer less than or equal to $\frac{N}{2}$.

Addition and deletion of edges and vertices

Applying the LC* rule does not change the Schmidt measure E_S. It is interesting to remark that other local changes to the graph, such as the deletion of edges or vertices, have only a limited effect on E_S. This fact is established by HEB in Ref. [9] in what they call the *edge/vertex rule*: On one hand, by deleting (or adding) an edge e between two vertices of a graph G the Schmidt measure of the resulting graph $G' = G \pm e$ can at most decrease (or increase) by 1. On the other hand, if a vertex v (including all its incident edges) is deleted, the Schmidt measure of the resulting graph $G' = G - v$ cannot increase, and will at most decrease by one. If $E_S(|G + e\rangle)$ denotes the Schmidt measure of the graph state corresponding to the graph $G + e$, then the previous rules can be summarized as

$$E_S(|G + e\rangle) \leq E_S(|G\rangle) + 1, \tag{6.12a}$$
$$E_S(|G - e\rangle) \geq E_S(|G\rangle) - 1, \tag{6.12b}$$
$$E_S(|G - v\rangle) \geq E_S(|G\rangle) - 1. \tag{6.12c}$$

We have used these rules in two ways: Firstly, as an internal test to check our calculations, comparing pairs of graphs connected by a sequence of addition or deletion of edges/vertices;

and secondly, as a useful tool that, in some graphs, has enabled us to go from a bounded to a determined value for the Schmidt measure, once again by comparison between a problematic graph G and a resulting graph G' (typically obtained by edge or vertex deletion) of a known Schmidt measure.

Schmidt measure in some special types of graphs

There are some special types of graph states in which lower and upper bounds for the Schmidt measure coincide (see Ref. [9]), giving directly a determined value for E_S. Since the maximal Schmidt rank for any state can be at most $\lfloor \frac{N}{2} \rfloor$, and restricting ourselves to states with coincident upper and lower bounds to E_S, it is true that $SR_{\max}(G) = E_S(|G\rangle) = PP(G) = VC(G) \leq \lfloor \frac{N}{2} \rfloor$. This is the case for GHZ states, and states represented by trees, rings with an even number of vertices, and clusters. In our work we have used the following results concerning GHZ states and trees:

(a) The Schmidt measure for any multipartite GHZ state is 1.

(b) A *tree* T is a graph that has no cycles. The Schmidt measure of the corresponding graph state $|T\rangle$ is the size of its minimal vertex cover: $E_S(|T\rangle) = VC(T)$.

There is another interesting kind of graphs for our purposes, the so-called *2-colorable graphs*. A graph is said to be 2-colorable when it is possible to perform a *proper 2-coloring* on it: This is a labeling $V \to \{1, 2\}$, such that all connected vertices are associated with a different element from $\{1, 2\}$, which can be identified with two colors. It is a well-known fact in graph theory that a necessary and sufficient criterion for a graph to be 2-colorable is that it does not contain any cycles of odd length. Mathematicians call these graphs *bipartite graphs* due to the fact that the whole set of vertices can be distributed into two disjoint subsets A and B, such that no two vertices within the same subset are connected, and therefore every edge connects a vertex in A with a vertex in B.

In Ref. [9], HEB provided lower and upper bounds for the Schmidt measure that could be applied to graph states represented by 2-colorable graphs:

$$\frac{1}{2}\text{rank}_{\mathcal{F}_2}(\Gamma) \leq E_S(|G\rangle) \leq \lfloor \frac{|V|}{2} \rfloor, \tag{6.13}$$

where Γ is the adjacency matrix of the 2-colorable graph. If Γ is invertible, then

$$E_S(|G\rangle) = \lfloor \frac{|V|}{2} \rfloor. \tag{6.14}$$

Besides, HEB pointed out that any graph G which is not 2-colorable can be turned into a 2-colorable one G' by simply deleting the appropriate vertices on cycles with odd length present in G. The identification of this graphical action with the effect of a σ_z measurement on qubits corresponding to such vertices yields new upper bounds for $E_S(|G\rangle)$:

$$E_S(|G\rangle) \leq E_S(|G'\rangle) + M \leq \lfloor \frac{|V - M|}{2} \rfloor + M \leq \lfloor \frac{|V| + M}{2} \rfloor, \tag{6.15}$$

where M is the number of removed vertices. We have used these new bounds in some graphs as a tool to check our calculations.

6.4 Final remarks, open problems, and future developments

To sum it all up, we have extended to 8 qubits the classification of the entanglement of graph states proposed in Ref. [9] for $n < 8$ qubits. Notice that for $n = 8$ we have 101 classes, while for $n < 8$ there are only 45 classes. For each of these classes we obtain a representative which requires the minimum number of controlled-Z gates for its preparation (see Fig. 6.2), and calculate the Schmidt measure for the 8-partite split (which measures the genuine 8-party entanglement of the class), and the Schmidt ranks for all bipartite splits (see Table 6.1).

This classification has been useful to obtain new all-versus-nothing proofs of Bell's theorem (Ref. [167]) and new Bell inequalities. Specifically, any 8-qubit graph state belonging to a class with a representative with 7 edges (i.e., a tree) has a specific type of Bell inequality (Ref. [172]). More generally, it has been helpful to investigate the non-locality (i.e., the non-simulability of the predictions of quantum mechanics by means of LHV models) of graph states in Ref. [171].

Extending the classification in Ref. [9] a further step sheds some light on the limitations of the method of classification. The criteria used in Ref. [9] to order the classes (see Sect. 6.2) already failed to distinguish all classes in $n = 7$. For instance, classes No. 40, No. 42, and No. 43 in Refs. [9, 11] have the same number of qubits, require the same minimum number of controlled-Z gates for the preparation, and have the same Schmidt measure and rank indexes. The same problem occurs between classes No. 110 and No. 111, between classes No. 113 and No. 114, and between classes No. 116 and No. 117 in our classification (see Table 6.1). Following Refs. [9, 11], we have placed the class with lower $|LC|$ in the first place. However, this solution is not satisfactory, since $|LC|$ is not related to the entanglement properties of the class. On the other hand, VDD have proposed a finite set of invariants that characterizes all classes (Ref. [12]). However, this set has more than 2×10^{36} invariants already for $n = 7$. We have addressed the problem of obtaining a minimum set of invariants capable of distinguishing all classes with $n \leq 8$ qubits in Ref. [217], and this work is the main issue of Chap. 7 of this thesis.

Another weak point in the method is that the precise value of E_S is still unknown for some classes. The good news is that, for most of these classes, the value might be fixed if we knew the value for the 5-qubit ring cluster state, which is the first graph state in the classification for which the value of E_S is unknown in Refs. [9, 11]. Unfortunately, we have not made any progress in calculating E_S for the 5-qubit ring cluster state.[5]

Table 6.1 shows that there are no 8-qubit graph states with rank indexes $RI_p = [\nu_j^p]_{j=p}^1$ with $\nu_j^p \neq 0$ if $j = p$, and $\nu_j^p = 0$ if $j < p$, i.e., with maximal rank with respect to all bipartite splits,

[5] There are other entanglement measures to specifically quantify the genuine multipartite entanglement in pure graph states (see footnote 30 on p. 118). Along with the Schmidt measure one can also consider, for instance, the relative entropy of entanglement and the geometric measure: this three quantities are extremely difficult to compute analytically. Interestingly, Hajdušek and Murao have recently presented in Ref. [211] a more graphical and intuitive perspective. In their approach they show that the problem of evaluating these three entanglement measures in pure graph states can be mapped directly to the well-known problem of identifying the maximum independent set in graph theory. For a given graph state $|G\rangle$, knowing the independence number $\alpha(G)$ of the graph G corresponds to knowing the upper bound for the three aforementioned entanglement measures, as well as whether the upper and lower bounds for each of them are equal. Moreover, identifying which qubits comprise the maximum independent set allows them to construct the minimal linear decomposition of $|G\rangle$ into product states as well as its closest separable and closest product state, which allow to calculate the measures. Unfortunately, they are able to evaluate the three entanglement measures only in the case when the lower and upper bounds coincide, which is not the case for the 5-qubit ring cluster state.

i.e., such that entanglement is symmetrically distributed between all parties. These states are robust against disentanglement by a few measurements. Neither there are 7-qubit graph states with this property (Refs. [9, 11]). This makes more interesting the fact that there is a single 5-qubit and a single 6-qubit graph state with this property (Refs. [9, 11]).

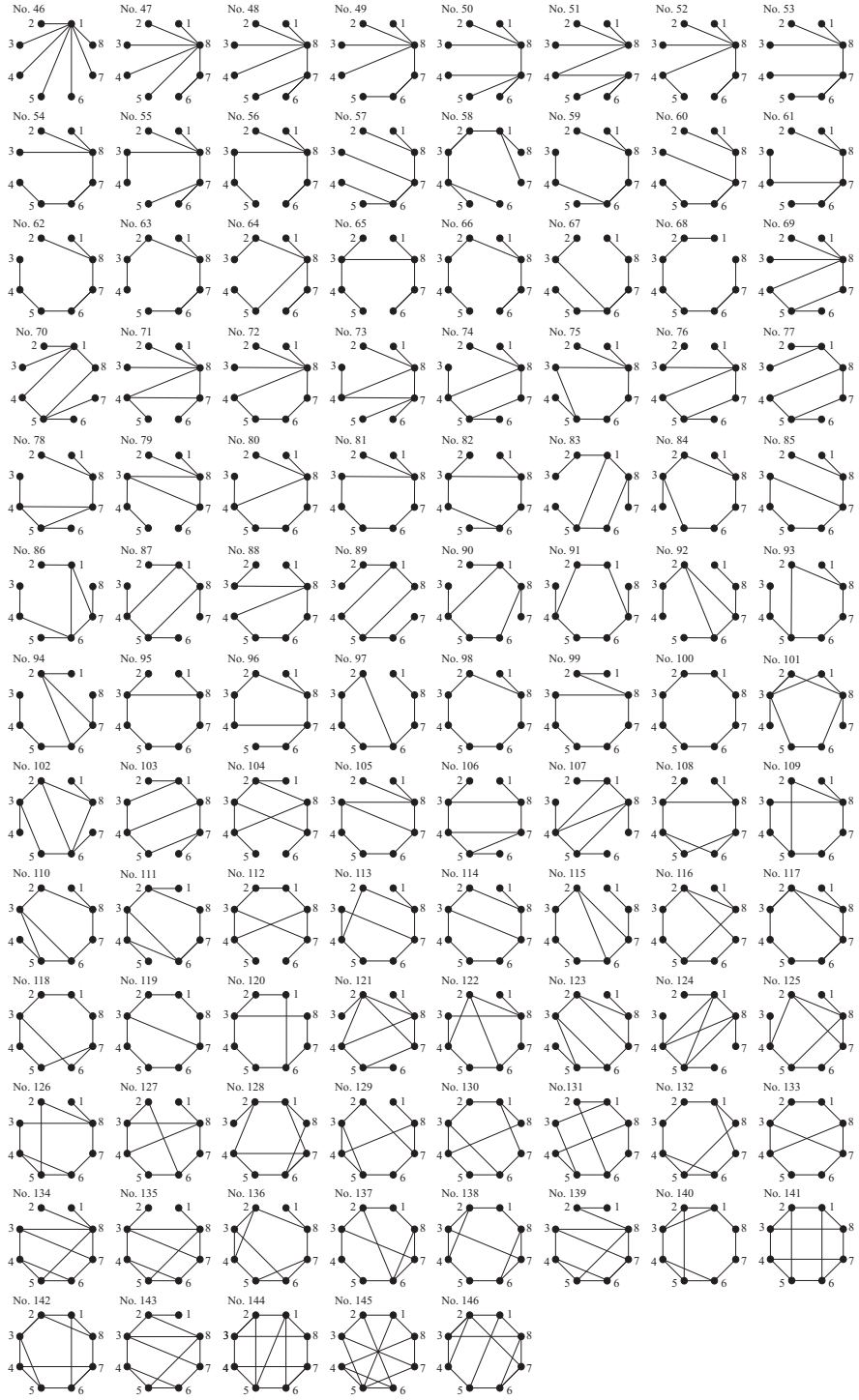

Figure 6.2: Graphs associated to the 101 classes on 8-qubit graph states inequivalent under local complementation and graph isomorphism. We have chosen as representative of the class the one (or one of those) with minimum number of edges and minimum maximum degree (i.e., number of edges incident with a vertex), which means that it requires the minimum number of controlled-Z gates in the preparation and minimum preparation depth.

Table 6.1: Entanglement of the 101 classes of 8-qubit graph states. No. is the number of the class; it is assigned attending to $|E|$, E_S, and RI_j; the numbering starts at the point in which the one in Refs. [9, 11] ends. $|LC|$ is the number of nonisomorphic elements of the class. $|E|$ is the number of edges of those representatives with the minimum number of edges. E_S is the Schmidt measure (or its lower and upper bounds). RI_j is the rank index with j qubits in the smaller bipartition (i.e., the number of bipartite splits in which a certain rank occurs; ranks appear in decreasing order from left to right). 2-col indicates whether or not a 2-colorable representative exists.

No.	$\|LC\|$	$\|E\|$	E_S	RI_4	RI_3	RI_2	2-col	No.	$\|LC\|$	$\|E\|$	E_S	RI_4	RI_3	RI_2	2-col
46	2	7	1	(0,0,0,35)	(0,0,56)	(0,28)	yes	97	154	8	4	(8,22,4,1)	(42,13,1)	(27,1)	no
47	6	7	2	(0,0,20,15)	(0,30,26)	(12,16)	yes	98	542	8	4	(8,22,5,0)	(42,14,0)	(27,1)	no
48	6	7	2	(0,0,30,5)	(0,45,11)	(15,13)	yes	99	300	8	4	(12,16,7,0)	(44,11,1)	(27,1)	yes
49	16	7	2	(0,0,30,5)	(0,45,11)	(17,11)	yes	100	214	8	4	(14,17,4,0)	(48,8,0)	(28,0)	yes
50	4	7	2	(0,0,34,1)	(0,48,8)	(16,12)	yes	101	14	9	3	(0,20,15,0)	(24,32,0)	(25,3)	no
51	16	7	2	(0,0,34,1)	(0,51,5)	(19,9)	yes	102	66	9	3	(0,28,7,0)	(32,24,0)	(25,3)	no
52	10	7	3	(0,12,16,7)	(16,28,12)	(20,8)	yes	103	66	9	3	(0,30,5,0)	(36,20,0)	(26,2)	yes
53	16	7	3	(0,12,22,1)	(16,34,6)	(20,8)	yes	104	6	9	3	(0,32,0,3)	(32,24,0)	(24,4)	yes
54	44	7	3	(0,12,22,1)	(16,35,5)	(21,7)	yes	105	57	9	$3 < 4$	(0,30,5,0)	(36,19,1)	(25,3)	no
55	16	7	3	(0,18,14,3)	(18,33,5)	(21,7)	yes	106	28	9	4	(8,18,9,0)	(38,18,0)	(25,3)	no
56	44	7	3	(0,18,14,3)	(22,29,5)	(23,5)	yes	107	17	9	4	(8,20,6,1)	(32,24,0)	(24,4)	no
57	10	7	3	(0,18,15,2)	(18,36,2)	(21,7)	yes	108	72	9	4	(8,20,7,0)	(36,20,0)	(25,3)	no
58	25	7	3	(0,18,16,1)	(18,36,2)	(22,6)	yes	109	87	9	4	(8,20,7,0)	(40,16,0)	(27,1)	no
59	44	7	3	(0,18,16,1)	(22,31,3)	(23,5)	yes	110	114	9	4	(8,22,5,0)	(40,16,0)	(26,2)	no
60	44	7	3	(0,24,9,2)	(24,30,2)	(23,5)	yes	111	372	9	4	(8,22,5,0)	(40,16,0)	(26,2)	no
61	26	7	3	(0,24,10,1)	(28,25,3)	(23,5)	yes	112	70	9	4	(8,24,2,1)	(40,16,0)	(26,2)	no
62	120	7	3	(0,24,10,1)	(28,26,2)	(24,4)	yes	113	264	9	4	(8,24,3,0)	(44,12,0)	(27,1)	no
63	66	7	3	(0,26,7,2)	(30,24,2)	(25,3)	yes	114	542	9	4	(8,24,3,0)	(44,12,0)	(27,1)	no
64	14	7	4	(8,12,12,3)	(32,18,6)	(24,4)	yes	115	156	9	4	(12,18,5,0)	(46,9,1)	(27,1)	no
65	25	7	4	(8,12,14,1)	(32,20,4)	(24,4)	yes	116	174	9	4	(12,20,3,0)	(46,10,0)	(27,1)	no
66	120	7	4	(8,14,12,1)	(34,19,3)	(25,3)	yes	117	542	9	4	(12,20,3,0)	(46,10,0)	(27,1)	no
67	72	7	4	(8,16,10,1)	(36,17,3)	(25,3)	yes	118	262	9	4	(12,20,3,0)	(48,8,0)	(28,0)	no
68	172	7	4	(8,18,8,1)	(38,16,2)	(26,2)	yes	119	802	9	4	(14,19,2,0)	(50,6,0)	(28,0)	no
69	10	8	2	(0,0,34,1)	(0,52,4)	(20,8)	yes	120	117	9	4	(16,16,3,0)	(50,6,0)	(28,0)	yes
70	10	8	2	(0,0,35,0)	(0,54,2)	(21,7)	yes	121	10	10	3	(0,32,2,1)	(32,24,0)	(24,4)	no
71	10	8	3	(0,12,22,1)	(16,36,4)	(20,8)	no	122	37	10	3	(0,32,3,0)	(40,16,0)	(27,1)	yes
72	21	8	3	(0,12,22,1)	(16,36,4)	(22,6)	no	123	36	10	4	(8,22,5,0)	(44,12,0)	(26,2)	no
73	10	8	3	(0,18,17,0)	(18,36,2)	(21,7)	no	124	7	10	4	(8,24,0,3)	(32,24,0)	(24,4)	no
74	44	8	3	(0,18,17,0)	(22,32,2)	(23,5)	yes	125	103	10	4	(8,24,3,0)	(42,14,0)	(26,2)	no
75	66	8	3	(0,18,17,0)	(22,33,1)	(24,4)	no	126	46	10	4	(8,24,3,0)	(44,12,0)	(27,1)	no
76	26	8	3	(0,20,14,1)	(24,30,2)	(24,4)	yes	127	170	10	4	(8,26,1,0)	(46,10,0)	(27,1)	no
77	26	8	3	(0,24,10,1)	(24,31,1)	(23,5)	yes	128	74	10	4	(12,20,3,0)	(46,10,0)	(27,1)	yes
78	28	8	3	(0,24,10,1)	(28,27,1)	(23,5)	no	129	340	10	4	(12,22,1,0)	(48,8,0)	(27,1)	no
79	44	8	3	(0,24,11,0)	(28,26,2)	(23,5)	no	130	254	10	4	(12,22,1,0)	(50,6,0)	(28,0)	no
80	132	8	3	(0,24,11,0)	(28,27,1)	(24,4)	no	131	433	10	4	(14,21,0,0)	(52,4,0)	(28,0)	no
81	114	8	3	(0,24,11,0)	(30,25,1)	(25,3)	yes	132	476	10	4	(16,18,1,0)	(52,4,0)	(28,0)	no
82	72	8	3	(0,26,9,0)	(30,26,0)	(25,3)	no	133	28	10	$4 < 5$	(12,22,0,1)	(48,8,0)	(28,0)	no
83	72	8	3	(0,28,6,1)	(32,23,1)	(25,3)	yes	134	9	11	$3 < 4$	(0,30,5,0)	(40,15,1)	(25,3)	no
84	198	8	3	(0,28,7,0)	(34,22,0)	(26,2)	yes	135	39	11	4	(8,26,1,0)	(44,12,0)	(26,2)	no
85	56	8	$3 < 4$	(0,30,4,1)	(34,21,1)	(25,3)	no	136	46	11	4	(12,20,3,0)	(50,6,0)	(27,1)	no
86	28	8	4	(8,16,10,1)	(32,22,2)	(24,4)	no	137	208	11	$4 < 5$	(16,18,1,0)	(52,4,0)	(28,0)	no
87	10	8	4	(8,16,10,1)	(32,24,0)	(24,4)	yes	138	298	11	$4 < 5$	(18,17,0,0)	(54,2,0)	(28,0)	no
88	56	8	4	(8,16,10,1)	(36,18,2)	(26,2)	no	139	24	11	$4 < 5$	(20,10,5,0)	(50,5,1)	(27,1)	no
89	66	8	4	(8,16,11,0)	(36,18,2)	(25,3)	yes	140	267	11	$4 < 5$	(20,14,1,0)	(54,2,0)	(28,0)	no
90	72	8	4	(8,18,9,0)	(34,22,0)	(25,3)	no	141	4	12	4	(28,0,7,0)	(56,0,0)	(28,0)	no
91	63	8	4	(8,18,9,0)	(36,20,0)	(26,2)	yes	142	22	12	$4 < 5$	(14,21,0,0)	(56,0,0)	(28,0)	no
92	66	8	4	(8,18,9,0)	(38,16,2)	(25,3)	no	143	46	12	$4 < 5$	(20,12,3,0)	(50,6,0)	(27,1)	yes
93	176	8	4	(8,18,9,0)	(38,17,1)	(26,2)	no	144	28	13	4	(28,4,3,0)	(56,0,0)	(28,0)	no
94	76	8	4	(8,20,6,1)	(36,19,1)	(25,3)	no	145	7	13	$4 < 5$	(16,18,1,0)	(56,0,0)	(28,0)	no
95	194	8	4	(8,20,7,0)	(38,18,0)	(26,2)	yes	146	51	13	$4 < 5$	(24,10,1,0)	(56,0,0)	(28,0)	no
96	352	8	4	(8,20,7,0)	(40,15,1)	(26,2)	no								

Chapter 7

Compact set of invariants characterizing graph states of up to eight qubits

In this chapter we present the results obtained in Ref. [217]. Below we provide a brief summary.

Summary:

The set of entanglement measures proposed by Hein, Eisert, and Briegel for n-qubit graph states [Phys. Rev. A **69**, 062311 (2004)] fails to distinguish between inequivalent classes under local Clifford operations if $n \geq 7$. On the other hand, the set of invariants proposed by Van den Nest, Dehaene, and De Moor [Phys. Rev. A **72**, 014307 (2005)] distinguishes between inequivalent classes, but contains too many invariants (more than 2×10^{36} for $n = 7$) to be practical. Here we solve the problem of deciding which entanglement class a graph state of $n \leq 8$ qubits belongs to by calculating some of the state's intrinsic properties. We show that four invariants related to those proposed by VDD are enough for distinguishing between all inequivalent classes with $n \leq 8$ qubits.

7.1 Introduction and main goal

Let us start, for the sake of convenience, with a quick overview of some of the results already presented in Chap. 5. This results are explained in more detail in Sect. 5.2.2:

Graph states play a fundamental role in the study of entanglement. Two quantum states have the same entanglement if they are equivalent under SLOCC. For $n = 3$, there are six classes under SLOCC (see Ref. [200]). For $n \geq 4$ the number of classes under SLOCC is infinite and is specified by an exponentially increasing number of parameters. However, if we focus on graph states of $n < 27$ qubits, then the discussion becomes simpler. On one hand, every two graph states which are SLOCC equivalent are also equivalent under LU operations (Ref. [205]). On the other hand, previous results suggest that, for graph states of $n < 27$ qubits, the notion of LU equivalence and LC equivalence coincide. The "LU⇔LC conjecture" states that "every two

LU-equivalent stabilizer states must also be LC equivalent." Ji *et al.* proved that the LU⇔LC conjecture is false in Ref. [206]. However, the LU⇔LC is true for several classes of n qubit graph states (Refs. [207, 208]) and the simplest counterexamples to the conjecture are graph states of $n = 27$ qubits in Ref. [206]. Indeed, Ji *et al.* "believe that 27 is the smallest possible size of counterexamples of LU⇔LC." In this part of our research we assume that deciding whether or not two graph states of $n < 27$ qubits have the same entanglement is equivalent to deciding whether or not they are LC equivalent.

The aim of this chapter is to solve the following problem: Given an n-qubit graph state with $n < 9$ qubits, decide which entanglement class it belongs to just by examining some of the state's intrinsic properties (i.e., without generating the whole LC class). The solution to this problem is of practical importance. If one needs to prepare a graph state $|G\rangle$ and knows that it belongs to one specific class, then one can prepare $|G\rangle$ by preparing the LC-equivalent state $|G'\rangle$ requiring the minimum number of entangling gates and the minimum preparation depth of that class (see Refs. [9, 11, 13]) and then transform $|G'\rangle$ into $|G\rangle$ by means of simple one-qubit unitary operations.[1] The problem is that, so far, we do not know a simple set of invariants which distinguishes between all classes of entanglement, even for graph states with $n \leq 7$ qubits.

In that regard recall that, as we already know from Chap. 6, the classification of graph states' entanglement has been achieved, up to $n = 7$ qubits, by HEB in Refs. [9, 11]. We have extended such classification to $n = 8$ qubits in Ref. [13]. The criteria for ordering the classes in Refs. [9, 11, 13], for each number of qubits, are based on several quantities: first, the minimum number of two-qubit gates required for the preparation of a member of the class; and second, some entanglement measures, namely, the Schmidt measure for the n-partite split (which measures the genuine n-party entanglement of the class, Ref. [214]), and the Schmidt ranks for all bipartite splits (or rank indexes, Refs. [9, 11]). The problem is that this set of entanglement measures *fails to distinguish between inequivalent classes* (i.e., between different types of entanglement). There is already an example of this problem for $n = 7$ in Refs. [9, 11], and the same occurs for $n = 8$ in Ref. [13] (see details in Sect. 6.4). Therefore, we cannot use these invariants for deciding which entanglement class a given state belongs to. Reciprocally, if we have such a set of invariants, then we can use it to unambiguously label each of the classes.

VDD proposed a finite set of invariants that characterizes all classes (Ref. [12]). However, already for $n = 7$, this set has more than 2×10^{36} invariants which are not explicitly calculated anywhere, so this set is not useful for classifying a given graph state. Indeed, VDD "believe that [their set of invariants] can be improved —if not for all stabilizer states then at least for some interesting subclasses of states" (Ref. [12]). Moreover, they state that "it is likely that only [some] invariants need to be considered in order to recognize LC equivalence" (Ref. [12]), and that "it is not unlikely that there exist smaller complete lists of invariants which exhibit less redundancies" (Ref. [12]). In this chapter we show that, if $n \leq 8$, then four invariants are enough to recognize the type of entanglement (Ref. [217]).

In Sect. 7.2, after outlining or referring to previous ideas allowing to follow the subsequent discussions, we introduce a new basic concept of the stabilizer formalism, namely, the support of a stabilizing operator (Sect. 7.2.1). This concept is necessary in order to review some of the

[1] This preparation procedure constitutes the issue of Chap. 8, where we take advantage of both the classification of graph states in LC equivalence classes (Chap. 6) and the identification of such classes on the basis of a compact set of LC invariants (main concern of the current chapter) to achieve optimality in the preparation.

results about the invariants proposed by VDD that will be useful in our discussion (Sect. 7.2.2). Then, in Sect. 7.3, we present the results of our research, and discuss their implications.

7.2 Basic concepts

In the following, we will take advantage of concepts and notation previously introduced in this thesis. In particular, we will base our discussion on the stabilizer formalism, since graph states are a special kind of stabilizer states:[2] we refer the reader to Sect. 5.1 for a condensed overview, and more specifically to the notions of Pauli group and generator of a group (Sect. 5.1.1), n-qubit stabilizer and stabilizer states (Sect. 5.1.3).

Of the two possible definitions of graph state, we are interested in this chapter in the algebraic characterization in the stabilizer formalism, which has been presented in Sect. 5.2.1, definition (II). Nevertheless, for convenience we recall it here: the graph state $|G\rangle$ associated to the graph G is the unique n-qubit state fulfilling

$$g_i|G\rangle = |G\rangle, \quad \text{for} \quad i = 1, \ldots, n, \tag{7.1}$$

where g_i are the generating operators of the state's stabilizer group, the latter defined as the set $\{s_j\}_{j=1}^{2^n}$ of all products of the generating operators. The generating operator g_i associated to the vertex i is defined by

$$g_i := X^{(i)} \bigotimes_{(i,j)\in E} Z^{(j)}, \tag{7.2}$$

where the product is extended to those vertices j which are connected with i and $X^{(i)}$ ($Z^{(i)}$) denotes the Pauli matrix σ_x (σ_z) acting on the ith qubit.

As we have seen, VDD found that the successive application of local complementation on the graph G associated to a graph state $|G\rangle$ is enough to generate the complete equivalence class of $|G\rangle$ under local unitary operations (orbit of $|G\rangle$) within the Clifford group (Ref. [10]). The details and the description of the graphical action of local complementation can be consulted in Sect. 5.2.2, item 6. For subsequent purposes we need to remember that, on the stabilizer, local complementation on the qubit i induces the map

$$Y^{(i)} \mapsto Z^{(i)}, Z^{(i)} \mapsto -Y^{(i)} \tag{7.3}$$

on the qubit i, and the map

$$X^{(j)} \mapsto -Y^{(j)}, Y^{(j)} \mapsto X^{(j)} \tag{7.4}$$

on the qubits j connected with i (Ref. [11]).

Finally, using local complementation one can generate the orbits of all LC-inequivalent n-qubit graph states. There are 45 orbits for $n \leq 7$ (Refs. [9, 11]) and 101 orbits for $n = 8$ (Ref. [13]).

With these tools, we are ready to introduce the new concept of support of a stabilizing operator.

[2] We also know from Chap. 5 that every stabilizer state is equivalent under LC operations to some (generally non unique) graph state (Ref. [158]).

7.2.1 Supports and classes of equivalence related to supports

Let $|\psi\rangle$ be a stabilizer state and $\mathcal{S}(|\psi\rangle)$ the corresponding stabilizer. Given a stabilizing operator $s_i = \alpha_i M_1^{(i)} \bigotimes \cdots \bigotimes M_n^{(i)}$, its *support* $\mathrm{supp}(s_i)$ is the set of all $j \in \{1, \ldots, n\}$ such that $M_j^{(i)}$ differs from the identity $\mathbb{1}$. Therefore, the support[3] of s_i is the set of the labels of the qubits on which the action of the Pauli matrices is non trivial (i.e., there is a X, Y, or Z Pauli matrix acting on the qubit). Notice that, according to Eqs. (7.3) and (7.4), the support of a stabilizing operator is preserved under the maps induced on the stabilizer by local complementation.

Let $\omega \subseteq \{1, \ldots, n\}$ be the support of a stabilizing operator s_i, $\mathrm{supp}(s_i) = \omega$. The *weight* of the operator s_i is the cardinality of its support, $|\omega|$. The identity operator $\mathbb{1} \bigotimes \cdots \bigotimes \mathbb{1}$, which is always present in a stabilizer due to the underlying group structure, fulfills $\omega = \{\emptyset\}$ and, therefore, is of weight zero.

The set of operators $\{s_i\}_{i=1}^{2^n}$ of a stabilizer $\mathcal{S}(|\psi\rangle)$ of a stabilizer state $|\psi\rangle$ can be classified into equivalence classes according to their supports, defining a partition in the stabilizer. We will say that two stabilizing operators s_i and s_j of $\mathcal{S}$ belong to the same equivalence class $[\omega]$ if they have the same support ω, i.e., $\mathrm{supp}(s_i) = \mathrm{supp}(s_j) = \omega$. We denote by $A_\omega(|\psi\rangle)$ the number of elements (stabilizing operators) $s_i \in \mathcal{S}(|\psi\rangle)$ with $\mathrm{supp}(s_i) = \omega$. In other words, $A_\omega(|\psi\rangle)$ is the cardinality of the equivalence class $[\omega]$.

Since any graph state $|G\rangle$ is a special type of stabilizer state, these definitions can also be applied to them.

7.2.2 Invariants of Van den Nest, Dehaene, and De Moor

The following theorem is a key result obtained by VDD in Ref. [12] that presents a finite set of invariants which characterizes the LC equivalence class of any stabilizer state (i.e., functions that remain invariant under the action of all LC transformations). We have chosen an adapted formulation of the theorem to group multiplication involving Pauli operators [see Eq. (7.5)], slightly different from VDD's original notation, which is based on the well-known equivalent formulation of the stabilizer formalism in terms of algebra over the field $\mathbb{F}_2 = \mathrm{GF}(2)$, where arithmetic is performed modulo 2 and each stabilizing operator is identified with a $2n$-dimensional binary index operator.

Theorem 1. Let $|\psi\rangle$ be a stabilizer state on n qubits corresponding to a stabilizer $\mathcal{S}_{|\psi\rangle}$. Let $r \in \mathbb{N}_0$ and consider subsets $\omega_k, \omega_{kl} \subseteq \{1, \ldots, n\}$ for every $k, l \in \{1, \ldots, r\}$, with $k < l$. Denote $\Omega := (\omega_1, \omega_2, \ldots, \omega_{12}, \omega_{13}, \ldots)$ and let $\mathcal{T}_{n,r}^{\Omega}(|\psi\rangle)$ be the set consisting of all tuples $(s_1, \ldots, s_r) \in \mathcal{S}_{|\psi\rangle} \times \ldots \times \mathcal{S}_{|\psi\rangle}$ satisfying

$$\mathrm{supp}(s_k) = \omega_k, \ \mathrm{supp}(s_k s_l) = \omega_{kl}. \tag{7.5}$$

Then, (i) $|\mathcal{T}_{n,r}^{\Omega}(|\psi\rangle)|$ is LC invariant and (ii) the LC equivalence class of $|\psi\rangle$ is completely determined by the values of all invariants $|\mathcal{T}_{n,n}^{\Omega}(|\psi\rangle)|$ (i.e., where $r = n$).

VDD provide another family of support-related invariants, based on a second theorem with the same formulation than the one above, except for the substitution of conditions (7.5) by new

[3] Let us remind the reader that, for a given stabilizer $\mathcal{S}$, the stabilized vector space $V_{\mathcal{S}}$ is of dimension 2^{n-k} when the cardinality of the generator $\gamma_{\mathcal{S}}$ is $|\gamma_{\mathcal{S}}| = k$. For simplicity we are assuming $k = n$ in the definition, but the concept of support we have just introduced can also be applied in case the stabilized space is not of dimension one, that is, in case that $\mathcal{S}$ does not fix a unique state $|\psi\rangle$.

constraints

$$\mathrm{supp}(s_k) \subseteq \omega_k,\ \mathrm{supp}(s_k s_l) \subseteq \omega_{kl}. \tag{7.6}$$

These new LC invariants are the dimensions of certain vector spaces and, in principle, are more manageable from a computational point of view because they involve the generator matrix of the stabilizer and rank calculation. Nevertheless, we will focus our attention on the first family of invariants, since they suffice to solve the problem we address in this chapter with no extra computational effort. To resort to the second family would be justified in case we had to use invariants with a high r value to achieve LC discrimination among graph states up to eight qubits. We refer the reader to Ref. [12] for a proof of Theorem 1 and the extension to the second family of LC invariants.

The invariants of Theorem 1 are the cardinalities of certain subsets $\mathcal{T}^{\Omega}_{n,r}(|\psi\rangle)$ of $\mathcal{S}_{|\psi\rangle}\cdots\mathcal{S}_{|\psi\rangle}$, which are defined in terms of simple constraints (7.5) on the supports of the stabilizing operators. VDD pointed out that, for $r = 1$, these invariants count the number of operators in the stabilizer with a prescribed support. Therefore, fixing $r = 1$, for every possible support $\omega_k \subseteq \{1, \ldots, n\}$, there is an invariant

$$|\{s \in \mathcal{S}_{|\psi\rangle} | \mathrm{supp}(s) = \omega_k\}|. \tag{7.7}$$

That is, the invariants for $r = 1$ are the $A_{\omega_k}(|\psi\rangle)$, i.e., the cardinalities of the equivalence classes $[\omega_k]$ of the stabilizer. The number of possible supports in a stabilizer of an n-qubit state is equal to 2^n and, therefore, there are 2^n VDD's invariants for $r = 1$. Many of them could be equal to zero. In fact, when dealing specifically with graph states, it can be easily seen that $A_{\omega_k}(|\psi\rangle) = 0$ when referred to supports fulfilling $|\omega_k| = 1$ because stabilizing operators of weight 1 are not present in the stabilizer of a graph state due to the inherent connectivity of the graphs associated to the states that rules out isolated vertices.

On the other hand, VDD consider the invariants $A_{\omega_k}(|\psi\rangle)$ as "local versions" of the so-called weight distribution of a stabilizer, a concept frequently used in classical and quantum coding theory. For $r \geq 2$, the new series of invariants involve r-tuples of stabilizing operators and their corresponding supports and constitute a generalization of the weight distribution. Let us denote

$$A_d(|\psi\rangle) = \sum_{\omega, |\omega|=d} A_\omega(|\psi\rangle), \tag{7.8}$$

the number of stabilizing operators with weight equal to d. According to this notation, the weight distribution of a stabilizer is the $(n+1)$-tuple

$$W_{|\psi\rangle} = \{A_d(|\psi\rangle)\}_{d=0}^{n}. \tag{7.9}$$

In principle, $W_{|\psi\rangle}$ could be a compact way to present the whole information about the invariants $A_\omega(|\psi\rangle)$, i.e., VDD's invariants with $r = 1$. This question will be addressed later.

In order to clarify the content of VDD's theorem, let us briefly discuss the way it works when applied to a particular graph state. We have chosen the three-qubit linear cluster state, $|\mathrm{LC}_3\rangle$, because of its simplicity, combined with a sufficient richness in the stabilizer structure. Table 7.1 shows the stabilizer of $|\mathrm{LC}_3\rangle$ with its eight stabilizing operators, $\{s_1, \ldots, s_8\}$. Three of them ($s_1 = g_1$, $s_2 = g_2$, and $s_3 = g_3$) constitute a generator. $|\mathrm{LC}_3\rangle$ is a three-qubit graph state, so there are $2^3 = 8$ possible supports (8 being the number of subsets in the set $\{1, 2, 3\}$):

$$\{\emptyset\}, \{1\}, \{2\}, \{3\}, \{1, 2\}, \{1, 3\}, \{2, 3\}, \{1, 2, 3\}. \tag{7.10}$$

Table 7.1: Stabilizer and supports for the graph state $|\mathrm{LC}_3\rangle$.

Stabilizing operators		Support	Weight
$XZ\mathbb{1}$	$s_1 = g_1$	$\{1,2\}$	2
ZXZ	$s_2 = g_2$	$\{1,2,3\}$	3
$\mathbb{1}ZX$	$s_3 = g_3$	$\{2,3\}$	2
$\mathbb{1}\mathbb{1}\mathbb{1}$	$s_4 = g_1 g_1$	$\{\emptyset\}$	0
YYZ	$s_5 = g_1 g_2$	$\{1,2,3\}$	3
$X\mathbb{1}X$	$s_6 = g_1 g_3$	$\{1,3\}$	2
ZYY	$s_7 = g_2 g_3$	$\{1,2,3\}$	3
$-YXY$	$s_8 = g_1 g_2 g_3$	$\{1,2,3\}$	3

(i) VDD's invariants for $r = 1$. In this case, $\Omega = (\omega_1)$. By Ω, we denote each of all the possible ways to choose a single support ω_1, so there are eight choices for Ω, which are those listed in Eq. (7.10). Given a particular choice of $\Omega = (\omega_1)$, the set $\mathcal{T}^{\Omega}_{n,1}(|\mathrm{LC}_3\rangle)$ contains all stabilizing operators s_1 for the $|\mathrm{LC}_3\rangle$ fulfilling

$$\mathrm{supp}(s_1) = \omega_1, \tag{7.11}$$

so, as a matter of fact, $\mathcal{T}^{\Omega}_{n,1}(|\mathrm{LC}_3\rangle)$ is the equivalence class $[\omega_1]$ associated to the support ω_1. Only five out of the eight possible supports are in fact present in the stabilizer of the state $|\mathrm{LC}_3\rangle$ (see the column "Support" in Table 7.1) and, therefore, we can distinguish between five non empty equivalence classes $[\omega]$. According to VDD's theorem, the LC invariants for $r = 1$, $|\mathcal{T}^{\Omega}_{n,1}(|\mathrm{LC}_3\rangle)|$, are the cardinalities $A_\omega(|\mathrm{LC}_3\rangle)$ of such equivalence classes $[\omega]$, namely,

$$A_{\{\emptyset\}}(|\mathrm{LC}_3\rangle) = 1, \tag{7.12a}$$
$$A_{\{1\}}(|\mathrm{LC}_3\rangle) = 0, \tag{7.12b}$$
$$A_{\{2\}}(|\mathrm{LC}_3\rangle) = 0, \tag{7.12c}$$
$$A_{\{3\}}(|\mathrm{LC}_3\rangle) = 0, \tag{7.12d}$$
$$A_{\{1,2\}}(|\mathrm{LC}_3\rangle) = 1, \tag{7.12e}$$
$$A_{\{1,3\}}(|\mathrm{LC}_3\rangle) = 1, \tag{7.12f}$$
$$A_{\{2,3\}}(|\mathrm{LC}_3\rangle) = 1, \tag{7.12g}$$
$$A_{\{1,2,3\}}(|\mathrm{LC}_3\rangle) = 4. \tag{7.12h}$$

(ii) VDD's invariants for $r = 2$. In this case, $\Omega = (\omega_1, \omega_2; \omega_{12})$. By Ω we denote each of all the possible different ways to choose two supports ω_1, ω_2, and then a third support ω_{12}. Let $M = 2^n$ be the number of possible supports and n being the number of qubits. On one hand, there are $\binom{M}{2}$ different combinations of two supports (ω_1, ω_2), plus M couples of the form $(\omega_1, \omega_2 = \omega_1)$. On the other hand, there are M possible choices for ω_{12}. As a consequence, there are $M\left[M + \binom{M}{2}\right]$ ways to choose Ω. For $n = 3$, this number is 288. Given a particular choice

of $\Omega = (\omega_1, \omega_2; \omega_{12})$, the set $\mathcal{T}^{\Omega}_{n,2}(|\mathrm{LC}_3\rangle)$ contains all the two-tuples of the stabilizing operators (s_1, s_2) of the state $|\mathrm{LC}_3\rangle$ fulfilling

$$\mathrm{supp}(s_1) = \omega_1,\ \mathrm{supp}(s_2) = \omega_2,\ \mathrm{supp}(s_1 s_2) = \omega_{12}. \tag{7.13}$$

Many of these sets $\mathcal{T}^{\Omega}_{n,2}(|\mathrm{LC}_3\rangle)$ could be empty because the stabilizer fails to fulfill any of the conditions (7.13). The cardinalities of the 288 sets, $|\mathcal{T}^{\Omega}_{n,2}(|\mathrm{LC}_3\rangle)|$, are the VDD's invariants that we are interested in. For instance, if we choose $\Omega = (\omega_1, \omega_2; \omega_{12})$ such that

$$\omega_1 = \{1, 2\},\ \omega_2 = \{1, 2, 3\},\ \omega_{12} = \{1, 2, 3\}, \tag{7.14}$$

then, according to the information in Table 7.1, there is only one operator with support ω_1, namely, s_1, and four operators with support ω_2: s_2, s_5, s_7, and s_8. We obtain $\mathcal{T}^{\Omega}_{n,2}(|\mathrm{LC}_3\rangle) = \{(\mathrm{s}_1, \mathrm{s}_2), (\mathrm{s}_1, \mathrm{s}_5), (\mathrm{s}_1, \mathrm{s}_7), (\mathrm{s}_1, \mathrm{s}_8)\}$ because these four two-tuples verify conditions (7.13), and the value of the corresponding VDD's invariant is the cardinality of the set, $|\mathcal{T}^{\Omega}_{n,2}(|\mathrm{LC}_3\rangle)| = 4$.

Another example. If we choose Ω such that $\omega_1 = \{1, 2\}$, $\omega_2 = \{2, 3\}$, and $\omega_{12} = \{1, 2, 3\}$, then the VDD's invariant is $|\mathcal{T}^{\Omega}_{n,2}(|\mathrm{LC}_3\rangle)| = 0$, because the two-tuple (s_1, s_3) defined by the supports ω_1 and ω_2 fulfills $s_1 s_3 = s_6$ and s_6 does not match with support ω_{12}.

7.3 Results and discussion

The number of VDD's invariants for an n-qubit graph state grows very rapidly with r (and, of course, with n). If $n = 3$, there are eight invariants for $r = 1$ and 288 invariants for $r = 2$. For an eight-qubit graph state, there are 256 invariants for $r = 1$ and 8421376 for $r = 2$. Obviously, the problem of calculating all the VDD's invariants for graph states up to eight qubits becomes completely unfeasible if there are no restrictions on r. The total number of VDD's invariants for a given n-qubit graph state, and all possible values of r, is $M + \sum_{r=2}^{n} C'(M, r)C'(M, P)$, where $M = 2^n$, $P = \binom{r}{2}$, and $C'(M, r)$ denotes the combinations with repetition of M elements choose r. For $n = 7$, this formula gives 2.18×10^{36}; for $n = 8$, it gives 1.88×10^{53}.

How many of them are needed to distinguish between all LC equivalence classes? VDD stated in Ref. [12] that "the LC equivalence class of $|\psi\rangle$ is completely determined by the values of all invariants $|\mathcal{T}^{\Omega}_{n,n}(|\psi\rangle)|$ (i.e., where $r = n$)". However, this number [i.e., $C'(M, r)C'(M, P)$ with $r = n$] is still too large to be practical. For $n = 7$ is 2.18×10^{36} and for $n = 8$ is 1.88×10^{53} (i.e., most of the invariants correspond to the case $r = n$). We are interested in the minimum value of r that yields a series of invariants sufficient to distinguish between all the 146 LC equivalence classes of graph states up to $n = 8$ qubits. In Ref. [12], the authors point out that there are examples of equivalence classes in stabilizer states which are characterized by invariants of small r; for instance, those equivalent to GHZ states. In addition, they remark that a characterization based on small r values could be feasible, at least for some interesting subclasses or subsets of stabilizer states. We have calculated the VDD's invariants for $r = 1$ for the 146 LC equivalence classes of graph states with up to $n = 8$ qubits. This implies calculating the cardinalities $A_{\omega}(|\psi\rangle)$ of the corresponding equivalence classes $[\omega]$ of the 146 representatives of the LC equivalence classes, 30060 invariants in total (since there are 1, 1, 2, 4, 11, 26, and 101 classes of two-, three-, four-, five-, six-, seven-, and eight-qubit graph states, respectively, and the

number of VDD's invariants with $r = 1$ is 2^n for each class). Our results confirm the conjecture that invariants with $r = 1$ are enough for distinguishing between the 146 LC equivalence classes for graph states up to eight qubits. It is therefore unnecessary to resort to families of VDD's invariants $|\mathcal{T}^{\Omega}_{n,r}(|\psi\rangle)|$ with $r \geq 2$.

Our goal is not to show the values of these 30060 invariants but to compress all this information and construct simple invariants from it. However, in order to do it properly, some requirements should be fulfilled. (I) The compacted information must be unambiguous and easily readable. (II) The compacted information must be LC invariant. (III) The compacted information concerning different LC equivalence classes must still distinguish between any of them.

Following the comments of VDD in Ref. [12] about considering the invariants $A_\omega(|\psi\rangle)$ as "local versions" of the weight distribution $W_{|\psi\rangle}$ of a stabilizer, we have calculated $W_{|\psi\rangle}$ for the 146 LC classes of equivalence, according to definition (7.9). It can easily be seen that, if $A_\omega(|\psi\rangle)$ is LC invariant, then $W_{|\psi\rangle}$ is also LC invariant and permits a compact way to compress the information of the invariants $A_\omega(|\psi\rangle)$. Unfortunately, $W_{|\psi\rangle}$ is not able to distinguish between any two LC classes of equivalence. Table 7.2 shows that the weight distribution fails to distinguish between LC classes starting from $n = 6$. Graph states with labels 13 and 15 in Refs. [9, 11] have the same weight distribution and this degeneration increases as the number of qubits grows, as we have checked out calculating $W_{|\psi\rangle}$ for all graph states up to eight qubits.

Table 7.2: Weight distribution for graph states up to six qubits.

Graph state	A_0	A_1	A_2	A_3	A_4	A_5	A_6
1	1	0	3				
2	1	0	3	4			
3	1	0	6	0	9		
4	1	0	2	8	5		
5	1	0	10	0	5	16	
6	1	0	4	6	11	10	
7	1	0	2	8	13	8	
8	1	0	0	10	15	6	
9	1	0	15	0	15	0	33
10	1	0	7	8	7	24	17
11	1	0	6	0	33	0	24
12	1	0	4	8	13	24	14
13	1	0	3	8	15	24	13
14	1	0	2	8	17	24	12
15	1	0	3	8	15	24	13
16	1	0	3	0	39	0	21
17	1	0	1	8	19	24	11
18	1	0	0	8	21	24	10
19	1	0	0	0	45	0	18

Therefore, we must look for a way to compress the information about the invariants $A_\omega(|\psi\rangle)$, which satisfies (I)–(III). The fact that the stabilizing operators of a stabilizer can be classified into equivalence classes according to their supports (equivalence classes $[\omega]$), and that the cardinalities of such classes $[\omega]$ are the invariants $A_\omega(|\psi\rangle)$, leads us to introduce two definitions. Two classes $[\omega_1]$ and $[\omega_2]$ are equipotent if and only if both have the same cardinality, i.e., $A_{\omega_1}(|\psi\rangle) = A_{\omega_2}(|\psi\rangle)$, regardless of whether their stabilizing operators have different weights $|\omega_1| \neq |\omega_2|$ or not. It is clear that the number of equipotent equivalence classes $[\omega]$ for a given cardinality $A_\omega(|\psi\rangle)$ is LC invariant. We will call it the A_ω multiplicity (or A_ω potency) and denote it by $M(A_\omega)$. For instance, if we take a look at the list of invariants $A_\omega(|\mathrm{LC}_3\rangle)$ [see Eqs. (7.12a)–(7.12h)] we find that the value 0 appears three times (so there are three equivalence classes $[\omega]$ with that cardinality), and then $M(0) = 3$. Using this criterion, $M(1) = 4$ and $M(4) = 1$ for the $|\mathrm{LC}_3\rangle$.

If we tabulate the values of $A_\omega(|\psi\rangle)$ together with the corresponding values of $M(A_\omega)$, we obtain a two-index compact information, which is LC invariant and, more importantly, LC discriminant, as required. The results are shown in Tables 7.3–7.5.

In Table 7.5 we can see that four numbers are enough to distinguish between all classes of graph states with $n = 8$ qubits: the multiplicities of the values 0, 1, 3, and 4. Indeed, in Tables 7.3 and 7.4 we see that these four numbers are enough to distinguish between all classes of graph states with $n \leq 8$ qubits.

Summarizing, we have shown that, to decide which entanglement class a graph state of $n \leq 8$ qubits belongs to, it is enough to calculate four quantities. These four LC invariants characterize any LC class of $n \leq 8$ qubits.

This result solves a problem raised in the classification of graph states of $n \leq 8$ qubits[4] developed in Refs. [9, 11, 13]. A compact set of invariants that characterize all inequivalent classes of graph states with a higher number of qubits can be obtained by applying the same strategy. This can be done numerically up to $n = 12$ qubits,[5] a number of qubits beyond the present experimental capability in the preparation of graph states (Ref. [195]).

We have also shown that the conjecture (Ref. [218]) that the list of LC invariants given in Eq. (7.6) is sufficient to characterize the LC equivalence classes of all stabilizer states, which is not true in general (Ref. [9]), is indeed true for graph states of $n \leq 8$ qubits. Moreover, we have shown that, for graph states of $n \leq 8$ qubits, the list of LC invariants given in Eq. (7.7), which is more restrictive than the list given in Eq. (7.6), is enough. This solves a problem suggested in Ref. [12], regarding the possibility of characterizing special subclasses of stabilizer states using subfamilies of invariants.

[4] See Sect. 6.4.

[5] As a matter of fact, this is one of the problems we address in Chap. 8, where the calculation of cardinality-multiplicity (C-M) invariants $A_\omega(|G\rangle)$ — $M(A_\omega)$ is extended to graph states $|G\rangle$ of up to 12 qubits, and whose effectiveness as discriminants among any LC classes of graph states is discussed as well.

Table 7.3: Invariants for the n-qubit graph states with $3 \leq n \leq 6$. Notation: $\text{value}_{\text{multiplicity}}$. The numeration of the classes is the one in Refs. [9, 11].

No.	Invariants
1	0_2, 1_1, 3_1
2	0_3, 1_4, 4_1
3	0_8, 1_7, 9_1
4	0_8, 1_3, 2_4, 5_1
5	0_{15}, 1_{16}, 16_1
6	0_{18}, 1_8, 2_3, 4_2, 10_1
7	0_{17}, 1_7, 2_6, 5_1, 8_1
8	0_{15}, 1_{11}, 3_5, 6_1
9	0_{32}, 1_{31}, 33_1
10	0_{38}, 1_{15}, 2_8, 8_2, 17_1
11	0_{41}, 1_{16}, 4_6, 24_1
12	0_{38}, 1_{14}, 2_7, 4_1, 5_2, 8_1, 14_1
13	0_{42}, 1_6, 2_8, 4_6, 5_1, 13_1
14	0_{37}, 1_{12}, 2_8, 3_4, 6_2, 12_1
15	0_{42}, 1_{12}, 4_6, 5_3, 13_1
16	0_{44}, 1_4, 2_{12}, 5_3, 21_1
17	0_{34}, 1_{18}, 2_6, 3_1, 5_4, 11_1
18	0_{33}, 1_{21}, 3_3, 4_6, 10_1
19	0_{47}, 1_1, 3_{15}, 18_1

Table 7.4: Invariants for the seven-qubit graph states. Notation: $\text{value}_{\text{multiplicity}}$. The numeration of the classes is the one in Refs. [9, 11].

No.	Invariants
20	0_{63}, 1_{64}, 64_1
21	0_{78}, 1_{32}, 2_{15}, 16_2, 34_1
22	0_{84}, 1_{32}, 4_8, 8_3, 40_1
23	0_{77}, 1_{31}, 2_{15}, 8_3, 17_1, 26_1
24	0_{87}, 1_{25}, 4_8, 5_6, 16_1, 25_1
25	0_{92}, 1_{12}, 2_8, 4_7, 5_4, 8_4, 20_1
26	0_{87}, 1_{16}, 2_{14}, 4_7, 8_1, 10_2, 28_1
27	0_{80}, 1_{25}, 2_{11}, 3_3, 4_3, 5_3, 8_1, 14_1, 23_1
28	0_{85}, 1_{15}, 2_{16}, 4_3, 6_7, 9_1, 18_1
29	0_{87}, 1_{12}, 2_{15}, 4_9, 5_3, 13_1, 22_1
30	0_{80}, 1_{21}, 2_{12}, 3_6, 4_1, 5_4, 8_3, 17_1
31	0_{86}, 1_{28}, 4_3, 5_4, 8_6, 20_1
32	0_{89}, 1_{12}, 2_{16}, 4_4, 5_4, 8_2, 32_1
33	0_{72}, 1_{40}, 2_3, 3_4, 4_4, 9_4, 18_1
34	0_{85}, 1_{14}, 2_{17}, 4_7, 5_1, 6_2, 13_1, 22_1
35	0_{79}, 1_{25}, 2_{12}, 4_2, 5_6, 8_3, 17_1
36	0_{86}, 1_{14}, 2_{17}, 4_4, 5_2, 6_2, 8_2, 26_1
37	0_{80}, 1_{21}, 2_{12}, 3_8, 4_1, 5_2, 6_2, 12_1, 21_1
38	0_{74}, 1_{32}, 2_8, 3_3, 4_5, 7_5, 16_1
39	0_{77}, 1_{22}, 2_{16}, 3_5, 4_2, 7_5, 16_1
40	0_{70}, 1_{36}, 2_7, 3_7, 6_7, 15_1
41	0_{78}, 1_{22}, 2_{14}, 3_5, 4_3, 5_4, 11_1, 20_1
42	0_{74}, 1_{26}, 2_{15}, 3_5, 6_7, 15_1
43	0_{84}, 1_8, 2_{21}, 3_7, 6_7, 15_1
44	0_{78}, 1_{24}, 2_3, 3_{15}, 4_6, 10_1, 19_1
45	0_{83}, 1_{22}, 3_{10}, 4_{10}, 6_2, 24_1

Table 7.5: Invariants for the eight-qubit graph states. Notation: $\text{value}_{\text{multiplicity}}$. The numeration of the classes is the one in Ref. [13].

No.	Invariants	No.	Invariants
46	0_{128}, 1_{127}, 129_1	97	0_{163}, 1_{44}, 2_{17}, 3_{14}, 4_5, 5_4, 7_2, 10_6, 22_1
47	0_{158}, 1_{63}, 2_{32}, 32_2, 65_1	98	0_{157}, 1_{55}, 2_{17}, 3_9, 4_4, 5_3, 6_3, 7_1, 9_4, 12_2, 24_1
48	0_{173}, 1_{64}, 4_{15}, 16_3, 84_1	99	0_{165}, 1_{40}, 2_{18}, 3_{17}, 4_4, 5_2, 6_2, 7_1, 9_4, 12_2, 24_1
49	0_{158}, 1_{62}, 2_{31}, 16_1, 17_2, 32_1, 50_1	100	0_{152}, 1_{59}, 2_{16}, 3_8, 4_{12}, 9_8, 21_1
50	0_{176}, 1_{63}, 8_{16}, 65_1	101	0_{168}, 1_{58}, 4_{18}, 8_3, 9_6, 12_2, 24_1
51	0_{176}, 1_{56}, 4_7, 5_8, 8_7, 32_1, 44_1	102	0_{177}, 1_{26}, 2_{26}, 3_4, 4_{11}, 5_2, 6_2, 8_6, 20_1, 32_1
52	0_{192}, 1_{24}, 2_{16}, 4_8, 5_7, 8_4, 16_4, 37_1	103	0_{174}, 1_{20}, 2_{40}, 3_9, 6_4, 7_2, 8_2, 12_4, 27_1
53	0_{180}, 1_{30}, 2_{30}, 4_8, 8_2, 10_2, 16_2, 17_1, 49_1	104	0_{200}, 1_{21}, 4_{24}, 5_6, 13_4, 57_1
54	0_{163}, 1_{54}, 2_{22}, 3_8, 8_4, 9_2, 18_1, 24_1, 42_1	105	0_{159}, 1_{58}, 2_{15}, 3_4, 4_{12}, 9_2, 10_4, 16_1, 34_1
55	0_{185}, 1_{32}, 2_{16}, 4_{13}, 8_7, 20_2, 44_1	106	0_{193}, 1_{19}, 2_{15}, 3_{12}, 6_{12}, 9_1, 12_3, 54_1
56	0_{181}, 1_{30}, 2_{23}, 4_6, 6_7, 8_3, 9_2, 12_2, 18_1, 30_1	107	0_{196}, 1_9, 2_{24}, 4_{12}, 5_4, 8_8, 13_2, 41_1
57	0_{191}, 1_{32}, 2_9, 4_{16}, 10_6, 16_1, 66_1	108	0_{180}, 1_{26}, 2_{26}, 3_4, 4_4, 6_{10}, 9_2, 12_3, 36_1
58	0_{176}, 1_{49}, 4_{14}, 5_{14}, 20_2, 41_1	109	0_{164}, 1_{40}, 2_{28}, 3_2, 4_8, 5_4, 6_1, 7_2, 10_6, 22_1
59	0_{183}, 1_{28}, 2_{25}, 4_6, 5_2, 6_3, 8_2, 10_2, 13_2, 14_1, 16_1, 34_1	110	0_{174}, 1_{32}, 2_{22}, 3_{13}, 4_4, 7_1, 8_2, 10_6, 11_1, 31_1
60	0_{179}, 1_{32}, 2_{25}, 4_9, 6_3, 8_3, 10_1, 14_2, 20_1, 38_1	111	0_{166}, 1_{40}, 2_{22}, 3_9, 4_9, 5_1, 6_1, 7_4, 10_1, 13_1, 16_1, 31_1
61	0_{186}, 1_{24}, 2_{20}, 4_{10}, 5_8, 8_2, 10_4, 16_1, 40_1	112	0_{168}, 1_{31}, 2_{32}, 3_9, 4_8, 5_1, 7_2, 13_4, 31_1
62	0_{169}, 1_{46}, 2_{15}, 3_7, 4_5, 5_7, 8_1, 9_2, 12_1, 15_1, 18_1, 33_1	113	0_{161}, 1_{46}, 2_{21}, 3_{10}, 4_4, 5_6, 6_1, 8_3, 11_2, 14_1, 26_1
63	0_{175}, 1_{27}, 2_{31}, 3_4, 4_6, 6_2, 8_7, 9_1, 14_2, 26_1	114	0_{158}, 1_{51}, 2_{20}, 3_{12}, 4_2, 5_3, 6_1, 7_2, 8_2, 11_4, 26_1
64	0_{200}, 1_8, 2_{14}, 4_{18}, 5_6, 8_6, 13_1, 14_2, 29_1	115	0_{164}, 1_{40}, 2_{28}, 3_2, 4_7, 5_6, 8_7, 14_1, 26_1
65	0_{188}, 1_{13}, 2_{28}, 4_{16}, 6_4, 9_2, 12_4, 33_1	116	0_{161}, 1_{38}, 2_{37}, 3_7, 4_2, 6_1, 7_3, 10_6, 28_1
66	0_{181}, 1_{20}, 2_{26}, 3_8, 4_8, 6_3, 7_4, 8_1, 10_3, 16_1, 28_1	117	0_{161}, 1_{43}, 2_{23}, 3_{14}, 4_4, 5_3, 6_1, 7_2, 10_2, 13_2, 28_1
67	0_{179}, 1_{24}, 2_{26}, 3_4, 4_8, 5_2, 6_8, 9_2, 12_1, 18_1, 30_1	118	0_{155}, 1_{55}, 2_{12}, 3_{16}, 4_9, 9_8, 21_1
68	0_{170}, 1_{35}, 2_{20}, 3_{12}, 4_7, 5_2, 7_4, 8_1, 10_2, 13_2, 25_1	119	0_{152}, 1_{59}, 2_{16}, 3_{10}, 4_9, 6_1, 8_6, 11_2, 23_1
69	0_{180}, 1_{54}, 4_8, 5_7, 16_4, 17_2, 37_1	120	0_{160}, 1_{42}, 2_{29}, 3_3, 4_{12}, 6_1, 8_6, 11_2, 23_1
70	0_{176}, 1_{62}, 8_{14}, 16_1, 17_2, 32_1	121	0_{192}, 1_{25}, 4_{24}, 5_6, 8_8, 41_1
71	0_{188}, 1_{22}, 2_{32}, 5_7, 8_4, 17_2, 69_1	122	0_{176}, 1_{24}, 2_{24}, 3_6, 4_{16}, 6_1, 7_2, 10_6, 22_1
72	0_{148}, 1_{84}, 2_8, 3_7, 8_4, 17_4, 35_1	123	0_{190}, 1_{28}, 2_{12}, 3_1, 5_{16}, 8_6, 11_2, 51_1
73	0_{185}, 1_{32}, 2_{15}, 4_{12}, 8_{10}, 16_1, 50_1	124	0_{200}, 1_5, 2_{32}, 5_6, 8_8, 13_4, 41_1
74	0_{178}, 1_{30}, 2_{26}, 4_9, 6_6, 8_3, 9_2, 24_1, 36_1	125	0_{169}, 1_{35}, 2_{28}, 3_4, 4_4, 5_6, 6_4, 8_1, 9_2, 12_2, 33_1
75	0_{166}, 1_{54}, 2_{14}, 4_6, 5_7, 8_4, 9_1, 14_2, 17_1, 29_1	126	0_{170}, 1_{44}, 2_{14}, 3_6, 5_{12}, 8_6, 10_1, 11_2, 26_1
76	0_{188}, 1_{26}, 2_{14}, 4_{14}, 5_2, 8_6, 9_2, 13_1, 14_2, 29_1	127	0_{161}, 1_{48}, 2_{19}, 3_6, 4_9, 5_4, 7_6, 10_1, 16_1, 28_1
77	0_{186}, 1_{28}, 2_{18}, 4_{12}, 5_4, 10_4, 14_2, 16_1, 40_1	128	0_{161}, 1_{42}, 2_{33}, 3_3, 4_6, 6_1, 7_3, 10_6, 28_1
78	0_{191}, 1_{24}, 2_{22}, 4_1, 5_8, 8_7, 14_2, 60_1	129	0_{160}, 1_{50}, 2_{18}, 3_8, 4_9, 6_3, 7_2, 9_4, 12_1, 30_1
79	0_{178}, 1_{32}, 2_{25}, 4_7, 6_6, 8_4, 12_3, 42_1	130	0_{156}, 1_{52}, 2_{19}, 3_9, 4_{10}, 6_1, 8_6, 11_2, 23_1
80	0_{166}, 1_{49}, 2_{15}, 3_6, 4_8, 5_6, 8_1, 9_1, 11_1, 14_1, 20_1, 35_1	131	0_{152}, 1_{59}, 2_{16}, 3_{12}, 4_6, 6_2, 7_4, 10_4, 25_1
81	0_{156}, 1_{70}, 2_3, 3_4, 4_{15}, 9_2, 10_1, 13_4, 28_1	132	0_{156}, 1_{52}, 2_{16}, 3_{13}, 4_{10}, 7_5, 10_2, 13_1, 25_1
82	0_{179}, 1_{27}, 2_{27}, 3_4, 4_6, 6_4, 8_2, 9_1, 12_5, 30_1	133	0_{148}, 1_{69}, 2_{12}, 3_2, 4_{16}, 9_8, 21_1
83	0_{179}, 1_{24}, 2_{26}, 3_4, 4_{10}, 5_2, 6_4, 8_2, 9_2, 12_1, 18_1, 30_1	134	0_{188}, 1_{34}, 3_{20}, 6_3, 9_{10}, 54_1
84	0_{165}, 1_{49}, 2_{14}, 3_6, 4_{10}, 7_6, 8_1, 10_2, 13_2, 25_1	135	0_{166}, 1_{44}, 2_{20}, 3_3, 4_{12}, 8_{10}, 35_1
85	0_{160}, 1_{56}, 2_{16}, 3_4, 4_{10}, 5_4, 8_1, 14_4, 32_1	136	0_{191}, 1_{30}, 2_3, 3_3, 4_{12}, 7_{15}, 10_1, 48_1
86	0_{190}, 1_{10}, 2_{30}, 4_{16}, 5_3, 9_2, 10_2, 16_2, 37_1	137	0_{154}, 1_{51}, 2_{26}, 3_8, 4_6, 6_2, 7_4, 10_4, 25_1
87	0_{200}, 1_9, 2_{16}, 4_{24}, 5_2, 13_4, 57_1	138	0_{154}, 1_{51}, 2_{24}, 3_{14}, 4_1, 6_5, 9_6, 27_1
88	0_{176}, 1_{28}, 2_{16}, 3_{14}, 4_{12}, 7_1, 8_4, 11_4, 23_1	139	0_{183}, 1_{12}, 2_{31}, 3_{10}, 5_{10}, 6_6, 12_3, 30_1
89	0_{174}, 1_{30}, 2_{32}, 4_4, 5_2, 6_6, 8_5, 14_2, 32_1	140	0_{160}, 1_{36}, 2_{34}, 3_9, 4_8, 6_4, 9_2, 12_2, 27_1
90	0_{175}, 1_{24}, 2_{33}, 3_4, 4_{10}, 6_2, 7_4, 8_1, 16_2, 34_1	141	0_{212}, 1_1, 3_{14}, 6_{28}, 45_1
91	0_{168}, 1_{28}, 2_{44}, 3_1, 4_2, 6_4, 7_2, 8_2, 12_4, 27_1	142	0_{184}, 1_{43}, 6_{28}, 45_1
92	0_{175}, 1_{27}, 2_{31}, 3_4, 4_8, 6_2, 8_1, 9_1, 10_6, 34_1	143	0_{179}, 1_{14}, 2_{35}, 3_{15}, 7_3, 8_8, 10_1, 32_1
93	0_{170}, 1_{33}, 2_{26}, 3_9, 4_4, 5_2, 6_6, 7_1, 9_1, 12_2, 15_1, 27_1	144	0_{172}, 1_9, 2_{56}, 3_6, 6_4, 8_8, 29_1
94	0_{182}, 1_{20}, 2_{26}, 3_8, 4_{10}, 5_2, 8_3, 10_1, 13_2, 16_1, 34_1	145	0_{188}, 1_{37}, 3_2, 6_{28}, 45_1
95	0_{164}, 1_{41}, 2_{28}, 3_6, 4_4, 5_4, 6_2, 7_2, 11_2, 14_2, 29_1	146	0_{164}, 1_{21}, 2_{56}, 3_2, 6_4, 8_8, 29_1
96	0_{167}, 1_{40}, 2_{23}, 3_7, 4_5, 5_5, 7_1, 8_4, 11_2, 14_1, 29_1		

Chapter 8

Optimal preparation of graph states

In this chapter we present the results obtained in Ref. [209]. Below we provide a brief summary.

Summary:

We show how to prepare any graph state of up to 12 qubits with: (a) the minimum number of controlled-Z gates, and (b) the minimum preparation depth. We assume only one-qubit and controlled-Z gates. The method exploits the fact that any graph state belongs to an equivalence class under local Clifford operations. We extend up to 12 qubits the classification of graph states according to their entanglement properties, and identify each class using only a reduced set of invariants. For any state, we provide a circuit with both properties (a) and (b), if it does exist, or, if it does not, one circuit with property (a) and one with property (b), including the explicit one-qubit gates needed.

8.1 Introduction

Building a quantum computer entails isolating atomic-scale systems, except when a controlled interaction (e.g., a logic gate) is applied. Isolation must be kept up until a subsequent controlled interaction is applied. Any undesirable coupling with the outside disrupts the quantum state of the systems and ruins the computation. Due to the enormous difficulties which keeping atomic-scale systems isolated and controlled entails, a main limiting factor preventing the development of quantum computing is the amount of time during which the systems must be kept isolated and controlled to achieve the computation. Therefore, the task of reducing this amount of time is an essential factor in the process of achieving the goal of building a quantum computer.

Another limiting factor for quantum computation is the number of entangling gates needed. While one-qubit gates can be built with fidelities higher than 99%, two-qubit entangling gates hardly reach 93%, and this becomes worse for three-qubit gates, etc. Therefore, since one- and two-qubit gates are enough for universal quantum computation, it is reasonable to focus on circuits with only one- and two-qubit gates, and having the least possible number of two-qubit gates.

Here we address the problem of preparing an important class of quantum states, namely, graph states, with circuits requiring (a) the minimum number of two-qubit entangling gates, and (b) the minimum preparation depth (i.e., requiring a minimum number of time steps). We assume that we can implement arbitrary one-qubit gates and one specific two-qubit entangling gate, the controlled-Z gate. The result can be easily extended to any other specific two-qubit gate.

8.1.1 Graph states: the graph as a blueprint for preparation

The subject of study in this chapter, as in the foregoing two ones, is the graph state. The reader interested in references about the most relevant applications of graph states in the field of quantum information, together with an outline of the experimental efforts devoted to the creation and testing of graph states of an increasing number of qubits, may find them in Sect.5.2. Likewise, Sect. 5.2.2 deals with the role of graph states in the theory of entanglement. Our contributions with respect to this topic are described in Chaps. 6–7, more specifically in Sect. 6.4 and Sect. 7.3.

Although two definitions of graph state have already been presented in detail in Sect. 5.2.1, it is convenient for our purposes recalling here definition (I), according to which the graph G provides a blueprint for preparing the graph state $|G\rangle$. Succinctly, an n-qubit graph state $|G\rangle$ is a pure state associated with a graph $G = (V, E)$ consisting of a set of n vertices $V = \{0, \ldots, n-1\}$ and a set of edges E connecting pairs of vertices, $E \subset V \times V$ (Refs. [9, 11]). Each vertex represents a qubit, whereas an edge $(i, j) \in E$ represents an Ising-type interaction between qubits i and j. To prepare $|G\rangle$, one first prepares each qubit in the state $|+\rangle = \frac{1}{\sqrt{2}}(|0\rangle + |1\rangle)$, i.e., the initial state will be $|\psi_0\rangle = \bigotimes_{i \in V} |+\rangle_i$. Then, for each edge $(i, j) \in E$ connecting two qubits i and j, one applies a controlled-Z gate between these qubits, i.e., the unitary transformation ${}^{C}Z = |00\rangle\langle 00| + |01\rangle\langle 01| + |10\rangle\langle 10| - |11\rangle\langle 11|$.

8.1.2 Preparation using only controlled-Z gates

Let us suppose that we have the state $|\psi_0\rangle = \bigotimes_{i=0}^{n-1} |+\rangle_i$, and we want to prepare the eight-qubit graph state $|G\rangle$ whose graph G is in Fig. 8.1, using only controlled-Z gates. One possible way is to follow the preparation procedure suggested by G, taking into account the possible restrictions in performing two or more controlled-Z gates simultaneously, and optimally distributing the controlled-Z gates to minimize the number of steps. The *preparation depth* of $|G\rangle$ is the *minimum* number of time steps required to prepare $|G\rangle$ (Ref. [216]).

The state $|\psi_0\rangle$ corresponds to a graph with n isolated vertices. The total number of edges in G gives a trivial upper bound to the preparation depth of $|G\rangle$, since each controlled-Z gate can be applied in a time step. To find the minimum number of time steps, we have to explore the possibility of applying two or more controlled-Z gates in a single time step.

Given a vertex i in G, the *neighborhood* of i, $\mathcal{N}(i)$, is the set of vertices connected to i. Now let us suppose that there is more than one element in $\mathcal{N}(i)$, i.e., $|\mathcal{N}(i)| > 1$, and let $j, k \in \mathcal{N}(i)$ be two of the neighbors. Then, to prepare the corresponding graph state $|G\rangle$ we must apply a controlled-Z gate to entangle qubits i and j, and another one to entangle qubits i and k. Applying a controlled-Z gate between qubits i and j in a certain time step implies that both

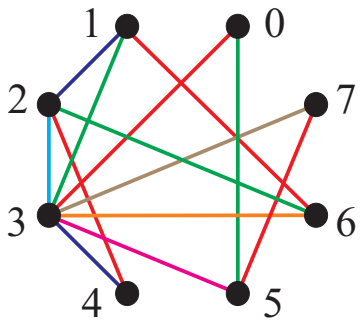

Figure 8.1: Graph corresponding to the 8-qubit graph state we want to prepare. Edges in the same color represent controlled-Z gates that can be performed in the same time step.

qubits are busy during this entangling interaction. If we focus on qubit i, we have to wait for a further time step to have qubit i free before applying another controlled-Z gate to entangle i and k. Nevertheless, vertex k could be connected to another vertex $l \neq \{i, j\}$ in G. If such is the case, we could in principle take advantage of the same time step we are using to entangle qubits i and j in order to do the same with qubits k and l, because both controlled-Z gates can be performed in parallel.

Remarkably, the problem of determining the *minimum* number of time steps with the restrictions that we have mentioned is related to an old problem in graph theory: given an edge (i, j) in G, let us use a certain color to mark (i, j) and those other edges of G corresponding to controlled-Z gates that can be performed at the same time step than that of (i, j), and use different colors for those edges related to controlled-Z gates that do not fulfill this condition. Since two controlled-Z gates can be performed at the same time step if and only if the four qubits involved do not coincide, then every edge incident to the same vertex must have a *different* color. In graph theory this color configuration is called a *proper edge coloring* or, to put it more concisely, the graph is said to be edge-colored. Hence, the preparation depth problem is equivalent to determining the minimum number of colors required to get a proper edge coloring of G. This problem is known as the determination of the *chromatic index* or *edge chromatic number* $\chi'(G)$.

Let us denote by $\Delta(G)$ the maximum degree of G (i.e., the maximum number of edges incident to the same vertex). Vizing's theorem (Ref. [219]) states that G can be edge-colored in either $\Delta(G)$ or $\Delta(G) + 1$ colors, and not fewer than that. Therefore, $\chi'(G)$ is either $\Delta(G)$ or $\Delta(G) + 1$. A proof can be found in Ref. [220]. The important point is that $\chi'(G)$ gives the preparation depth of $|G\rangle$ (Refs. [216, 221]).

Graphs requiring $\Delta(G)$ colors are called class-1 graphs, and those requiring $\Delta(G) + 1$ colors are called class-2 graphs. For instance, the four-qubit fully connected graph state is represented by a graph of four vertices, six edges, and maximum degree equal to 3: it is a class-1 graph, so that its preparation depth coincides with its maximum degree: 3. On the other hand, the three-qubit fully connected graph state is represented by a graph of three vertices with three

edges and maximum degree equal to 2: it is the smallest class-2 graph and, as a consequence, its preparation depth is also 3.

The graph in Fig. 8.1 is a class-1 graph: it can be edge-colored with $\Delta(G) = 7$ colors (this number corresponds to the degree of vertex 3). Hence, if we use only controlled-Z gates, the minimum preparation depth of the corresponding graph state is 7. For instance, one of the optimal distributions of the 13 controlled-Z gates is given in the circuit of Fig. 8.2, which has seven time steps.

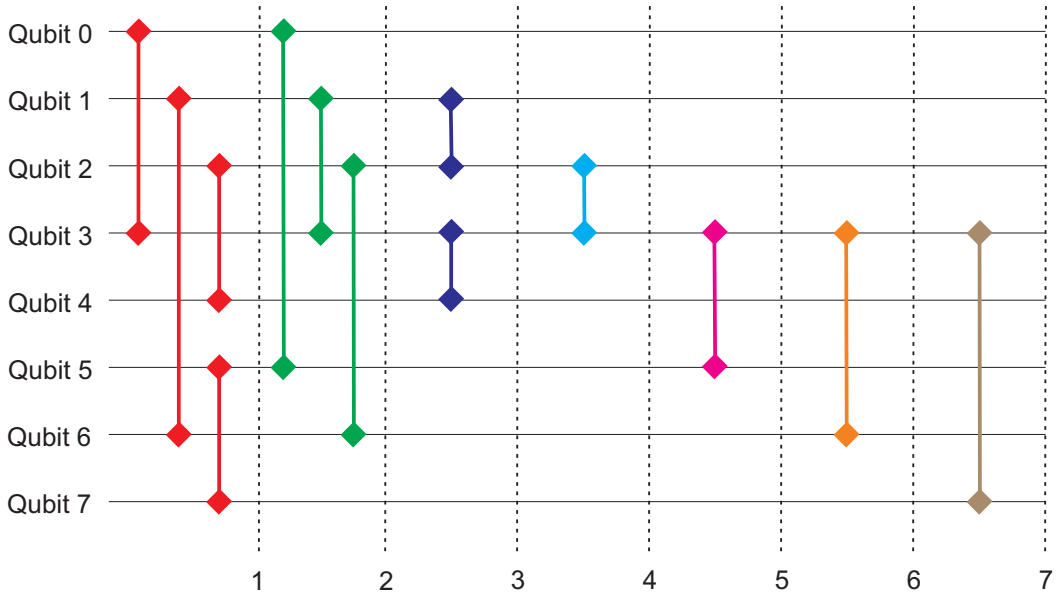

Figure 8.2: A circuit with minimum preparation depth for the graph state corresponding to Fig. 8.1, using only controlled-Z gates. In the circuit, a qubit (vertex of the graph) is represented by a horizontal wire, and a controlled-Z gate (edge in the graph) by a vertical segment with diamond-shaped ends connecting the qubits involved in the operation. Time steps are separated by vertical dashed lines.

However, if we are allowed to use one-qubit gates, in most cases it is possible to get the desired graph state with a lower number of two-qubit gates and less preparation depth. For that purpose, one has to take into account the degree of entanglement of the state we want to prepare.

8.1.3 Optimum preparation

Let us recall that two graph states have the same degree of entanglement[1] if and only if they are equivalent under local unitary LU operations (Ref. [205]), so that they belong to the

[1]This paragraph is a condensed summary of results that we have previously presented in a more extensively way in Sect. 5.2.2.

same LU equivalence class. Moreover, previous results suggest that, for graph states of up to 26 qubits (Ref. [206]), the notions of LU equivalence and LC equivalence coincide and, therefore, entanglement classes are in fact LC equivalence classes (or LC classes, for short). This implies a remarkable simplification, since it is possible to carry out a graphical description of the action of LC transformations on graph states (Ref. [10]): the successive application of a simple graph transformation rule, the so called *local complementation*, on a certain graph G and on those that are obtained from G, allows us to generate the whole LC class of $|G\rangle$. The entire set of graphs connected to a given G by a sequence of local complementations is usually referred to as the *orbit* of G (in correspondence with the LC orbit or LC class of $|G\rangle$).

Any of the graph states belonging to a given LC class could be used as a representative for that orbit, but there is a practical advantage in taking one requiring: (a) the minimum number of controlled-Z gates, or (b) the minimum preparation depth of the class. If we can identify which LC class a given $|G\rangle$ belongs to, then we can prepare $|G\rangle$ by preparing instead the LC-equivalent state $|G'\rangle$ requiring (a) and (b), and then transform $|G'\rangle$ into $|G\rangle$ by means of single-qubit Clifford operations corresponding to a sequence of local complementations carried out on G'. This last transformation from $|G'\rangle$ to $|G\rangle$ requires only one additional time step, since the local complementation at vertex a is equivalent (Refs. [9, 11]) to the unitary operation

$$U_a^\tau(G) = \exp\left(-i\frac{\pi}{4}\sigma_x^{(a)}\right) \prod_{b\in\mathcal{N}(a)} \exp\left(i\frac{\pi}{4}\sigma_z^{(b)}\right), \tag{8.1}$$

where $\sigma_x^{(a)}$ is the Pauli matrix σ_x acting on qubit a, $\sigma_z^{(b)}$ is the Pauli matrix σ_z acting on qubit b, and $\mathcal{N}(a)$ is the neighborhood of a. Operations on different qubits commute, and therefore one can group together a sequence of unitary operations $U_a^\tau(G)$ corresponding to local complementations into n one-qubit gates R_i (with $i = 0, \ldots, n-1$), which can be jointly performed in a single step.

The preparation procedure of a graph state $|G\rangle$ through the optimum LC representative $|G'\rangle$ provides an advantage in time steps when compared to the standard graph-based controlled-Z procedure[2] when

$$\chi'(G) - \chi'(G') > 1, \tag{8.2}$$

since the preparation depth for the standard procedure is $\chi'(G)$, while the preparation depth through the optimum LC representative is $\chi'(G')+1$, that is, the sum of the preparation depth of the optimum LC representative plus a unit of time corresponding to the one-qubit gates. This means that the preparation depth through the optimum LC representative provides an advantage for most graph states. For instance, as we will see, for the graph state of Fig. 8.1, the optimum preparation circuit requires only seven controlled-Z gates and three time steps: saving six controlled-Z gates and requiring four time steps fewer than in the standard procedure.

However, the preparation through the optimum LC representative requires us to identify which LC class $|G\rangle$ belongs to. To be practical, this must require us to identify the simplest signature of the class.

In Sect. 8.2, we classify all LC classes for graph states up to $n = 12$ qubits. This classification is based on a reduced set of invariants which allows us to identify which class a given state belongs

[2] I.e., the one that uses G as a blueprint for the preparation of $|G\rangle$, described above.

to. In Sect. 8.3, we provide a representative of the class with both properties (a) and (b), if it exists, or, if it does not, one with property (a) and one with property (b). All these results, which occupy several hundreds of megabytes, are organized in two tables, one for $n < 12$ and one for $n = 12$, and presented as supplementary material in Ref. [14]. Finally, in Sect. 8.4, we explain how to obtain the one-qubit gates needed, and provide as supplementary material a computer program in Ref. [15] to, given the graph G corresponding to the state we want to prepare, generate a sequence of local complementations which connect G to the corresponding optimum graph(s). In Sect. 8.5, the whole method is illustrated with an example.

8.2 Classification of graph states in terms of entanglement

The classification of the entanglement of graph states has been achieved up to $n = 7$ in Refs. [9, 11], and we have extended it to $n = 8$ in Ref. [13] (see Chap. 6). There are 45 LC classes[3] for graph states up to seven qubits, and 101 LC classes for eight-qubit graph states, which are ordered according to certain criteria based on several entanglement measures, which are invariant under LC transformations.

Here we extend the classification up to $n = 12$. The number of orbits for $n \leq 8$ qubits is 146. For $n = 9$, there are 440 orbits; for $n = 10$, there are 3 132 orbits; for $n = 11$, there are 40 457; and, for $n = 12$, there are 1 274 068. All the information about each LC class is presented as supplementary material in Ref. [14].

For each LC class we give the number of nonisomorphic graphs in the associated LC* class (size of the orbit), $|LC|$. Then, the orbits are classified according to the number of vertices (qubits), $|V|$; the minimum number of edges of a graph belonging to the class (controlled-Z gates needed for the preparation), $|E|$; the Schmidt measure, E_S (upper and lower bounds are given where the exact value is unknown); and for $n/2 \geq i \geq 2$, the rank indexes RI_i for bipartite splits with i vertices in the smallest partition. The classifying labels $|V|$, $|E|$, E_S, and RI_i are applied in this order. Additionally, we include the information regarding the existence (or not) of a two-colorable graph belonging to the class (a piece of data which is useful, in some cases, to calculate lower and upper bounds for the Schmidt measure).

However, these numbers, which were (almost) enough to identify every class if $n \leq 8$, are not enough to identify every class if $n > 8$. In other words, the set of entanglement measures for n-qubit graph states used in Refs. [9, 11, 13] failed to distinguish between inequivalent classes under LC operations if $n > 8$: different LC classes had coincident values for those entanglement measures. In fact, the number of problematic LC classes increases with n. Therefore, using these invariants for deciding which entanglement class a given state belongs to is unreliable. A finite set of invariants that characterizes all classes has been proposed in Ref. [12]. However, already for $n = 7$, this set has more than 2×10^{36} invariants which are not explicitly calculated anywhere, and hence this set is not useful for classifying a given graph state.

[3] In this and subsequent sections, as we have done in previous chapters, we use again the abbreviation LC* for local complementation on graphs, the graphical counterpart of local Clifford (LC) operations on graph states. Nevertheless, sometimes it is arguable, and the reader may overlook this notation (perhaps unnecessary) when dealing in the same paragraph or argument with LC orbits of graph states and LC* orbits of the associated graphs, given that there is a direct correspondence, and the meaning is clear from the context.

Nevertheless, a compact set of invariants related to those proposed in Ref. [12] is enough to distinguish among all inequivalent LC classes with $n \leq 8$ qubits: the 4 two-index invariants called cardinalities-multiplicities (C-M hereafter) in Ref. [217]. There is a straightforward procedure for calculating these four invariants using the information contained in the graphs (see Chap. 7).

We have analyzed the utility and limitations of the C-M invariants as LC-class discriminants for graph states up to 12 qubits, a question that was left as an open problem in Ref. [217] (see Chap. 7, p. 141), where it was conjectured that four of these C-M invariants would be enough to label and discriminate all the LC classes. Our results show that for graph states of $n \geq 9$ qubits the C-M invariants fail to distinguish between inequivalent LC classes: the smallest counterexample of the conjecture corresponds to a pair of nine-qubit orbits that have exactly the same entire list of C-M invariants. These are the only problematic orbits for $n = 9$ qubits. As an alternative for discriminating between them, we have calculated the whole list of VDD invariants of type $r = 1$ (Ref. [12]) for these two orbits, and once again these invariants coincide. In order to determine the number of C-M and VDD "problematic" (undistinguishable) orbits, we have extended our calculations up to $n = 12$ qubits. The ratio $p_f(n)$ of the number of graphs belonging to problematic orbits and the overall number of graphs for each n, gives the probability that a randomly chosen graph state falls in one of the problematic orbits. The values of $p_f(n)$ are, fortunately, quite low (see Table 8.1). Therefore, the first step of the procedure of preparation, i.e., the identification of the orbit, resorts to C-M invariants (and, sometimes, type $r = 1$ VDD invariants), and works in most cases. For those rare states whose orbit identification through C-M or VDD ($r = 1$) invariants is not univocal, one would resort to VDD invariants of higher order r (Ref. [12]). However, the computational effort of this task makes this procedure less efficient than simply generating the whole LC* orbit of the graph.

Table 8.1: Orbits for which C-M and VDD invariants are not good LC discriminants.

n	No. of orbits	No. of problematic orbits	$p_f(n)$
≤ 8	146	0	0
9	440	2	0.0012218
10	3 132	8	0.0006996
11	40 457	78	0.0011929
12	1 274 068	472	0.0000949

In the supplementary material (see Ref. [14]), those LC classes which have the same set of quantities $\{|V|, |E|, E_S, RI_i\}$ are ordered according to the C-M invariants, going from the smallest cardinality (zero) to the biggest one, and increasing the value of the associated multiplicity of each cardinality. For those orbits with the same set of quantities $\{|V|, |E|, E_S, RI_i, \text{C-M invariants}\}$, orbits are ordered by the increasing size of the orbit, $|LC|$. We do not apply any subsequent classifying criteria, in case there were undistinguishable LC classes left.

C-M invariants are given as an ordered list of multiplicities M_i, for $i = 0, \ldots, x$. The value M_i is the multiplicity of the cardinality i. We do not list all 2^n possible multiplicities, but only the multiplicities of cardinalities $0, \ldots, x$, where x is the smallest number such that

all"non-problematic" orbits are distinguished. This may not be the smallest possible set of C-M invariants. For instance, only the cardinalities $\{0, 1, 3, 4\}$ are needed for $n \leq 8$, but, for simplicity's sake, we have included the continuous list $\{0, 1, 2, 3, 4\}$.

8.3 Optimum representative

We have determined the optimum representatives for all the orbits up to 12 qubits, initially defined as one of those with the minimum number of edges in the orbit and, among them, one of those with the minimum chromatic index. In the supplementary material (Ref. [14]), we have included a column labeled $\min(|E|, \chi', \#)$ for each LC* class, where $|E|$ is the minimum number of edges in the class, χ' is the minimum chromatic index of the graphs with $|E|$ edges, and $\#$ is the number of nonisomorphic graphs with $|E|$ edges and chromatic index χ'. The value of χ' coincides with the preparation depth of those representative states and indicates how much more efficient the preparation procedure we are proposing is than the standard one [it is $\chi'(G')$ in Eq. (8.2)].

While carrying out the LC* classification, an interesting observation arose: the optimum representative of a certain orbit was determined by the application of two filters to the orbit *in a certain order*. First, we looked for the graph with the minimum number of edges (which implies a minimum number of two-qubit entangling operations), $|E|$, and second the minimum chromatic index χ' fixed that $|E|$ (which means a minimum preparation depth given those graphs with $|E|$ edges). However, if we commute the order of the filters, for $n \leq 7$ qubits, the result of the permutation of the filters gives the same graph, but this is not the case for $n > 7$. We get the simplest example of non coincidence between the final optimum representatives for $n = 8$, where there is only one orbit (LC* class number 136) in which the permutation of the filters does not produce the same final graph. There are two graphs in this orbit with $|E| = 11$ and $\chi' = 4$, and one graph with $\chi' = 3$ and $|E| = 12$ (see Fig. 8.3). For each $n \leq 12$, we calculated the number of orbits with different final representatives when we applied the filters in different order: the ratio of the number of "exceptional" orbits and the entire number of orbits increases with n, for $n \geq 9$ (Table 8.2).

Table 8.2: Orbits for which a different order of the filters relating the minimum number of edges and minimum chromatic index produces a non-coincident representative graph.

n	# of orbits	# of exceptional orbits
≤ 7	45	0
8	101	1
9	440	3
10	3 132	65
11	40 457	2 587
12	1 274 068	136 518

Moreover, we have included in our tables (see supplementary material Ref. [14]), beside the

column labeled $\min(|E|, \chi', \#)$, another column labeled $\min(\chi', |E|, \#)$, with a 3-tuple of values $(\chi', |E|, \#)$, where χ' is now the minimum chromatic index in the class, $|E|$ is the minimum number of edges of the graphs with chromatic index χ', and $\#$ is the number of nonisomorphic graphs with chromatic index χ' and $|E|$ edges. Checking the coincidence of χ' and $|E|$ in both columns directly tells us if a certain orbit is exceptional or not. In case of coincidence, we have left the second column blank. From an experimental point of view, the appropriate order for the filters is something that the experimentalists should elucidate, since it is related to the physical substrate used to implement the qubits, and the resources at their disposal. If minimizing the number of two-qubit entangling operations is a critical factor, because the fidelity in performing such quantum gates is lower than desirable, then the appropriate order is $(|E|, \chi')$: once the number of gates is minimized, then it is the turn of reducing the preparation depth.

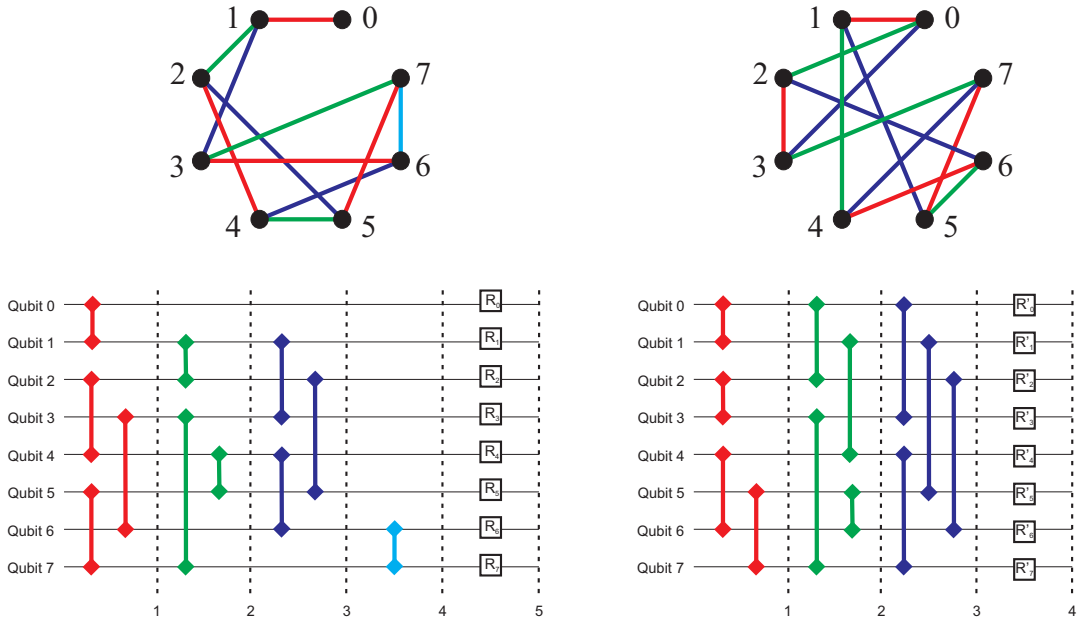

Figure 8.3: Two optimum representatives for LC* class number 136 (up). The graph on the left is obtained by applying over the entire orbit the filter $\min(|E|, \chi')$, i.e., first minimizing over $|E|$ and then over χ', whereas the one on the right is obtained by applying the filter $\min(\chi', |E|)$. Any graph state belonging to LC class number 136 could be prepared by means of the circuits depicted under those representatives. The circuit on the left prioritizes a lower number of entangling gates; the one on the right prioritizes a lower preparation depth. R_i and R'_i are one-qubit gates. They are specific for the state of the class 136 we want to prepare.

To complete our results in Ref. [14] we provide, in the two final columns for each LC* class, an optimum graph resulting from the filters applied in the order $\min(|E|, \chi', \#)$, and another

one applying the filters as $\min(\chi', |E|, \#)$ (if it is not coincident with the former; in case of coincidence, the second final column is left blank). The edges of the graph are listed, with vertices indexed as $0, \ldots, n-1$. Moreover, edges are divided in classes (enclosed by parentheses) that define a proper edge-coloring (with χ' colors). This information is equivalent to providing an *optimum circuit* [with a number of time steps equal to $\chi'(G')$] for preparing the optimum representative graph G' of the class. The graphs and circuits in Fig. 8.3 have been designed according to the information in the supplementary material in Ref. [14] for LC* class number 136.

8.4 One-qubit gates

Assuming that an experimentalist has prepared the optimum representative graph state $|G'\rangle$ corresponding to the desired state $|G\rangle$, he or she needs to know at least one sequence of local complementations connecting G' with G. The length of this LC* sequence is not relevant, due to the possibility of implementation of the corresponding local operations as one-qubit gates in only one time step, as was already discussed above. However, finding a way in the orbit from $|G'\rangle$ to $|G\rangle$ is a hard task. To make the entire orbit-based preparation procedure practical, we have designed a computer program that accomplishes this task. Very briefly, it uses the information about the graph G related to the state $|G\rangle$ that one wishes to obtain. The input is the information about the edges. The program finds the optimal graph(s) G' with respect to both the number of edges and chromatic index (these two quantities are also part of the output), and provides a sequence of LC* mapping G' onto G (corresponding to LC operations transforming $|G'\rangle$ into $|G\rangle$). This computer program is included as supplementary material in Ref. [15].

8.5 Example

In order to clarify the whole process, we go back to the graph in Fig. 8.1. As we mentioned, G is a class-1 graph. Therefore, the preparation depth of $|G\rangle$ using only controlled-Z gates is 7. The orbit-based procedure allows us to reduce significatively the preparation depth and the number of controlled-Z gates. It consists of the following steps:

(I) To identify the orbit or LC equivalence class the graph state $|G\rangle$ belongs to, we calculate the C-M invariants (Ref. [217]). The result is: $\{0_{170}, 1_{35}, 3_{12}, 4_7\}$. Therefore, after consulting Ref. [14], we conclude that the graph state $|G\rangle$ belongs to the LC class number 68.

(II) Also in Ref. [14] we find the optimum representative graph G': it is the eight-vertex linear cluster LC_8 (see Fig. 8.4). Graph LC_8 is a class-1 graph, whose maximum degree is $\Delta(G') = 2$. Hence its preparation depth is 2, which means a remarkable saving in the preparation depth compared to that of $|G\rangle$.

(III) Therefore, it is worth preparing $|G\rangle$ by preparing $|G'\rangle$ and then applying suitable one-qubit gates. The program in Ref. [15] outputs a sequence of local complementations which connects G' to G. For instance, the sequence of LC* operations applied on vertices 6, 7, 4, 5, and 2 in graph G' enables us to obtain G. Denoting the corresponding series of LC operations by $\tau(G')$, we have $|G\rangle = \tau(G')|G'\rangle$. Applying Eq. (8.1) and re-arranging terms so that

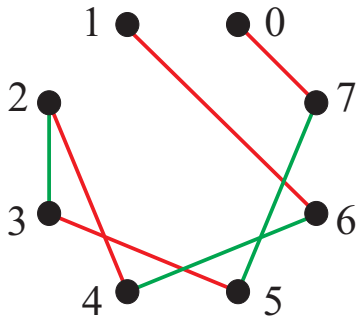

Figure 8.4: Graph state LC_8, optimum representative of orbit 68.

$\tau(G') = \prod_{i\in V} R_i$, where R_i is a specific gate on qubit i, we obtain that

$$R_0 = \exp\left(i\frac{\pi}{2}\sigma_z^{(0)}\right), \tag{8.3a}$$

$$R_1 = \exp\left(i\frac{3\pi}{4}\sigma_z^{(1)}\right), \tag{8.3b}$$

$$R_2 = \exp\left(-i\frac{\pi}{4}\sigma_x^{(2)}\right)\exp\left(i\frac{\pi}{4}\sigma_z^{(2)}\right), \tag{8.3c}$$

$$R_3 = \exp\left(i\frac{\pi}{2}\sigma_z^{(3)}\right), \tag{8.3d}$$

$$R_4 = \exp\left(i\frac{\pi}{4}\sigma_z^{(4)}\right)\exp\left(-i\frac{\pi}{4}\sigma_x^{(4)}\right)\exp\left(i\frac{\pi}{4}\sigma_z^{(4)}\right), \tag{8.3e}$$

$$R_5 = \exp\left(-i\frac{\pi}{4}\sigma_x^{(5)}\right)\exp\left(i\frac{\pi}{4}\sigma_z^{(5)}\right), \tag{8.3f}$$

$$R_6 = \exp\left(i\frac{\pi}{2}\sigma_z^{(6)}\right)\exp\left(-i\frac{\pi}{4}\sigma_x^{(6)}\right), \tag{8.3g}$$

$$R_7 = \exp\left(i\frac{\pi}{4}\sigma_z^{(7)}\right)\exp\left(-i\frac{\pi}{4}\sigma_x^{(7)}\right). \tag{8.3h}$$

In addition, the number of controlled-Z gates necessary to get $|G\rangle$ is remarkably reduced (six two-qubit gates fewer than in the standard preparation method). The optimum circuit for preparing $|G\rangle$, with a preparation depth equal to 3, is the one in Fig. 8.5.

8.6 Further developments: Hypergraph states as generalizations of graph states

Hitherto, we have considered graph states as a special family of stabilizer states (see Chap. 5). In this ending section, we will devote a few lines to discuss another natural way in which graph states can be embedded into a more general set of quantum states: quantum *hypergraph states*.

Graph states can be created in an n-qubit system using only particular two-qubit interactions, implemented for instance as controlled-Z gates. Nevertheless, a strictly larger set of n-qubit

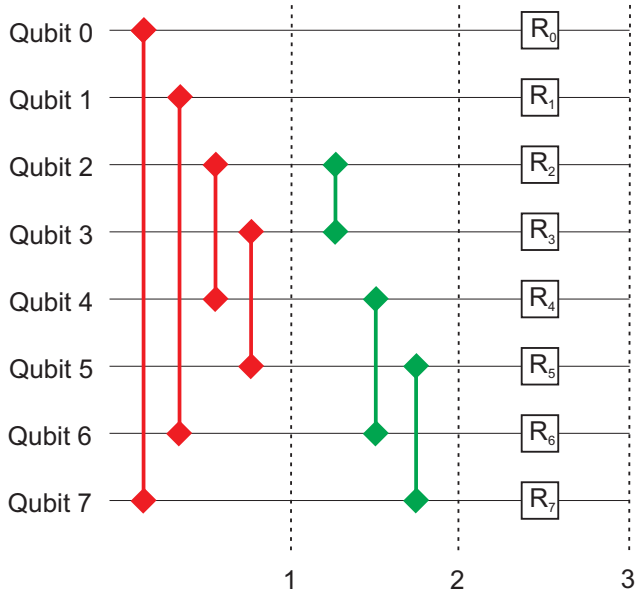

Figure 8.5: Optimum circuit for preparing the graph state corresponding to Fig. 8.1.

entangled quantum states can be generated considering up to n-qubit interactions of a certain kind among the qubits. This line of thought leads to the introduction of the so-called hypergraph states (Refs. [222, 223]), which also admit an intuitive graphical representation that serves as a possible blueprint for their preparation, and an algebraic characterization based on the fact that they are stabilized by operators which constitute appropriate generalizations of the stabilizing operators of graph states.

Following Ref. [222], to account for k-qubit interactions ($1 \leq k \leq n$), let us consider a general controlled-Z gate, denoted by ${}^{C}Z^{(k)}_{i_1 i_2 \ldots i_k}$, acting on the k qubits labeled by $i_1 i_2 \ldots i_k$. By definition we take ${}^{C}Z^{(1)}_{i_1} \equiv Z_{i_1}$. Algebraically, ${}^{C}Z^{(k)}_{i_1 i_2 \ldots i_k}$ introduces a minus sign to the input state $|11\ldots1\rangle_{i_1 i_2 \ldots i_k}$, i.e.,

$$ {}^{C}Z^{(k)}_{i_1 i_2 \ldots i_k} |11\ldots1\rangle_{i_1 i_2 \ldots i_k} = -|11\ldots1\rangle_{i_1 i_2 \ldots i_k}, \tag{8.4} $$

and leaves all the other components of the computational basis unchanged. Hence the action of the controlled-Z gate is invariant under permutations of the n qubits in the computational basis, which means that any of the k qubits on which ${}^{C}Z^{(k)}_{i_1 i_2 \ldots i_k}$ acts can be considered as the target qubit.[4] Trivially, the usual 2-qubit controlled-Z gate is just an instance of the general controlled-Z gate, that is, ${}^{C}Z = {}^{C}Z^{(2)}_{i_1 i_2}$.

To define the concept of hypergraph state we need a previous definition: a *hypergraph* $G_{\leq n} = \{V, E\}$ is a set of n vertices V with a set of hyperedges E of any order $k, 1 \leq k \leq n$. In other

[4] For consistency in the definitions, it is also assumed in Ref. [222] that ${}^{C}Z^{(0)} \equiv -1$.

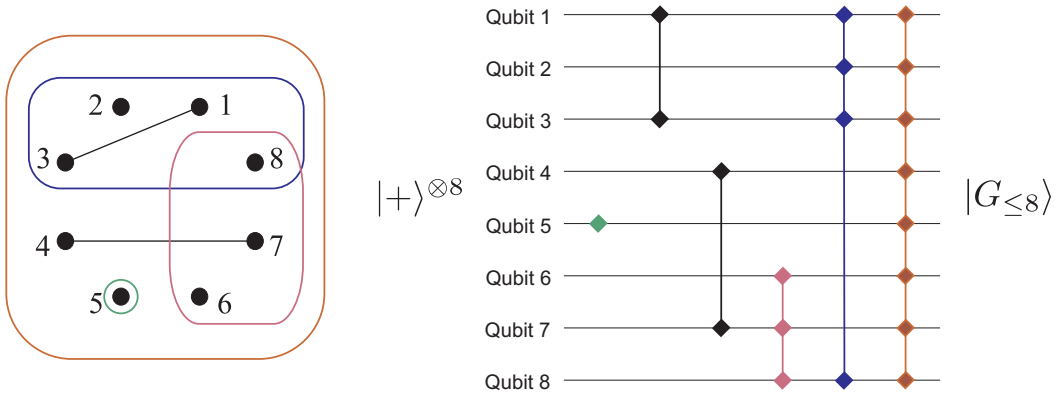

Figure 8.6: Correspondence between a 8-vertex hypergraph (left) and the circuit of preparation of the corresponding 8-qubit hypergraph state (right). The hypergraph $|G_{\leq 8}\rangle$ has one 1-hyperedge $\{5\}$, two 2-hyperedges $\{1,3\}$ and $\{3,4\}$, one 3-hyperedge $\{6,7,8\}$, one 4-hyperedge $\{1,2,3,4\}$, and one 8-hyperedge $\{1,2,3,4,5,6,7,8\}$. Note that in the circuit of preparation there is a local Z gate acting on qubit $\{5\}$, whereas the rest of the operations are standard and general controlled-Z gates affecting different sets of qubits. The symbols are self-explained.

words, E is a set of non-empty subsets of V, so a hyperedge can connect any number of vertices (a hyperedge connecting k vertices is called a k-hyperedge).

With the action of the general controlled-Z gate in Eq. (8.4) and the definition of hypergraph at hand, we arrive at the two definitions of hypergraph state:

(I) Given a hypergraph $G_{\leq n}$ as a blueprint, the recipe for the preparation of the corresponding quantum hypergraph state $|G_{\leq n}\rangle$ is the following: Assign to each vertex a qubit, and first prepare each qubit in the state $|+\rangle = \frac{1}{\sqrt{2}}(|0\rangle + |1\rangle)$, i.e., the initial n-qubit state will be $|\psi_0\rangle = |+\rangle^{\otimes n}$. Then, for each hyperedge, perform a general controlled-Z operation between all connected qubits. Formally, if the qubits $i_1, i_2, \ldots, i_k$ are connected by a k-hyperedge, then perform the operation ${}^{C}Z^{(k)}_{i_1 i_2 \ldots i_k}$. Eventually, and according to this, the corresponding hypergraph state can be written as

$$|G_{\leq n}\rangle = \prod_{k=1}^{n} \prod_{\{i_1,i_2,\ldots,i_k\}\in E} {}^{C}Z^{(k)}_{i_1 i_2 \ldots i_k} |+\rangle^{\otimes n}, \tag{8.5}$$

where $\{i_1, i_2, \ldots, i_k\} \in E$ denotes k vertices which are connected by a k-hyperedge. Notice that the product of $k = 1, 2, \ldots, n$ accounts for different types (sizes or cardinalities) of hyperedges in the hypergraph.

We illustrate the correspondence between hypergraphs and hypergraph states with an example in Fig. 8.6.

(II) The algebraic characterization on the basis of a generalized stabilizer formalism is the following: The hypergraph state $|G_{\leq n}\rangle$ associated to a given hypergraph $G_{\leq n}$ is the unique

n-qubit state which fulfills

$$K_i|G_{\leq n}\rangle = |G_{\leq n}\rangle, \;\; \forall i = 1, 2, \ldots, n. \tag{8.6}$$

For any vertex i, K_i is the correlation operator given by

$$K_i = X_i \otimes \prod_{k=1}^{n} {}^{C}Z_{\mathcal{N}(i)}^{(k-1)} = X_i \otimes \prod_{k=1}^{n} \prod_{(i_1,i_2,\ldots,i_{k-1})\in\mathcal{N}(i)} {}^{C}Z_{i_1 i_2 \ldots i_{k-1}}^{(k-1)}, \tag{8.7}$$

where the product over k takes into account all kinds of hyperedges that may appear in $G_{\leq n}$. For any value of k, the neighborhood $\mathcal{N}(i)$ of the vertex i is defined as

$$\mathcal{N}(i) = \{(i_1, i_2, \ldots, i_{k-1}) | \{i, i_1, i_2, \ldots, i_{k-1}\} \in E\}. \tag{8.8}$$

Different kinds of neighborhoods can obviously appear in this scenario (ranging from single vertices to $k-1$-tuples), depending on the order k of the hyperedges that connect the vertex i to other vertices.

A k-uniform hypergraph is a hypergraph such that all its hyperedges have size k (in other words, it is a collection of sets of size k). Therefore, graphs constitute the family of 2-uniform hypergraphs. Accordingly, the set of graph states is the subset of 2-uniform hypergraph states. This fact poses the question whether the classification of graph states in equivalence classes under LC operations that we have dealt with in Chaps. 5–8 admits an extension for the broader family of hypergraph states. We can give a positive answer: the exploration of the entanglement properties and nonclassical features of hypergraph states has been carried out very recently in Ref. [223]. The authors identify the equivalence classes under LU transformations for hypergraph states of up to four qubits (providing also simple representatives for each class), as well as important classes of five- and six-qubit states, and determine various entanglement properties of these classes. They also present general conditions under which the local unitary equivalence of hypergraph states can simply be decided by considering a finite set of transformations with a clear graph-theoretical interpretation (Pauli operations). Moreover, they consider the question whether hypergraph states and their correlations can be used to reveal contradictions with classical hidden variable theories (thereby extending a previous work in Ref. [165]), and show that the generalized stabilizer formalism of hypergraph states can be used to derive various NC and Bell inequalities.

A natural extension of our contribution in this chapter, namely, the analysis of the preparation depth of a given hypergraph state $|\mathcal{H}\rangle$ and its possible optimal preparation procedure, would rely upon the unambiguous identification of the LU equivalence class $|\mathcal{H}\rangle$ belongs to, the knowledge of the simplest representative hypergraph state $|\mathcal{H}_0\rangle$ of that class, and a sequence of LU operations (possibly local Pauli operations) connecting both of them. For that purpose, we would resort to elements of graph theory: the chromatic index $\chi'(\mathcal{H})$ of a hypergraph $\mathcal{H}$ is the least number of colors needed to color the hyperedges so that no intersecting hyperedges (hyperedges with some common vertices) have the same color. This number is a measure of the preparation depth of $|\mathcal{H}\rangle$ since it takes into account the fact that, during the action of a general controlled-Z gate on a set of qubits, all of them are busy (unavailable) for another multi-qubit interaction. This is a possible issue for future research.

Chapter 9

Proposed experiment for the quantum "Guess My Number" protocol

In this chapter we present the results obtained in Ref. [224]. Below we provide a brief summary.

Summary:

An experimental realization of the entanglement-assisted "Guess My Number" protocol for the reduction of communication complexity, introduced by Steane and van Dam, would require producing and detecting three-qubit GHZ states with an efficiency $\eta > 0.70$, which would require single photon detectors of efficiency $\sigma > 0.89$. We propose a modification of the protocol which can be translated into a real experiment using present-day technology. In the proposed experiment, the quantum reduction of the multiparty communication complexity would require an efficiency $\eta > 0.05$, achievable with detectors of $\sigma > 0.47$, for four parties, and $\eta > 0.17$ ($\sigma > 0.55$) for three parties.

9.1 Introduction

In foregoing chapters, we have focused our attention on graph states, an important family of multipartite quantum states (which includes among its members GHZ and cluster states) useful for applications in quantum information science, some of which have been outlined in Sect. 5.2. Such a list of applications was not intended to be exhaustive, but significant in relation to the possible uses of graph states. Among them, we mentioned communication complexity (Ref. [174]), for which graph states constitute interesting and advantageous resources due to their genuine multipartite entanglement. The goal of this chapter is to present, in a straightforward manner, an experimental protocol of reduction of communication complexity based on the use of quantum resources, known as the "Guess My Number" (GMN) protocol. The key point is that the participants in the GMN protocol share an entangled quantum state, and this quantum state is precisely a graph state, the 3-qubit or 4-qubit GHZ state, respectively, whose associated

graphs are the complete graphs K_3 or K_4, belonging to the LC classes of graph states Nos. 2 and 3 in Refs. [9, 11]. This protocol will serve as an example to additionally motivate the usefulness and importance of graph states in quantum information theory.

First of all, we will quickly review some basic concepts relating communication complexity. Then, we will describe the original GMN protocol in Sect. 9.2. In subsequent sections we present our contributions: first, our modified version of the GMN protocol in Sect. 9.3, and finally our results and conclusions in Sect. 9.4.

9.1.1 Reduction of communication complexity in a nutshell

Communication complexity is an abstract model for the paradigm of distributed computation (Ref. [41]). Its main purpose is to study the amount of information, in terms of bits or qubits (quantum communication complexity), that two spatially separated computing devices need to exchange in order to perform some computational task. Andrew Yao in 1979 was the first to introduce and study the topic of classical communication complexity in Ref. [225]. Yao himself, in 1993, considered how the situation might change if separated devices (or parties, Alice and Bob) were allowed to exchange qubits rather than classical bits (Ref. [226]). In principle, there are apparently convincing reasons to believe that quantum information should not provide any advantage when compared with classical communication: Holevo's theorem (Ref. [227]), a result about the classical information capacity of quantum channels, states that, for any classical message, the cost of transmitting it from one party (Alice) to another party (Bob) in terms of qubits is the same as the cost of transmitting it in terms of classical bits. In other words, if the computational task requires transmitting k bits on average, then it also requires k qubits on average.[1]

Notwithstanding, such belief turns out to be incorrect: quantum mechanics can be used to obtain remarkable advantages for such information/computation tasks. In fact, one of the most impressive applications of quantum resources for information processing is precisely the reduction of the communication complexity required for certain computations (Refs. [174, 229, 230, 231, 232]).

Following Ref. [41], in order to understand why quantum information can provide an advantage in communication and, nonetheless, not to contradict Holevo's theorem, let us consider first a *communication scenario*, the most basic one. Such scenario is illustrated in Fig. 9.1, which is taken also from Ref. [41]: there are two parties, Alice and Bob. Alice receives an input consisting of an n-bit string $x \in \{0,1\}^n$, and her task is to transmit it to Bob. She is only allowed to send him a message, and with that information at disposal Bob must output x. In this so simple scenario it is true that messages based on quantum resources are not more efficient than classical ones, according to Holevo's theorem. As a consequence, Alice will have to send n qubits in order to achieve the task (classically, she would have to send the entire n-bit string x): quantum information does not provide an advantage.

Nevertheless, the situation with respect to a possible advantage in the use of quantum re-

[1] To put it another way, and following G. Brassard (Ref. [228]), no more than n bits of expected classical information can be communicated between *unentangled* parties by the transmission of n qubits. Yao's original model implicitly assumed that Alice and Bob were not allowed to share prior entanglement in the initialization phase.

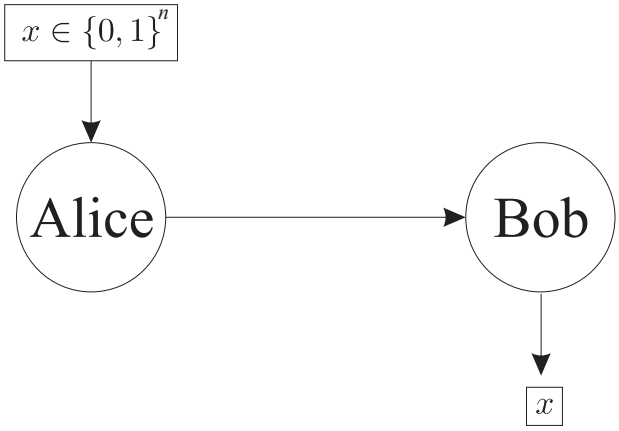

Figure 9.1: The basic communication scenario (the one underlying Holevo's theorem). Alice receives as input an n-bit string x, and then sends a message to Bob, who must output x. Sending a quantum message in not more efficient than sending a classical one, according to Holevo (Ref. [227]). Figure taken from Ref. [41].

sources instead of classical ones is different when one considers a more elaborated communication scenario for Alice and Bob, with a different computational task: imagine that Bob's goal is not to output Alice's n-bit string x (unknown for him), but to determine some information that is a function $f(x, y)$ of x which may depend on other data y (for instance, another n-bit string) at Bob's disposal but unknown for Alice. It is assumed that the form of the function f is known both to Alice and to Bob prior to the execution of the information protocol. Obviously, there is a trivial solution for this problem: Alice sends Bob her input x, and Bob subsequently computes $f(x, y)$. Remarkably, in this more involved scenario, quantum information enables Alice and Bob to attain the task with less qubit communication than would be required if the protocol were restricted to convey only classical bit communication. An scenario of the class we have just described, following Ref. [41], is usually referred to as a *communication complexity* scenario, and is illustrated in Fig. 9.2, which is also taken from Ref. [41].

The issue in classical communication complexity is to evaluate how much classical communication is required to compute the value of the function $f(x, y)$. To accomplish the task, the parties may not only exchange bits, but also use shared or local randomness. In quantum communication complexity the parties may instead use quantum resources. There are basically two approaches: the quantum communication model (Ref. [226]), in which parties can communicate qubits, and the entanglement model (Ref. [174]), where the parties share entangled states and are allowed to communicate classical bits.[2] Interestingly, the entanglement model is connected

[2]Both models are essentially equivalent *if* one allows the parties in the quantum communication model to share entangled states as well, since in that case one qubit in the quantum communication model can be replaced by two bits and one maximally entangled 2-qubit state (an EPR pair, v.g., $|\Phi^+\rangle = \frac{1}{\sqrt{2}}(|0\rangle|0\rangle + |1\rangle|1\rangle)$) in the entanglement model, and conversely one bit can be simulated by one qubit (Ref. [41]).

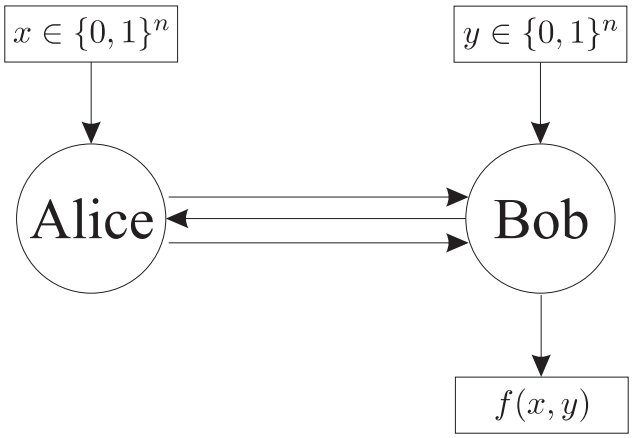

Figure 9.2: The basic communication complexity scenario. Both Alice and Bob receive n-bit strings, x and y respectively (x unknown to Bob, y unknown to Alice), and their goal is to compute certain function $f(x,y)$, that will be Bob's output. For some tasks with this structure, communication based on quantum messages is much more efficient than communication restricted to classical messages. The number of qubits can be exponentially smaller than the number of bits. Figure taken from Ref. [41].

with fundamental problems: in Ref. [125] it is proven that for every Bell's inequality, including those which are not yet known, there always exists a communication complexity problem, for which a protocol assisted by states which violate the inequality (therefore, entangled) is more efficient than any classical protocol. Violation of Bell's inequalities is the necessary and sufficient condition for quantum protocols to beat the classical ones.

In this chapter we are interested precisely in the second approach: Let us suppose that two or more separated parties need to compute a function of a number of inputs distributed among them. Using the best classical strategy, this would require a certain minimum amount of classical communication to be transmitted between the parties. However, if the parties initially shared some entangled states, then the amount of classical communication required for the computation would be a great deal smaller than if no entanglement were present. The quantum advantage usually grows with the number of parties involved (Ref. [229]). Entanglement-assisted reduction of classical communication complexity has numerous potential applications in computer networks, VLSI circuits, and data structures (Ref. [233]).

Graph states, like other entangled quantum states, constitute a valuable resource that may be shared by the participants in those scenarios corresponding to the entanglement model of communication complexity. They can provide surprising increases in communication efficiency in some protocols and tasks, outperforming the best classical yield. Our purpose in the next sections is to present in detail one of those scenarios, involving a communication protocol based on the GMN game, with the peculiarity that the contestants share specifically a graph state (in particular, a GHZ state of 3 or 4 qubits). We analyze the difficulties of an experimen-

tal realization of the entanglement-assisted GMN protocol for the reduction of communication complexity, and then propose certain changes that make the modified version of the GMN protocol experimentally feasible. We discuss the best classical strategy (exchanging bits and using shared randomness), the alternative quantum strategy (exchanging bits on the basis of a clever use of the shared graph state), and then make a comparison between their yields to determine the quantum versus classical advantage, through the analysis of the probability of success in the game. Finally, we discuss the photon detection efficiency requirements needed to perform the experiment in the laboratory, and make a concrete proposal for such an experiment.

9.2 The original *Guess My Number* protocol. Experimental requirements

A particularly attractive, thought-provoking, and stimulating way to show the quantum advantage was proposed by Steane and van Dam as a method for always winning the television contest "Guess My Number" in Ref. [232]. A team of three contestants (Alice, Bob, and Charlie), each of them isolated in a booth, is given an integer number $n = n_A + n_B + n_C$ of apples (where $n_j = 0$, 1/2, 1, or 3/2). One of the contestants must guess whether the number is odd or even just by receiving one bit from the other two contestants. The best classical strategy would allow the contestants to win in 75% of the cases. However, they can win in 100% of the cases if they initially share three-qubit GHZ states (Refs. [162, 234]). The same game can be played with four contestants and the quantum versus classical advantage is the same: 100% vs 75%. Steane and van Dam stressed that "A laboratory demonstration of entanglement-enhanced communication would be (...) a landmark in quantum physics and quantum information science" (Ref. [232]). So far, however, the requirements for an experimental implementation of the quantum GMN protocol have impeded further progress. Some progress has been reported on simpler schemes of quantum reduction of classical communication complexity. For instance, Xue *et al.* presented an experiment on quantum reduction of two-party communication complexity based on two-qubit entanglement (Ref. [235]). Galvão proposed a protocol requiring only one qubit and a detection efficiency $\sigma > 0.33$ (Ref. [236]). More recently, Brukner, Żukowski, and Zeilinger have introduced a quantum reduction of two-party communication complexity based on the entanglement between two qutrits (Ref. [237]).

The main obstacle for an experimental realization of the quantum GMN protocol is the high detection efficiency required. The required setup would consist of a source of GHZ states, single qubit operations, and single qubit detectors. If we define the overall efficiency η as the number of three-qubit (or four-qubit) joint detections corresponding to GHZ states, divided by the number of three-qubit (or four-qubit) systems emitted by the source, then, assuming that when no joint detection occurs the probability of winning the game is only 1/2, the experimental probability of winning the GMN game using GHZ states is

$$P_{\text{exp}}(\eta) = \eta + (1 - \eta)\frac{1}{2}. \tag{9.1}$$

Therefore, the quantum advantage could be detected if an overall efficiency $\eta > 0.50$ could be achieved. In the three-qubit case, the experiment would require threefold coincidences between

detectors so that each individual detector should have an efficiency $\sigma = 0.79$ (since $\sigma = \eta^{1/c}$, c being the number of qubits). Moreover, in order to obtain an experimental quantum probability of winning the GMN game 10% higher than the best classical probability, we would need $\eta > 0.70$, which would require detectors of efficiency $\sigma > 0.89$.

Quantum optics provides the best way to produce qubits in a GHZ state and distribute them to various spacetime regions. However, the first experiments producing three-photon polarization-entangled GHZ states (Refs. [238, 239]) did not satisfy the demands of the GMN protocol, because only a tiny fraction of the ensemble of photon triplets was detected (Ref. [232]). Further experiments producing four-photon GHZ states (Ref. [240]) yield a fourfold coincidence with a success probability 4 times higher than that of previous three-photon experiments. Moreover, recent experiments (Ref. [241]) report a fourfold coincidence rate 2 orders of magnitude brighter than in Ref. [240]. We shall show that in the very near future this technology could allow an experimental demonstration of a quantum reduction of a genuine three or four-party communication complexity.

9.3 The modified *Guess My Number* protocol

In this section, we introduce a modified version of the quantum GMN protocol which is experimentally feasible with current technology. We shall describe a quantum reduction of three-party (four-party) communication complexity in which the quantum advantage is clear, provided we can produce three (four) qubits in a GHZ state and detect them all separately with an overall efficiency $\eta > 0.17$, which would require detectors of efficiency $\sigma > 0.55$ ($\eta > 0.05$ and $\sigma > 0.47$, for four qubits). The main goal of this proposal is to note that the absence of perfect sources and detectors does not prevent us from performing an experimental demonstration of a quantum reduction of a genuine multiparty communication complexity and to stimulate experimental work along these lines.

The modified GMN game preserves all the essential features of the original game, but includes rules that relax the detection requirements to experimentally show the quantum advantage. The modified GMN game features one referee (and a fourth contestant in the $c = 4$ version). We shall discuss in detail the four-party version of the modified protocol; similar rules apply to the three-party version. During the game, each of four contestants (Alice, Bob, Charlie, and David) is isolated in a booth. Before the game starts, they can take anything they want with them into the booths, but once they are in, they will not be able to communicate with each other or with anybody else, save for the referee. Once they are in the booths, the referee distributes among them a randomly chosen integer number n of apples in four portions, $n = n_A + n_B + n_C + n_D$, such that $n_j = 0$, 1/2, 1, or 3/2. Then, the referee asks each and everyone whether or not they are ready to play the game; if all contestants say yes, then the referee asks Bob, Charlie, and David to give him a bit. Then, the referee adds (modulo 2) the three bits, and hands the result over to Alice. The team wins if Alice ascertains whether the total number of distributed apples is even or odd. If any contestant refuses to play the game, then the referee distributes a new number $n' = n'_A + n'_B + n'_C + n'_D$ of apples and asks the four contestants again whether or not they are ready to play the game, etc. If the referee distributes N rounds of apples, then the contestants are forced to play the game for at least r rounds (hereafter referred as "the played

Table 9.1: The 19 integer combinations of 0, 1/2, 1, and 3/2, and their corresponding 128 variations. In 64 of them $n_i + n_j + n_k + n_l$ is an odd number while in the other 64 it is an even number.

$\{n_i, n_j, n_k, n_l\}$	$n_i + n_j + n_k + n_l$	number of variations
$\{0, 0, 0, 0\}$	0	1
$\{0, 0, 0, 1\}$	1	4
$\{0, 0, 1/2, 1/2\}$	1	6
$\{0, 0, 1/2, 3/2\}$	2	12
$\{0, 0, 1, 1\}$	2	6
$\{0, 1/2, 1/2, 1\}$	2	12
$\{1/2, 1/2, 1/2, 1/2\}$	2	1
$\{0, 0, 3/2, 3/2\}$	3	6
$\{0, 1/2, 1, 3/2\}$	3	24
$\{0, 1, 1, 1\}$	3	4
$\{1/2, 1/2, 1/2, 3/2\}$	3	4
$\{1/2, 1/2, 1, 1\}$	3	6
$\{0, 1, 3/2, 3/2\}$	4	12
$\{1/2, 1/2, 3/2, 3/2\}$	4	6
$\{1/2, 1, 1, 3/2\}$	4	12
$\{1, 1, 1, 1\}$	4	1
$\{1/2, 3/2, 3/2, 3/2\}$	5	4
$\{1, 1, 3/2, 3/2\}$	5	6
$\{3/2, 3/2, 3/2, 3/2\}$	6	1

rounds"). The contestants know $p = r/N$ before the game starts. In addition, the referee must ensure that each of the 128 possible variations of apples (see Table 9.1) occurs with the same frequency in the played rounds.

9.3.1 Maximum classical probability of winning

In the modified GMN game, if the referee forces the contestants to play in $r = pN$ of the N rounds, the contestants can refuse to play between the first and the $N - r$ round, but then they are forced to play in the remaining r rounds. If they decide to play without being forced to do so then, every time they play, they will postpone in one round the moment they have to play compulsorily. The maximum classical probability of winning is obtained by combining two strategies. The first one applies in the rounds in which they play without being forced to do so, and can be designed in a way such that the contestants know when they must play and success is guaranteed when they do play (this happens, at best, once in every 32 rounds, on average, if $c = 4$, and once in every 8 rounds, on average, if $c = 3$). The second strategy applies when they are forced to play. It could be any of the best classical strategies of the original GMN game, giving a probability of success of 3/4 (for instance, each contestant would give the referee a bit

value 0 if she/he had received $n_j = 0$ or $1/2$, or a bit value 1 if she/he had received $n_j = 1$ or $3/2$). From all this follows that, for the modified GMN game, the best classical strategies (of which there are several) give the following maximum probability of winning for $c = 3$ or $c = 4$ contestants being forced to play in at least p of the rounds,

$$\begin{aligned} P_C(c,p) &= \lim_{N\to\infty}\left[\frac{(1-\mu)^{N-pN}}{4pN}\sum_{j=0}^{pN}(j+3pN)\mu^j \right. \\ &\quad \times \begin{pmatrix} N-pN+j-1 \\ j \end{pmatrix} \\ &\quad \left. + \sum_{j=pN+1}^{N}(1-\mu)^{N-j}\mu^j \begin{pmatrix} N \\ j \end{pmatrix}\right], \end{aligned} \tag{9.2}$$

where

$$\mu = \frac{8}{2^{2c}}. \tag{9.3}$$

For $c = 3$ and $c = 4$, this probability is represented as a function of p in Fig. 9.3. In addition, Fig. 9.3 contains numerical simulations of the probability that the team with $c = 3$ and $c = 4$ wins when using the best classical strategy for games of $N = 100$ rounds.

Note that, in both cases, if the referee forces the team to play all the rounds, the probability of winning by using the best classical strategy is $3/4$ while, if the referee forces them to play in at least one of every 100 rounds, then the probability of success using the best classical strategy is approximately 1.

9.3.2 Best entanglement-assisted strategy

Let us now see what the probabilities of winning are when using the best entanglement-assisted strategy. The contestants will always win if they use the following method:

(1) Each contestant carries a qubit belonging to a four-qubit system initially prepared in the GHZ state

$$|\mathrm{GHZ}\rangle = \frac{1}{\sqrt{2}}(|\bar{0}\bar{0}\bar{0}\bar{0}\rangle + |\bar{1}\bar{1}\bar{1}\bar{1}\rangle), \tag{9.4}$$

where $|\bar{0}\bar{0}\bar{0}\bar{0}\rangle = |\bar{0}\rangle \otimes |\bar{0}\rangle \otimes |\bar{0}\rangle \otimes |\bar{0}\rangle$, where $|\bar{0}\rangle = (1/\sqrt{2})(|0\rangle + |1\rangle)$ and $|\bar{1}\rangle = (1/\sqrt{2})(|0\rangle - |1\rangle)$.

(2) Each contestant j applies to her/his qubit the rotation

$$R(n_j) = |\bar{0}\rangle\langle\bar{0}| + e^{in_j\pi}|\bar{1}\rangle\langle\bar{1}|, \tag{9.5}$$

where n_j is her/his number of apples.

(3) Then, each contestant measures her/his qubit in the computational basis $\{|0\rangle, |1\rangle\}$.

(4) If, due to the inefficiency of the detectors, a contestant does not obtain a result, then she/he will tell the referee that she/he will not play the game, and the referee will therefore abort that round. Note that, in the aborted rounds, Alice does not receive any bits from the referee. If all contestants consent to play that round, then Bob, Charlie, and David will give their outcomes to the referee, who will add them up, and give the result to Alice.

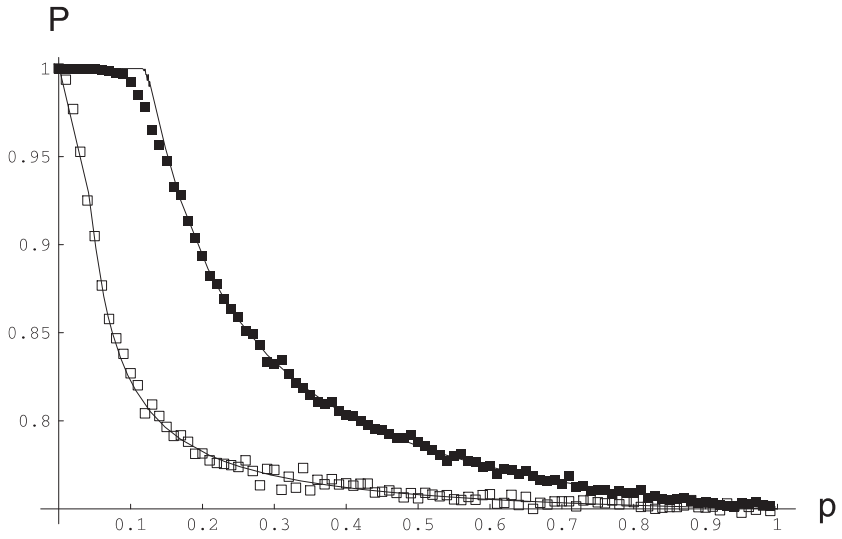

Figure 9.3: Exact and numerical simulations of the probability of the contestants winning the modified GMN game using the best classical strategy, as a function of the minimum percentage of rounds the referee forces them to play, for the three-contestant game (black squares) and four-contestant game (white squares). In the numerical simulations the referee distributes $N = 100$ rounds. The exact probabilities are given by Eq. (9.2). Interestingly, for $c = 3$ contestants forced to play in at least $p = 0.17$ of the rounds, the best classical probability of winning is only $P_C = 0.92$. For $c = 4$ contestants forced to play in at least $p = 0.05$ of the rounds, the best classical probability of winning is only $P_C = 0.90$.

In this case Alice can give the correct answer with probability 1 because state (9.4) has the following property: for any $n_A + n_B + n_C + n_D$ integer (where $n_j = 0,\ 1/2,\ 1,$ or $3/2$),

$$\begin{aligned} &R(n_A) \otimes R(n_B) \otimes R(n_C) \otimes R(n_D)|\mathrm{GHZ}\rangle \\ &\quad = \begin{cases} |\mathrm{GHZ}\rangle & \text{if } n_A + n_B + n_C + n_D \text{ is even,} \\ |\mathrm{GHZ}^{\perp}\rangle & \text{if } n_A + n_B + n_C + n_D \text{ is odd,} \end{cases} \end{aligned} \tag{9.6}$$

where $|\mathrm{GHZ}\rangle$ and $|\mathrm{GHZ}^{\perp}\rangle$ can be reliably distinguished by local measurements in the computational basis:

$$\begin{aligned} |\mathrm{GHZ}\rangle &= \frac{1}{2\sqrt{2}}(|0000\rangle + |0011\rangle + |0101\rangle + |0110\rangle \\ &\quad +|1001\rangle + |1010\rangle + |1100\rangle + |1111\rangle), \end{aligned} \tag{9.7}$$

$$\begin{aligned} |\mathrm{GHZ}^{\perp}\rangle &= \frac{1}{2\sqrt{2}}(|0001\rangle + |0010\rangle + |0100\rangle + |0111\rangle \\ &\quad +|1000\rangle + |1011\rangle + |1101\rangle + |1110\rangle). \end{aligned} \tag{9.8}$$

Table 9.2: Examples of single photon detection efficiency requirements for the modified GMN protocol. c is the number of parties, $P_Q - P_C$ is the difference between the quantum and classical probabilities of winning, η is the number of joint detections divided by the number of systems emitted by the source, and σ is the corresponding single photon detection efficiency.

c	$P_Q - P_C$	η	σ
3	0.250	1	1
4	0.250	1	1
3	> 0.214	> 0.50	> 0.79
4	> 0.218	> 0.20	> 0.67
3	> 0.107	> 0.20	> 0.58
4	> 0.177	> 0.10	> 0.56
3	> 0.077	> 0.17	> 0.55
4	> 0.097	> 0.05	> 0.47

9.4 Results and discussion

Assuming that, when all four contestants obtain a result, this corresponds to a GHZ state (i.e., assuming that any error in the preparation is negligible), then having an experimental efficiency η allows the team to play the modified GMN game with $p = \eta$. Now let us go back to the probabilities illustrated in Fig. 9.3. In the first place we shall compare the experimental requirements for the original GMN game with three qubits to those of the modified protocol. The most important point is that, while in the original GMN protocol the difference between the quantum and classical probabilities of winning could be detected only if the experimental setup has an overall efficiency $\eta > 0.50$ (that is, a single qubit detection efficiency $\sigma = 0.79$), in the modified protocol the difference between the quantum and classical probabilities *can be detected for almost any efficiency*. Moreover, as seen above, to obtain an experimental quantum probability of winning 10% higher than the best classical probability in the original GMN protocol, the setup would need to have $\eta > 0.70$ (that is, a single qubit detection efficiency $\sigma > 0.89$). However, to obtain a difference between the quantum and classical probabilities of winning higher than 7.7% in the modified protocol, the setup would only require $\eta > 0.17$ (that is, detectors of efficiency $\sigma > 0.55$). On the other hand, since sources of four-photon GHZ states (9.4) are currently available (Refs. [240, 241]), then it is interesting to note that, for $c = 4$ contestants and an experimental setup with an overall efficiency $\eta > 0.05$ (that is, with detectors of efficiency $\sigma > 0.47$), it would be possible to obtain a difference between the quantum and classical probabilities higher than 9.7%. Photodetectors of $\sigma > 0.47$ are currently available. Other examples for different values of σ can be found in Table 9.2. An interesting advantage of all these experiments is that the expected quantum probabilities are 1, which implies that the error of the experimental results, given by the standard deviation $\sqrt{P(1-P)}/r$, where r is the number of coincidences (i.e., played rounds), should be very low.

The proposed experiment would consist of a source emitting three (or four) polarization-entangled photons in a GHZ state generated in a parametric-down conversion process (Refs. [240,

241]), coupled into three (four) single mode optical fibers which distribute the photons to different regions, where each photon suffers a randomly chosen rotation of the type (9.5), and a linear polarization measurement (typically the horizontal and vertical states represent the computational basis). If all photons are detected, then two (three) of the contestants send their result to the referee who adds them up and sends the result to the third (fourth) contestant, who adds it to her result and gives the answer.

To sum up, while testing the advantage of the original quantum GMN protocol involving three parties would require detectors of an efficiency *at least* $\sigma > 0.79$ (or $\sigma > 0.89$ to obtain an experimental quantum probability of winning 10% higher than the best classical probability), we have introduced a modified quantum GMN protocol involving three or four parties and preserving all the essential features of the original one, but with the remarkable property that the quantum vs classical advantage is detectable for *any* σ. To be specific, $\sigma > 0.55$ would allow us to obtain an experimental quantum probability of winning at least 7.7% higher than the best classical probability in the three-party case, and $\sigma > 0.47$ would allow us to obtain an experimental quantum probability of winning at least 9.7% higher than the best classical probability in the four-party case.

As a final remark, our hope that this proposal stimulated experimental work to detect the quantum reduction of a genuine multiparty communication complexity was made into reality in 2007 by Zhang *et al.* in Ref. [16]. The authors present an experimental demonstration of a modified version of the entanglement-assisted GMN protocol for the reduction of communication complexity among three separated parties. The parties take advantage of the properties of the GHZ state they share. As expected, the results of experimental measurements imply that the separated parties can compute a function of distributed inputs by exchanging less classical information than it is required by using any classical strategy. Moreover, the results also demonstrate the advantages of entanglement-enhanced communication, which is very close to quantum communication. In Figs. 9.4 and 9.5, reproduced with permission of the authors, we show the experimental setup and the measurement results of the modified quantum three-party GMN experiment.

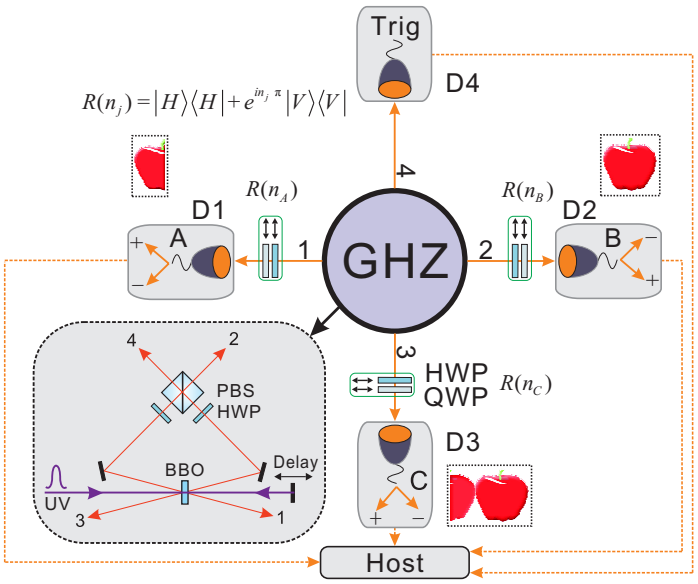

Figure 9.4: Diagram of Hefei's experimental setup for the three-party modified GMN game using three-photon entanglement. Reproduced from Zhang *et al.*, Phys. Rev. A **75**, 022302 (2007), with permission of the authors.

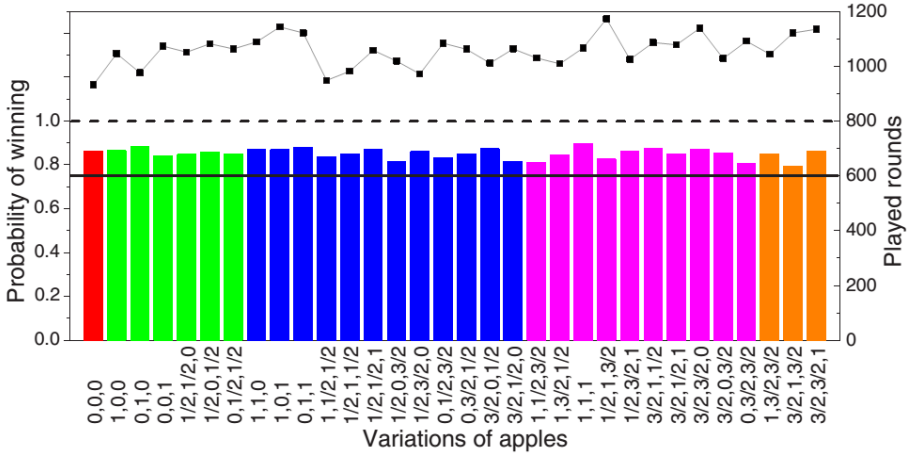

Figure 9.5: Measurement results of Hefei's quantum three-party GMN experiment, for the 32 possible variations. Square dots represent the number of played rounds (corresponding to the right y axis). The dashed line at 1.0 and the solid line at 0.75 represent the theoretical maximum quantum and classical probabilities of winning the modified GMN game, respectively. The histogram (referred to the left y axis) shows the experimental probabilities of winning, which turn out to be significantly higher than the maximum classical probabilities. Reproduced from Zhang *et al.*, Phys. Rev. A **75**, 022302 (2007), with permission of the authors.

Exclusivity graphs and graph states: What is the connection?

Last but not least, we conclude with a final remark that gives internal coherence to our work. Recall what we said at the beginning of this work, on p. 27: Throughout this thesis, graphs have been the ubiquitous mathematical entity upon which we have based all our research. That being true, we must highlight the fact that this thesis is divided into two parts where graphs *mean very different things* and play diverse roles. In the first part, devoted to exclusivity graphs of NC inequalities, graphs account for experiments in which some measurements are carried out on states: vertices represent events while edges describe relations of mutual exclusivity between events, and on the basis of such graphs we construct NC inequalities and calculate their bounds from some combinatorial numbers specific of the graphs. In the second part, devoted to graph states, graphs represent entangled multi-qubit quantum states. The graph not only provides an aid to write the generator of a graph state, but also serves as a blueprint for its preparation: vertices represent qubits (each of them initialized at the state $|+\rangle$) and edges describe subsequent entangling 2-qubit operations (v.g., controlled-Z gates). This proves how fruitful and versatile graph theory becomes when applied to some fundamental problems in QT (one of the main thrusts of the thesis), but at the same time causes us a slight nuisance: the scope of the thesis is too wide to be captured in a meaningful, precise and relatively short title, and this explains why we have chosen that of *Quantum correlations and graphs*, an intentionally broad-range title with which we try to cover all the aspects of our research.

Nevertheless, between these apparently non-linked parts of the thesis there is in fact a profound connection. So, the question is: Exclusivity graphs and graph states, what is the connection?

Such a question is frequently formulated in workshops and meetings on quantum information theory when the topic of exclusivity graphs of NC inequalities is part of the programme, since most people in the field usually have acquired prior familiarity with graph states. In the following we elucidate the answer to this question succinctly, on the basis of previous results obtained by other authors.

A connection between exclusivity graphs and graph states

(I) The first key result comes from Ref. [165]: any graph state corresponding to a connected graph violates local realism, i.e., all graph states feature nonlocal correlations unexplainable

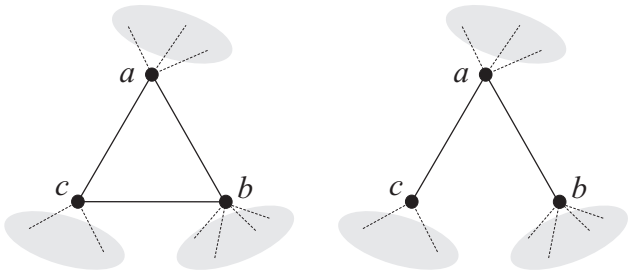

Figure 9.6: Connected subgraphs on 3 vertices of a given graph G that give rise to a violation of local realism by the corresponding graph state $|G\rangle$.

with LHV theories. For instance, the non-trivial 2-qubit graph state is LC equivalent to the singlet state and hence violates the original Bell inequality, Ref. [37]. Moreover, for a connected graph state with more than two vertices, any connected subgraph on three vertices yields a contradiction when trying to explain the observed correlations with LHV theories (see Fig. 9.6).

A quick reminder: recall (Sect. 5.2.1) that a graph state $|G\rangle$ associated to graph G is the unique common eigenvector to all stabilizing (generating) operators g_i, i.e., $g_i|G\rangle = |G\rangle$ for all $i \in \{1, ..., n\}$. Regarding correlations, from a physical point of view, the graph G describes all the perfect correlations of the state $|G\rangle$, since $\langle G|g_i|G\rangle = 1$ for all $i \in \{1, ..., n\}$. By considering the set of operators that can be obtained from products of generating operators (5.44), one obtains a commutative group featuring 2^n elements, the so-called stabilizer group, defined as

$$\mathcal{S}(G) = \{s_j\}_{j=1,...,2^n}, \qquad s_j = \prod_{i \in I_j(G)} g_i, \tag{9.9}$$

where $I_j(G)$ denotes any of the 2^n subsets of the vertices of the graph G. All the stabilizing operators are of the form

$$s_i = \bigotimes_{j=1}^{n} O_j^{(i)}, \tag{9.10}$$

where operators $O_j^{(i)} \in \{\mathbb{1}, \pm X_j, \pm Y_j, \pm Z_j\}$ are one-qubit Pauli operators.

In order to prove that all graph states feature nonlocal correlations (Ref. [165]; see also Ref. [164], specifically for cluster states of qubits with respect to their nonlocal properties, where it is proven that a GHZ argument always holds for any cluster state), we can proceed to generate Bell inequalities by adding all elements of the stabilizer group $\mathcal{S}(G)$. We eventually arrive at the operator

$$\mathcal{B}(G) = \sum_{i=1}^{2^n} s_i = \sum_{i=1}^{2^n} \bigotimes_{j=1}^{n} O_j^{(i)}. \tag{9.11}$$

It is then possible to define a Bell inequality based on the above Bell operator, and to compute its local bound

$$L(G) = \max_{\text{LHV}} |\langle \mathcal{B} \rangle| \tag{9.12}$$

Note that the graph state $|G\rangle$ reaches the value of 2^n (i.e., the algebraic maximum) for Bell inequality (9.12), since $s_i|G\rangle = |G\rangle$ for all $i \in \{1, ..., 2^n\}$. However, it turns out that $L(G) < 2^n$ for any graph G. Therefore, for all graph states it is possible to construct a Bell inequality, which the graph state itself violates maximally.

Bell inequalities of the type (9.12), in principle, are not optimal in the following sense (Ref. [171]): note that they involve the entire set of 2^n stabilizing operators of $\mathcal{S}(G)$. Nevertheless, for a given graph state associated to a connected graph of $n \geq 3$ qubits, if one considers the Bell operator involving the whole set of stabilizing operators, then one always have a violation of a Bell inequality (Ref. [165]), but not the maximum one according to a specific measure, namely, the ratio $\mathcal{D}$ between the quantum value of the Bell operator and its bound in LHV theories (Refs. [165, 171]). Such a violation occurs because that Bell operator contains inside a simpler Bell operator (i.e., involving a smaller number of stabilizing operators) giving the maximum violation according to $\mathcal{D}$. Moreover, the maximum violation (measured by $\mathcal{D}$) can be obtained for Bell operators with a different number of terms: in that case, one can choose the one with the lowest number, since the other inequalities contain this inequality and require more measurements, according to Ref. [171].

Anyway, we conclude that for graph states it is always possible to derive Bell inequalities maximally violated by them.

(II) The second key result comes from Ref. [242]: it is possible to transform the Bell operator (9.11), which is written as a sum of mean values of stabilizing operators, into a sum of probabilities of events, and then apply CSW's graph-theoretic approach from Refs. [6, 7] in order to construct the graph associated with the Bell inequality[3] (9.12). The procedure is the following (Ref. [242]):

Let G be a graph on n vertices and $|G\rangle$ the corresponding n-qubit graph state. Let $\mathcal{S}(G)$ be the stabilizer group of G. For each $s_i \in \mathcal{S}(G)$, with $s_i = \bigotimes_{j=1}^{n} O_j^{(i)}$, let $w_i = |\{O_j^{(i)} : O_j^{(i)} \neq \mathbb{1}\}|$ be the weight[4] of s_i. Let $\mathcal{E}_i = \{\mathcal{E}_{(k,i)} : k = 1, 2, \ldots, 2^{w_i - 1}\}$ be the set of the *events* of s_i, *i.e.* the measurement outcomes that occur with non-zero probability when the system is in state $|G\rangle$ and the stabilizing operators s_i are measured with single-qubit measurements. The set of all events is $\mathcal{E} = \bigcup_{i=1,2,\ldots,2^n-1} \mathcal{E}_i$. Hence, two events are *exclusive* if there exists a $j \in \{1, \ldots, n\}$ for which the same single-qubit measurement gives a different outcome. Therefore, the exclusivity graph of the inequality (9.12) is the graph $H(G)$ in which vertices represent the events in $\mathcal{E}$ and edges link pairs of mutually exclusive events.

This method has a remarkable feature: when it is applied to two graphs G_1 and G_2 belonging to the same orbit under local complementation, it eventually leads to the *same exclusivity graph* $H(G)$. In other words, there is an unique exclusivity graph $H(G)$ for each LC orbit (and consequently for each LC class of equivalence of graph states), and one can choose any arbitrary graph of the orbit as a representative to generate $H(G)$ (for instance, the simplest representatives in the classifications provided in Refs. [9, 11, 13, 209]).

Another important point concerns the characteristics of the exclusivity graph: given an n-qubit graph state $|G\rangle$, let H be the exclusivity graph corresponding to its LC orbit. Then, for

[3] We know from Sect. 1.3 that Bell inequalities are special instances of NC inequalities, in particular, when the tests involved in a NC inequality are not only compatible but also space-like separated.

[4] See Sect. 7.2.1.

$n > 2$,

$$\alpha(H) < \vartheta(H) = \alpha^*(H) = 2^n - 1, \tag{9.13}$$

where $\alpha(H)$, $\vartheta(H)$ and $\alpha^*(H)$ are the independence number, the Lovász number and the fractional packing number of H, respectively.[5] In other words, the graph G violates the corresponding Bell inequality (9.12) up to its algebraic maximum.

Let us recall, from Sect. 1.4.6, that those graphs G fulfilling $\alpha(G) < \vartheta(G) = \alpha^*(G)$ are called QFCGs, and for them there is a NC inequality in which the maximum quantum violation cannot be higher without violating the E principle, Ref. [7]. Moreover, in Chap. 3 we refer to quantum correlations achieving $\alpha^*(G)$ as quantum *fully contextual* correlations. Finally, it turns out that exclusivity graphs associated to LC orbits of graph states belong to such noteworthy family of QFCGs.

A final remark: the foregoing connection between exclusivity graphs and graph states suggests a possible generalization that deserves future research. In Sect. 8.6 we have outlined the concept of hypergraph states. The identification of equivalence classes of hypergraph states under LU transformations for up to four qubits, as well as important classes of five- and six-qubit states has been carried out in Ref. [222]. The question whether hypergraph states and their correlations can be used to reveal contradictions with classical hidden variable theories has also been considered, and various NC inequalities and Bell inequalities have been derived in Ref. [222]. It would be interesting to generate the corresponding exclusivity graphs and study their properties, in particular their combinatorial numbers: we cannot dismiss the possibility that the results on hypergraph states shed new light on the nature and limits of quantum correlations.

[5] See definitions in Sect. 1.4.4.

Conclusiones

En esta tesis hemos tratado diversos aspectos de la teoría cuántica (TC), que comprenden tanto problemas de índole fundamental como aplicada. Todos ellos comparten un rasgo distintivo común: se trata de problemas adecuados para abordarlos mediante una descripción basada en conceptos, métodos y herramientas propios de la teoría de grafos. Tal descripción proporciona una capacidad de percepción adicional en la búsqueda de soluciones a los problemas planteados. Nuestros resultados confirman el poder, versatilidad y utilidad del enfoque basado en teoría de grafos que hemos seguido. Esto se hace patente tanto en la Parte I, donde el principal objeto de interés es el grafo de exclusividad de una desigualdad no contextual (NC) y la conexión de sus números combinatorios característicos con los límites de las correlaciones clásicas, cuánticas y más generales; como en la Parte II, donde la atención se centra primordialmente en los estados grafo, su clasificación de acuerdo con sus propiedades de entrelazamiento, y la formulación de un procedimiento óptimo de preparación. Y no sólo eso: la conexión entre ambas partes de la tesis (p. 171) revela nuevos aspectos que a primera vista pasan desapercibidos pero que, una vez desvelados, dan soporte a la idea ya mencionada: la TC y la teoría de grafos son disciplinas que se impulsan mutuamente en obvia sinergia.

En línea con estas consideraciones, y a fin de dar fin a la tesis, presentamos a continuación el resumen con las conclusiones obtenidas a partir de aquellos capítulos que corresponden a los resultados innovadores de nuestro trabajo:

- Capítulo 1

  Los Resultados 1 y 2 de la Ref. [7], correspondientes a la aproximación a las correlaciones cuánticas mediante teoría de grafos de Cabello-Severini-Winter (CSW), permitirían diseñar experimentos con contextualidad cuántica "a la carta" mediante la selección de grafos G con las relaciones deseadas entre el número de independencia $\alpha(G)$, el número de Lovász $\vartheta(G)$ y el número de empaquetamiento fraccionario $\alpha^*(G)$, grafos para los cuales CSW proporcionan un método general para construir desigualdades NC.

  Siguiendo la propuesta de CSW, nosotros hemos abordado la elaboración de la clasificación de los llamados grafos cuánticos contextuales (QCG), que se definen como aquéllos para los que $\alpha(G) < \vartheta(G)$. En la Ref. [8] proporcionamos una lista ordenada que contiene G, $\alpha(G)$, $\vartheta(G)$, y $\alpha^*(G)$ para todos los grafos de menos de 11 vértices tales que $\alpha(G) < \vartheta(G)$. La Tabla 1.1 presenta el número total de grafos simples conexos no isomorfos para un número de vértices entre 2 y 10; además, el número de ellos que son QCG [$\alpha(G) < \vartheta(G)$], y para éstos últimos, el número de ellos que son grafos cuánticos completamente contextuales [QFCG, es decir, aquéllos para los que $\alpha(G) < \vartheta(G) = \alpha^*(G)$].

No existen QCG con un número de vértices menor que 5. En la Fig. 1.5 presentamos una muestra con los 37 QCG de menor orden, aquéllos correspondientes a un número de vértices entre 5 y 7. El QCG más simple es el pentágono o 5-ciclo, C_5, que es el grafo de exclusividad asociado a las desigualdades NC de Wright y Klyachko-Can-Binicioğlu-Shumovsky (véanse Refs. [49, 74]). Una cuidadosa inspección de la figura revela que todos los grafos mostrados en ella contienen a C_5 como subgrafo inducido, con la excepción de dos de ellos: el heptágono o 7-ciclo (C_7) y su complemento ($\overline{C_7}$). Estos tres grafos pertenecen a una familia bien conocida en teoría de grafos: los llamados *holes* y *antiholes* impares. Un análisis posterior de los QCG de hasta 10 vértices sugiere que todos los QCG podrían contener necesariamente holes y/o antiholes impares como subgrafos inducidos. Resolvemos este problema en la Ref. [78] (y dicha solución es nuestro principal interés en el Cap. 2).

No hay ningún QFCG con menos de 10 vértices. Los más simples son los cuatro grafos de 10 vértices que se muestran en la Fig. 1.6. Dado que para tales grafos se tiene que $\alpha(G) < \vartheta(G) = \alpha^*(G)$, hay una desigualdad NC asociada a cada uno de ellos en la cual la máxima violación cuántica no puede ser mayor sin violar el principio de exclusividad (E), es decir, que la suma de las probabilidades de un conjunto de eventos mutuamente excluyentes dos a dos no puede ser mayor que 1. Alcanzar tal máxima violación cuántica revelaría, por tanto, correlaciones cuánticas completamente contextuales. El grafo (a) en la Fig. 1.6, llamado por nosotros S_3, es el grafo de exclusividad que corresponde a la desigualdad NC capaz de revelar correlaciones cuánticas completamente contextuales más simple desde el punto de vista de la dimensión del sistema cuántico requerido (Ref. [89]; véanse también las conclusiones del Cap. 3). El grafo (d) en la Fig. 1.6 es el conocido como grafo de Johnson, $J(5, 2)$, que es el grafo de exclusividad correspondiente a la desigualdad *twin* de Cabello en la Ref. [90]: se trata de la desigualdad NC capaz de revelar correlaciones cuánticas completamente contextuales más simple desde el punto de vista del número de experimentos (test sí/no) necesario. Los grafos (b) y (c) son esencialmente como el grafo (a) más una o dos aristas extra, y no superan a los grafos (a) ó (d) en lo referente al número de experimentos necesario o la dimensión del sistema cuántico requerido.

En consecuencia, finalmente podemos concluir que la clasificación completa de los QCG de hasta 10 vértices que proporcionamos en la Ref. [8] nos permite identificar escenarios experimentales con correlaciones "a la carta" mediante la selección de grafos con las propiedades requeridas, y clasificar las correlaciones cuánticas a través del estudio de los números combinatorios de dichos grafos.

- Capítulo 2

  Hemos demostrado que la TC únicamente viola un tipo particular de desigualdades NC: aquéllas cuyos grafos de exclusividad contienen ciertos subgrafos inducidos básicos, los ciclos impares con cinco o más vértices y sus complementos (Resultado 1, p. 64). También hemos demostrado que la presencia de algunos de estos subgrafos proporciona una cota inferior a la dimensión mínima que debe tener un sistema cuántico para hacer que la desigualdad NC correspondiente sea experimentalmente comprobable (Resultado 2, p. 67).

  Por otro lado, hemos mostrado que hay una familia de desigualdades NC violada por la

TC cuyos grafos de exclusividad son precisamente los ciclos de orden impar (Resultado 3, p. 68). Este resultado no es nuevo (véanse Refs. [6, 1, 47]). El resultado interesante es que hemos demostrado que existe otra familia de desigualdades NC violadas por la TC cuyos grafos de exclusividad son los complementos de los ciclos de orden impar (Resultado 4, p. 68), y además hemos descrito cómo alcanzar el máximo valor cuántico para cada miembro de esta familia.

Finalmente, hemos aportado evidencias que sugieren que la máxima violación cuántica de las desigualdades correspondientes a los Resultados 3 y 4 es seleccionada por el principio E. Esto añade nuevos ejemplos a la lista de desigualdades cuyo máximo valor cuántico es seleccionado por dicho principio (véase Ref. [19]). El hecho de que los grafos de exclusividad de estas desigualdades NC básicas están presentes como subgrafos inducidos en el grafo de exclusividad de *cualquier* desigualdad NC violada por la TC (Resultado 1) sugiere que el principio E puede resultar fundamental para explicar las correlaciones cuánticas.

- Capítulo 3

  Hemos aplicado la aproximación de CSW a las correlaciones cuánticas mediante teoría de grafos (Refs. [6, 7]) sobre la base de nuestra clasificación de los QCG proporcionada en la Ref. [8], con la finalidad de diseñar un experimento con contextualidad cuántica "a la carta" mediante la búsqueda y selección de grafos con las propiedads deseadas. Este procedimiento nos ha permitido identificar y después llevar a cabo un experimento con test cuánticos compatibles y secuenciales, que produce correlaciones con la mayor contextualidad permitida bajo la suposición de *no-disturbance* (ND) expresada por la Ec. (1.20), que se asume como válida también para teorías post-cuánticas.

  Para tal propósito, hemos utilizado nuestra clasificación de QCG para seleccionar aquel QFCG con menos de 11 vértices (hay sólo cuatro grafos de esta clase) que requiriese un sistema cuántico con la mínima dimensión necesaria para alcanzar la máxima violación cuántica de la desigualdad NC asociada a tal grafo. Además, hemos proporcionado la desigualdad NC, el estado cuántico y el conjunto de medidas conducentes a dicha máxima violación cuántica.

  Asumiendo que los fotones detectados constituyen una muestra representativa y fiel de los emitidos por la fuente, y asumiendo también que la compatibilidad de los test secuenciales es perfecta, las correlaciones observadas en nuestro experimento exhiben la mayor contextualidad de la que nunca antes se haya informado en ningún experimento previo sobre desigualdades de Bell o desigualdades NC: correlaciones experimentales en las cuales la fraccción de correlaciones no contextuales es menor que 0.06. Se trata, pues, de correlaciones experimentales que proporcionan una evidencia convincente de la existencia de correlaciones completamente contextuales (i. e., aquéllas sin contenido no contextual) en la naturaleza.

  Además, con todo ello hemos demostrado la utilidad de la aproximación de CSW a las correlaciones cuánticas basada en teoría de grafos (Refs. [6, 7]), a la hora de identificar experimentos con ciertas propiedades deseables. Ello sugiere que desarrollos posteriores según estas líneas de trabajo proporcionarán mejores herramientas para identificar y observar fenómenos de especial interés físico.

- Capítulo 4

  Una red social (RS) suele describirse típicamente mediante un grafo en el cual los vértices representan actores de la red y las aristas representan el resultado de su mutua interacción, pero tal grafo no plasma la naturaleza de las interacciones ni explica por qué un actor se conecta o no a otros actores de la RS. Para solventar esa carencia en la descripción habitual, hemos introducido un enfoque físico de las RS en el cual cada actor viene caracterizado por un test sí/no realizado sobre un sistema físico. Este enfoque nos ha permitido considerar RS más generales (RSG), que van más allá de las que se originan por interacciones basadas en propiedades preexistentes, como ocurre en una RS clásica (RSC). Hemos confrontado RSG y RSC descritas por el mismo grafo, y hemos puesto de manifiesto la diferencia entre ellas por medio de una tarea simple para la cual los rendimientos correspondientes, medidos a través de la probabilidad promedio de éxito en la tarea, están acotados superiormente de manera diferente dependiendo de la naturaleza de las interacciones que definen cada tipo de RS.

  Hemos introducido también las RS cuánticas (RSQ) como un ejemplo de RS más allá de las RSC: hemos demostrado que las RSQ superan a las RSC en la tarea mencionada previamente y para ciertos grafos específicos. Presentamos todos los grafos no isomorfos de menos de 11 vértices (alrededor de 10^6) para los que las RSQ superan a las RSC en la Ref. [142]. Hemos identificado los grafos más simples con esta característica, y hemos demostrado que los grafos para los cuales las RSQ superan a las RSC son cada vez más frecuentes a medida que el número de vértices crece.

  Además, hemos considerado grafos para los cuales las RSQ superan a las RSC, pero tales que ninguna RSG descrita por uno de tales grafos supera a la mejor RSQ con el mismo grafo, y hemos identificado todos los grafos de menos de 11 vértices con esa propiedad. La Tabla 4.1 muestra el número de grafos no isomorfos con un número dado de vértices, hasta 10 vértices; el número de ellos en que las RSQ superan a las RSC, y para éstos últimos, el número de aquéllos para los cuales ninguna RSG supera a la mejor RSQ.

  Finalmente, hemos considerado grafos para los que la ventaja cuántica es independiente del estado cuántico, y hemos identificado el grafo más simple de este tipo.

- Capítulo 5

  Al ser este capítulo una introducción a la segunda parte de la tesis, consistente en la recopilación de aspectos conceptuales junto con resultados de otros autores, no hay conclusiones asociadas a él.

- Capítulo 6

  Hemos extendido hasta $n = 8$ qubits la clasificación del entrelazamiento de los estados grafo con $n < 8$ qubits propuesta por Hein, Eisert y Briegel (HEB) en la Ref. [9]. Para $n = 8$ hay 101 clases de equivalencia bajo operaciones locales de Clifford (LC), también conocidas como clases LC u *órbitas*, en tanto que para $n < 8$ hay sólo 45 clases LC.

  Para cada una de estas clases LC hemos obtenido un representante cuya preparación requiere el mínimo número de puertas controlled-Z y, además, la mínima profundidad de

preparación. Dichos representantes se corresponden con grafos con el mínimo número de aristas y el mínimo grado máximo (véase la Fig. 6.2). También hemos calculado, para cada clase LC, la medida de Schmidt para la partición 8-partita (que mide el entrelazamiento genuino 8-partito de la clase LC), y los rangos de Schmidt para todas las particiones bipartitas (Tabla 6.1).

Esta clasificación ha resultado útil para obtener nuevas demostraciones *todo-o-nada* del teorema de Bell en la Ref. [167], y nuevas desigualdades de Bell. Concretamente, cualquier estado grafo de 8 qubits que pertenezca a una clase LC con un grafo representante de 7 aristas (i. e., un árbol) conlleva un tipo específico de desigualdad de Bell (Ref. [172]). De modo más general, la clasificación ha sido útil para investigar la no localidad (i. e., la no reproducibilidad de las predicciones de la TC por medio de modelos de variables ocultas locales—modelos LHV por su acrónimo en inglés) de los estados grafo en la Ref. [171].

Los criterios utilizados en la Ref. [9] para etiquetar y ordenar las clases LC ya fallaban al distinguir todas las clases para $n = 7$. Hemos comprobado que el mismo problema surge con $n = 8$, entre las clases No. 110 y No. 111, entre las clases No. 113 y No. 114, y entre las clases No. 116 y No. 117 de nuestra clasificación (véase la Tabla 6.1). Por otra parte, Van den Nest, Dehaene y De Moor (VDD) han propuesto en la Ref. [12] un conjunto finito de invariantes que caracteriza todas las clases, pero dicho conjunto contiene demasiados invariantes (más de 2×10^{36} para $n = 7$) para resultar práctico. Este hecho plantea el problema de obtener un conjunto mínimo de invariantes bajo operaciones LC capaz de distinguir todas las clases con $n \leq 8$ qubits (éste es el principal asunto tratado en el Cap. 7 de esta tesis).

El valor preciso de la medida de Schmidt E_S es todavía desconocido para algunas clases. Sin embargo, para la mayoría de estas clases, dicho valor podría quedar fijado si se conociera el valor para el estado cluster anular de 5 qubits (correspondiente al grafo pentagonal o 5-ciclo), que es el primer estado grafo de la clasificación para el cual el valor de E_S se desconoce (Refs. [9, 11]). Desafortunadamente, nosotros no hemos hecho ningún progreso en el cálculo de E_S para dicho estado grafo.

No hay estados grafo de 8 qubits con índices de rango $RI_p = [\nu_j^p]_{j=p}^1$ con $\nu_j^p \neq 0$ si $j = p$, y $\nu_j^p = 0$ si $j < p$, i. e., con rango máximo con respecto a todas las biparticiones, es decir, tales que el entrelazamiento esté simétricamente distribuido entre todas las partes (Tabla 6.1). Estos estados son robustos contra el desentrelazamiento producido por unas pocas medidas. Tampoco hay estados grafo de 7 qubits con esta propiedad (Refs. [9, 11]). Esto hace más interesante el hecho de que haya únicamente un estado grafo de 5 qubits y otro de 6 qubits con esta propiedad (Refs. [9, 11]).

- Capítulo 7

  El conjunto de medidas de entrelazamiento propuesto por HEB en la Ref. [9] para estados grafo de n qubits falla al distinguir entre clases LC no equivalentes si $n \geq 7$ (Ref. [13]). El conjunto de invariantes propuesto por VDD en la Ref. [12] sí distingue entre clases LC no equivalentes, pero contiene demasiados invariantes (más de 2×10^{36} para $n = 7$) para resultar práctico.

Hemos resuelto el problema de decidir a qué clase de entrelazamiento pertenece un estado grafo de $n \leq 8$ qubits mediante el cálculo de algunas de las propiedades intrínsecas del estado, y por tanto sin generar la clase LC completa.

En primer lugar, hemos confirmado la conjetura formulada en la Ref. [12] de que los invariantes de VVD de tipo $r = 1$ son suficientes para distinguir entre las 146 clases de equivalencia bajo operaciones LC para estados grafo de hasta ocho qubits. No obstante, el número de dichos invariantes para estados grafo de hasta ocho qubits es aún demasiado grande para propósitos prácticos (30060 invariantes). Posteriormente, hemos comprobado que la distribución de pesos, que constituye una forma compacta de comprimir la información relativa a los invariantes de VDD de tipo $r = 1$, no resuelve el problema de distinguir entre cualesquiera dos clases de equivalencia LC: de hecho, ya no lo hace para estados grafo de 6 qubits.

A continuación, hemos introducido un nuevo conjunto compacto de invariantes bajo operaciones LC relacionados con los propuestos por VDD, a los que hemos denominado invariantes cardinalidad-multiplicidad (C-M), y hemos demostrado que basta con cuatro invariantes C-M para distinguir entre todas las clases LC no equivalentes de estados grafo con $n \leq 8$ qubits. Este resultado resuelve el problema surgido en la clasificación de los estados grafo de $n \leq 8$ qubits desarrollada en las Refs. [9, 11, 13].

También hemos demostrado que la conjetura formulada en la Ref. [218], según la cual la lista de invariantes bajo operaciones LC dados por la Ec. (7.6) es suficiente para caracterizar las clases de equivalencia LC de todos los estados de estabilizador, que no es cierta en general (Ref. [9]), es de hecho cierta para estados grafo de $n \leq 8$ qubits. Además hemos demostrado que para estados grafo de $n \leq 8$ qubits, la lista de invariantes bajo operaciones LC que vienen dados por la Ec. (7.7), que es más restrictiva que la lista de los que vienen dados por la Ec. (7.6), es suficiente. Esto resuelve un problema apuntado por VDD en la Ref. [12], en relación con la posibilidad de caracterizar subclases especiales de estados de estabilizador usando subfamilias de invariantes.

Se puede obtener un conjunto compacto de invariantes C-M que caracterice todas las clases LC no equivalentes para estados grafo con un número mayor de qubits aplicando la misma estrategia. Esto puede llevarse a cabo numéricamente hasta $n = 12$, un número de qubits más allá de la actual capacidad experimental de preparación de estados grafo (Ref. [195]). En este capítulo, la cuestión tocante a si estos invariantes conservan su eficacia para discriminar de manera no ambigua entre diferentes clases LC, queda abierta para futura investigación, y finalmente es resuelta en el Cap. 8.

- Capítulo 8

  Hemos propuesto un procedimiento para la preparación óptima de cualquiera de los más de 1.65×10^{11} estados grafo de hasta 12 qubits, basado en sus propiedades de entrelazamiento. Aquí por preparación óptima entendemos una preparación con (a) un número mínimo de puertas de entrelazamiento y (b) un número mínimo de pasos o etapas de tiempo, cuando es posible; o bien, eligiendo entre (a) o (b) en los otros casos. La preferencia dependerá del sistema físico particular que estemos considerando. Nuestro principal objetivo ha sido proporcionar en un único paquete todas las herramientas necesarias para identificar con

rapidez la clase de entrelazamiento a la que pertenece el estado diana, y a continuación encontrar fácilmente el circuito (o los circuitos) óptimo(s) correspondiente(s) de puertas de entrelazamiento, y finalmente las puertas de un qubit explícitas adicionales necesarias para preparar el estado diana; todo ello a partir de un estado puro producto inicial, y asumiendo únicamente puertas de un qubit arbitrarias y puertas controlled-Z, lo que constituye el escenario más común para propósitos prácticos.

Los resultados publicados en la Ref. [209] y presentados en este capítulo van más allá de los que se obtienen en las Refs. [9, 11, 13, 217]: la clasificación en virtud del entrelazamiento de una familia muy relevante de estados puros (estados grafo, y por extensión, estados de estabilizador) de 9, 10, 11 y 12 qubits. En total, se introducen casi 1.3×10^6 clases de entrelazamiento.

Hemos analizado la utilidad y las limitaciones de los invariantes C-M como discriminantes de las clases LC para estados grafo de hasta 12 qubits, una cuestión que se dejó como problema abierto en la Ref. [217] (véase Cap. 7), donde se conjeturaba que cuatro de tales invariantes C-M bastarían para etiquetar y discriminar todas las clases LC. Nuestros resultados muestran que para estados grafo de $n \geq 9$ qubits los invariantes C-M fallan al distinguir entre clases LC no equivalentes: el contraejemplo de menor tamaño para la conjetura corresponde a un par de órbitas de nueve qubits que tienen exactamente la misma lista completa de invariantes C-M. Éstas son las únicas órbitas problemáticas para $n = 9$ qubits. Como alternativa para discriminar entre ellas hemos calculado la lista completa de invariantes de VDD de tipo $r = 1$ (véase Ref. [12]) para las dos órbitas, y una vez más estos invariantes coinciden. A fin de determinar el número de órbitas "problemáticas" (indistinguibles) desde el punto de vista de los invariantes C-M y VDD, hemos extendido nuestros cálculos hasta $n = 12$ qubits. La ratio $p_f(n)$ entre el número de grafos pertenecientes a órbitas problemáticas y el número total de grafos para cada valor de n, da la probabilidad de que un estado grafo escogido al azar caiga en una de las órbitas problemáticas. Los valores calculados de $p_f(n)$ son, afortunadamente, bastante bajos (véase la Tabla 8.1). Por tanto, el primer paso en el procedimiento de preparación, i. e., la identificación de la órbita, recurre a invariantes C-M (y, a veces, a invariantes de VDD tipo $r = 1$), y funciona en la mayoría de los casos. Para aquellos casos poco frecuentes en los que la identificación de la órbita a través de invariantes C-M o de VDD ($r = 1$) no fuera unívoca, uno podría recurrir a invariantes de VDD de mayor orden r (Ref. [12]). Sin embargo, el esfuerzo computacional de dicha tarea hace este procedimiento menos eficiente que simplemente generar la órbita LC completa del estado grafo.

Los resultados obtenidos tienen relevancia experimental. Por ejemplo, imaginemos un físico experimental en el campo de los iones atrapados que quisiera preparar estados grafo. El físico experimental sabe que puede mantener, v. g., nueve iones (qubits) aislados de influencias externas por un período de tiempo dado, y sabe que durante ese tiempo puede llevar a cabo un máximo de m operaciones de entrelazamiento de dos qubits con una eficiencia por encima de un cierto valor umbral. El físico experimental quiere saber qué clases de estados grafo (qué clases de entrelazamiento) son una diana razonable con estos recursos. Nuestros resultados en este capítulo le permiten responder a esta cuestión: si $m = 8$, él puede preparar 47 clases diferentes (las clases 147–193 en la Ref. [14]); si $m = 9$,

puede preparar $47 + 95 = 142$ clases diferentes (las clases 147–288 en la Ref. [14]), etc. Además, nuestro trabajo le dice cuál es la secuencia óptima de láseres (puertas) requerida para preparar cualquier estado de cada clase.

Y lo que es más interesante: consideremos que el físico experimental quiere preparar un estado grafo específico de nueve qubits. Nuestra contribución proporciona el protocolo conocido más simple para identificar a qué clase de entrelazamiento pertenece el estado grafo diana, y da el circuito más simple para prepararlo, donde más simple significa en la mayoría de los casos aquél que requiere el mínimo número de puertas de entrelazamiento de dos qubits y mínimo número de pasos de computación; en aquellos casos en que tal circuito no existe, nuestra contribución proporciona un circuito que requiere el mínimo número de puertas de entrelazamiento, y también otro circuito que requiere mínima profundidad.

- Capítulo 9

  El protocolo original asistido por entrelazamiento para la reducción de la complejidad de la comunicación conocido como "Guess My Number" (GMN), que fue introducido por Steane y van Dam en la Ref. [232], plantea algunas dificultades para su realización experimental: requeriría producir y detectar estados de Greenberger-Horne-Zeilinger (GHZ) de tres qubits con una eficiencia $\eta > 0.70$, lo que a su vez conllevaría disponer de detectores de un fotón con eficiencia $\sigma > 0.89$.

  Hemos elaborado una versión modificada del protocolo GMN: los cambios que hemos introducido finalmente hacen que el protocolo GMN modificado sea factible experimentalmente. Discutimos la mejor estrategia clásica (que implica intercambio de bits y uso de aleatoriedad compartida); la estrategia cuántica alternativa (en que se intercambian bits sobre la base de un uso ingenioso de un estado entrelazado compartido por los participantes en el protocolo, que es además un estado grafo); y a continuación realizamos una comparación entre sus rendimientos para determinar la ventaja cuántica respecto a la variante clásica, mediante el análisis de la probabilidad de éxito en el protocolo (que puede visualizarse como un juego).

  Nuestros resultados indican que, mientras que la comprobación de la ventaja del protocolo cuántico GMN original con tres participantes precisa de detectores con una eficiencia de *al menos* $\sigma > 0.79$ (ó $\sigma > 0.89$ para obtener una probabilidad experimental cuántica de éxito un 10% mayor que la mejor probabilidad clásica), nuestro protocolo cuántico GMN modificado con tres o cuatro participantes conserva todas las características esenciales del original, pero con la destacable propiedad de que la ventaja cuántica respecto a la variante clásica es detectable para *cualquier* σ.

  Para ser más específicos, una eficiencia $\sigma > 0.55$ nos permitiría obtener una probabilidad experimental cuántica de éxito al menos un 7.7% mayor que la mejor probabilidad clásica, en el caso de tres participantes; y $\sigma > 0.47$ nos permitiría obtener una probabilidad experimental cuántica de éxito al menos un 9.7% mayor que la mejor probabilidad clásica, en el caso de cuatro participantes en el protocolo.

  Esta propuesta ha estimulado posterior esfuerzo experimental para la detección de la reducción cuántica de una complejidad de comunicación multipartita genuina, lo que finalmente ha llevado a la realización del experimento (véase la Ref. [16]), con los resultados

esperados: los participantes en el protocolo cuántico modificado pueden computar una función de inputs distribuidos mediante el intercambio de menos información clásica de la que se requeriría utilizando cualquier estrategia clásica.

Con estas consideraciones, damos fin a las conclusiones de la tesis doctoral.

Conclusions

In this thesis we have dealt with several topics in quantum theory (QT), encompassing both fundamental and applied issues, all of them sharing a common feature: they are suitable for a description based on concepts, methods and tools taken from graph theory, and such description provides additional insight in search of solutions to the problems raised. Our results confirm the power, versatility and usefulness of the graph-theoretic approach we have followed. This is patent both in Part I, where the main subject of interest is the exclusivity graph of a non-contextuality (NC) inequality and the connection of its characteristic combinatorial numbers with the limits of classical, quantum and more general correlations; and in Part II, where attention is primarily focused on graph states, their classification according to entanglement properties, and the formulation of an optimal preparation procedure. Moreover, the connection between both parts of the thesis (p. 171) reveals new aspects that at first sight go unnoticed but, once uncovered, support the aforementioned idea: QT and graph theory are disciplines that mutually boost each other in obvious synergy.

In line with these considerations, and in order to close this thesis, we present below the summary of conclusions drawn from those chapters which correspond to innovative results of our work:

- Chapter 1

  According to Cabello-Severini-Winter's (CSW) graph-theoretic approach to quantum correlations, Results 1 and 2 in Ref. [7] would allow to design experiments with quantum contextuality on demand by selecting graphs G with the desired relationships between the independence number $\alpha(G)$, the Lovász number $\vartheta(G)$ and the fractional packing number $\alpha^*(G)$, graphs for which a general method to construct NC inequalities is provided.

  Following that suggestion, we have addressed the elaboration of a classification of quantum contextual graphs (QCGs, for which $\alpha(G) < \vartheta(G)$). An ordered list containing G, $\alpha(G)$, $\vartheta(G)$, and $\alpha^*(G)$ for all graphs with less than 11 vertices for which $\alpha(G) < \vartheta(G)$ is provided in Ref. [8]. Table 1.1 presents the total number of non-isomorphic simple connected graphs for a number of vertices ranging from 2 to 10; the number of them which are QCGs $[\alpha(G) < \vartheta(G)]$, and for the latter, the number of those which are quantum fully contextual graphs [QFCGs, fulfilling $\alpha(G) < \vartheta(G) = \alpha^*(G)$].

  There are no QCGs with a number of vertices less than 5. In Fig. 1.5 we present a sample with the 37 simplest QCGs, those corresponding to a number of vertices ranging from 5 to 7. The simplest QCG is the pentagon or 5-cycle, C_5, which is the exclusivity graph

corresponding to the Wright and Klyachko-Can-Binicioğlu-Shumovsky NC inequalities (see Refs. [49, 74]). A careful inspection of the figure reveals that all the graphs shown in it contain C_5 as induced subgraph, with the exception of two: the heptagon or 7-cycle (C_7) and its complement ($\overline{C_7}$). This three graphs belong to a well-known family in graph theory: the so-called *odd holes* and *odd antiholes*. A subsequent analysis of the QCGs of up to 10 vertices suggests that all QCGs might necessarily contain odd holes and/or odd antiholes as induced subgraphs, Ref. [78] (this issue is our main interest in Chap. 2).

There is no QFCG with less than 10 vertices. The simplest ones are the four 10-vertex graphs depicted in Fig. 1.6. Given that for such graphs $\alpha(G) < \vartheta(G) = \alpha^*(G)$, there is an NC inequality associated to each of them in which the maximum quantum violation cannot be higher without violating the exclusivity (E) principle (namely, that the sum of probabilities of a set of pairwise exclusive events cannot be higher than 1). Achieving such maximum quantum violation would reveal, therefore, fully contextual quantum correlations. Graph (a) in Fig. 1.6, called S_3, is the graph corresponding to the simplest NC inequality capable of revealing fully contextual quantum correlations, from the viewpoint of the dimensionality of the required quantum system, Ref. [89] (see conclusions of Chap. 3). Graph (d) in Fig. 1.6 is the Johnson graph $J(5, 2)$, which is the exclusivity graph corresponding to Cabello's twin-inequality in Ref. [90], the simplest NC inequality capable of revealing fully contextual quantum correlations, from the viewpoint of the number of experiments (yes-no tests) needed. Graphs (b) and (c) are essentially as graph (a) plus one or two extra edges, and do not outperform (a) nor (d) regarding the number of experiments needed or the dimensionality of the quantum system required.

Consequently, we finally conclude that the complete classification of QCGs up to 10 vertices provided in Ref. [8] allows to identify experimental scenarios with correlations on demand by picking out graphs with the required properties, and classify quantum correlations through the study of their graph combinatorial numbers.

- Chapter 2

  We have proven that QT only violates a particular kind of NC inequalities: those whose exclusivity graph contains some basic induced subgraphs, odd cycles with five or more vertices and their complements (Result 1, p. 64). We have also shown that the presence of some of these subgraphs provides a lower bound to the minimum dimension that a quantum system must have to make the corresponding NC inequality experimentally testable (Result 2, p. 67).

  In addition, we have shown that there is a family of NC inequalities violated by QT whose exclusivity graphs are precisely odd cycles (Result 3, p. 68). This result is not new (see Refs. [6, 1, 47]). The interesting result is that we have shown that there is another family of NC inequalities violated by QT whose exclusivity graphs are the complements of odd cycles (Result 4, p. 68). We have described how to reach the maximum quantum value for each member of this family.

  Finally, we have shown evidences that suggest that the maximum quantum violation of the inequalities in Results 3 and 4 are singled out by the E principle. This adds new examples to the list of inequalities whose maximum quantum value is singled out by this principle

(see Ref. [19]). The fact that the exclusivity graphs of these NC inequalities are present in the exclusivity graph of *any* NC inequality violated by QT (Result 1) suggests that the E principle may be fundamental for quantum correlations.

- Chapter 3

  We have applied CSW's graph-theoretic approach in Refs. [6, 7] on the basis of our classification in Ref. [8] of QCGs to design an experiment with quantum contextuality on demand, by selecting graphs with the desired properties. This procedure has allowed us to identify and perform an experiment with sequential quantum compatible tests, which produces correlations with the largest contextuality allowed under the no-disturbance (ND) assumption (1.20), which is assumed to be valid also for post-quantum theories.

  For that purpose, we have used our classification of QCGs to select the QFCG with less than 11 vertices (there are only four of them) requiring a quantum system with the minimum dimension needed to achieve the maximum quantum violation of the NC inequality associated to the graph. Moreover, we have provided the NC inequality, the quantum state and the measurements leading to the maximum quantum violation.

  Assuming that the detected photons are a fair sample of those emitted by the source and assuming that the compatibility of the sequential tests is perfect, the correlations observed in our experiment exhibit the largest contextuality ever reported in any experiment of Bell or NC inequalities (experimental correlations in which the fraction of non-contextual correlations is less than 0.06), and provide compelling evidence of the existence of fully contextual correlations (i.e., those without non-contextual content) in nature.

  Moreover, we have demonstrated the usefulness of the approach to quantum correlations based on graph theory (Refs. [6, 7]) in identifying experiments with properties on demand. This suggests that further developments along these lines will provide better tools to identify and observe phenomena of physical interest.

- Chapter 4

  A social network (SN) is typically described by a graph in which vertices represent actors and edges represent the result of their mutual interactions, but such graph does not capture the nature of the interactions or explain why an actor is linked or not to other actors of the SN. To account for that lack in the usual description, we have introduced a physical approach to SNs in which each actor is characterized by a yes-no test on a physical system. This approach has allowed us to consider more general SNs (GSNs) beyond those originated by interactions based on pre-existing properties, as in a classical SN (CSN). We have confronted GSN and CSN described by the same graph and evidenced the difference between them by means of a simple task for which the corresponding yields, measured through the average probability of success, are upper bounded differently depending on the nature of the interactions defining the SN.

  We have also introduced quantum SNs (QSNs) as an example of SNs beyond CSNs: we have shown that QSNs outperform CSNs for the aforementioned task and some specific graphs. All non-isomorphic graphs with less than 11 vertices (around 10^6) in which QSNs outperform CSNs are presented in Ref. [142]. We have identified the simplest of these

graphs and shown that graphs in which QSNs outperform CSNs are increasingly frequent as the number of vertices increases.

Moreover, we have considered graphs for which QSNs outperform CSNs but no GSN outperforms the best QSN, and identified all the graphs with less than 11 vertices with that property. Table 4.1 contains the number of non-isomorphic graphs with a given number of vertices, up to 10 vertices; the number of them in which QSNs outperform CSNs, and for the latter, the number of those for which no GSN outperforms the best QSN.

Finally, we have considered graphs for which the quantum advantage is independent of the quantum state, and identified the simplest graph of this kind.

- Chapter 5

  Being this chapter a compilation of conceptual issues and results of other authors, there are no conclusions associated to this chapter.

- Chapter 6

  We have extended to 8 qubits the classification of the entanglement of graph states proposed in Ref. [9] for $n < 8$ qubits. For $n = 8$ there are 101 local Clifford (LC) classes of equivalence (orbits), while for $n < 8$ there are only 45 classes.

  For each of these classes we have obtained a representative which requires the minimum number of controlled-Z gates for its preparation and, in addition, the minimum preparation depth. This representatives correspond to graphs with minimum number of edges and minimum maximum degree (Fig. 6.2). We have also calculated for each class the Schmidt measure for the 8-partite split (which measures the genuine 8-party entanglement of the class), and the Schmidt ranks for all bipartite splits (Table 6.1).

  This classification has been useful to obtain new all-versus-nothing proofs of Bell's theorem in Ref. [167] and new Bell inequalities. Specifically, any 8-qubit graph state belonging to a class with a representative with 7 edges (i.e., a tree) has a specific type of Bell inequality (Ref. [172]). More generally, it has been helpful to investigate the nonlocality (i.e., the non-simulability of the predictions of quantum mechanics by means of local hidden variable (LHV) models) of graph states in Ref. [171].

  The criteria used in Ref. [9] to label and order the classes already failed to distinguish all classes in $n = 7$. We have checked that the same problem occurs between classes No. 110 and No. 111, between classes No. 113 and No. 114, and between classes No. 116 and No. 117 in our classification (see Table 6.1). On the other hand, Van den Nest, Dehaene, and De Moor (VDD) have proposed a finite set of invariants that characterizes all classes in Ref. [12], but contains too many invariants (more than 2×10^{36} for $n = 7$) to be practical. This fact poses the problem of obtaining a minimum set of LC invariants capable of distinguishing all classes with $n \leq 8$ qubits (main issue of Chap. 7 of this thesis).

  The precise value of the Schmidt measure E_S is still unknown for some classes. Nevertheless, for most of these classes, the value might be fixed if we knew the value for the 5-qubit ring cluster state, which is the first graph state in the classification for which the

value of E_S is unknown (Refs. [9, 11]). Unfortunately, we have not made any progress in calculating E_S for the 5-qubit ring cluster state.

There are no 8-qubit graph states with rank indexes $RI_p = [\nu_j^p]_{j=p}^1$ with $\nu_j^p \neq 0$ if $j = p$, and $\nu_j^p = 0$ if $j < p$, i.e., with maximal rank with respect to all bipartite splits, i.e., such that entanglement is symmetrically distributed between all parties (Table 6.1). These states are robust against disentanglement by a few measurements. Neither there are 7-qubit graph states with this property (Refs. [9, 11]). This makes more interesting the fact that there is a single 5-qubit and a single 6-qubit graph state with this property (Refs. [9, 11]).

- Chapter 7

  The set of entanglement measures proposed by Hein, Eisert and Briegel (HEB) in Ref. [9] for n-qubit graph states fails to distinguish between inequivalent classes under LC operations if $n \geq 7$ (Ref. [13]). The set of invariants proposed by VDD in Ref. [12] distinguishes between inequivalent classes, but contains too many invariants (more than 2×10^{36} for $n = 7$) to be practical.

  We have solved the problem of deciding which entanglement class a graph state of $n \leq 8$ qubits belongs to by calculating some of the state's intrinsic properties, thus without generating the whole LC class.

  First, we have confirmed the conjecture in Ref. [12] that VVD's invariants of type $r = 1$ are enough for distinguishing between the 146 LC equivalence classes for graph states up to eight qubits. Nevertheless, the number of such invariants for graph states of up to eight qubits is still too large for practical purposes (30060 invariants). Subsequently, we have checked that the weight distribution, a compact way to compress the information regarding VDD invariants of type $r = 1$, does not solve the problem of distinguishing between any two LC classes of equivalence: it already fails for 6-qubit graph states.

  Then, we have introduced a new compact set of LC invariants related to those proposed by VDD, the so-called cardinality-multiplicity (C-M) invariants, and shown that four C-M invariants are enough for distinguishing between all inequivalent classes with $n \leq 8$ qubits. This result solves the problem raised in the classification of graph states of $n \leq 8$ qubits developed in Refs. [9, 11, 13].

  We have also shown that the conjecture in Ref. [218] that the list of LC invariants given in Eq. (7.6) is sufficient to characterize the LC equivalence classes of all stabilizer states, which is not true in general (Ref. [9]), is indeed true for graph states of $n \leq 8$ qubits. Moreover, we have shown that, for graph states of $n \leq 8$ qubits, the list of LC invariants given in Eq. (7.7), which is more restrictive than the list given in Eq. (7.6), is enough. This solves a problem suggested in Ref. [12], regarding the possibility of characterizing special subclasses of stabilizer states using subfamilies of invariants.

  A compact set of C-M invariants that characterize all inequivalent classes of graph states with a higher number of qubits can be obtained by applying the same strategy. This can be done numerically up to $n = 12$, a number of qubits beyond the present experimental capability in the preparation of graph states (Ref. [195]). The question whether these invariants keep their effectiveness to unambiguously discriminate among different LC classes

is left open for future research (and solved in Chap. 8).

- Chapter 8

  We have proposed a procedure for the optimal preparation of any of the more than 1.65×10^{11} graph states with up to 12 qubits, based on their entanglement properties. Optimal means with both (a) a minimum number of entangling gates and (b) a minimum number of time steps, when possible, or choosing between (a) or (b), in the other cases. The preference will depend on the particular physical system we are considering. The main goal has been to provide in a single package all the tools needed to rapidly identify the entanglement class the target state belongs to, and then easily find the corresponding optimal circuit(s) of entangling gates, and finally the explicit additional one-qubit gates needed to prepare the target, starting with a pure product state and assuming only arbitrary one-qubit gates and controlled-Z gates, which constitutes the most common scenario for practical purposes.

  The results published in Ref. [209] and presented in this chapter go beyond those in Refs. [9, 11, 13, 217]: the classification of entanglement for a highly relevant family of qubit pure states (graph states and, by extension, stabilizer states) of 9, 10, 11, and 12 qubits. In total, almost 1.3×10^6 entanglement classes are introduced.

  We have analyzed the utility and limitations of the C-M invariants as LC-class discriminants for graph states up to 12 qubits, a question that was left as an open problem in Ref. [217] (see Chap. 7), where it was conjectured that four of these C-M invariants would be enough to label and discriminate all the LC classes. Our results show that for graph states of $n \geq 9$ qubits the C-M invariants fail to distinguish between inequivalent LC classes: the smallest counterexample of the conjecture corresponds to a pair of nine-qubit orbits that have exactly the same entire list of C-M invariants. These are the only problematic orbits for $n = 9$ qubits. As an alternative for discriminating between them, we have calculated the whole list of VDD invariants of type $r = 1$ (see Ref. [12]) for these two orbits, and once again these invariants coincide. In order to determine the number of C-M and VDD "problematic" (undistinguishable) orbits, we have extended our calculations up to $n = 12$ qubits. The ratio $p_f(n)$ of the number of graphs belonging to problematic orbits and the overall number of graphs for each n, gives the probability that a randomly chosen graph state falls in one of the problematic orbits. The values of $p_f(n)$ are, fortunately, quite low (see Table 8.1). Therefore, the first step of the procedure of preparation, i.e., the identification of the orbit, resorts to C-M invariants (and, sometimes, type $r = 1$ VDD invariants), and works in most cases. For those rare states whose orbit identification through C-M or VDD ($r = 1$) invariants is not univocal, one would resort to VDD invariants of higher order r (Ref. [12]). However, the computational effort of this task makes this procedure less efficient than simply generating the whole LC orbit of the graph state.

  The results have experimental relevance. For example, imagine an experimentalist in the field of trapped ions who wants to prepare graph states. The experimentalist knows that he can keep, e.g., nine ions (qubits) isolated from external influences for a given period of time, and knows that during this time he can perform a maximum of m two-qubit entangling operations with an efficiency above a certain threshold. The experimentalist wants to know which classes of graph states (which classes of entanglement) are a reasonable target with

these resources. Our results in this chapter allow him to answer this question: if $m = 8$, he can prepare 47 different classes (classes 147–193 in Ref. [14]); if $m = 9$, he can prepare $47 + 95 = 142$ different classes (classes 147–288 in Ref. [14]), etc. Moreover, our work tells the experimentalist which is the optimum sequence of lasers (gates) required for preparing any state of each class.

More interestingly, consider that the experimentalist wants to prepare a specific nine-qubit graph state. Our contribution provides the simplest known protocol to identify which entanglement class the target state belongs to, and give the simplest circuit to prepare it, where simplest means in most cases the one requiring the minimum number of entangling gates and computational steps or, in those cases in which such a circuit does not exist, gives a circuit requiring the minimum number of entangling gates, and a circuit requiring minimum depth.

- Chapter 9

  The original entanglement-assisted "Guess My Number" (GMN) protocol for the reduction of communication complexity, introduced by Steane and van Dam in Ref. [232], poses some difficulties for an experimental realization: it would require producing and detecting three-qubit Greenberger-Horne-Zeilinger (GHZ) states with an efficiency $\eta > 0.70$, which in turn would require single photon detectors of efficiency $\sigma > 0.89$.

  We have elaborated a modified version of the GMN protocol: the changes we have introduced eventually make the modified GMN protocol experimentally feasible. We discuss the best classical strategy (exchanging bits and using shared randomness), the alternative quantum strategy (exchanging bits on the basis of a clever use of the shared entangled state, which is a graph state), and then make a comparison between their yields to determine the quantum versus classical advantage, through the analysis of the probability of success in the game.

  Our results indicate that while testing the advantage of the original quantum GMN protocol involving three parties requires detectors of an efficiency *at least* $\sigma > 0.79$ (or $\sigma > 0.89$ to obtain an experimental quantum probability of winning 10% higher than the best classical probability), our modified quantum GMN protocol involving three or four parties preserves all the essential features of the original one, but with the remarkable property that the quantum vs classical advantage is detectable for *any* σ.

  To be specific, $\sigma > 0.55$ would allow us to obtain an experimental quantum probability of winning at least 7.7% higher than the best classical probability in the three-party case, and $\sigma > 0.47$ would allow us to obtain an experimental quantum probability of winning at least 9.7% higher than the best classical probability in the four-party case.

  This proposal has stimulated subsequent experimental work to detect the quantum reduction of a genuine multiparty communication complexity, which has resulted in the realization of the experiment (see Ref. [16]), with the expected results: the parties involved in the modified quantum protocol, can compute a function of distributed inputs by exchanging less classical information than it is required by using any classical strategy.

With this, we put and end to the conclusions of our PhD thesis.

Publications and contributions directly related to the thesis

Articles published in peer-reviewed journals

1. A. Cabello and A. J. López-Tarrida,
   Proposed experiment for the quantum "Guess My Number" protocol,
   Phys. Rev. A **71**, 020301(R) (2005).

2. A. Cabello, A. J. López-Tarrida, P. Moreno, and J. R. Portillo,
   Entanglement in eight-qubit graph states
   Phys. Lett. A **373**, 2219 (2009); ibid. **374**, 3991 (2010).

3. A. Cabello, A. J. López-Tarrida, P. Moreno, and J. R. Portillo,
   Compact set of invariants characterizing graph states of up to eight qubits
   Phys. Rev. A **80**, 012102 (2009).

4. A. Cabello, L. E. Danielsen, A. J. López-Tarrida, and J. R. Portillo,
   Optimal preparation of graph states
   Phys. Rev. A **83**, 042314 (2011).

5. A. Cabello, L. E. Danielsen, A. J. López-Tarrida, and J. R. Portillo,
   Quantum social networks
   J. Phys. A: Math. Theor. **45**, 285101 (2012).

6. E. Amselem, L. E. Danielsen, A. J. López-Tarrida, J. R. Portillo, M. Bourennane, and A. Cabello,
   Experimental fully contextual correlations
   Phys. Rev. Lett. **108**, 200405 (2012).

7. A. Cabello, L. E. Danielsen, A. J. López-Tarrida, and J. R. Portillo,
   Basic exclusivity graphs in quantum correlations
   Phys. Rev. A **88**, 032104 (2013).

Other contributions

1. A. Cabello, y A. J. López-Tarrida,

   Propuesta experimental para implementar el protocolo cuántico "Guess My Number"

   XXX Reunión Bienal de la Real Sociedad Española de Física (Orense, España, septiembre de 2005). *Libro de actas de la XXX Bienal de la Real Sociedad Española de Física* (Universidad de Vigo, 2005), p. 663.

2. A. Cabello, J. R. Portillo, A. J. López-Tarrida, y P. Moreno,

   Entrelazamiento en estados grafo de 8 qubits

   I Workshop Matemática Discreta Algarve Andalucía y VI Encuentros Andaluces de Matemática Discreta. *Avances en Matemática Discreta en Andalucía y en El Algarve* (Instituto Superior de Engenharia da Universidade Do Algarve, Galaroza, Huelva, España, 2009), p. 71. ISBN: 978-972-97073-7-7.

3. A. Cabello, A. J. López-Tarrida, P. Moreno, y J. R. Portillo,

   Conjunto compacto de invariantes que permiten caracterizar estados grafo de hasta ocho qubits

   XXXII Reunión Bienal de la Real Sociedad Española de Física (Ciudad Real, España, 7-11 de septiembre de 2009). M. A. López de la Torre, J. A. de Toro y J. González, *Libro de actas de la XXXII Bienal de la Real Sociedad Española de Física* (Real Sociedad Española de Física, Madrid, 2009), p. 540-541.

4. A. Cabello, A. J. López-Tarrida, P. Moreno, and J. R. Portillo,

   Compact set of invariants characterizing graph states up to eight qubits

   QIPC 2009. International Conference on Quantum Information Processing and Communication (September 21-25, 2009, Rome, Italy). Book of abstracts, p. 39.

5. A. Cabello, J. R. Portillo, A. J. López-Tarrida, and P. Moreno,

   Classification of the entanglement properties of eight qubit graph states

   JCCGG 2009. The 7th Japan Conference on Computational Geometry and Graphs (Kanazawa, Japan, November 11-13, 2009). Book of abstracts (Japan Advanced Institute of Science and Technology, Kanazawa, 2009), pp. 105-106.

6. A. Cabello, L. E. Danielsen, A. J. López-Tarrida, and J. R. Portillo,

   Optimal preparation of quantum graph states

   ACCOTA 2010. International Workshop on Combinatorial and Computational Aspects of Optimization, Topology and Algebra (Playa del Carmen, Quintana Roo, México, 2010). Book of abstracts, pp. 58-59.

7. A. Cabello, L. E. Danielsen, A. J. López-Tarrida, y J. R. Portillo,

   Aproximación mediante grafos a las teorías clásicas, la mecánica cuántica y las teorías probabilísticas generales

XXXIII Reunión Bienal de la Real Sociedad Española de Física (Santander, España. 19-23 septiembre 2011). *XXXIII Reunión Bienal de la Real Sociedad Española de Física*, Vol. 4, p. 185-186. ISBN: 978-84-86116-40-8.

8. J. R. Portillo, A. Cabello, A. J. López-Tarrida, and L. E. Danielsen,

   Quantum Social Networks

   ACCOTA 2012. International Workshop on Combinatorial and Computational Aspects of Optimization, Topology and Algebra (Huatulco, Oaxaca, México, 2012).

9. A. Cabello, L. E. Danielsen, A. J. López-Tarrida, y J. R. Portillo,

   Grafos de exclusividad en correlaciones cuánticas

   VIII Encuentros Andaluces de Matemática Discreta (IMUS, Universidad de Sevilla, 2013).

Index of acronyms

BS	50/50 beam splitter
C-M	Cardinality-multiplicity (invariants)
C-NOT	Controlled NOT (gate, operation)
CHSH	Clauser-Horne-Shimony-Holt
COM	Commutativity
CSN	Classical social network
CSW	Cabello-Severini-Winter
E	Exclusivity (principle)
EPR	Einstein-Podolski-Rosen
GHZ	Greenberger-Horne-Zeilinger
GMN	Guess My Number (protocol)
GSN	General social network
HEB	Hein-Eisert-Briegel
HWP	Half-wave plate
JM	Joint measurability
KS	Kochen-Specker
LC	Local Clifford (equivalence, operation)

LC*	Local complementation
LHV	Local hidden variables
LO	Local Orthogonality (principle)
LOCC	Local operations assisted by classical communication
LU	Local unitary (equivalence, operation, transformation)
NC	Non-contextuality (inequality)
ND	No-Disturbance (principle, assumption)
NCHV	Non-contextual hidden variables
OR	Orthonormal representation
PBS	Polarizing beam splitter
POVM	Positive-operator-valued measure
PVM	Projection-valued measure
QCG	Quantum contextual graph
QFCG	Quantum fully contextual graph
QNCG	Quantum non-contextual graph
QSN	Quantum social network
QT	Quantum theory
SLOCC	Stochastic local operations assisted by classical communication
SN	Social network
VDD	Van den Nest-Dehaene-De Moor
VLSI	Very-large-scale integration

Bibliography

[1] Y.-C. Liang, R. W. Spekkens and H. M. Wiseman, Phys. Rep. **506**, 1 (2011). 18, 28, 37, 53, 177, 186

[2] M. Nawareg, F. Bisesto, V. D'Ambrosio, E. Amselem, F. Sciarrino, M. Bourennane and A. Cabello, (2013), arXiv:1311.3495. 18, 28, 37, 53

[3] J. Barrett, N. Linden, S. Massar, S. Pironio, S. Popescu and D. Roberts, Phys. Rev. A **71**, 022101 (2005). 18, 28, 37, 44

[4] L. Masanes, A. Acín and N. Gisin, Phys. Rev. A **73**, 012112 (2006). 18, 28, 37, 44

[5] M. P. Seevinck, *Parts and holes. An inquiry into quantum and classical correlations*, PhD thesis, Utrecht University, 2008, arXiv:0811.1027v3. 18, 28, 37

[6] A. Cabello, S. Severini and A. Winter, (2010), arXiv:1010.2163. 19, 28, 37, 43, 49, 50, 52, 53, 56, 64, 68, 69, 70, 71, 77, 82, 88, 173, 177, 186, 187

[7] A. Cabello, S. Severini and A. Winter, Phys. Rev. Lett. **112**, 040401 (2014). 19, 20, 28, 29, 37, 49, 50, 52, 53, 55, 56, 57, 58, 64, 71, 75, 77, 173, 174, 175, 177, 185, 187

[8] A. Cabello, L. E. Danielsen, A. J. López-Tarrida and J. R. Portillo, http://www.ii.uib.no/~larsed/quantum_graphs/. 20, 29, 59, 73, 75, 78, 175, 176, 177, 185, 186, 187

[9] M. Hein, J. Eisert and H. J. Briegel, Phys. Rev. A **69**, 062311 (2004). 22, 23, 24, 31, 32, 33, 95, 108, 109, 115, 117, 118, 119, 121, 122, 124, 125, 126, 127, 128, 129, 131, 134, 135, 140, 141, 142, 143, 146, 149, 150, 160, 173, 178, 179, 180, 181, 188, 189, 190

[10] M. Van den Nest, J. Dehaene and B. D. Moor, Phys. Rev. A **69**, 022316 (2004). 22, 31, 115, 122, 135, 149

[11] M. Hein, W. Dür, J. Eisert, R. Raussendorf, M. Van den Nest and H. J. Briegel, *Entanglement in graph states and its applications*, in *Quantum Computers, Algorithms and Chaos*, 2006, edited by G. Casati, D.L. Shepelyansky, P. Zoller and G. Benenti (IOS Press, Amsterdam, 2006), arXiv:quant-ph/0602096v1. 22, 24, 32, 33, 108, 109, 115, 116, 117, 118, 121, 122, 124, 125, 128, 129, 131, 134, 135, 140, 141, 142, 143, 146, 149, 150, 160, 173, 179, 180, 181, 189, 190

[12] M. Van den Nest, J. Dehaene and B. D. Moor, Phys. Rev. A **72**, 014307 (2005). 23, 32, 128, 134, 136, 137, 139, 140, 141, 150, 151, 179, 180, 181, 188, 189, 190

[13] A. Cabello, A. J. López-Tarrida, P. Moreno and J. R. Portillo, Phys. Lett. A **373**, 2219 (2009); ibid. **374**, 3991 (2010). 24, 33, 117, 121, 134, 135, 141, 144, 150, 173, 179, 180, 181, 189, 190

[14] A. Cabello, L. E. Danielsen, A. J. López-Tarrida and J. R. Portillo, http://www.ii.uib.no/~larsed/entanglement/. 24, 33, 150, 151, 152, 153, 154, 181, 182, 191

[15] A. Cabello, L. E. Danielsen, A. J. López-Tarrida and J. R. Portillo, http://www.ii.uib.no/~larsed/entanglement/findoptimal.c. 24, 33, 150, 154

[16] J. Zhang, X.-H. Bao, T.-Y. Chen, T. Yang, A. Cabello and J.-W. Pan, Phys. Rev. A **75**, 022302 (2007). 25, 34, 169, 182, 191

[17] E. P. Specker, Dialectica **14**, 239 (1960). 37, 40, 48, 53, 63, 70

[18] E. P. Specker, 2009, https://vimeo.com/52923835. 37, 40, 70

[19] A. Cabello, Phys. Rev. Lett. **110**, 060402 (2013). 37, 53, 58, 63, 70, 71, 177, 187

[20] B. Yan, Phys. Rev. Lett. **110**, 260406 (2013). 37, 53, 58

[21] B. Amaral, M. Terra Cunha and A. Cabello, Phys. Rev. A **89**, 030101(R) (2014). 37, 58, 72

[22] R. Ramanathan, A. Soeda, P. Kurzyński and D. Kaszlikowski, Phys. Rev. Lett. **109**, 050404 (2012). 43, 51

[23] R. F. Werner and M. M. Wolf, Quant. Inf. Comp. **1 (3)**, 1 (2001), arXiv:quant-ph/0107093v2. 45

[24] A. Peres, *Quantum Theory: Concepts and Methods*, (Kluwer, Dordrecht, 1995), p. 203. 46, 48, 73, 89, 105

[25] C. Heunen, T. Fritz and M. L. Reyes, Phys. Rev. A **89**, 032121 (2014). 46

[26] A. Cabello, Nature **474**, 456 (2011). 47

[27] M. Sadiq, P. Badziąg, M. Bourennane and A. Cabello, Phys. Rev. A **87**, 012128 (2013). 47, 55, 71

[28] D. Reeb, D. Reitzner and M. M. Wolf, J. Phys. A: Math. Theor. **46**, 462002 (2013). 47, 48

[29] J. S. Bell, Rev. Mod. Phys. **38**, 447 (1966). 48, 63

[30] S. Kochen and E. P. Specker, J. Math. Mech. **17**, 59 (1967). 48, 63, 89, 91

[31] C. J. Isham, *Lectures on Quantum Theory. Mathematical and Structural Foundations*, (Imperial College Press, London, 1995). 48

[32] O. Gühne, M. Kleinmann, A. Cabello, J.-Å. Larsson, G. Kirchmair, F. Zähringer, R. Gerritsma and C. F. Roos, Phys. Rev. A **81**, 022121 (2010). 48, 81

[33] G. Kirchmair, F. Zähringer, R. Gerritsma, M. Kleinmann, O. Gühne, A. Cabello, R. Blatt and C. F. Roos, Nature (London) **460**, 494 (2009). 49, 83

[34] M. Michler, H. Weinfurter and M. Żukowski, Phys. Rev. Lett. **84**, 5457 (2000). 49

[35] H. Bartosik, J. Klepp, C. Schmitzer, S. Sponar, A. Cabello, H. Rauch and Y. Hasegawa, Phys. Rev. Lett. **103**, 040403 (2009). 49

[36] E. Amselem, M. Rådmark, M. Bourennane and A. Cabello, Phys. Rev. Lett. **103**, 160405 (2009). 49, 79, 83

[37] J. S. Bell, Physics **1**, 195 (1964). 49, 172

[38] J. Barrett, L. Hardy and A. Kent, Phys. Rev. Lett. **95**, 010503 (2005). 49

[39] A. Acín, N. Brunner, N. Gisin, S. Massar, S. Pironio and V. Scarani, Phys. Rev. Lett. **98**, 230501 (2007). 49

[40] S. Pironio, A. Acín, S. Massar, A. Boyer de la Giroday, D. N. Matsukevich, P. Maunz, S. Olmschenk, D. Hayes, L. Luo, T. A. Manning and C. Monroe, Nature (London) **464**, 1021 (2010). 49

[41] H. Buhrman, R. Cleve, S. Massar and R. de Wolf, Rev. Mod. Phys. **82**, 665 (2010). 49, 63, 160, 161, 162

[42] R. W. Spekkens, D. H. Buzacott, A. J. Keehn, B. Toner and G. J. Pryde, Phys. Rev. Lett. **102**, 010401 (2009). 49, 63

[43] T. S. Cubitt, D. Leung, W. Matthews and A. Winter, Phys. Rev. Lett. **104**, 230503 (2010). 49, 88

[44] K. Svozil, *Bertlmann's chocolate balls and quantum type cryptography*, in *Physics and Computation 2010*, edited by H. Guerra (University of Azores, Portugal, Ponta Delgada, 2010), p. 235, arXiv:0903.0231v2. 49

[45] A. Cabello, V. D'Ambrosio, E. Nagali and F. Sciarrino, Phys. Rev. A **84**, 030302(R) (2011). 49, 63

[46] J. F. Clauser, M. A. Horne, A. Shimony and R. A. Holt, Phys. Rev. Lett. **23**, 880 (1969). 49, 51, 55, 73

[47] M. Aráujo, M. T. Quintino, C. Budroni, M. Terra Cunha and A. Cabello, Phys. Rev. A **88**, 022118 (2013). 50, 177, 186

[48] P. Kurzyński, R. Ramanathan and D. Kaszlikowski, Phys. Rev. Lett. **109**, 020404 (2012). 51

[49] R. Wright, *The state of a pentagon*, in *Mathematical Foundations of Quantum Mechanics*, edited by A. R. Marlow (Academic, San Diego, 1978), p. 255. 52, 53, 55, 59, 70, 176, 186

[50] L. Hardy, (2001), quant-ph/0101012. 52

[51] L. Hardy, (2011), arXiv:1104.2066. 52

[52] B. Dakić and Č. Brukner, *Quantum theory and beyond: Is entanglement special?*, in *Deep Beauty. Understanding the Quantum World through Mathematical Innovation*, edited by H. Halvorson (Cambridge University Press, New York, 2011), p. 365. 52

[53] L. Masanes and M. P. Müller, New J. Phys. **13**, 063001 (2011). 52

[54] G. Chiribella, G. M. D'Ariano and P. Perinotti, Phys. Rev. A **84**, 012311 (2011). 52

[55] L. Masanes, M. P. Müller, R. Augusiak and D. Pérez-García, PNAS **110**, 16373 (2013). 52

[56] C. A. Fuchs and A. Peres, Phys. Today **53**(3), 70 (2000). 53

[57] C. A. Fuchs and B. C. Stacey, (2014), arXiv:1401.7254. 53

[58] S. Popescu and D. Rohrlich, Found. Phys. **24**, 379 (1994). 53, 55

[59] W. van Dam, *Nonlocality and Communication Complexity*, PhD thesis, Department of Physics, University of Oxford, 2000. 53

[60] W. van Dam, Nat. Comput. **12**, 9 (2013). 53

[61] M. Pawłowski, T. Paterek, D. Kaszlikowski, V. Scarani, A. Winter and M. Żukowski, Nature (London) **461**, 1101 (2009). 53, 63

[62] M. Navascués and H. Wunderlich, Proc. R. Soc. A **466**, 881 (2009). 53, 63

[63] R. Gallego, L. E. Würflinger, A. Acín and M. Navascués, Phys. Rev. Lett. **107**, 210403 (2011). 53

[64] T. H. Yang, D. Cavalcanti, M. L. Almeida, C. Teo and V. Scarani, New J. Phys. **14**, 013061 (2012). 53

[65] T. Fritz, A. B. Sainz, R. Augusiak, J. Bohr Brask, R. Chaves, A. Leverrier and A. Acín, Nature Communications **4**, 2263 (2013). 53, 70

[66] M. Navascués, Y. Guryanova, M. J. Hoban and A. Acín, (2014), arXiv:1403.4621. 53

[67] A. Cabello, (2013), arXiv:1303.6523v1. 53

[68] C. E. Shannon, IRE Trans. Inform. Theory **2**, 8 (1956). 53, 54, 55, 65, 71, 88

[69] M. Grötschel, L. Lovász and A. Schrijver, J. of Combinatorial Theory B **40**, 330 (1986). 54, 55, 56

[70] R. Diestel, *Graph Theory*, *Graduate Texts in Mathematics* **173** (Springer, Heidelberg, 2010). 54, 88

[71] L. Lovász, IEEE Trans. Inf. Theory **25**, 1 (1979). 54, 55, 87, 88

[72] M. Grötschel, L. Lovász and A. Schrijver, Combinatorica **1**, 169 (1981). 54

[73] B. Cirel'son [Tsirelson], Lett. Math. Phys. **4**, 93 (1980). 55

[74] A. A. Klyachko, M. A. Can, S. Binicioğlu and A. S. Shumovsky, Phys. Rev. Lett. **101**, 020403 (2008). 55, 59, 63, 73, 176, 186

[75] M. Grötschel, L. Lovász and A. Schrijver, *Geometric Algorithms and Combinatorial Optimization* (Springer, Berlin, 1988). 56

[76] J. L. Ramírez-Alfonsín and B. A. Reed (Eds.), *Perfect graphs*, (John Wiley & Sons, 2001). 56

[77] A. Cabello, (2012), arXiv:1212.1756. 58, 70

[78] A. Cabello, L. E. Danielsen, A. J. López-Tarrida and J. R. Portillo, Phys. Rev. A **88**, 032104 (2013). 58, 60, 63, 176, 186

[79] B. D. McKay, `nauty` *User's Guide (Version 2.4)*, (Department of Computer Science, Australian National University, Canberra, Australia, 2007). 58, 78, 90

[80] http://www.wolfram.com/mathematica/. 58, 78, 90

[81] http://sedumi.ie.lehigh.edu/. 58, 78, 90

[82] http://www.mcs.anl.gov/hs/software/DSDP/. 58, 78, 90

[83] S. J. Benson, Y. Ye and X. Zhang, SIAM J. Optimiz. **10**, 443 (2000). 58, 78, 90

[84] `MACE` (MAximal Clique Enumerator). 58, 78, 90

[85] K. Makino and T. Uno, *New algorithms for enumerating all maximal cliques*, in *Proceedings of the 9th Scandinavian Workshop on Algorithm Theory (SWAT 2004)*, (Springer-Verlag, 2004), p. 260. 58, 78, 90

[86] F. Harary, *Graph Theory*, (Addison-Wesley, Reading, Massachusetts, 1994). 59, 84, 86

[87] K. Briggs, *The* `very_nauty` *Graph Library (Version 1.1)*. 59, 90

[88] L. T. Kou, L. J. Stockmeyer and C. K. Wong, Commun. ACM **21**, 135 (1978). 59, 90

[89] E. Amselem, L. E. Danielsen, A. J. López-Tarrida, J. R. Portillo, M. Bourennane and A. Cabello, Phys. Rev. Lett. **108**, 200405 (2012). 60, 73, 75, 176, 186

[90] A. Cabello, Phys. Rev. A **87**, 010104(R) (2013). 60, 73, 176, 186

[91] A. K. Ekert, Phys. Rev. Lett. **67**, 661 (1991). 63, 108

[92] J. Anders and D. E. Browne, Phys. Rev. Lett. **102**, 050502 (2009). 63

[93] E. Nagali, V. D'Ambrosio, F. Sciarrino and A. Cabello, Phys. Rev. Lett. **108**, 090501 (2012). 63, 73, 83

[94] A. Cabello, S. Filipp, H. Rauch and Y. Hasegawa, Phys. Rev. Lett. **100**, 130404 (2008). 63

[95] A. Cabello, Phys. Rev. Lett. **101**, 210401 (2008). 63, 83

[96] P. Badziąg, I. Bengtsson, A. Cabello and I. Pitowsky, Phys. Rev. Lett. **103**, 050401 (2009). 63

[97] J. Oppenheim and S. Wehner, Science **330**, 1072 (2010). 63

[98] C. Berge, Wiss. Z. Martin-Luther Univ. Halle-Wittenberg **10**, 114 (1961). 65

[99] R. J. Nowakowski and D. F. Rall, Discussiones Mathematicae Graph Theory **16**(1), 53 (1996). 65

[100] M. Chudnovsky, N. Robertson, P. Seymour and R. Thomas, Ann. Math. **164**, 51 (2006). 65

[101] L. Lovász, Discr. Math. **2**, 253 (1972). 65

[102] D. E. Knuth, Electr. J. Comb. **1**, A1 (1994). 65, 88

[103] M. W. Padberg, Math. Programming **6**, 180 (1974). 66

[104] M. W. Padberg, Linear Algebra Appl. **15**, 69 (1976). 66

[105] M. Preissmann and A. Sebö, *Some Aspects of Minimal Imperfect Graphs*, in *Perfect Graphs*, edited by B. A. Reed and J. L. Ramírez-Alfonsín (Wiley, Chichester, 2001), p. 185. 66

[106] J. Petersen, Acta Mathematica **15**, 193 (1891). 70

[107] J. Henson, (2012), arXiv:1210.5978v3. 70

[108] B. Codenotti, I. Gerace and G. Resta, Ars Combinatoria **66**, 243 (2003). 71, 72

[109] E. R. Scheinerman and D. H. Ullman, *Fractional Graph Theory*, *Wiley-Interscience Series in Discrete Mathematics and Optimization* (John Wiley & Sons, New York, 1997). 71, 86

[110] M. Rosenfeld, Proc. Am. Math. Soc. **18**, 315 (1967). 71

[111] T. Bohman and R. Holzman, IEEE Transactions on Information Theory **49**, 721 (2003). 71

[112] A. Vesel and J. Žerovnik, Discrete Math. **12**, 333 (1998). 72

[113] A. Vesel and J. Žerovnik, Inf. Process. Lett. **81**, 277 (2002). 72

[114] N. D. Mermin, Phys. Rev. Lett. **65**, 1838 (1990). 73, 108

[115] A. Cabello, J. M. Estebaranz and G. García-Alcaine, Phys. Lett. A **212**, 183 (1996). 73, 89

[116] V. D'Ambrosio, I. Herbauts, E. Amselem, E. Nagali, M. Bourennane, F. Sciarrino and A. Cabello, Phys. Rev. X **3**, 011012 (2013). 73, 83

[117] S. Yu and C. H. Oh, Phys. Rev. Lett. **108**, 030402 (2012). 73

[118] M. Kleinmann, C. Budroni, J.-Å. Larsson, O. Gühne and A. Cabello, Phys. Rev. Lett. **109**, 250402 (2012). 73

[119] A. Peres, J. Phys. A **24**, L175 (1991). 73

[120] J. Barrett, A. Kent and S. Pironio, Phys. Rev. Lett. **97**, 170409 (2006). 76

[121] L. Aolita, R. Gallego, A. Acín, A. Chiuri, G. Vallone, P. Mataloni and A. Cabello, Phys. Rev. A **85**, 032107 (2012). 82

[122] A. E. Lita, B. Calkins, L. A. Pellouchoud, A. J. Miller and S. W. Nam, Proc. SPIE Int. Soc. Opt. Eng.7681, 76810D (2010). 82

[123] D. Fukuda, G. Fuji, T. Numata, K. Amemiya, A. Yoshizawa, H. Tsuchida, H. Fujino, H. Ishii, T. Itatani, S. Inoue and T. Zama, Opt. Express **19**, 870 (2011). 82

[124] A. Cabello, L. E. Danielsen, A. J. López-Tarrida and J. R. Portillo, J. Phys. A: Math. Theor. **45**, 285101 (2012). 83

[125] Č. Brukner, M. Żukowski, J.-W. Pan and A. Zeilinger, Phys. Rev. Lett. **92**, 127901 (2004). 83, 162

[126] J. Scott, *Social Network Analysis*, (Sage, London, 1991). 84

[127] S. Wasserman and K. Faust, *Social Network Analysis: Methods and Applications*, (Cambridge University Press, Cambridge, 1994). 84

[128] L. C. Freeman, *The Development of Social Network Analysis*, (Empirical Press, Vancouver, 2006). 84

[129] R. Albert and A.-L. Barabási, Phys. Rev. Lett. **85**, 5234 (2000). 84

[130] R. Albert and A.-L. Barabási, Rev. Mod. Phys. **74**, 47 (2002). 84

[131] A.-L. Barabási, Science **325**, 412 (2009). 84

[132] R. D. Luce and A. D. Perry, Psychometrika **14**, 95 (1949). 86

[133] L. Lovász, M. Saks and A. Schrijver, Linear Algebra Appl. **114/115**, 439 (1989). 87

[134] R. Duan, S. Severini and A. Winter, IEEE Trans. Inf. Theory 59(2), 1164 (2013). 88

[135] U. Feige and R. Krauthgamer, SIAM J. Comput. **32**, 345 (2003). 88

[136] N. Alon and J. H. Spencer, *The Probabilistic Method*, (Wiley, New York, 2000). 88

[137] F. Juhász, Combinatorica **2**, 153 (1982). 88

[138] J. Zimba and R. Penrose, Stud. Hist. Phil. Sci. **24**, 697 (1993). 89

[139] A. Cabello and G. García-Alcaine, J. Phys. A **29**, 1025 (1996). 89

[140] A. Cabello, J. M. Estebaranz and G. García-Alcaine, Phys. Lett. A **339**, 425 (2005). 89

[141] M. Pavičić, J.-P. Merlet, B. D. McKay and N. D. Megill, J. Phys. A **38**, 1577 (2005). 89

[142] A. Cabello, L. E. Danielsen, A. J. López-Tarrida and J. R. Portillo, http://www.ii.uib.no/~larsed/qsn/. 90, 178, 187

[143] M. Aspelmeyer and J. Eisert, Nature **455**, 180 (2008). 96

[144] R. Raussendorf and H. J. Briegel, Phys. Rev. Lett. **86**, 5188 (2001). 96, 108

[145] M. Van den Nest, A. Miyake, W. Dür and H. J. Briegel, Phys. Rev. Lett. **97**, 150504 (2006). 96, 108

[146] D. Gottesman, *Stabilizer codes and quantum error correction*, PhD thesis, California Institute of Technology, 1997, arXiv:quant-ph/9705052v1. 96, 104, 105

[147] R. Cleve, D. Gottesman and H.-K. Lo, Phys. Rev. Lett. **83**, 648 (1999). 96

[148] D. Fattal, T. S. Cubitt, Y. Yamamoto, S. Bravyi and I. L. Chuang, (2004), arXiv:quant-ph/0406168v1. 96

[149] G. Wang and M. Ying, Phys. Rev. A **75**, 052332 (2007). 96

[150] M. B. Elliott, *Stabilizer states and local realism*, PhD thesis, University of New Mexico, 2008, arXiv:0807.2876v1. 96, 98, 99, 100, 102, 105, 107, 109

[151] B. Eastin, *Error channels and the threshold for fault-tolerant quantum computation*, PhD thesis, The University of New Mexico, 2007, arXiv:0710.2560v1. 97, 104, 105

[152] M. A. Nielsen and I. L. Chuang, *Quantum Computation and Quantum Information*, (Cambridge University Press, Cambridge, England, 2000). 101, 104, 105, 107

[153] D. Gottesman, Phys. Rev. A **57**, 127 (1998). 104, 105

[154] S. Aaronson and D.Gottesman, Phys. Rev. A **70**, 052328 (2004). 105

[155] M. B. Elliott, B. Eastin and C. M. Caves, Phys. Rev. A **77**, 042307 (2008). 105

[156] D. Gottesman, Phys. Rev. A **54**, 1862 (1996). 108

[157] D. Schlingemann and R. F. Werner, Phys. Rev. A **65**, 012308 (2001). 108

[158] D. Schlingemann, Quantum Inf. Comput. **2**(4), 307 (2002). 108, 114, 135

[159] Y.-J. Han, R. Raussendorf and L.-M. Duan, Phys. Rev. Lett. **98**, 150404 (2007). 108

[160] W. Dür, H. Aschauer and H.-J. Briegel, Phys. Rev. Lett. **91**, 107903 (2003). 108

[161] J. Dehaene, M. Van den Nest, B. De Moor and F. Verstraete, Phys. Rev. A **67**, 022310 (2003). 108

[162] D. Greenberger, M. Horne and A. Zeilinger, *Going beyond Bell's theorem*, in *Bell's Theorem, Quantum Theory and Conceptions of the Universe*, 1989, edited by M. Kafatos (Kluwer Academic, Dordrecht, Holland, 1989), p. 69, arXiv:0712.0921. 108, 163

[163] D. P. DiVincenzo and A. Peres, Phys. Rev. A **55**, 4089 (1997). 108

[164] V. Scarani, A. Acín, E. Schenck and M. Aspelmeyer, Phys. Rev. A **71**, 042325 (2005). 108, 172

[165] O. Gühne, G. Tóth, P. Hyllus and H. J. Briegel, Phys. Rev. Lett. **95**, 120405 (2005). 108, 158, 171, 172, 173

[166] A. Cabello, Phys. Rev. Lett. **95**, 210401 (2005). 108

[167] A. Cabello and P. Moreno, Phys. Rev. Lett. **99**, 220402 (2007). 108, 117, 128, 179, 188

[168] M. Ardehali, Phys. Rev. A **46**, 5375 (1992). 108

[169] G. Tóth, O. Gühne and H. J. Briegel, Phys. Rev. A **73**, 022303 (2006). 108

[170] L.-Y. Hsu, Phys. Rev. A **73**, 042308 (2006). 108

[171] A. Cabello, O. Gühne and D. Rodríguez, Phys. Rev. A **77**, 062106 (2008). 108, 117, 128, 173, 179, 188

[172] O. Gühne and A. Cabello, Phys. Rev. A **77**, 032108 (2008). 108, 117, 128, 179, 188

[173] C. H. Bennett, G. Brassard, C. Crépeau, R. Jozsa, A. Peres and W. K. Wootters, Phys. Rev. Lett. **70**, 1895 (1993). 108

[174] R. Cleve and H. Buhrman, Phys. Rev. A **56**, 1201 (1997). 108, 159, 160, 161

[175] M. Żukowski, A. Zeilinger, M. A. Horne and H. Weinfurter, Acta Phys. Pol. A **93**, 187 (1998). 108

[176] D. Markham and B. C. Sanders, Phys. Rev. A **78**, 042309 (2008). 108

[177] P. Walther, K. J. Resch, T. Rudolph, E. Schenck, H. Weinfurter, V. Vedral, M. Aspelmeyer and A. Zeilinger, Nature (London) **434**, 169 (2005). 108

[178] N. Kiesel, C. Schmid, U. Weber, O. Gühne, G. Tóth, R. Ursin and H. Weinfurter, Phys. Rev. Lett. **95**, 210502 (2005). 108

[179] C.-Y. Lu, X.-Q. Zhou, O. Gühne, W.-B. Gao, J. Zhang, Z.-S. Yuan, A. Goebel, T. Yang and J.-W. Pan, Nat. Phys. **3**, 91 (2007). 108

[180] C.-Y. Lu, W.-B. Gao, O. Gühne, X.-Q. Zhou, Z.-B. Chen and J.-W. Pan, Phys. Rev. Lett. **102** 030502 (2009). 108

[181] J. K. Pachos, W. Wieczorek, C. Schmid, N. Kiesel, R. Pohlner and H. Weinfurter, New J. Phys. **11**, 083010 (2009). 108

[182] P. G. Kwiat, J. Mod. Opt. **44**, 2173 (1997). 108

[183] P. G. Kwiat and H. Weinfurter, Phys. Rev. A **58**, R2623(R) (1998). 108

[184] C. Cinelli, M. Barbieri, R. Perris, P. Mataloni and F. De Martini, Phys. Rev. Lett. **95**, 240405 (2005). 108

[185] T. Yang, Q. Zhang, J. Zhang, J. Yin, Z. Zhao, M. Żukowski, Z.-B. Chen and J.-W. Pan, Phys. Rev. Lett. **95**, 240406 (2005). 108

[186] J. T. Barreiro, N. K. Langford, N. A. Peters and P. G. Kwiat, Phys. Rev. Lett. **95**, 260501 (2005). 108

[187] M. Barbieri, F. De Martini, P. Mataloni, G. Vallone and A. Cabello, Phys. Rev. Lett. **97**, 140407 (2006). 108

[188] G. Vallone, E. Pomarico, P. Mataloni, F. De Martini and V. Berardi, Phys. Rev. Lett. **98**, 180502 (2007). 108

[189] H. Weinfurter and M. Żukowski, Phys. Rev. A **64**, 010102(R) (2001). 108

[190] M. Eibl, S. Gaertner, M. Bourennane, C. Kurtsiefer, M. Żukowski and H. Weinfurter, Phys. Rev. Lett. **90**, 200403 (2003). 108

[191] S. Gaertner, M. Bourennane, M. Eibl, C. Kurtsiefer and H. Weinfurter, Appl. Phys. B **77**, 803 (2003). 108

[192] M. Bourennane, M. Eibl, S. Gaertner, C. Kurtsiefer, A. Cabello and H. Weinfurter, Phys. Rev. Lett. **92**, 107901 (2004). 108

[193] P. Walther, M. Aspelmeyer, K. J. Resch and A. Zeilinger, Phys. Rev. Lett. **95**, 020403 (2005). 108

[194] S. Gaertner, M. Bourennane, C. Kurtsiefer, A. Cabello and H. Weinfurter, Phys. Rev. Lett. **100**, 070504 (2008). 108

[195] W.-B. Gao, C.-Y. Lu, X.-C. Yao, P. Xu, O. Gühne, A. Goebel, Y.-A. Chen, C.-Z. Peng, Z.-B. Chen and J.-W. Pan, Nat. Phys. **6**, 331 (2010). 108, 117, 141, 180, 189

[196] W.-B. Gao, X.-C. Yao, P. Xu, O. Gühne, A. Cabello, C.-Y. Lu, Z.-B. Chen and J.-W. Pan, unpublished. 108

[197] T. Monz, P. Schindler, J. T. Barreiro, M. Chwalla, D. Nigg, W. A. Coish, M. Harlander, W. Hänsel, M. Hennrich and R. Blatt, Phys. Rev. Lett. **106**, 130506 (2011). 108

[198] C. H. Bennett, S. Popescu, D. Rohrlich, J. A. Smolin and A. V. Thapliyal, Phys. Rev. A **63**, 012307 (2000). 112

[199] G. Vidal, J. Mod. Opt. **47**, 355 (2000). 112

[200] W. Dür, G. Vidal and J. I. Cirac, Phys. Rev. A **62**, 062314 (2000). 112, 113, 133

[201] N. Linden and S. Popescu, Fortsch. Phys. **46**, 567 (1998), arXiv:quant-ph/9711016. 112

[202] J. Kempe, Phys. Rev. A **60**, 910 (1999). 112

[203] H.-K. Lo and S. Popescu, Phys. Rev. A **63**, 022301 (2001). 113

[204] F. Verstraete, J. Dehaene, B. De Moor and H. Verschelde, Phys. Rev. A **65**, 052112 (2002). 113

[205] M. Van den Nest, J. Dehaene and B. D. Moor, *Local equivalence of stabilizer states*, in *Proceedings of the 16th International Symposium on Mathematical Theory of Networks and Systems (MTNS 2004)*, (Katholieke Universiteit Leuven, Belgium, 2004). 114, 133, 148

[206] Z. Ji, J. Chen, Z. Wei and M. Ying, Quantum Inf. Comput. **10**(1&2), 97 (2010). 114, 115, 134, 149

[207] M. Van den Nest, J. Dehaene and B. D. Moor, Phys. Rev. A **71**, 062323 (2005). 115, 134

[208] B. Zeng, H. Chung, A. W. Cross and I. L. Chuang, Phys. Rev. A **75**, 032325 (2007). 115, 134

[209] A. Cabello, L. E. Danielsen, A. J. López-Tarrida and J. R. Portillo, Phys. Rev. A **83**, 042314 (2011). 117, 145, 173, 181, 190

[210] L. E. Danielsen, *Database of Self-Dual Quantum Codes*, http://www.ii.uib.no/~larsed/vncorbits/. 117, 121

[211] M. Hajdušek and M. Murao, New J. Phys. **15**, 013039 (2013). 118, 128

[212] X.-Y. Chen, J. Phys. B: At. Mol. Opt. Phys. **43(8)**, 085507 (2010). 118

[213] C. Wang, L. Jiang and L. Wang, J. Appl. Math. Phys. **1**, 51 (2013). 118

[214] J. Eisert and H. J. Briegel, Phys. Rev. A **64**, 022306 (2001). 123, 134

[215] S. Severini, Phys. Lett. A **356**, 99 (2006). 123

[216] M. Mhalla and S. Perdrix, (2004), *8th Workshop Quantum Information Processing, QIP'05*, (Boston, January 2005), arXiv:quant-ph/0412071. 125, 146, 147

[217] A. Cabello, A. J. López-Tarrida, P. Moreno and J. R. Portillo, Phys. Rev. A **80**, 012102 (2009). 128, 133, 134, 151, 154, 181, 190

[218] A. Bouchet, Discrete Math. **114**, 75 (1993). 141, 180, 189

[219] V. G. Vizing, Diskret. Analiz. **3**, 25 (1964), (in Russian). 147

[220] J. Misra and D. Gries, Inform. Process. Lett. **41**, 131 (1992). 147

[221] A. Broadbent and E. Kashefi, Theor. Comput. Sci. **410**, 2489 (2009). 147

[222] M. Rossi, M. Huber, D. Bruß and C. Macchiavello, New J. Phys. **15**, 113022 (2013). 156, 174

[223] O. Gühne, M. Cuquet, F. E. S. Steinhoff, T. Moroder, M. Rossi, D. Bruß, B. Kraus and C. Macchiavello, (2014), arXiv:1404.6492v1. 156, 158

[224] A. Cabello and A. J. López-Tarrida, Phys. Rev. A **71**, 020301(R) (2005). 159

[225] A. C.-C. Yao, *Some complexity questions related to distributed computing*, in *Proceedings of the 11th Annual ACM Symposium on Theory of Computing, STOC'79*, (New York, 1979). 160

[226] A. C.-C. Yao, *Quantum circuit complexity*, in *Proceedings of the 34th Annual IEEE Symposium on Foundations of Computer Science*, (Palo Alto, California, 1993). 160, 161

[227] A. S. Holevo, Probl. Peredachi Inf. **9**:3, 3 (1973). 160, 161

[228] G. Brassard, (2001), arXiv:quant-ph/0101005v1. 160

[229] H. Buhrman, R. Cleve and A. Wigderson, *Quantum vs. classical communication and computation*, in *Proceedings of the 30th Annual ACM Symposium on the Theory of Computing (STOC98)*, (ACM Press, New York, 1998), p. 63. 160, 162

[230] H. Buhrman, W. van Dam, P. Høyer and A. Tapp, Phys. Rev. A **60**, 2737 (1999). 160

[231] R. Raz, *Exponential separation of quantum and classical communication complexity*, in *Proceedings of the 31st Annual ACM Symposium on the Theory of Computing (STOC99)*, 1999, (ACM Press, New York, 1999), p. 358. 160

[232] A. M. Steane and W. van Dam, Phys. Today **53** (2), 35 (2000). 160, 163, 164, 182, 191

[233] E. Kushilevitz and N. Nisan, *Communication Complexity*, (Cambridge University Press, Cambridge, England, 1997). 162

[234] D. M. Greenberger, M. A. Horne, A. Shimony and A. Zeilinger, Am. J. Phys. **58**, 1131 (1990). 163

[235] P. Xue, Y.-F. Huang, Y.-S. Zhang, C.-F. Li and G.-C. Guo, Phys. Rev. A **64**, 032304 (2001). 163

[236] E. F. Galvão, Phys. Rev. A **65**, 012318 (2002). 163

[237] Č. Brukner, M. Żukowski and A. Zeilinger, Phys. Rev. Lett. **89**, 197901 (2002). 163

[238] D. Bouwmeester, J.-W. Pan, M. Daniell, H. Weinfurter and A. Zeilinger, Phys. Rev. Lett. **82**, 1345 (1999). 164

[239] J.-W. Pan, D. Bouwmeester, M. Daniell, H. Weinfurter and A. Zeilinger, Nature (London) **403**, 515 (2000). 164

[240] J.-W. Pan, M. Daniell, S. Gasparoni, G. Weihs and A. Zeilinger, Phys. Rev. Lett. **86**, 4435 (2001). 164, 168, 169

[241] Z. Zhao, T. Yang, Y.-A. Chen, A.-N. Zhang, M. Żukowski and J.-W. Pan, Phys. Rev. Lett. **91**, 180401 (2003). 164, 168, 169

[242] A. Cabello, M. G. Parker, G. Scarpa and S. Severini, J. Math. Phys. **54**, 072202 (2013). 173